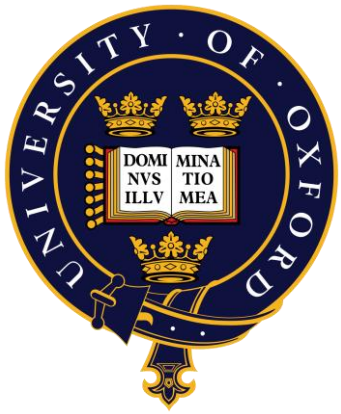
Investigating and modelling early upper gastro-intestinal neoplasia



Michael Joseph White

Magdalen College

University of Oxford

A thesis submitted for the degree of

Doctor of Philosophy in Clinical Medicine

Hilary 2022

Declaration

All the work presented in this thesis is the result of my own work except where otherwise explicitly stated. This work has not been submitted as part of another thesis unless stated otherwise, although some figures feature in the published work Owen & White et al. 2018. The work presented in this thesis was performed whilst I was a graduate student at the Ludwig Institute for cancer research, under the supervision of Professor Xin Lu and Professor Mark Middleton.

Acknowledgements

It has been a long and challenging road to get to this point, full of the highest of highs and the lowest of lows. There are so many people that I need to thank for their help and support along the way.

Xin and Professor Middleton, thank you for guiding me throughout the years of research and thank you for your unwavering support during the COVID 19 pandemic with my difficulties juggling clinical work, having a young family and writing up my thesis. You were understanding and gave me support when it was most needed and for this, I am eternally grateful.

From a pastoral point of view, I would really like to thank Professor Rob Gilbert and Professor Sarah De Val for their support, understanding, faith and belief in me and my ability to get this done after multiple extensions and developing long COVID.

I would like to thank my wife Lucie, for her support with writing my thesis whilst working full time as a surgical trainee, and at the same time as going through the desperate times of the pandemic, moving house and having our beautiful son Freddie. Freddie, perhaps one day you will read this, I would like you to know that you brought me so much joy every day, when I was struggling you gave me strength to keep pushing and getting my thesis done.

I would like to thank my parents for always pushing and encouraging me to set my sights high and believing in me when I have had difficulties. My siblings James and Philippa who were always a great source of support.

I would like to thank my lab mates: Richard Owen, David Severson, Gopi, Ludo, Stefanie, Zinaida, Liz Slee, Imogen and Carlos for the helpful chats, brainstorming, teamwork and generally being a fantastic sounding board for ideas. I would

particularly like to thank Gopi for his important mentorship in the lab despite only overlapping for 18 months in the lab his method of rigorously planning every experiment, in an effort to make every experiment into usable data.

I would like to give a huge thank you to Indi, Mark, Richard Lisle, Shan, Stan, Professor Rob Goldin, Dr Lai-Mun Wang, Dr Adam Bailey, Dr Barbara Braden, Dr Beth Bird-Lieberman, Dr James East, Mr Nick Maynard, Mr Bob Marshall, Mr Bruno Sgromo, Paul Sopp, Angie Green, Paolo Piazza, David Buck, Richard Bryant,

Lastly, but by no means least the whole of the OUH endoscopy unit, the Biobank team, the Wellcome Trust Centre for Human Genetics Functional genomics unit, the Human Developmental Biology Resource in Edinburgh and the Whole of the Oxford branch of the Ludwig Institute for Cancer research.

NB: A significant proportion of Chapter 4 and 5 have been included in publication (Owen, White et al. 2018). I have gained consent from Dr Richard Owen and Dr David Severson for inclusion of some published material in my thesis.

Publications

- Owen RP*, **White MJ***, Severson DT*, Braden B, Bailey A, Goldin RD, Wang LM, Maynard N, Green A, Piazza P, Buck D, Middleton M, Ponting C, Schuster-Boeckler B, Lu X. Single cell RNA-seq reveals profound transcriptional similarity between Barretts esophagus and esophageal glands. Nature communications 9 (1), 4261 (*these authors are joint first authors)
- Severson DT, Owen RP, **White MJ**, Lu X, Schuster-Böckler B. BEARscc determines robustness of single-cell clusters using simulated technical replicates. Nature communications 9 (1), 1187
- Morris EV, Cerundolo L, Lu M, Verrill C, Fritzsche F, **White MJ**, Thalmann GN, Ten Donkelaar CS, Ratnayaka I, Salter V, Hamdy FC, Lu X, Bryant RJ. Nuclear iASPP may facilitate prostate cancer progression. Cell Death Dis. 2014 Oct 23; 5:e1492. PMID: 25341046
- Verrill C, Cerundolo L, Mckee C, **White M**, Kartsonaki C, Fryer E, Morris E, Brewster S, Ratnayaka I, Marsden L, Lilja H, Muschel R, Lu X, Hamdy F, Bryant RJ. Altered expression of epithelial-to-mesenchymal transition proteins in extraprostatic prostate cancer. Oncotarget. 2016 Jan 12; 7(2):1107-19. doi:10.18632/oncotarget. 6689
- Dedeić Z, Sutendra G, Hu Y, Chung K, Slee EA, **White MJ** , Zhou FY, Goldin RD, Ferguson DJP, McAndrew D, Schneider JE, Lu X. Cell autonomous role of iASPP deficiency in causing cardiocutaneous disorders. Cell Death & Differentiation, 1
- Zhou FY, Ruiz-Puig C, Owen RP, **White MJ**, Rittscher J, Lu X. Motion sensing superpixels (MOSES) is a systematic computational framework to quantify and discover cellular motion phenotypes. eLife 8, e40162

Abstract

In recent years, gastro-oesophageal cancers have increased in incidence in the western world with no known cause. Barrett's oesophagus (BO) is a premalignant lesion induced by chronic biliary reflux. The cell of origin of BO has been greatly contested yet elusive. Non-dysplastic BO is a poorly understood but highly heterogeneous metaplastic tissue with deranged differentiation and a high incidence of early P53 mutations. Intestinal metaplasia (IM) is an internationally accepted defining criterion for BO diagnosis. In this thesis, I have examined the role of early P53 mutation in the development of gastro-oesophageal cancers by using a combined P53 mutant transgenic mouse in combination with a biliary reflux model. Although gastric cancers did not consistently occur, I found evidence that P53 mutations may potentiate inflammation in non-dysplastic BO. Further investigation of BO cellular complexity using sc-RNA-seq also found that BO shared transcriptional similarity with a subset of oesophageal cells, but not with gastric or duodenal cells, and identified a number of potential biomarkers. Lastly, I have developed organoid models for BO, and demonstrated their ability to differentiate into cell populations see in the scRNA-seq data. In conclusion, my findings reveal a striking similarity between normal OSG cells and BO cells with the high expression of LEFTY1 and TFF3. I identify potential early markers for goblet cell differentiation, SPINK4 and ITLN1 and OLFM4 expression as a marker of BO progenitor cells, which may have clinical implications.

List of abbreviations

AB	Alcian Blue
BO	Barrett's Oesophagus
CLE	Columnar lined epithelium
GIM	Gastric Intestinal metaplasia
GOJ	Gastro-oesophageal junction
GORD	Gastro-oesophageal Reflux disease
IF	Immunofluorescence
IHC	Immunohistochemistry
IM	Intestinal metaplasia
ISH	*In situ* hybridisation
MLE	Multi-layered epithelium
NDBO	Non dysplastic Barrett's oesophagus
OAC	Oesophageal Adenocarcinoma
OSG	Oesophageal submucosal gland
PAS	Periodic Acid Schiff
SCJ	Squamo-columnar junction
sc-RNA-seq	Single cell RNA sequencing

Table of Contents

DECLARATION **1**

ACKNOWLEDGEMENTS **2**

PUBLICATIONS **4**

ABSTRACT **5**

LIST OF ABBREVIATIONS **6**

CHAPTER 1: INTRODUCTION **12**

1.1 ANATOMY OF THE HUMAN UPPER GASTRO-INTESTINAL TRACT 12

1.1.1 Oesophagus *12*

1.1.2 Stomach *13*

1.1.3 Duodenum *14*

1.2 DIFFERENCES BETWEEN THE MOUSE AND HUMAN UPPER GI TRACT 15

1.3 BIOLOGY OF THE OESOPHAGUS 16

1.3.1 Oesophageal development *16*

1.3.2 Oesophageal epithelium *19*

1.3.3 Native oesophageal submucosal glands (OSGs) *20*

1.4 BIOLOGY OF THE STOMACH 21

1.4.1 Gastric development *21*

1.4.2 Gastric epithelium *23*

1.4.3 Gastric cardia native or acquired? *24*

1.5 BIOLOGY OF THE DUODENUM 26

1.5.1 Duodenal development *26*

1.5.2 Goblet cells *27*

1.6 BARRETT'S OESOPHAGUS (BO) 28

1.6.1 Diagnosis of BO *30*

1.6.2 Pathology of BO *31*

1.7 GASTRO OESOPHAGEAL REFLUX DISEASE (GORD) 32

1.8 METAPLASIA 33

1.8.1 Squamous metaplasia *35*

1.8.2 Intestinal metaplasia (IM) *35*

1.9 UPPER GASTRO-INTESTINAL CANCERS 37

1.9.1 Oesophageal carcinoma *38*

1.9.2 Gastric carcinoma *39*

1.9.3 Gastro-oesophageal junctional carcinoma *39*

1.10 GENETIC SUSCEPTIBILITY TO BO AND OAC 40

1.11 UNDERSTANDING MALIGNANT PROGRESSION IN BO 42

1.12 Genomic studies of BO and OAC 48
1.13 Animal models of GORD, BO, OAC and GAC 49
1.14 Transgenic models of gastro-oesophageal cancer 51
1.14.1 Developmental gene models 51
1.14.2 TGF β pathway transgenic models 52
1.14.3 Inflammatory gene models 53
1.14.4 Parietal cell targeting models 54
1.14.5 Combined Helicobacter-transgenic models 54
1.15 Mixed transgenic and surgical models 55
1.16 Rodent surgical models 56
1.17 Cellular origins of BO 57
1.17.1 Squamous hypothesis transdifferentiation versus transcommitment 57
1.17.2 Gastric stem cell hypothesis 60
1.17.3 Submucosal gland hypothesis 62
1.17.4 Circulating bone marrow cells 66
1.17.5 Residual embryonic cell hypothesis 67
1.17.6 Transitional cells hypothesis 68
1.18 Summary 70
AIMS 71
CHAPTER 2: METHODS 72
2.1 Materials 72
2.1.1 Reagents 72
2.1.2 Cell lines 75
2.2 Tissue culture 75
2.2.1 Culture of cell lines 76
2.2.2 Storage of cells in liquid nitrogen 76
2.2.3 Organotypic culture 77
2.2.4 Human organoid culture 78
2.3 Human tissue 80
2.3.1 Biobanking 80
2.3.2 Preparation of single cells from endoscopic biopsies 80
2.3.3 Cell isolation for flow cytometry 81
2.3.4 sc-RNA-seq 83
2.3.5 Sequencing data analysis 83
2.3.6 Foetal tissue samples 83
2.4 Murine studies 84
2.4.1 Breeding 84
2.4.2 Genotyping 84
2.4.3 Biliary reflux mouse model 85

2.4.4 Necropsy, dissection, fixation and embedding *85*
2.5 HISTOLOGICAL METHODS 85
2.5.1 Haematoxylin and eosin staining *85*
2.5.2 Alcian blue staining *86*
2.5.3 Immunohistochemistry *86*
2.5.4 Tissue/ cell immunofluorescence *87*
2.5.5 Table of primary antibodies used for staining *88*
2.5.6 Table of secondary antibodies used for staining *89*
2.5.7 Quantification of immunohistochemical staining H-score *90*
2.5.8 RNA in situ hybridisation (RNAscope™) *90*
2.6 MOLECULAR METHODS 92
2.6.1 Quantitative polymerase chain reaction (PCR) *92*
2.6.2 Table of QPCR primers *92*
2.6.3 Expression plasmid transfection *93*
CHAPTER 3: RESULTS – DEVELOPING A TRANSGENIC/ BILIARY REFLUX MODEL TO EXAMINE GASTRIC CARCINOGENESIS 94
3.1 INTRODUCTION 94
3.1.1 The P53 family *95*
3.1.2 P53 mutation in upper GI cancer *96*
3.1.3 The ASPP family *98*
3.2 ASPP EXPRESSION IN THE UPPER GI TRACT 99
3.3 INVESTIGATING AN UPPER GI PHENOTYPE OF iASPP AND ASPP2 TRANSGENIC MICE 101
3.4 INVESTIGATING AN UPPER GI PHENOTYPE OF P53 TRANSGENIC MICE 103
3.5 *p53^{R172H}* MICE HAVE INCREASED INCIDENCE OF CARCINOMAS 104
3.6 *p53^{R172H}* MICE DEMONSTRATE SOME EVIDENCE OF IM 107
3.7 *p53$^{R172H/+}$* EXPRESS MUC2 IN THEIR STOMACHS 109
3.8 EXAMINING THE POTENTIAL ROLE FOR EARLY *P53* MUTATION IN GOJ CANCERS WITH BILIARY REFLUX MODEL 111
3.9 SURVIVAL OF DCA AND UNTREATED GROUPS 111
3.10 INCREASED EXPRESSION OF INFLAMMATORY MEDIATORS IN MICE EXPOSED TO HIGH DOSE BILE SALTS 115
3.11 INCREASED EXPRESSION OF PNFKB IN *P53$^{R172H/+}$* DCA TREATED MICE 117
3.12 COX2 EXPRESSION IN *P53$^{R172H/+}$* AND DCA TREATED MICE 117
3.13 *P53^{R172H}* IN A MOUSE MODEL OF BILIARY REFLUX DOES NOT INDUCE GASTRIC ADENOCARCINOMA DEVELOPMENT 120
3.14 DCA TREATED MICE DEVELOPED EVIDENCE OF HEPATITIS AND LIVER TUMOURS 122
3.16 DISCUSSION 125
3.17 LIMITATIONS 127

CHAPTER 4: DISSECTING CELL POPULATIONS WITHIN BO 129

4.1 INTRODUCTION 129

4.2 CREATING A BIOBANK OF UPPER GI BIOPSIES 130

4.3 EPCAM HIGH AND EPCAM LOW CELL POPULATIONS WERE SEEN IN OESOPHAGEAL CELLS 132

4.4 IDENTIFYING CELL POPULATIONS IN NORMAL UPPER GI EPITHELIUM 133

4.4.1 Obtaining cells 133

4.4.2 Analysis of sc-RNA-seq data 135

4.5 HIGH LEFTY1 AND KRT7 EXPRESSION DEFINE BO EPITHELIAL CELLS 139

4.6 VALIDATION COHORT TO ESTABLISH EXPRESSION PATTERNS WITHIN BO 142

4.7 EXAMINATION OF LEFTY1 EXPRESSION IN THE GI TRACT 144

4.8 OSGS SHARE AN EXPRESSION PROFILE WITH BO 146

4.9 SPINK4 AND ITLN1 ARE NOVEL MARKERS OF GOBLET CELLS IN BO 149

4.10 SPINK4 AND ITLN1 MARK DIFFERENT CELLS WITHIN A GOBLET CELL POPULATION 151

4.11 SPINK4 AND ITLN1 MAY BE MARKERS OF EARLY COLONIC GOBLET CELL DIFFERENTIATION 153

4.12 OSGS SHOW MARKERS OF SQUAMOUS, TRANSITIONAL AND GOBLET CELL DIFFERENTIATION 154

4.13 GOBLET CELL DIFFERENTIATION IN DUODENAL ORGANOIDS 156

4.14 EFFECT OF Ɣ SECRETASE INHIBITION ON *SPINK4*, *ITLN1* AND *MUC2* EXPRESSION IN CELL LINES 158

4.15 INDUCING *SPINK4* OR *ITLN1* EXPRESSION DOES NOT DRIVE GOBLET CELL DIFFERENTIATION IN CELL LINES 159

4.17 DISCUSSION 161

4.18 LIMITATIONS 165

CHAPTER 5: RESULTS – IDENTIFICATION OF STEM-LIKE CELLS IN BO AND OSGS 168

5.1 SC-RNA-SEQ IDENTIFIES CANDIDATE PROGENITOR MARKERS 168

5.2 COMBINED ANALYSIS OF BO AND OSGS SUGGESTS *OLFM4* AS A POSSIBLE PROGENITOR CELL MARKER 170

5.3 EXAMINING OLFM4 EXPRESSION IN THE GASTRO-INTESTINAL TRACT 172

5.4 EXAMINING OLFM4 EXPRESSION IN OESOPHAGEAL EPITHELIUM 174

5.5 EXAMINING CO-EXPRESSION IN OLFM4+ CELLS 175

5.6 RNA *IN SITU* HYBRIDISATION SUGGESTS *OLFM4/ LGR5* CO-EXPRESSION IN OSGS 176

5.7 RNA *IN SITU* HYBRIDISATION TO EXAMINE *OLFM4* AND *LGR5* EXPRESSION IN BO 178

5.8 USING ORGANOTYPIC MODELS TO EXAMINE CELL DIFFERENTIATION IN BO 179

5.9 ORGANOID MODELS DEVELOPED TO SUPPORT LGR5+ POPULATIONS 182

5.10 BO ORGANOIDS RECAPITULATE CRYPT/GLAND STRUCTURE SEEN *IN VIVO* 183

5.11 BO ORGANOIDS SHOW DIFFERENTIATION OF ALL CELL TYPES SEEN IN SC-RNA-SEQ DATA 185

5.12 RNA *IN SITU* HYBRIDISATION IN BO ORGANOIDS 186

5.13 Culture of EpCAM+ cells from oesophageal biopsies 188
5.14 Discussion 189
5.15 Limitations 191
CHAPTER 6: RESULTS – LINKING BO WITH COLUMNAR LINED OESOPHAGUS OF DEVELOPMENTAL ORIGINS 193
6.1 Morphology of the human foetal oesophagus 193
6.2 Expression of BO markers in the foetal oesophagus 195
6.3 Immunofluorescence co-staining of P63, KRT5 and KRT7 in the early foetal oesophagus 197
6.4 Immunofluorescence co-staining of, KRT7, KRT5 and P63 in the 18 week foetal oesophagus 199
6.5 LEFTY1 and TFF3 expression in the foetal oesophagus 200
6.6 *LGR5* and *OLFM4* localisation in the foetal duodenum 201
6.7 Expression of *LGR5* and *OLFM4* in the foetal oesophagus 203
6.8 KRT7 and P63 expression in oesophageal inlet patches 205
6.9 Expression of BO markers in oesophageal inlet patches 206
6.10 Discussion 207
6.11 Limitations 210
CHAPTER 7: DISCUSSION 211
7.1 Investigating the role of early p53 mutation in GOJ carcinogenesis 211
7.1.1 Discussion 211
7.1.2 Future directions 212
7.2 Identification of cell populations within BO 213
7.2.1 Discussion 213
7.2.2 Future directions 216
7.3 OLFM4 and LGR5 expression in the adult oesophagus 217
7.3.1 Discussion 217
7.3.2 Future directions 218
7.4 Human foetal oesophagus and OIPs may have links to BO 219
7.4.1 Discussion 219
7.4.2 Future directions 220
CHAPTER 8: CONCLUSION 223
BIBLIOGRAPHY 225

Chapter 1: Introduction

Cancer of the gastro-oesophageal junction is a complex and multifactorial disease, which disproportionately effects the populations of the United Kingdom and is associated with significant mortality and high morbidity (Walters, Nur et al. 2010, Thrift and Whiteman 2012). BO is metaplastic precursor to oesophageal adenocarcinoma (OAC), existing as a stepping-stone between normal epithelium and malignancy (Curtius, Rubenstein et al. 2020). This project aims to examine possible origins of this metaplastic precursor and to develop methods to model it.

1.1 Anatomy of the human upper gastro-intestinal tract

1.1.1 Oesophagus

The oesophagus is a tubular luminal organ, which extends from the oropharynx to the stomach. The primary role of the oesophagus is to transport food boli from the mouth to the stomach. In adults, the oesophagus is 25-40 centimetres long (Oezcelik and DeMeester 2011). The oesophagus comprises primarily of proliferative cells with small populations of secretory cells. Histologically the oesophagus consists of a non-keratinized stratified squamous epithelium, flat round cells layered 10-20 cell layers deep from the deep basal layer to most superficial (Oezcelik and DeMeester 2011). The cells comprising the basal layer are arranged 3-4 cells thick and are immature, whereas the “stratified” cell layers nearer to the luminal surface exhibit markers of maturation. Eventually mature, terminally differentiated squamous cells on the luminal surface slough off in the lumen. Other cell populations within the oesophagus include melanocytes, secretory endocrine cells, oesophageal submucosal cells (Woods

and Carey 2014). At the distal end of the oesophagus the lower oesophageal sphincter (LOS).

1.1.2 Stomach

The stomach is a luminal organ in the left upper quadrant of the abdomen, below the diaphragm and between the liver and the spleen. Its primary roles include protection from potentially harmful ingested bacteria, digestion, and a signalling/endocrine role to the rest of the gastrointestinal tract and other parts of the body (Wilson and Stevenson 2019). Endoscopically the gastro-oesophageal junction (GOJ) can be delineated by using the top of the rugal fold as the landmark for the beginning of the stomach, or the distal end of the palisade vessels as the end of the oesophagus (Peck-Radosavljevic, Püspök et al. 1999). However, both can be obscured by inflammation or distention of the top of the stomach. Endoscopically the Z-line can be observed, representing the transition point from squamous oesophageal epithelium to the columnar gastric epithelium, in disease the demarcation of the Z-line can become obscured (Wallner, Sylvan et al. 2002).

The stomach has five histologically defined epithelial regions; the cardia, fundus, body, antrum and the pylorus (Wilson and Stevenson 2019). These regions vary by their gland structure, their cell composition, location in the stomach and role. Gastric epithelial cells are classified as either secretory or proliferative cells. The stomach is lined with a columnar epithelium with a glandular crypt structure. The glands of all regions of the stomach are primarily lined with surface mucus cells and mucus neck cells to varying degrees (Peck-Radosavljevic, Püspök et al. 1999). These mucus cells produce mucous and bicarbonate to protect the epithelium from gastric acid and are histologically distinct from goblet cells. Many other specialised cells exist within the histologically unique regions of the stomach: cardia, fundus, body, antrum and

pylorus. Each region harbours different by the specialist cell types. The gastric cardia contains parietal cells (also known as oxyntic cells) and enterochromaffin-like cells. Parietal cells are located deep in the glands of the cardia and secrete hydrochloric acid (HCL) and intrinsic factor (involved in the absorption of vitamin B12). Enterochromaffin-like cells are often found adjacent to parietal cells, and release histamine to stimulate parietal cell acid secretion (Ban 2013). The fundus and body have parietal cells too but additionally contains chief cells, which secrete pepsinogen, a pro-enzyme that converts into the digestive protease pepsin upon exposure to acid and gastric lipase (Ban 2013). The pyloric and antral regions possess enteroendocrine cells including G cells, which produce and secrete the hormone gastrin. Gastrin works by stimulating parietal cells to produce gastric acid and D cells, which secrete somatostatin to inhibit gastric acid secretion (Ban 2013).

1.1.3 Duodenum

The duodenum, the first section of the small intestine, is a luminal organ that connects the pylorus of the stomach to the jejunum, a continuation of the small bowel. The duodenum largely plays a role of neutralising stomach acid and initialising the enzymatic breakdown of proteins and lipids. Anatomically, the duodenum is separated into four parts (D1, D2, D3 and D4). D1 and D2 derive from the embryological foregut; D3 and D4 derive from the embryological midgut (Shames 2019). The first part is a continuation of the pylorus after the pyloric sphincter and receives acidified gastric content. The pancreatic duct and common bile duct join the second part of the duodenum at the major duodenal papilla (Shames 2019). This landmark delineates the transition from foregut to midgut. Bile and pancreatic juice mix with the acidic gastric content at the ampulla, requiring the duodenal epithelium to be specially adapted to its caustic luminal contents. The duodenum comprises of cells that can be functionally

categorised as proliferative, secretory or absorptive cells (Shames 2019). The duodenum has a villous mucosa, with intestinal glands in a crypt villous formation. Columnar enterocytes, which have an absorptive role, make up the majority of the luminal surface and are specialised to withstand the extremes of acidity and alkalinity. As with other epithelial organs, the duodenum consists of many other cell types. When the pyloric sphincter opens releasing the gastric chime into the duodenum the drop in pH and presence of lipids stimulates enteroendocrine cells (Shames 2019). Mucins have a gel-like property which when secreted across an epithelial surface, acts as a lubricant and protective film. Paneth cells are another secretory cell population which exist at the bottom of intestinal crypts, which play an antibacterial role by producing lysozyme as well as a critical role in maintaining the stem cell niche at the bottom of intestinal crypts (Shames 2019). Deep to the muscularis mucosa, Brunner's glands unique to the duodenum secrete mucin and bicarbonate to help neutralised the gastric acid and protect the surface epithelium (Shames 2019).

1.2 Differences between the mouse and human upper GI tract

Many studies utilise murine models to study development and disease within the upper GI tract. In mice a single basal layer exists with four to six layers of cells (Treuting, Clifford et al. 2012, Zhang, Jiang et al. 2017, Kabir, Karami et al. 2022).. The mouse oesophagus does not contain papillae the basal layer of the epithelium (Seery and Watt 2000, Barbera, di Pietro et al. 2015). The squamo-columnar junction in mice is not at the anatomical boundary of the oesophagus and the stomach, as it is in humans (Treuting, Arends et al. 2018). In mice, the squamo-columnar epithelial junction is in the middle of the anatomical stomach, giving rise to the squamous forestomach in rodents. In mice oesophageal stratified squamous epithelium develops

layers of acellular keratin, much like human skin, which is absent in the human oesophagus, this keratinised layer will protect the oesophagus from acidic or biliary reflux (Liu, Lin et al. 2013, Treuting, Arends et al. 2018). In mice, when the muscular layer of the oesophagus forms, most of the smooth muscle is replaced with striated muscle, except for the distal oesophagus and lower oesophageal sphincter (Treuting, Arends et al. 2018). Mice are quadrupedal, therefore, gravity has a different effect on gastro-oesophageal physiology (Treuting, Arends et al. 2018). These differences in gravity and musculature along with differences in rodent enteric neuronal signalling pathways explains why rodents are unable to vomit or experience acid reflux.

1.3 Biology of the oesophagus

1.3.1 Oesophageal development

The oesophagus arises from the anterior foregut, which also gives rise to the lungs and trachea. Respiratory oesophageal separation (ROS) occurs between the fourth and sixth week of gestation. Failure of normal ROS is pathological and leads to oesophageal atresia and tracheoesophageal fistulae. The molecular signalling that takes place during development defines orientation, epithelial cell differentiation and boundaries between the structures adjacent to the oesophagus. The early separation of the oesophagus and the trachea is controlled by co-ordinated expression of multiple signalling pathways (Zhang, Bailey et al. 2021).

SHH expression is high in the ventral foregut before ROS takes place. In the corresponding adjacent mesenchyme, SHH pathway targets GLI2 and GLI3 are highly expressed. Transgenic murine models demonstrate that knockout of *SHH*, *GLI2*, *GLI3*, or *FOXF1* in mice leads to the development of oesophageal atresia

and/or tracheoesophageal fistulae suggesting their roles are critical for respiratory-oesophageal separation (Litingtung, Lei et al. 1998, Mahlapuu, Pelto-Huikko et al. 1998, Motoyama, Liu et al. 1998, Pepicelli, Lewis et al. 1998). Further studies demonstrated that loss of GLI2 and GLI3 leads to loss of mesenchymal expression of WNT2, WNT2B and BMP4 (Rankin, Han et al. 2016). Similarly upstream of SHH signalling, inhibition or ablation of retinoic acid signalling leads to loss of endodermal SHH expression impairing lung epithelial development and reduced mesenchymal expression of WNT2, BMP4 and FOXF1. This demonstrates that retinoic acid signalling is critical for the development of endodermal and mesodermal components during early foregut development. (Desai, Malpel et al. 2004, Wang, Dollé et al. 2006, Rankin, Han et al. 2016). Further to the role of BMP4 signalling in the mesenchymal foregut, studies have shown that loss of BMP4 during early murine embryonic development leads to loss of lung development (Li, Gordon et al. 2008). During normal ROS, BMP receptor 1a (BMPR1A) activation by BMP4 leads to phosphorylation of SMAD1/5/8. This triggers NKX2.1 expression and lung epithelial differentiation in the ventral foregut, giving rise to the lung buds (Domyan, Ferretti et al. 2011). *BMPR1a* null mice demonstrate a complete absence of *Nkx2.1* expression, and as a result, ROS never occurs and the anterior foregut remains a single tube (Domyan, Ferretti et al. 2011). Similar to the way that *Nkx2.1* determines lung epithelial development, SOX2 is a transcription factor that determines oesophageal epithelial differentiation (Domyan, Ferretti et al. 2011). Domyan and colleagues that in *Bmpr1a* -/- mice, which do not normally develop lungs, additional knockout of SOX2 rescues this phenotype leading to normal ROS (Domyan, Ferretti et al. 2011). This suggests that BMP signalling promotes lung epithelial specification through repression of SOX2 activity in early lung development (Zhang, Bailey et al. 2021).

Overexpression of BMP signalling is also detrimental to normal ROS. Humans born with tracheoesophageal fistulae are rarely found to possess variants in the Noggin gene (NOG), a BMP antagonist (Murphy, Li et al. 2012). Deletion of *Nog* leads to failure of ROS with oesophageal atresia and tracheoesophageal fistulae in effected mice (Que, Choi et al. 2006, Li, Litingtung et al. 2007). This phenotype in Noggin knockout mice can be rescued by additional deletion of BMP4 or BMP7 demonstrating that too much or too little BMP signalling can be detrimental in early foregut development (Zhang, Bailey et al. 2021).

WNT signalling is also critical for the early development of the anterior foregut. *Wnt2* and *Wnt2b* knockout mice both fail to develop lungs *in utero* (Goss, Tian et al. 2009), and deletion of key WNT effector β-catenin also leads to complete loss of lung development (Goss, Tian et al. 2009, Harris-Johnson, Domyan et al. 2009, Hou, Ma et al. 2019). Mesenchymal gene *BARX1* interacts with WNT signalling during ROS (Woo, Miletich et al. 2011): *Barx1* knockout mice fail to develop separate lungs and oesophagus, instead have a foregut lined with Nkx2.1 expressing pulmonary progenitor cells (Woo, Miletich et al. 2011). Loss of *Barx1* reduces expression of sFRP1 and sFRP2 in the mesenchyme, which usually act as WNT inhibitors. Thus reduced *Barx1* expression leads reduced inhibition of Wnt signalling, promoting development of respiratory progenitor cells instead of oesophageal progenitors in the dorsal foregut (Woo, Miletich et al. 2011). Sox2 and Nkx2.1 have antagonising roles for normal respiratory oesophagus separation to occur balance needs to be achieved between Hedgehog, Retinoic acid, BMP, and WNT signalling. Conditional deletion of *Sox2*, using $Foxa2^{CreER}$; $Sox2^{loxp/loxp}$ mice at E6.5 (embryonic age; weeks) causes a complete loss of oesophageal development, highlighting that *Sox2* expression is imperative for oesophageal development in mice (Trisno, Philo et al. 2018). Further

experiments from the same group using human pluripotent stem cells to derive oesophageal organoids demonstrated that SOX2 is also required for the specification of human oesophageal cells (Trisno, Philo et al. 2018). Many of the genes discussed have been implicated in the development of BO throughout the literature and their roles in normal development of the foregut will be referred to later on in this thesis.

1.3.2 Oesophageal epithelium

Following separation of the trachea and oesophagus, the embryonic oesophagus is lined by pseudostratified columnar cells. These nascent oesophageal progenitor cells express squamous markers, SOX2 and P63, but also columnar markers SOX9 and KRT8 (Zhang, Yang et al. 2018). At E13 in mice, the developing oesophageal epithelial cells express Krt7 (a marker for simple glandular epithelium). This leads to the beginning of squamous development of the oesophagus, the basal layer cells begin expressing p63/Krt5/Krt14 and the suprabasal cells express Krt4/Krt13 (Yu, Slack et al. 2005, Jiang, Li et al. 2017, Zhang, Jiang et al. 2017, Zhang, Yang et al. 2018, Zhang, Bailey et al. 2021). Development of the stratified epithelium in both mice and humans is regulated by Notch and BMP signalling and key transcription factors Yes-Associated protein (YAP) and Kruppel-like factor 4 (Klf4) (Zhang, Bailey et al. 2021).

The epithelium of the oesophagus turns over in the human adult every eleven days and in mice every three to four days. To maintain the tissue there must be coordination between proliferation and differentiation of basal cells (Marques-Pereira and Leblond 1965, Doupé, Alcolea et al. 2012, Pan, Nicholson et al. 2013).

1.3.3 Native oesophageal submucosal glands (OSGs)

OSGs are columnar lined glands which are found in the normal oesophagus with higher population densities near the upper and lower oesophageal sphincters (van Nieuwenhove, Destordeur et al. 2001, Lorinc and Oberg 2015). OSGs are similar in structure to salivary glands and secrete bicarbonate and mucins to neutralise stomach acid, protect the surface squamous epithelium and lubricate food transit (Al Yassin and Toner 1977). OSGs also secrete epidermal growth factor and prostaglandins (van Nieuwenhove, Destordeur et al. 2001). An excretory duct perforates the muscularis mucosa and the epithelium to transport the secreted products to the surface (Lorinc and Oberg 2015, von Furstenberg, Li et al. 2017). The deep portion of the OSG duct is closest to the acinar gland and is lined by a simple columnar epithelium early embryonic oesophagus, while the duct nears the lumen the duct becomes lined by an epithelium expressing classical markers of squamous epithelial differentiation (Lorinc, Mellblom et al. 2015).

The distribution of OSGs through the oesophagus is heterogeneous (Al Yassin and Toner 1977). While OSGs can occur throughout the proximal and distal oesophagus, they are not visible at endoscopy and therefore cannot be intentionally sampled in a standard oesophageal mucosal biopsy *in vivo* (Al Yassin and Toner 1977). Examination of squamous biopsies taken suggest that OSGs are found in between 4% and 50% of biopsies from patients undergoing an endoscopic examination (Long and Orlando 1999). Although there is some limited evidence that OSGs have a higher population density in the distal oesophagus and that OSGs are found more readily in biopsies from patients with GORD, the significance of OSG morphology and distribution remains unknown (Long and Orlando 1999).

1.4 Biology of the stomach

1.4.1 Gastric development

After the initial patterning, driven by HOX genes, the posterior foregut is further divided into distinct organs (the stomach, duodenum, pancreas, liver and biliary tree). However, the molecular mechanism driving the definition of the gastro-oesophageal junction is poorly understood. While studies have tended to assume that the boundaries between adjacent organs occur by binary fate decisions based on gene expression, the reality is that there is much more nuance that this. SHH expression by endodermal and mesodermal components are critical in oesophageal and squamous forestomach development (Fukuda and Yasugi 2005, Kim and Shivdasani 2016, McCracken and Wells 2017). However, distal to the squamous columnar junction (SCJ) Indian hedgehog (IHH) expression predominates (Bitgood and McMahon 1995). Studies have shown that deletion of mesenchymal *Hoxa5* expression in mice leads to disruption of this Shh-Ihh expression boundary at the SCJ and effects the position of the forestomach-hindstomach boundary (Aubin, Déry et al. 2002). Deletion of *Shh* in mouse models has been individually shown to disrupt the SCJ in the stomach (Drubbel, Pirard et al. 2021). In transgenic mice where both *Hoxa5* and *Shh* are knocked out, the columnar lined hindstomach develops intestinal differentiation (Ramalho-Santos, Melton et al. 2000). No specific "master regulator" of gastric development exists, although the patterning depends on several factors. GATA binding protein 4 (Gata4), a zinc finger transcription factor is highly expressed in the columnar hind-stomach of mice but not at all in the squamous forestomach, the same pattern is seen in humans either side of the SCJ (Jacobsen, Narita et al. 2002, Jacobsen, Mannisto et al. 2005). Although Sox2 expression is critical of the development of the normal oesophagus and is highly expressed in the gastric

epithelium throughout development, gastric epithelial differentiation is unaffected by *Sox2* deletion *in vivo* (Que, Okubo et al. 2007*).*

The molecular mechanisms that direct early embryonic development of the stomach appear to be conserved across vertebrate species. Much like in oesophageal development, SOX2 is highly expressed in the embryonic stomach, whereas CDX2, not SOX2 is expressed in early duodenal development (Gao, White et al. 2009, Grainger, Savory et al. 2010). The gastric-duodenal epithelial junction at the pylorus is molecularly underpinned by the SOX2-CDX2 expression boundary. When ectopic expression of *Sox2* is induced in the small intestine it induces gastric differentiation (Raghoebir, Bakker et al. 2012). In transgenic models where *Cdx2* is overexpressed in murine stomachs, mice develop foci of intestinal differentiation (Silberg, Sullivan et al. 2002). However, balance between SOX2 and CDX2 expression is not all that defines the junction between the stomach and the intestine at the pylorus. *Sox2* knockout mice have a relatively normal gastric development and epithelium (Que, Luo et al. 2009). There is a redundancy network co-ordinated by SOX B family members ensuring that when *SOX2* expression is lost its role is fulfilled (Miyagi, Kato et al. 2009). Timing of loss of *Cdx2* in mouse models is critical. In constitutive mutants, *Cdx2* loss in the early murine endoderm results in colonic atresia and foci of oesophageal epithelium developing in the distal intestine, but this has not shown to cause loss or disruption of epithelial junctions (Gao, White et al. 2009, Grainger, Savory et al. 2010). Loss of *Cdx2* expression later on in using an inducible *Vil1-CreER* mouse model leads to the development of gastric pyloric glands in the duodenum (Grainger, Savory et al. 2010). Although *in vitro* loss of *Cdx2* in intestinal stem cells impairs intestinal epithelial differentiation, *in vivo* loss of *Cdx2* causes widespread gastric differentiation throughout the intestines (Verzi, Shin et al. 2010,

Stringer, Duluc et al. 2012). This is due to effects of the mesenchymal-epithelial interaction in the in vivo setting. There are still unidentified factors which have a role in the delineation epithelial junctions in the GI tract (McCracken and Wells 2017). BARX1, known for its role in the development of the oesophagus by moderating WNT signalling in the early oesophageal mesenchyme is also expressed in the gastric mesenchyme, but not the intestine. BARX1-mediated WNT inhibition is specifically required in the gastric epithelium to suppress intestinal transformation. However, in murine models ectopic *Barx1* expression in the intestine does not influence intestinal differentiation (Jayewickreme and Shivdasani 2015). However, the timing of WNT activation is important in the delineation of the gastric-intestinal epithelial boundary (McCracken and Wells 2017).

1.4.2 Gastric epithelium

Within the stomach, disparate epithelial regions exist. Pancreatic and duodenal homeobox gene 1 (PDX1) is a transcription factor in the Parahox gene cluster. In addition to its role in the development of the pancreas and duodenum, PDX1 has a role in the epithelial patterning of the gastric antral epithelium. PDX1 expression is critical for the development of Gastrin producing G cells in the antrum. However, *Pdx1* knockout mice do not have a grossly abnormal gastric phenotype (Fujitani, Fujitani et al. 2006) . Similarly, Nkx6.3, an antrum specific transcription factor, is essential for the development of G cells, but *Nkx6.3* knockout mice do not confer loss of gastric antral differentiation (Choi, Romer et al. 2008). As with early foregut epithelial development, mesenchymal signalling plays a critical role in the differentiation of distinctive epithelial regions in the stomach. NKX3.2 is a transcription factor highly expressed in the mesenchyme surrounding the distal stomach and duodenum. Deletion of *Nkx3.2* in a murine model lead to loss of the

gastric antrum specialisation including loss of parietal cell differentiation (Verzi, Stanfel et al. 2009). Studies in an avian model suggests that Nkx3.2 acts to repress Wnt5a and Bmp4 signalling (Nielsen, Murtaugh et al. 2001). This suggests that Nkx3.2 may work to modulate WNT and BMP signalling in mammalian gastric epithelial patterning. Other studies have demonstrated the importance of WNT signalling in gastric regional epithelial patterning, and repression of WNT signalling is required in antral development (Kim, Buchner et al. 2005, Cervantes, Yamaguchi et al. 2009, Matsuyama, Aizawa et al. 2009). Deletion of the WNT effector β-catenin prior to gastric epithelial patterning leads to increased expression of Pdx1 throughout the stomach, antralisation of the proximal stomach and loss of the fundic gland differentiation (McCracken, Aihara et al. 2017). The same group have demonstrated that gastric epithelial phenotype can be switched with or without active WNT signalling in an organoid (McCracken, Aihara et al. 2017, Broda, McCracken et al. 2019). A more recent study demonstrates that fundic, body or antral gland specification is determined by Noggin, BMP and epidermal growth factor (EGF) expression gradients in mesenchyme immediately adjacent to the glands (Wölffling, Daddi et al. 2021).

1.4.3 Gastric cardia native or acquired?

GCM is glandular epithelium in the proximal stomach without the presence of parietal cells. This epithelium is thought to act as a buffer zone between the true stomach and the true squamous oesophagus in order to prevent damage to the stratified squamous epithelium. Some indirect evidence suggests that the gastric cardia mucosa (GCM) is acquired as a result of gastro oesophageal reflux (Chandrasoma 1997, Oberg, Peters et al. 1997, Spechler 1999, Spechler 2018). Analysis of patients without GORD they found that no true GCM existed and glands containing parietal cells often came

directly into contact with the squamous epithelium of the oesophagus proper (Oberg, Peters et al. 1997). Another study found evidence of OSGs underneath rugal folds from 10 oesophagectomy specimens, suggesting that the endoscopic landmark of rugae are not an appropriate boundary for the gastro-oesophageal junction (Chandrasoma, Lokuhetty et al. 2000). They concluded that a columnar lined metaplastic epithelial region known as the "squamo-oxyntic gap" existed in the lower oesophagus, which acted as a marker for the severity of GORD (Oberg, Peters et al. 1997). The cardia has frequently been found to demonstrate IM exhibiting molecular markers of intestinal differentiation such as villin1, and CDX2 expression (El-Serag, Sonnenberg et al. 1999). In a study of healthy volunteers pH manometry showed that a larger mean abdominal circumference was associated with more reflux (Robertson, Derakhshan et al. 2013). All GCM examined were inflamed regardless of waist circumference, although subjects with larger waists had a longer GCM (Robertson, Derakhshan et al. 2013). In a separate study, the same group showed that patients with hiatus hernia also had longer GCM (Robertson, Derakhshan et al. 2017). When directly comparing GCM and BO inflammation in the same patients, they were consistently found to have similar levels of inflammation, no histological differences were found between GCM from healthy volunteers and the GCM from patients with BO (Chandrasoma 1997). The reliability of biopsying the true GCM endoscopically is low as several studies have demonstrated the GCM to be <3mm in length (Chandrasoma 1997, Chandrasoma, Lokuhetty et al. 2000, Robertson, Derakhshan et al. 2013, Robertson, Derakhshan et al. 2017). However, in a separate study the GOJ was examined in 100 paediatric autopsy specimens, without a history of GORD, all had evidence of GCM without any evidence of inflammation (Zhou, Greco et al. 2001, Derdoy, Bergwerk et al. 2003). Two independent studies of paediatric GOJs

have found similar results. (Kilgore, Ormsby et al. 2000) This suggests there is a native component of GCM which in some paediatric specimens may be as short as 0.1mm. Evidence suggests that a native GCM does exist, however, findings from these various studies indicate that the GCM expands with age, obesity and GORD.

1.5 Biology of the duodenum

1.5.1 Duodenal development

The duodenum originates from the distal foregut and the anterior midgut. During early development, many cells lining the gut tube are phenotypically homogeneous with epithelial- mesenchymal cross talk, particularly involving WNT, NOTCH and BMP signalling to guide the tissue towards duodenal morphology. In the duodenum, as in the gastric antrum, absence of mesenchymal BARX1 leads to increased WNT signalling activity. CDX1and CDX2 are parahox genes with overlapping function important for normal intestinal epithelial development (Eda, Osawa et al. 2002, Gao, White et al. 2009, Savory, Pilon et al. 2009, Grainger, Savory et al. 2010). *Cdx2* heterozygous mice develop colonic polyps and studies of conditional *Cdx2* knockout mice demonstrate that early *Cdx2* loss impairs normal intestinal development (Chawengsaksophak, James et al. 1997, Tamai, Nakajima et al. 1999, Gao, White et al. 2009). From E15 in mice, the intestinal epithelium develops into a rudimental crypt-villus pattern, where proliferating cells localise to the inter-villus areas. Transcription Factor 3 (TCF3) expressed in the embryonic villus is an important β-catenin partner and effector of WNT signalling (Kim, Mao et al. 2007). As the epithelium matures, the precursor stem cells localise to the primitive crypts and through asymmetrical cell division drive an upward movement of the crypt-villus

junction, through mesenchymal cell movement. Both Wnt and BMP signalling are important for crypt formation (Calvert and Pothier 1990). Once the structure of the crypt and villus has developed, the intestinal epithelial differentiation program drives cells down broadly two paths absorptive and secretory. Intestinal stem cells exist in a controlled stem cell niche at the base of the crypt. The Notch signalling pathway plays a critical role in cell fate by regulating cell allocation to absorptive or secretory fates. Loss of Notch activity and deletion of notch effectors Dll1 and Dll4 in mouse models lead to a drive towards secretory lineages and loss of proliferative progenitor cells (Pellegrinet, Rodilla et al. 2011). Notch induces stem cells to produce Hairy and enhancer of split-1 (Hes1), which represses Atonal BHLH transcription factor 1 (Atoh1) and directs them towards enterocyte differentiation (Pellegrinet, Rodilla et al. 2011). Atoh1 expressing secretory progenitor cells co-express Notch ligand, Dll1 (Pellegrinet, Rodilla et al. 2011).

1.5.2 Goblet cells

Goblet cells are abundant within intestinal crypts. Goblet cells produce intestinal specific mucins such as Mucin 2 (MUC2) which provide a protective layer of mucous across the epithelium. Goblet cells share an intermediate progenitor with Paneth cells which expresses SAM pointed Domain Containing ETS Transcription factor (SPDEF) (Gregorieff, Stange et al. 2009, Noah, Kazanjian et al. 2010). Krupple like Factor 4 (KLF4) has been implicated in goblet cell development, as *Klf4* deletion in mouse embryos leads to abnormal goblet cell differentiation throughout the stomach which persists into later life (Zheng, Pritchard et al. 2009). However, inducible loss of *Klf4* expression in adult mice is not able to demonstrate a similar phenotype either in normal differentiation or in induced goblet cell differentiation with a gamma secretase

inhibitor (Zheng, Pritchard et al. 2009). This suggests that Klf4 has distinct roles in developing and mature intestinal differentiation and as such may well have a role in the development of pathological processes involving intestinal differentiation. The WNT pathway has also been shown to control goblet cell differentiation by regulating Notch effectors Atoh1 and Hes1 (Nakamura, Tsuchiya et al. 2007, Peignon, Durand et al. 2011).

1.6 Barrett's oesophagus (BO)

First described by Norman Barrett in 1950 as a "peptic ulceration of the oesophagus", BO is an example of an acquired metaplasia (Barrett 1950, Bremner, Lynch et al. 1970, Spechler and Goyal 1996, Chandrasoma 1997, Spechler 2002). In BO, the native adult squamous epithelium of the lower oesophagus is replaced with columnar epithelium (Barrett 1950). BO develops following chronic inflammation from GORD. The mixture of acid and bile in chronic GORD results in mucosal injury, inflammation, and cellular oxidative stress leading to the production of Reactive Oxygen Species (ROS) (Sihvo, Salminen et al. 2002, Dvorak, Payne et al. 2007). The replacement of squamous epithelium to columnar epithelium is considered an adaptive response to the inflammation (Spechler and Goyal 1996). Over time exposure to the ROS damages cellular proteins, lipids, mitochondria and DNA (Sihvo, Salminen et al. 2002, Dvorak, Payne et al. 2007). In turn, this changes cellular metabolism, gene expression and induces mutations, which plays part a role in the epithelial transformation (Sihvo, Salminen et al. 2002, Dvorak, Payne et al. 2007). Contention exists over the histological definition of BO (Fitzgerald, di Pietro et al. 2014). The American definition requires the presence of goblet cell differentiation, whereas the British definition describes a columnar lined oesophagus and does not

require the presence of goblet cells (Kelty, Gough et al. 2007, Srivastava, Odze et al. 2007, Ramus, Caygill et al. 2008, Spechler, Sharma et al. 2011, Fitzgerald, di Pietro et al. 2014). While the annual risk of developing OAC in BO patients is low (approximately 0.1- 0.3% per year) the lifetime risk of progression is at least 10-fold that of the general population (Thomas, Abrams et al. 2007, Hvid-Jensen, Pedersen et al. 2011, Thrift 2021). BO is the initial step in the progression from metaplasia to low-grade dysplasia, high-grade dysplasia and OAC (Jankowski, Wright et al. 1999). Although BO is the major risk factor leading to OAC, the large majority of OAC cases patients are never formally diagnosed with BO even at surgical resection (Van der Burgh, Dees et al. 1996, Kelty, Gough et al. 2007, Spechler 2013). The reason for this is poorly understood.

The majority of BO involves the gastro-oesophageal junction (GOJ), at the intersection between the distal oesophagus and the gastric cardiac epithelium (Jung, Talley et al. 2011). In cases when BO is not contiguous with the GOJ, isolated pink "islands" of BO epithelium centimetres from the GOJ surrounded by squamous epithelium can be seen (Sharma, Morales et al. 1998, Coad, Woodman et al. 2005, Nakanishi, Saka et al. 2007, Leedham, Preston et al. 2008, Lorinc, Mellblom et al. 2015, Epstein, Cosby et al. 2017). Nevertheless, the debate continues regarding the possible origin of BO and how it may develop. There are six main theories about the BO cell of origin. The first is that in response to the reflux induced inflammation the native squamous epithelial cells of the oesophagus transdifferentiate and become columnar cells (Minacapelli, Bajpai et al. 2017, Wang 2017, Agoston, Pham et al. 2018). The second is that localised inflammation signalling leads to recruitment of circulating bone marrow derived stem cells, which implant in the epithelium and differentiate into columnar epithelial cells (Epperly, Guo et al. 2004, Sarosi, Brown et

al. 2008, Hutchinson, Stenstrom et al. 2011). The third hypothesis suggests a role for native oesophageal submucosal gland cells , which migrate onto the lumen surface leading to BO (Van Nieuwenhove and Willems 1998, Glickman, Chen et al. 2001, Leedham, Preston et al. 2008, Lorinc, Mellblom et al. 2015, Garman 2017). The fourth proposed source is the migration of cells from the gastric epithelium (Quante, Bhagat et al. 2012, Lavery, Nicholson et al. 2014). The fifth is reactivation of a dormant population of residual embryonic stem cells at the SCJ (Wang, Ouyang et al. 2011). The most recent sixth theory implies activation of a transitional columnar epithelium that exists at the boundary between the squamous and columnar epithelium (Jiang, Li et al. 2017).

1.6.1 Diagnosis of BO

During endoscopic examination of the lower oesophagus, BO is inspected with high definition white light endoscopy and targeted biopsies of the epithelium can be taken. The Seattle protocol suggests quadrantic biopsies should be taken every 2cm, starting from the upper end of the gastric rugae for the area that is suspected of being columnarised. The Seattle protocol has demonstrated better detection of dysplastic area compared to random biopsies or reliance on endoscopist's recognition of a dysplastic pit pattern (Reid, Blount et al. 2000, Fitzgerald, Saeed et al. 2001, Abela, Going et al. 2008). Guidance on endoscopic diagnosis of BO varies depending on country; some professional bodies specify a certain length of the segment of columnarised epithelium is required to be classified as BO. All classifications agree that ≥1cm segments of columnar lined epithelium may be endoscopically described as BO pending histological analysis of biopsies as there is always potential for a hiatus hernia to distort the true boundary between the oesophagus and stomach (Riddell and

Odze 2009, Thota, Vennalaganti et al. 2017). The Prague C & M criteria is used as a means of endoscopically monitoring extent of BO within the oesophagus by measuring the circumferential length of BO and the maximal length of BO as a proxy for the area of the lesion (Sharma, Dent et al. 2006). Many studies have been carried out examining the effects of size of BO epithelium and if it correlates with the degree of progression risk (Hamade, Vennelaganti et al. 2019).

1.6.2 Pathology of BO

Contention exists over the pathological criteria for the diagnosis of BO. For the British definition of BO, a columnar lined oesophagus alone is required, where the American pathological definition requires presence of intestinal specific goblet cells on the histological examination to verify BO (Spechler, Sharma et al. 2011, Fitzgerald, di Pietro et al. 2014). The diagnostic challenge is that sometimes the segment of true BO that is biopsied does not contain evidence of IM. Yield of IM within a biopsy is directly proportional to the number of biopsies taken of a given BO segment (Harrison, Perry et al. 2007, Bennett, Moayyedi et al. 2015). Studies have shown that short-segment BO without IM is associated with a very low cancer risk and therefore routine surveillance of these patients is not recommended by any western gastroenterological society (Hamade, Vennelaganti et al. 2019). Guidelines also suggest that very short segment BO (<1cm in length) should not be biopsied as finding the true Z line of the gastro-oesophageal junction is endoscopist dependent (Kelty, Ackroyd et al. 2004, Odze 2005, Ramus, Caygill et al. 2008). BO should not be confused with IM of the gastric cardia (El-Serag, Sonnenberg et al. 1999). 18% of patients with reflux disease have been found to have IM of the gastric cardia and it is

not associated with increased risk of developing gastro-oesophageal junctional adenocarcinoma in humans (Hirota, Loughney et al. 1999, Rubio, Hirota et al. 2004).

1.7 Gastro oesophageal reflux disease (GORD)

In GORD, gastric acid, bile salts and pepsin present in gastric juice reflux up the oesophagus which is not physiologically adapted for an acidic environment, over time this triggers chronic inflammation (Winkelstein, Wolf et al. 1954). Complications of reflux oesophagitis include oesophageal ulceration, structuring, and the development of BO. The incidence of GORD is higher in developed countries due to the association with obesity, which leads to higher intra-abdominal pressure in patients and a propensity for reflux. In the USA 20% of adults report symptoms of heartburn at least once a week (El-Serag, Sweet et al. 2014). In Japan, the incidence of GORD has almost doubled from 10% in the 1990s to 19% in 2010, this rise has been put down to rising obesity and a more westernised diet (El-Serag, Sweet et al. 2014, Nirwan, Hasan et al. 2020). The traditional concept of reflux oesophagitis believed that gastric acid and pepsin induced damage leads to cell-cell junctions becoming permeable, exposing the deep epithelium to further damage by pepsin and hydrogen ions (Winkelstein, Wolf et al. 1954). This kills the superficial cell layer leading to localised inflammation and infiltration of neutrophils and eosinophils, driving hyperplasia of the basal epithelial layer (Winkelstein, Wolf et al. 1954). The mechanism of reflux related oesophagitis was investigated with a rat surgical oesophago-duodenostomy model to induce reflux like injury to the rat oesophagus (Souza, Huo et al. 2009). Reflux related epithelial changes took weeks to develop and did not start with erosion of the mucosa as Winkelstein and others had postulated (Winkelstein, Wolf et al. 1954). In this rat model, inflammation did not start at the

mucosa, in fact after one week the surface epithelium was intact. Further *in vitro* experiments on cultured primary human oesophageal squamous cells suggested that bile salts specifically were responsible for inducing Interleukin 1β (IL-1β) and Interleukin 8 (IL-8) expression (Souza, Huo et al. 2009). IL-8 expression was found in the *in vivo* model to have induced the migration of the T cell to the rat's oesophagi (Souza, Huo et al. 2009). This led to the hypothesis that oesophagitis may develop through a cytokine mediated injury instead of the classical caustic ulceration model of reflux oesophagitis (Souza, Huo et al. 2009). The authors suggest that epithelial ulceration then results as the effect of chronic exposure to chemokines damaging cell-cell adhesions. Furthermore, the importance of biliary constituents not gastric acid in refluxate has been demonstrated in a number of clinical and experimental studies (Kivilaakso, Fromm et al. 1980, Gillen, Keeling et al. 1988, Gotley, Morgan et al. 1988, Jankowski, Hopwood et al. 1993, Kaur, Ouatu-Lascar et al. 2000, Pera, Brito et al. 2000, Zhang, Altorki et al. 2001). The presence of bile acids in gastric content contributes to oesophageal injury and further the development of BO and OAC (Miwa, Segawa et al. 1994, Miwa, Sahara et al. 1996, Lagergren, Bergstrom et al. 1999).

1.8 Metaplasia

Epithelial tissues cover and line every organ and cavity in the body. While epithelial cells can derive from the mesoderm, ectoderm and endoderm, the epithelium of the GI tract develops from the endoderm. A complex array of local and systemic hormonal signalling and nutrient distribution direct epithelial cell cycle, metabolism, transcription, apoptosis and tissue homeostasis. Cellular plasticity refers to the ability of a cell to alter its phenotype, this is particularly important during embryonic

development and tissue regeneration. During mesenchymal to epithelial transformation (MET), cells migrate in a mesenchymal state during organogenesis before becoming epithelial cells. Conversely malignant cells are thought to invade by means of epithelial to mesenchymal transformation (EMT) (Takahashi, Tanabe et al. 2007, Goldenring and Mills 2021, Tata, Chow et al. 2021). Tissue resident stem cells are plastic, allowing differentiation pathways to be flexible in response to cell signalling and environmental cues.

Metaplasia is the replacement of one differentiated epithelial cell type with another. The definition importantly differs from transdifferentiation (Slack 1985, Slack and Tosh 2001). Transdifferentiation is the process whereby one differentiated cell type transforms into another (Beresford 1990). There are many examples of metaplasia in differentiated adult epithelial cell types. In the majority of examples, the metaplastic stimulant (such as cigarette smoke, acid or alkali induced damage, hormones or alcohol) leads to inflammation, which triggers metaplasia. Continued long term exposure to the inflammation can lead the metaplasia to become dysplasia then cancer due to an accumulation of DNA damage (Giroux and Rustgi 2017). Cells can adapt to such an environmental stimulus. However, removing the stimulus alone may only stabilise the metaplasia reducing the malignant progression into dysplasia and cancer; it is not clear whether reversal of metaplasia can occur by simply removing the metaplastic stimulus. The development of metaplasia from normal epithelium can be viewed as an adaptive response: the metaplasia is a stable epithelial transformation despite some driver mutations being present, and the vast majority of patients with metaplasia will never proceed to malignant transformation (Giroux and Rustgi 2017). Investigation of the development of metaplasia has always focused on cellular plasticity and migration, whereas progression to dysplasia and cancer from metaplasia

is perceived as a stepwise oncogenic process (Giroux and Rustgi 2017). There are three types of metaplasia; squamous metaplasia, acinar ductal metaplasia and intestinal metaplasia (Tosh and Slack 2002).

1.8.1 Squamous metaplasia

Squamous metaplasia most commonly occurs in the lungs and in the cervix (Nucci and Crum 2007). In the lung, regular prolonged exposure to tobacco smoke can lead to squamous metaplasia of the alveoli and bronchi (Greenberg, Yee et al. 2002, Giroux and Rustgi 2017). Lung neoplasia such as squamous cell carcinoma and cystic keratinizing epithelioma can develop from regions of squamous metaplasia and are often associated with localised inflammation (Greenberg, Yee et al. 2002). In the cervix, at the junction of the squamous, ectocervix and the columnar endocervix there is a squamous columnar junction (Nucci and Crum 2007). At these epithelial transition zones, the epithelial boundary is delineated during embryological development (Tata, Chow et al. 2021). Here low vaginal pH and human papilloma virus infection induce a chronic inflammation that leads to squamous metaplasia at the transition zone, leading to the presence of squamous cells in the endocervix (Schottenfeld and Beebe-Dimmer 2006, Nucci and Crum 2007). The regulation of these epithelial boundaries is believed to be critical in understanding the biology of metaplasia both in the cervix and in the oesophagus (Tata, Chow et al. 2021).

1.8.2 Intestinal metaplasia (IM)

IM is defined as the presence of intestinal specific differentiation outside of the intestine (Spechler and Goyal 1996, Gutierrez-Gonzalez and Wright 2008). Like

many other differentiated tissues, it is a morphological feature that can also be determined by expression of specific molecular markers for intestinal lineages. IM is found in the distal oesophagus or GOJ as BO, in the glandular epithelium of the stomach or in the pancreas (Spechler and Goyal 1996, Gutierrez-Gonzalez and Wright 2008). In the glandular stomach, chronic *helicobacter pylori* (*H.pylori*) infection, which is present in approximately 50% of the world population, can lead to loss of parietal and chief cells and reduction in gastric acid secretion (Parsonnet 1995, Correa, Piazuelo et al. 2010). The most common pathology in response to *H.pylori* infection is atrophic gastritis (Kawaguchi, Haruma et al. 1996). In gastric intestinal metaplasia (GIM) the metaplastic cells express trefoil factor 2 (TFF2) (Busuttil and Boussioutas 2009). *H.pylori* colonisation is the leading risk factor for GIM but others include bile reflux through from the duodenum, tobacco smoking, low dietary fruit, vegetable and vitamin C intake and high dietary salt intake (Gutierrez-Gonzalez and Wright 2008, Busuttil and Boussioutas 2009, Correa, Piazuelo et al. 2010, Zhang, Zheng et al. 2021). Autoimmune gastritis can also lead to atrophic gastritis and IM. Initially GIM occurs in small foci throughout the antrum and body (Busuttil and Boussioutas 2009). GIM is classified into two different pathological subtypes, incomplete and complete (Leung and Sung 2002, Busuttil and Boussioutas 2009). Incomplete GIM resembles colonic epithelium, with incomplete mucin expression and the absence of a brush border (Leung and Sung 2002). Continued exposure to the metaplastic agents may lead to further DNA damage and the development of dysplastic foci within the GIM (Farinati, Cardin et al. 1998). The actual frequency of progression to adenocarcinoma in the stomach is difficult to ascertain, however, when the underlying cause of GIM is allowed to continue disease may progress to low grade dysplasia, high-grade dysplasia (Li, Bautista et al. 2016). There is international

disagreement how and if GIM should be monitored (Huang, Ende et al. 2020, Shah, Gawron et al. 2020). Two competing models exist for the development of GIM. GIM may arise from TFF2 positive SPEM cells, from chief cells, or from gastric isthmus stem cells (Gutierrez-Gonzalez and Wright 2008). Gastric stem cells are identified by expression of the adult stem cell marker, LRG5 (Leucine-rich repeat-containing G-protein coupled receptor 5) (Wang, Yeoh et al. 2012). LRG5+ cells have been identified in the many adult stem cell niches (Barker, van Es et al. 2007, Barker, Rookmaaker et al. 2012, Schuijers and Clevers 2012). Although LGR5 is a widely accepted stem cell marker, there are several other adult stem cell markers proposed (BMI-1 and OLFM4) which mark slightly different cell populations (Mills and Shivdasani 2011). LGR5+ cells have properties of self-renewal and often co-express OLFM4 (Barker, van Es et al. 2007). They are located throughout the stomach and give rise to long-lived gastric glands *in vitro* which can give rise to all cell lineages found *in vivo* (Sato, van Es et al. 2011). In humans and mice, Chief cells expressing LRG5 have been isolated and can initiate epithelial repair after injury *in vitro* (Wu, Xie et al. 2013). The cell of origin for GIM remains uncertain. Despite LGR5 positive cells having the ability to give rise to early gastric adenocarcinomas in mouse models, IM within this model and others has not been demonstrated (Fu, Wang et al. 2020).

1.9 Upper gastro-intestinal cancers

80% of human cancers are epithelial in origin, primarily as epithelial cells cover our body and line every organ, creating the major interface between our environment and our body. In the traditional classification of tumours in the gastro-intestinal tract, diseases are classified by tissue of origin and histology. Previously there has been

little ambiguity in defining oesophageal and gastric cancers as separate malignancies; however, the lines are blurred now more than ever. There are two main types of oesophageal cancer; squamous cell carcinoma (OSCC) and adenocarcinoma (OAC) Gastric malignancies also have different subtypes; however, I will focus on the carcinogenesis of oesophageal and gastric adenocarcinoma (GAC). Adenocarcinomas of the gastro-intestinal tract share similar endodermal developmental origins and exposure to common insults promote their carcinogenesis. Interestingly OAC and GAC are linked by almost inverse epidemiology.

1.9.1 Oesophageal carcinoma

Each year 6,900 people are diagnosed with and 6,200 die from oesophageal cancer making it the sixth most common cause of cancer death (Yousef, Cardwell et al. 2008). Oesophageal cancers have poor prognosis with the 5-year survival rate of 19% across all stages at diagnosis and only 0.9% for patients who are diagnosed with disseminated disease (Malhotra, Yanala et al. 2017). OSCC is the most frequent oesophageal cancer in the world, with the highest incidence in eastern Asia and parts of Africa (Malhotra, Yanala et al. 2017). The main risk factors for OSCC are tobacco and alcohol consumption; however, other environmental factors play a part in carcinogenesis such as consumption of hot beverages, nutritional deficiencies and low dietary intake of fresh fruit and vegetables (Sheikh, Poustchi et al. 2019). OAC is the most common subtype of oesophageal cancer in western countries, whose frequency continues to increase. Although, the incidence of OAC is extremely low in some areas of the world, its incidence has increased between 4% and 10% year on year in developed countries since the 1970’s. The reason for the increased incidence are

primarily due to increasing incidence of obesity and GORD (El-Serag, Sweet et al. 2014).

1.9.2 Gastric carcinoma

Gastric carcinoma is the third highest cause of cancer deaths worldwide (Thrift and El-Serag 2020). GAC is most prevalent in developing countries, particularly in Asia, Central America, and South America. The majority of gastric cancers are adenocarcinomas, which can be described histologically by the Lauren classification into intestinal and diffuses subtypes have also been subtyped by the TCGA (Bass, Thorsson et al. 2014, Oue, Sentani et al. 2019). The World Health Organisation (WHO) uses a different classification, which groups GAC into papillary, tubular, mucinous and poorly cohesive carcinomas. The utility of classifications based on histological appearance has not proven itself, instead more important molecular classification allows us to understand the detailed biology of the tumours and therefore, shed light on which mode of therapy might be most likely to provide benefits to patients. The most predominant types are intestinal-type tumours of the gastric body and antrum. Most gastric cancers are associated with pathogens such as *H. pylori* and the Epstein - Barr virus (EBV). Subclinical *H. pylori* and EBV infection are highly prevalent throughout the population; identification of cancer causing strains has shed more light on the carcinogenic potential of these pathogens (Bass, Thorsson et al. 2014).

1.9.3 Gastro-oesophageal junctional carcinoma

The incidence of Gastro-oesophageal Junctional Adenocarcinomas (GOJAC) has increased dramatically in western countries at a similar time as the decrease in non-

cardia gastric cancers (Quante, Wang et al. 2022). GOJAC tumours are classified by Siewart and stein based on the location of the tumour (Siewert and Stein 1996). As is discussed below the true junction of the oesophagus and stomach can be debated along anatomical, endoscopic and histologic landmarks. Type I tumours are adenocarcinomas of the distal third of the oesophagus; these usually arise from BO, which may involve the native squamous columnar junction from above. Type II tumours are carcinomas that arise most likely from the gastric cardiac epithelium at the GOJ. Type III tumours are adenocarcinomas originating distal to the gastric cardia, which infiltrate the GOJ and oesophagus distal to proximal. Type I and type II tumours are treated as OACs and type III tumours are thought of as GACs. The incidence of gastric cardia cancer has been increasing. *H. pylori* infection is associated with atrophic gastritis of the gastric cardia and is a risk factor for GAC, particularly in countries where *H. pylori* infection is most prevalent (Hosokawa, Kinoshita et al. 2012). In *H. pylori* negative gastric cardia adenocarcinomas and GOJAC, there is no association with gastric atrophy. These tumours occur most frequently in developed countries and are increasingly common in developing countries. *H. pylori* is a negative gastric cancers are strongly associated with GORD and obesity, suggesting similarities between *H. pylori* negative gastric cardia cancer and the pathogenesis of BO and OAC (Bornschein, Quante et al. 2021).

1.10 Genetic susceptibility to BO and OAC

Susceptibility to BO is likely to develop from a cumulative effect of environmental risk factors, germline polymorphisms and somatic genetic variants. Studies have revealed a cluster of predisposing factors suggesting that inherited factors including circulating cytokine levels have value in predicting likelihood of development and

progression of BO (Sun, Zhang et al. 2017, Dong, Buas et al. 2018, Dong, Levine et al. 2018). Germline polymorphisms have been investigated by Genome wide association studies (GWAS) which overall have demonstrated that germline genetic susceptibility factors make up approximately 35% of the heritability of BO and about 25% of the heritability of OAC (Ek, Levine et al. 2013). These large-scale population-based studies have also been able to determine polygenic factors that increase likelihood of developing BO or OAC. These polygenic factors also known as single nucleotide polymorphisms (SNPs) which have demonstrated large overlap in the risk of developing BO and OAC suggesting they share genetic susceptibility (Ek, Levine et al. 2013). These SNPs are in genes known to play important roles during oesophageal development: FOXF1, FOXP1 and BARX1, by interacting with WNT/BMP signalling (Su, Gay et al. 2012, Buas, Onstad et al. 2015, Dai, de Dieu Tapsoba et al. 2015, Gharahkhani, Fitzgerald et al. 2016). Other prominent SNPs conferring BO risk relate to ion transport (cystic fibrosis transmembrane conductance regulator (CFTR)) and immune regulation, with SNPs associated with major histocompatibility (MHC) genes and MGST1 (microsomal glutathione transferase 1) (Su, Gay et al. 2012, Buas, Onstad et al. 2015, Gharahkhani, Fitzgerald et al. 2016). As previously discussed, inflammation induced by GORD has a significant role in the development of BO and OAC. Further analyses demonstrated that people with a Body mass index (BMI) >30kg/m^2 together with a specific SNP confers a three times greater risk of developing BO versus a person with the same SNP and a BMI<25kg/m^2 (Böhmer, Hecker et al. 2020). Other combinations of specific SNP variants with a history of tobacco smoking or recurrent reflux symptoms similarly lead to a significant increase in OAC risk (Dong, Buas et al. 2018). In a recent study, data aggregated from several previous GWAS studies demonstrates that obesity

driven GORD is associated increase incidence in BO and OAC but not depression associated GORD (Ong, An et al. 2021).

1.11 Understanding malignant progression in BO

The transformation of BO to dysplasia and onto OAC necessitates accumulation of (epi)genetic modifications and mutations, which enable metaplastic cells to develop the adaptive advantages of tumour cells (Hanahan and Weinberg 2011). In absolute terms, conversion from BO to OAC occurs infrequently, however BO remains the most potent risk factor for OAC development and provides the best insight into OAC carcinogenesis (Shaheen, Crosby et al. 2000).

The risk of progression to OAC increases dramatically with dysplastic BO. Duits et al reported in a study of patients with low grade dysplasia likelihood of progression to high grade dysplasia or OAC was between 9.1% and 13.4% per patient per year (Duits, van der Wel et al. 2017). In patients with high grade dysplasia the progression rate is 25% per patient per year (Duits, van der Wel et al. 2017). The difficulty to monitoring and understanding who will progress still lies with endoscopic examination of patients with non-dysplastic BO in endoscopic surveillance programmes. Studies examining short segment versus long segment BO have suggested that the longer the BO lesion up the oesophagus conveys a higher risk of progression to dysplasia or adenocarcinoma. Pohl et al examined 240 patients with short segment BO and 573 patients with long segment BO, showing cancer progression risk to be 0.03% and 0.22% respectively (Pohl, Pech et al. 2016). However, Bhat et al followed over 8500 patients, reporting no link between BO length and disease progression, in this study only approximately 1500 patients had

BO segments measured (Bhat, Coleman et al. 2011). Most recently, Nour et al. examined 1883 patients from 7 centres in America, patients with non-dysplastic BO were followed up for a median of 6.4 years and rigorously measured according to the Prague classification (Hamade, Vennelaganti et al. 2019). Endoscopic surveillance does not have unanimous support in the literature, however, a meta-analysis by Qiao et al., of 51 studies, which included more than 11000 patients demonstrated that routine biopsy surveillance of patients with non-dysplastic BO increased the identification of early neoplasia within the BO and reduced OAC related mortality by 61% (Qiao, Hyder et al. 2015). Another a prospective multicentre study supporting the results from Qiao et al (Kastelein, Van Olphen et al. 2016). Recent studies have suggested that narrow band imaging with modern generation endoscopes may reduce numbers of biopsies and lead to more accurate detection of dysplasia based on endoscopist's experience in identifying dysplastic pit patterns (Elsheaita, El-Bially et al. 2020). In most examples, this has been found to sample the majority of the heterogeneity within the BO lesion, however, genetic studies heterogeneity of BO have shed more light on the clonal evolution within BO.

Genetic Studies examining the transition from BO to low grade dysplasia, high grade dysplasia and OAC have largely focused on *P53* and *P16* genes (Weaver, Ross-Innes et al. 2014, Ross-Innes, Becq et al. 2015, Stachler, Taylor-Weiner et al. 2015). From these studies by the Bass and Fitzgerald labs two models have been proposed for BO progression. One study published by Maley et al. suggests that an initial mutation usually a *P16* and *P53* mutations are common throughout BO lesions, Maley et al. suggests that they confer a selective advantage to a clonal cell population, which then expands throughout BO, the so called "selective sweep hypothesis" (Maley, Galipeau et al. 2004). A separate study by Leedham and colleagues proposed a different model

whereby several clones could develop independently within the BO lesion and their expansion and evolution is regulated through clonal competition (Leedham, Preston et al. 2008). Agrawal and colleagues carried out whole exome sequencing on eleven OAC samples, 2 with paired BO, surprisingly high mutation rates were found in the BO samples, with many identical to the adjacent OAC sample from the same patient (Agrawal, Jiao et al. 2012). The Fitzgerald group has also investigated the chronology of mutational accumulation in OAC. In their study, Weaver et al. examined 112 BO, LGD, HGD and OAC samples by means of whole genome sequencing (WGS) (Weaver, Ross-Innes et al. 2014). These results demonstrated that a large number of tumour suppressor genes and oncogenes commonly mutated in OAC are also found in BO. P53 mutations are is often found in dysplastic and non-dysplastic BO, suggesting that P53 mutation has a role in early carcinogenesis of OAC, in contrary to colorectal cancer where P53 mutation is considered a later event (Hamelin, Fléjou et al. 1994). This suggests that many potentially cancer causing mutations exist within non-dysplastic BO and that the use of histopathological scoring, which is the current clinical standard of care, may not be the best means of predicting likelihood of malignant progression. In another study, mutational analysis of skin from healthy eyelids suggested that levels of mutations in known cancer-causing genes can be surprisingly high in benign tissues (Martincorena, Roshan et al. 2015). In the context of BO, mutational profiles cannot be used as a marker of likely disease progression. In paired analysis of BO and OAC from the same patients, Ross-Innes et al. demonstrate that in more than fifth percent of cases there is only a twenty percent concordance between the mutational profile of the BO and the adjacent OAC sample. Progression from BO to OAC is clearly linked to copy number alterations, which were only rarely found in BO (Ross-Innes, Becq et al. 2015). 9pLOH was frequently seen in BO. *P53*

mutations were found to occur in 83% of OAC cases compared to 39% of BO cases. Mutational profiling of multiple sites per lesion, was able to confirm the hypothesis that BO is a polyclonal disease, analysis has shown that multiple heterogeneous clones arising within the BO lesion and compete with other clones in the epithelial lesion, some progress to dysplasia, some to OAC and others remain non-dysplastic BO (Ross-Innes, Becq et al. 2015). At a similar time, another group published whole exome analysis of 25 pairs of BO and OAC (Stachler, Taylor-Weiner et al. 2015). In this study, they suggest two possible pathways for the progression of BO to OAC (Stachler, Taylor-Weiner et al. 2015). The first is the genome doubling pathway, whereby *P53* mutation occurs early in non-dysplastic BO, this then leaves the door open for further mutations to accumulate and genome doubling, which leads to genomic instability, oncogenic amplifications, copy number alterations and aneuploidy. The second route from BO to OAC that Stachler proposes in the "Non-genome doubling pathway", which describes a steady accumulation of mutations in tumour suppressor genes, including *CDKN2A, SMAD4* and *P53* function loss leading to oncogenic activation, genomic instability, copy number alterations and aneuploidy (Stachler, Taylor-Weiner et al. 2015). Furthermore they carried out a case cohort study of BO examining the temporo-spatial evolution of BO (Li, Galipeau et al. 2014). More than 95% of patients with BO will never progress to OAC, but again 9pLOH was frequently observed as in the study from the Fitzgerald Lab (Li, Galipeau et al. 2014, Ross-Innes, Becq et al. 2015). In those patients who did progress to OAC, loss of genomic stability was observed as the likely "threshold moment" before BO progressed to dysplasia and OAC leading to copy number alterations, chromosomal rearrangement and genomic doubling as identified by Stachler and colleagues. They conclude that whilst the majority of BO patients have genomically stable lesions, a

catastrophic genomic event such as a *P53* or C*DKN2A* mutation occurs allowing chromothriptic events to occur enabling evolution of BO to OAC to occur within a few years (Li, Galipeau et al. 2014). In a more recent study, Martinez and colleagues carried out in situ hybridisation on cytosponge "pseudobiopsies", these data support again the model by which patients who progress to OAC from BO have identifiable regions of cells with genetic instability before malignant transformation has occurred (Martinez, Timmer et al. 2016). A follow up study by Stachler carried out whole genome sequencing on FFPE samples in an attempt to risk stratify BO progressors again they identified the high incidence of *P53, CDKN2A*, chromosomal rearrangements are often seen in non-dysplastic BO, but not all lead to OAC (Stachler, Camarda et al. 2018). The six main studies discussed all agree that chromosomal instability and often genomic doubling are significant and frequent events which likely hail the early development of OAC from BO. *CDKN2A*, *CTNNB1*, *CDH1*, *GPX3*, *NOX5* all likely play important roles in BO progression to OAC. *P53* mutation is the most notable and most frequently occurring mutation in OAC and occurs in histologically non-dysplastic BO more than expected. Clinically P53 immunohistochemistry staining is used as an adjunct to the phenotypic criteria for dysplasia diagnosis; indeed *P53* mutations are very common in OAC. However, immunohistochemistry studies looking at BO patients who progress to OAC, suggest that P53 protein expression is only found in 7% of NDBO and 18% of OAC (Snyder, Dunbar et al. 2019). A prospective study looking predicting progression to OAC in BO patients determined that whereas aberrant P53 expression suggests presence of dysplasia that otherwise may be missed with random biopsies the only biomarker that predicted progression to OAC was presence of aneuploidy in the biopsies (Hadjinicolaou, van Munster et al. 2020). Further studies looking a targeted analysis

of SNPs in genes highly mutated in OAC was carried out using data from the BEACON (Barrett's and oesophageal adenocarcinoma consortium) data were carried out. 13 *P53* SNPs and 24 *CDKN2A* SNPs. Despite none of the *P53* polymorphisms having an association with OAC risk; three SNPs within the *CDKN2A* region correlated with 10-16% reduced risk for developing OAC (Buas, Levine et al. 2014). Further in vitro experiments went on to explain this effect by overexpressing one of the *CDKN2A* SNPs in cell lines, when expressed it reduced micro-RNA mediated repression of *CDKN2A* gene expression, allowing better *CDKN2A* function and improved tumour suppression effects (Buas, Levine et al. 2014).

High mutational burden, genomic rearrangements and competing clonal populations describe the evolving mutational landscape in BO. Longitudinal studies have described BO progressing to OAC as occurring either through a gradual accumulation of mutations, a chromothriptic event which leads to early genomic instability in the BO cells or an early cluster of critical mutations in genes such as *P53, CDKN2A, ARID1A* and *SMARCA4* (Weaver, Ross-Innes et al. 2014, Noorani, Li et al. 2020). Although we discuss OAC and GAC as anatomically distinct cancers there is increasing data that biologically they overlap. Combined analysis of OAC and GAC data from the Cancer genome atlas demonstrates that it is difficult to discern between chromosomally unstable GAC and OAC (Cancer Genome Atlas Research, Analysis Working Group: Asan et al. 2017). Epigenetic changes within BO predicting progression to OAC add further nuance and complexity to the predictive value of mutational profiles. Recently a multi-omic study examining NDBO, Dysplastic BO and OAC. This study demonstrated that the majority of genomic rearrangements (Katz-Summercorn, Jammula et al. 2022)

1.12 Genomic studies of BO and OAC

Alexandrov and colleagues initially described a means of disentangling mutations and their mutagens computationally introducing the concept of mutational signatures produced by certain mutagens, for example smoking, ultraviolet light etc. (Alexandrov, Nik-Zainal et al. 2013). Within the context of OAC, Secrier et al identified signature 17A, previously unassigned to a precise mutagen as the most likely mutational pattern caused by gastric reflux (Secrier, Li et al. 2016, Frankell, Jammula et al. 2019). This signature is specific to oesophageal and GOJ adenocarcinomas and is defined by T to G or T to C substitution in a CTT context, a mutational profile that is likely to be due to reflux induced oxidative stress (Nones, Waddell et al. 2014, Tomkova, Tomek et al. 2018). Although this mutational signature is seen throughout the OAC genome, the two most frequently mutated genes are *P53*, mutated in 72% of cases and *CDKN2A* (cyclin dependent kinase inhibitor 2A) mutated in 12% of cases). P53 is a tumour suppressor and co-ordinator of cellular apoptosis. *CDKN2A*, also known as P16, acts as part of the P53 pathway, regulates cell cycle and has p53-independent role, therefore is classed as a tumour suppressor. Other genes such as *ELMO1* and *DOCK2*, which act as intracellular mediators of the Rho family, and co-ordinated cell motility and invasion in tumours (Dulak, Stojanov et al. 2013). Other commonly mutated gene pathways in BO and OAC include chromatin remodelling, RAS and ATK pathways, DNA methylation, WNT, NOTCH, SMAD and TGF-β family pathways (Dulak, Stojanov et al. 2013, Weaver, Ross-Innes et al. 2014, Ross-Innes, Becq et al. 2015, Secrier, Li et al. 2016). Recently, a multi-omic cross-sectional study looking a BO progressors and non-progressors (Katz-Summercorn, Jammula et al. 2022). This study showed that genomic complexity occurs early in BO with early *P53* and *CDKN2A* mutations with chromothripsis often

occurring before clonal expansion. Transcriptional and epigenetic data showed widespread suppression of the WNT pathway and cell cycle genes (Katz-Summercorn, Jammula et al. 2022). Indeed, many mutations have been found in known morphogenic, and developmentally important pathways this has informed the development of many murine models that have been developed to attempt to model BO, OAC and GAC.

1.13 Animal models of GORD, BO, OAC and GAC

Many attempts have been made to create the ideal animal models for the development of BO and OAC. Porcine, canine and rodent surgical models of BO have already been discussed. Epithelial tumours are much less common in mice than humans, murine gastric lymphomas and sarcomas are much more frequently described. Most existing genetic models of upper gastro-intestinal cancers recreate much of the stepwise stages of carcinogenesis associated with intestinal-type gastric adenocarcinoma. This is usually initiates with gastritis and goes on to gastric gland atrophy followed by IM, dysplasia and malignant transformation with invasion into the submucosa. There are however, some critical differences between described transgenic murine models of gastric adenocarcinoma and the human disease that they are attempting to model.

The majority of transgenic murine models have been generated on the C57BL/6 or mixed genetic backgrounds. In cancers that are known to be in part driven by oestrogen receptor signalling such as gastric carcinomas we often see a gender bias. As previously mentioned, there is an increasing understanding about the role of tumour micro environmental signalling in carcinogenesis and metastatic progression. Immune signalling is critical part of the carcinogenic milieu particularly in

inflammation driven gastric and oesophageal cancers and therefore likely to be affected by the genetic background of the mouse used in the model. Compared with C57BL/6 mice, mice with the BALB/C genetic background have been shown to have a predisposition towards autoimmune gastritis (Baxter, Jordan et al. 2005). Given that many epithelial cancers are initiated by or driven by inflammation, mouse strain differences should also be considered in their predisposition to cancer development and could be utilised to develop inflammatory cancer models. For an ideal in vivo model there has to be genetic relevance to the human disease; similarities in the anatomy of the squamous columnar junction and physiologically relevant induction of inflammation (Kararli 1995).

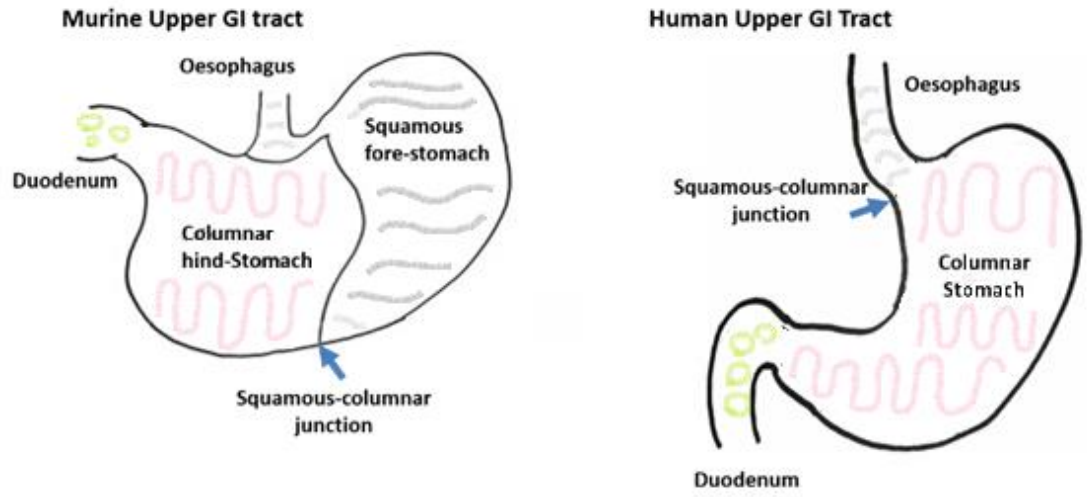


Figure 1.1 Diagram to show the differences between the murine and the human upper gastro-intestinal tracts

Left: is a diagram of the murine upper GI tract. This diagram demonstrates an oesophagus and fore-stomach lined by a stratified squamous epithelium and a columnar hind stomach with a glandular structure. In the middle of the stomach lies the squamous columnar junction, which the blue arrow delineates.

Right: is a diagram of the human upper GI tract. This diagram demonstrates an oesophagus lined by a stratified squamous epithelium and a columnar stomach with a glandular structure. At the site of the anatomical oesophago-gastric junction lies the squamous columnar junction, which the blue arrow delineates. Diagrams are not to scale.

1.14 Transgenic models of gastro-oesophageal cancer

1.14.1 Developmental gene models

An early transgenic model attempting to recreate BO was a *Cdx2* transgenic mouse, using the β subunit of the H+/K+ ATPase promoter to overexpress Cdx2 in a targeted manner in parietal cells (Mutoh, Hakamata et al. 2002). The mice were developed on a C57BL/6 background and reared in a pathogen free environment. At 12 weeks old, mice demonstrated hypergastrinaemia and incomplete GIM. At 2 years old, these mice all had gastric tumours. These mice developed malignant transformation with Apc and *P53* mutations mimicking those seen in human gastric adenocarcinomas, but no metastases. *Cdx1* transgenic mice did not develop gastric tumours but demonstrated complete IM with several secretory cell lineages including entero-endocrine cells and Paneth cells.

WNT's critical role in intestinal development implicates its role in BO development. Mouse models overexpressing β-catenin show instances multifocal gastric dysplasia (Coste, Freund et al. 2007). *Apc* mutant mice develop gastric tumours in low frequency, compared with the more frequently observed colonic lesions (Fox, Dangler et al. 1997). These tumours are primarily of the gastric antrum (Tomita, Yamada et al. 2007). Forkhead homolog 6 (FKH6) has been shown to be upstream of WNT signalling in gut development (Perreault, Katz et al. 2000). Mouse models show germline loss of Fkh6 leads early death of pups. Gastric hyperplasia, cyst formation, mucous cell metaplasia and increased cell proliferation were seen. Transforming Growth Factor alpha (TGFα) transgenic mice, in which over expression of TGFα drives gastric hyperplasia with glandular cystic proliferation mimicking human, Ménétrier's Disease (Nomura, Settle et al. 2005). The fundic crypt structure become more like antral crypts with expression of Pdx1 (pancreatic and duodenal homeobox

gene 1) in the fundus however they do not demonstrate IM. In human squamous cells inhibition of Notch signalling has been demonstrated to increase expression of columnar cytokeratins and gastric mucins via KLF4 expression (Vega, Giroux et al. 2014). In mice, complete knockout of *Klf4* is lethal, so a conditional deletion of Klf4 was developed in gastric epithelium (Katz, Perreault et al. 2005). After 26 weeks gastric epithelial hyperplasia, mucous metaplasia was seen, however, the mice did not develop inflammation, dysplasia or adenocarcinoma. Sonic Hedgehog (Shh) is another gene critical in embryological development and differentiation. After 3 weeks Shh knockout mice have intestinal differentiation within gastric epithelium without IM (Sancho, Batlle et al. 2004).

1.14.2 TGF β pathway transgenic models

The Transforming growth factor β (TGFβ) superfamily has been linked with the development of BO in many studies. Through their involved in cell proliferation and tissue development TGFβ, associated receptors and the SMAD signalling are all considered tumour suppressor genes. Mutations in genes associated with this pathway lead to neoplasia, invasion and metastasis (Derynck, Akhurst et al. 2001). Normal tissues cells produce TGFβ1 as an autocrine and paracrine signal either stimulate or suppress production of extracellular matrix providing a cellular scaffold, enabling cell polarisation, cell division, proliferation and differentiation within a tissue. TGFβ alterations have been shown in BO and OAC (Singh, Singh et al. 2019). The inactivating homozygous TGFβ1 mutant mice die within 3 weeks of birth (Shull, Ormsby et al. 1992). Phenotyping deceased pups demonstrated evidence of gastric inflammation, ulceration, metaplasia and hyperplasia (Shull, Ormsby et al. 1992). This suggested that TGFβ1 might play a significant role in the development of upper

GI metaplasia and cancer formation (Boivin, O'Toole et al. 1995). Targeting the same pathway, a dominant negative mutant of the TGFβII receptor was created expressed in the stomach by inserting it onto the *Tff1* promoter (Hahm, Lee et al. 2002). The dominant negative mutant pairs with WT TGFβ receptor subunits in gastric epithelial cells, in turn this reduces response to TGFβ ligand signalling. The mice have no gastric phenotype however they have a more exaggerated response to *H. pylori* infection with gastric dysplasia and adenocarcinoma. Bone morphogenic proteins (BMP) are part of the TGF beta superfamily. Noggin is an endogenous BMP antagonist, which when knocked out or mutated leads to constitutively active *Bmpr1a* mice also develop to adulthood with CLE (Rodriguez, Da Silva et al. 2010). When BMPR1a is knocked-out epithelial stratification occurs however, normal squamous differentiation is inhibited (Rodriguez, Da Silva et al. 2010). SMAD4 is downstream of TGFβ signalling. A transgenic model was developed demonstrating that *Smad4* heterozygous mice developed gastric polyps and adenocarcinomas (Xu, Brodie et al. 2000). Further work by found that this phenotype was caused by Smad4 loss in murine T cells, which drove malignant transformation (Kim, Li et al. 2006). This demonstrates that aberrations in the TGF β signalling pathway may be used by the tumour microenvironment to promote tumour development.

1.14.3 Inflammatory gene models

Trefoil Factors are secretory peptides that are expressed in a regionally specific way throughout the gastro-intestinal tract. TFF1 is expressed in gastric mucus cells and has a role in barrier function and epithelial regeneration. In *Tff1*, knockout mice developed dysplastic lesions and gastric antral adenocarcinomas (Tomasetto, Masson et al. 2000). Loss of Tff1 expression led to increased cyclo-oxygenase -2 (COX2)

expression in the gastric stroma. In this model a selective COX2 inhibitor demonstrated the role for COX2 in driving malignant transformation in polyps (Saukkonen, Tomasetto et al. 2003). Indeed COX2 and NFκB signalling have been demonstrated to be important in the development of mouse models of junctional carcinogenesis in other studies (Quante, Bhagat et al. 2012). In another model, the COX2 and WNT1 gene cassettes were inserted downstream of the K19 promoter (Oshima, Matsunaga et al. 2006). This model develops inflammation, dysplasia and adenocarcinoma with submucosal invasion. Upstream of TFF1 is the gp130 receptor, which binds IL-6 and IL-11 in the stomach. Mutation of the gp130 gene leads to gastric tumourigenesis. This is driven by a gp130 dependent induction of interleukin signalling in the gastric epithelium and a downregulation of the SHP-2/RAS/ERK/AP-1 pathway (Judd, Alderman et al. 2004). This phenotype may be epithelial or stromally driven.

1.14.4 Parietal cell targeting models

Parietal cells present in gastric fundic crypts secrete hydrochloric acid. These cells have been targeted to develop experimental models of increased acid secretion to mimic reflux and induce gastric cancer. However, none of the models have successfully demonstrated malignant transformation, instead demonstrated hypergastrinaemia and hyperplasia of the gastric epithelium (Schultheis, Clarke et al. 1998, Toh, Sentry et al. 2000, Heitzmann, Grahammer et al. 2004, Gawenis, Greeb et al. 2005) .

1.14.5 Combined Helicobacter-transgenic models

In mice with neutral gastric pH gastric infection of *H.felis* has been shown to have a synergistic effect driving gastric tumorigenesis (Wang, Dangler et al. 2000). P53 is a transcription factor that works as a master regulator of apoptosis, proliferation and

DNA damage repair. Loss of heterozygosity mutations in P53 have been described in oesophageal and gastric cancers along with their premalignant lesions. Studies have examined mice that were heterozygous for P53 in the gastric mucosa alone. After 26 weeks mice with this gastric specific knockout developed epithelial hypertrophy, hyperproliferation, mucous metaplasia, atrophy and polypoid lesions of the gastric fundus and antrum (Fox, Li et al. 1996). When combined with *H.felis* infection P53 heterozygous mice develop dysplasia or cancer development (Fox, Li et al. 1996).

1.15 Mixed transgenic and surgical models

Oesophago-jejunostomies were carried out with a total gastrectomy on *p53* knockout mice with a C57BL/6 background exposing the lower oesophagus to bile (Fein, Peters et al. 1999). Mice died by 25 weeks due to development of haematological malignancy. Only 4 out of 12 mice survived passed 24 weeks. Two mice developed OAC and one mouse developed oesophageal squamous cell carcinoma. In another more recent study 28 out of 32 *P53-/-* mice died before 20 weeks, again due to haematological malignancy (Hao, Liu et al. 2009). Hao et al. studied the effects of germline mutations in *p53* and *Cdkn2a* combined with the oesophago-jejunostomies on a C57BL/6 background. In this study, none of the mice developed a columnar lined oesophagus, IM or OAC, one mouse developed OSCC (Hao, Liu et al. 2009). In a further study, oesophago-jejunostomy surgery on *p27-/-* mice with or without oral nitrosamine exposure. This study reported 26% incidence of CLE and 23.3% of mice developed OAC (Ellis Jr, Xu et al. 2001).

1.16 Rodent surgical models

A wide spectrum of animals have been utilised in the quest for the ideal animal model of BO and OAC. Although none to date have proven ideal, all are useful and each in some way sheds light on the pathogenesis of BO and OAC. Canine and porcine models are viewed as more physiologically and anatomically relevant to humans, however, with current constraints transgenic canine and porcine models are impractical in many ways. Primates are the only animals known to fulfil the criteria of genetic and anatomical similarity with humans and naturally experience gastro-oesophageal reflux.

Rodents have been shown to lack the ability to vomit or experience reflux (Kararli 1995). Surgical models have given insight into the role of gastric and duodenal reflux onto squamous oesophageal epithelium. All of these models created in mice rats and dogs proceeded to columnarisation of the oesophagus in the post-operative period and haled as models of BO by the authors. Some animals had evidence of IM which defined by expression of Trefoil factors or dysplasia and OAC. The adenocarcinomas that develop lack the invasiveness and metastases so are unable to model human cancer progression. Following a oesophago-jejunostomy peri-anastomotic columnarisation of squamous epithelium is more likely due to wound healing (Agoston, Pham et al. 2018). BO was found to develop in between 3 and 77% of cases between 20 and 70 weeks post-op. In rats that proceeded to OAC, this was reported in between 7 to 83% of animals requiring between 30 and 70 weeks post op (Miyashita, Shah et al. 2011, Miyashita, Miwa et al. 2013, Miyashita, Shah et al. 2013). However, in these surgical models rodents and mice have never exhibited presence of islands of columnar epithelium surrounded by squamous cells. This may be due to lack for gland structures deep to the squamous epithelium. Some studies were also designed with

utilisation of exogenous carcinogens such as nitrosamines, high iron diets and high fat diets to promote carcinogenesis. Duodeno-oesophageal anastomosis alone lead to development of CLE in 42.4% of mice and OAC in 6%. Carcinogen alone lead to OAC 13% of the time (Xu, LoCicero III et al. 2000). Duodeno-oesophageal anastomosis surgery and carcinogen exposure lead to CLE in 42% of cases and OAC 37%. In another study, mice with BALB/C background they demonstrated CLE in 60% of mice after 16 weeks post duodeno-oesophageal anastomosis surgery and OAC in 55% of mice at 20 weeks post op (Raggi, Langer et al. 2010). C57BL/6 mice and demonstrated that CLE incidence was 7% at 52 weeks (Pham, Genta et al. 2014). One study carried out an experiment where BALB/C and C57BL/6 mice were directly compared following side to side (Babu, Meng et al. 2008). C57BL/6 mice were found to have a reduced inflammatory response to reflux, this is likely due to immune differences between C57BL/6 mice and BALB/C mice leading to variation phospholipase A2 expression. Aikou and colleagues presented a model which suggests the involvement of bone marrow derived stem cells in the development of BO (Aikou, Aida et al. 2013).

1.17 Cellular origins of BO

1.17.1 Squamous hypothesis transdifferentiation versus transcommitment

For squamous epithelial cells to be the cell of origin of BO it would require reprogramming of squamous cells giving rise to a columnar lined oesophagus (Slack and Tosh 2001). This has been hypothesized to occur in either of two ways transdifferentiation or transcommitment (Wang and Souza 2016, Wang 2017). The process of transdifferentiation would require a terminally differentiated squamous cell

to become a columnar cell (Takahashi, Tanabe et al. 2007, Mills and Sansom 2015, Wang 2017). Transcommitment involves reprogramming of squamous progenitor cells leading to a columnar gene expression driving columnar differentiation (Wang and Souza 2016). Several studies have described multi-layered epithelium (MLE) which doesn't ascribe itself to the classical morphology of a stratified squamous epithelium or a simple columnar epithelium and expressed both squamous and columnar differentiation markers (Glickman, Chen et al. 2001, Chen, Qin et al. 2008, Langner, Wolf et al. 2014). These studies suggest that the MLE may demonstrate a cell population undergoing transdifferentiation or transcommitment. These cells were not found at the GOJ in healthy volunteers without BO, but are a specific to the GOJs of patients with BO (Boch, Shields et al. 1997). Further examination of the cytokeratin profiles of the MLE cells, revealing that they basal layer of cells expresses squamous markers KRT4 and KRT13, yet the more superficial cells express columnar cytokeratins such as KRT19. Using a rat model of BO, Chen and colleagues developed a rat surgical model of reflux by carrying out oesophago-duodenal anastomosis, allowing bile exposure to the squamous rat foregut (Chen, Qin et al. 2008). At the neo-squamo-columnar junction produced by the surgery a MLE type cell population was seen similar to what Boch and colleagues had previously described in humans (Boch, Shields et al. 1997, Chen, Qin et al. 2008). Chen et al. conclude that as rats do not have any native submucosal glands the MLE must derive from the native oesophageal squamous cells in response to their exposure to bile (Chen, Qin et al. 2008). Further studies proposing evidence for potential trans-commitment from squamous to columnar epithelium is demonstrated by using the model of the embryonic mouse oesophagus (Yu, Slack et al. 2005). During normal oesophageal development i*n utero*, the mouse oesophagus is columnar lined

expressing KRT8 and KRT18, which becomes squamous expressing KRT14 half way through gestation (Yu, Slack et al. 2005). Yu and colleagues grew *ex vivo* day 11.5 mouse oesophageal cells to mimic oesophageal development *in vitro* (Yu, Slack et al. 2005). During the late stages of oesophageal development some cells were found to co-express the columnar marker KRT8 and squamous marker KRT14 (Yu, Slack et al. 2005). This proves that it is possible for a columnar cell to transdifferentiate during development, they demonstrate that there is a biological precedent for transdifferentiation but they do not directly demonstrate squamous to columnar transdifferentiation in a model that mimics BO.

Another example of transdifferentiation is SPEM (Spasmolytic polypeptide expressing metaplasia) in the murine gastric epithelium (Que, Garman et al. 2019). In SPEM as a response to injury induced by *H.pylori* or chemical exposure chief cells are able to de differentiate re-enter the cell cycle and become Trefoil Factor 2 (TFF2) expressing cells (Goldenring and Nam 2010, Goldenring, Nam et al. 2011, Radyk, Burclaff et al. 2018, Goldenring and Mills 2021). Mills and colleagues proposed that this may be a means by which squamous epithelium could develop into BO (Jin and Mills 2018, Willet, Lewis et al. 2018). There has been no study with data to directly support transdifferentiation, transcommitment where reflux alters gene expression driving naïve cells down a columnar differentiation pathway has more support. The presence of ectopic IM in the oesophagus is itself evidence of transcommitment as goblet cells are not normally present in the oesophagus (Que, Garman et al. 2019).

1.17.2 Gastric stem cell hypothesis

Norman Barrett's original description of BO included a suggestion that these lesions were caused migration of cells from the proximal stomach (Barrett 1957). A recent study examining the epigenetic profile of BO and OAC demonstrated a chromatin states demonstrating a pattern between that of gastric and intestinal epithelium this has been used to infer a gastric cell of origin for BO (Singh, Ha et al. 2021). BO has been shown to contain specialised differentiation, including expression of gastric specific genes, Claudin18 and TFF2 (Jovov, Van Itallie et al. 2007, Lavery, Nicholson et al. 2014). If gastric cells were the BO progenitor cells they are most likely to have migrated from the most adjacent gastric epithelium, the cardia. BO glands include a very diverse differentiation pattern including pyloric, antral, fundic and less frequently pancreatic specific expression. MacDonald and colleagues suggest the range of gland phenotypes and their distribution within BO suggests an evolution from cardia type glands at the SCJ towards intestinal type glands more proximally (McDonald, Lavery et al. 2015). Gland expression patterns in BO are primarily gastric with MUC5AC+/TFF1+ glands, MUC6+/TFF2+ glands predominating, particularly in BO adjacent to the GOJ (McDonald, Lavery et al. 2015). Other studies have demonstrated specialised gastric differentiation in human BO with gastrin receptor (Cholecystokinin 2 receptor, CCK2R) expression (Abdalla, Lao-Sirieix et al. 2004). Some groups have used expression of gastric stem cell marker, LGR5 to support the hypothesis that Barrett's has a gastric cell of origin as no native oesophageal LGR5+ population has yet been found. Quante and colleagues carried out a study demonstrating that LGR5 positive cells from the mouse gastric cardia migrate proximal to the SCJ in response to inflammation in the squamous epithelium (Quante, Bhagat et al. 2012). However, LGR5 is the most widely accepted adult stem

cell marker present throughout the gastro-intestinal tract (Barker, van Es et al. 2007, Barker, Huch et al. 2010). In their study, Quante and colleagues created a combined transgenic and reflux model was used. These mice overexpressed IL-1β squamous epithelial cells and were then treated with the bile salt, deoxycholic acid (DCA) to mimic biliary reflux (Quante, Bhagat et al. 2012). After 12 months of DCA consumption mice were found to have inflammation of their proximal squamous forestomach and determined to have a BO-like epithelium at the SCJ (Quante, Bhagat et al. 2012). In some mice, the BO-like epithelium also progressed to dysplasia and adenocarcinoma. However, this model does not demonstrate a columnar lined forestomach or a columnar lined oesophagus. In both Quante's model and in human BO an increased expression of Krt19 and Tff2 were seen, neither are usually expressed in cells adjacent to the SCJ. Quante and colleagues suggest that BO cells is likely to be the result of gastric cardia stem cell migrating up the oesophagus. In a separate study carried out by Lavery, patients with BO and associated adenocarcinoma were treated with Iodo-deoxyuridine (IdU) at different time points prior to oesophagectomy (Lavery, Nicholson et al. 2014). Detailed post-operative histological analysis of the resection specimens showed the presence of LRG5+ cells in BO. Location of the LRG5+ cells in the BO crypts co-localised with IdU tracing showed that the proliferative population was in the middle of the gland this crypt phenotype is not intestinal-type, but suggests a gastric antral LGR5+ position within the BO crypt. These data are used by Lavery and colleagues to suggest that the pattern LRG5 expression in BO is most similar to gastric epithelium (Lavery, Nicholson et al. 2014). Studies examining patients after oesophagectomy develop a new cardia type mucosa at the distal oesophagus within 2 years, intestinal type glands appear after 5 years post-operation (Lord, Wickramasinghe et al. 2004, O'riordan, Tucker et al.

2004). In a recent study Nowicki-osuch and colleagues carried out a comprehensive molecular profiling of normal oesophagus, OSGs, gastric cardia, and BO and found that transcriptional similarities were most profound between gastric cardia and BO (Nowicki-Osuch, Zhuang et al. 2021).

1.17.3 Submucosal gland hypothesis

One potential origin of BO are OSGs. OSGs are found throughout the human oesophagus deep to the stratified squamous epithelium. They harbour the only population of columnar cells native to the oesophagus. Their role is to produced bicarbonate and mucin in order to neutralise gastric acid and lubricate transition of the food bolus (Treuting, Arends et al. 2018). OSGs drain through ducts lined by cuboidal cells which transition to squamous cells before meeting the stratified squamous epithelium of the oesophagus. Several studies have described islands of BO epithelium surrounded by squamous epithelium and conversely squamous islands surrounded by BO (Sharma, Morales et al. 1998, Coad, Woodman et al. 2005, Epstein, Cosby et al. 2017). In a Japanese study of 131 oesophagostomy specimens from patients with squamous cell carcinomas Barrett's islands were seen in 57% of specimens (Nakanishi, Saka et al. 2007). The islands can be several centimetres proximal to the SCJ (Nakanishi, Saka et al. 2007). The presence of BO islands in the mid oesophagus puts into question that BO can only be caused by gastric cells migrating up the oesophagus. Studies on human oesophagostomy specimens mapping OSGs have showed an increased density of OSGs below the Barrett's- squamous boundary (neo-SCJ) (Lörinc and Öberg 2012). In another study, oesophagectomy specimens containing BO, 15 specimens demonstrated neo-squamous islands that were continuous with OSG ducts suggesting they arise from the OSGs (Coad,

Woodman et al. 2005) The same study also saw 21 oesophagectomy specimens where BO was continuous with the OSG ducts (Coad, Woodman et al. 2005). Beyond these observational studies, several important clonality studies have been carried out. Paulson and colleagues carried out microdissection and genetic analysis of 20 specimens of squamous islands surrounded by BO, in most cases no shared mutations were seen between the OSGs and the squamous islands nor the OSGs and the BO above. 1 specimen showed the same p16 mutation shared between the squamous island and the BO, which was not seen in the adjacent normal oesophagus and was not a germline mutation suggesting that in that instance the BO and the squamous island shared the same progenitor (Paulson, Xu et al. 2006). Further work by Leedham and colleagues demonstrated that similar to previous studies neo-squamous islands were often found above OSGs. In 1 of 3 cases the p53 mutations in BO did not match the p53 mutations seen in the neo-squamous islands or the OSG. However, in 1 of 3 specimens the p16 mutation found in the BO epithelium was also seen in the OSG duct continuous with the BO at the surface (Leedham, Preston et al. 2008). Another study examined mitochondrial DNA mutations for clone tracing and in 1 patient found shared mitochondrial mutations between the squamous and BO mucosa, suggesting that they share the same progenitor (Nicholson, Graham et al. 2012).They found that OSGs had missed clonal cell populations, demonstrating OSGs may contain more than one progenitor cell. Taken together suggested that BO and squamous epithelium can derive from OSGs in a clonal manner.

A key limitation examining OSG biology is *in vivo* modelling. Rodents do not have OSGs, however, pigs and dogs do. Porcine models for examining the role of OSGs in the development of BO are useful as the density of OSGs throughout the oesophagus

is much higher than in humans (Krüger, Gonzalez et al. 2017, von Furstenberg, Li et al. 2017) The Garman laboratory developed a pig model of radiofrequency ablation (RFA) induced oesophageal injury where cell proliferation during repair was tracked by examining uptake of 5-thynyl-2'-deoxyuridine (EdU). Expectedly, high EdU uptake was seen in the basal squamous epithelium, as the wound healing response was activated. However, high EdU uptake was also demonstrated in the submucosal gland ducts in pigs with oesophageal injury (von Furstenberg, Li et al. 2017). This suggests a population of stem cells exist within OSGs. The OSGs of the pigs were then micro dissected out and cultured as organoids which, demonstrated two different phenotypes some expressed squamous genes and others expressed columnar genes. Transcriptional comparison of columnar OSG organoids from matched the transcriptional profile BO associated genes (such as *AGR2, SOX9, KRT8, KRT18, MUC1* and *MUC13*) (Krüger, Gonzalez et al. 2017, von Furstenberg, Li et al. 2017). When comparing the cultured OSGs to the transcriptional profiles of the dissected OSGs the higher mucin gene expression in the *in vitro* cells were the only genes significantly different. Garman's group suggest that the OSG progenitor cell populations exist within the OSG duct expressing both columnar markers (KRT7) and squamous markers (P63, KRT5) these cells may have the ability to give rise to squamous and columnar cell linages following oesophageal epithelial injury. However, which cell population within OSGs has this ability remains a mystery, and whether or not one cell has the multipotency to be able to produce columnar and squamous lineages remains to be seen. OSGs have been shown to undergo acinar ductal metaplasia in response to chronic inflammation, demonstrating that GORD effects OSG cells (Garman, Kruger et al. 2015).

Another study has used canine model of chronic GORD by creating a surgical "cardioplasty" and a fixed hiatus hernia to promote gastric content reflux and induce inflammation (Gillen, Keeling et al. 1988). Squamous epithelium was endoscopically resected to create two $2cm^2$ areas of de-epithelised oesophagus one patch at the GOJ and the other 2cm proximal leaving 2cm of normal squamous epithelium between. In a canine model, jejuno-gastric anastomoses were done to increase the bile component of the refluxate. In other dogs, Gastrin analogues were administered to increase gastric acid production and increase propensity for reflux. The lower oesophagi and GOJs of the dogs were examined after 3 months. Dogs from both the gastrin supplemented group and the surgical group were found to have columnar epithelium develop in the distal de-epithelised area at the GOJ, compared to control animals who received no endoscopic mucosal resection demonstrated only normal stratified squamous epithelium with mild reflux related inflammatory changes (Gillen, Keeling et al. 1988). Remarkably, 30% of dogs in the gastrin group developed columnar epithelium in the proximal area of stripped epithelium 4cm proximal from the GOJ with 2cm of squamous epithelium and the other 2cm denuded area between. From these results, it is clear that cells have not migrated up from the gastric cardia skipping the patch of squamous epithelium. Histological analysis revealed that the regions of neo-columnar lined oesophagus 4cm away from the GOJ were continuous with OSGs. The OSGs are therefore the likely source of the columnar lined oesophagus in this experiment (Gillen, Keeling et al. 1988).

In a recent, study using scRNA sequencing of mouse and Human upper GI tracts, OSG specific *HOXA13* was found to be highly expressed in BO and in a cell population at the SCJ (Janmaat, Nesteruk et al. 2021). Lineage tracing studies in

animals with OSGs and studies to isolate and sequence OSGs need to be carried out to further characterise OSGs.

1.17.4 Circulating bone marrow cells

Several studies have suggested that multipotent stem cells from the bone marrow exist in the peripheral circulation and may be recruited to and contribute to the regeneration of inflammatory lesions. In support of this hypothesis, bone marrow derived stem cells have been reported to contribute to the regeneration of many other tissues such as: skin, gastric epithelium, lung, muscle, intestine, brain, liver, heart and endothelium. Specifically, one study has shown that radiation induced oesophageal injury in mice in infiltrated and repaired by transplanted bone marrow derived cells (Epperly, Guo et al. 2004). A potential role for bone marrow derived cells by first lethally irradiating female rats to destroy the bone marrow, then transfusing the female rats with age and strain matched male rat blood (Sarosi, Brown et al. 2008). Rodents were then randomly assigned to undergo a sham procedure or oesophagojejunostomies (attaching a loop of jejunum to the oesophagus) this was shown to acts as a reflux model by bathing the oesophagus in a bile rich mixture of gastric and pancreatic juices (Sarosi, Brown et al. 2008). They suggested that this leads to a "Barrett's-like model", where chronic inflammation leads to oesophageal columnarisation and IM. Eight weeks after oesophagojejunostomy DNA Fluorescence *in situ* Hybridisation (FISH) was carried out looking for evidence of the Y chromosome (male sex chromosome). Results suggested that Y-chromosomes from the male rats had incorporated in the nuclei of the female epithelial cells in the region of oesophageal inflammation. Y chromosome staining was seen in both squamous and the "metaplastic" columnar cells. There remains no evidence that bone marrow

derived cells directly differentiate into oesophageal epithelial cells. The immune localisation due to localised inflammation leads to recruitment of male leukocytes. These leukocytes may have their nuclei incorporated into the epithelial cells, or it may simply be artefact from the Y chromosome containing cells dying and leaving Y chromosome remnants in the epithelium, which were stained positively during the FISH assay. Hutchinson and colleagues demonstrated findings of a male patient with acute myeloid leukaemia, who underwent bone marrow irradiation followed by bone marrow transplantation with his sister as the donor. A decade later the same patient went on to develop a distal oesophageal adenocarcinoma, FISH examination demonstrated that the tumour contained cells with 2X chromosomes, suggesting that the bone marrow contributed to the tumour. Hutchinson and colleagues also carried out an in vivo experiment where irradiated mice underwent a bone marrow transplant with cells expressing β-Galactosidase, then went on to have a oesophago-jejunostomy (Hutchinson, Stenstrom et al. 2011). Within twenty weeks 30% of mice demonstrated columnarisation of their oesophagus containing β-galactosidase expressing cells. This data is thought provoking, however, it is difficult to draw conclusions from this data that fit with the larger body of data in the literature and how it pertains to what we see clinically as BO.

1.17.5 Residual embryonic cell hypothesis

Two recent studies have defined a cell population that exists at the SCJ, which may give rise to IM. The first is Frank McKeon's work on the Residual Embryonic Cell (RECs) population, which exists at the squamous columnar junction (SCJ), has provided important molecular insight into the development of IM within BO (Wang, Ouyang et al. 2011). As previously mentioned the anatomy of the rodent and human

upper gastro-intestinal (GI) tract differs significantly. Along with the absence of OSGs in rodents, mice have their SCJ in the middle of their stomach, so the GOJ and SCJ are at different sites and the murine gastric fundus or forestomach is a stratified squamous epithelium. This limits comparisons that can be made between the human disease and murine *in vivo* models. In the *Tp63-/-* mouse model to examine squamous epithelial development in the upper GI tracts. The mice die shortly after birth due to their lack of a stratum corneum in their skin so they lack the barrier function that skin provides, leading to loss of tissue fluid through the dermis. Upon examination of the murine stomachs, a simple columnar epithelium exists with IM with the presence of positive alcian blue (AB) staining. By tracing cell populations during embryological development, Wang and colleagues identified a cell niche at the SCJ where P63 negative Carbonic anhydrase 4 (CAR4) positive cells lay dormant as an embryonic remnant (Wang, Ouyang et al. 2011). In *Tp63-/-* mice, this CAR4+ KRT7+ population were suggested to be responsible for proliferating and lining the mouse stomach, giving rise to goblet cell differentiation shown by the AB staining. Wang and colleagues suggest that inflammation interrupts the equilibrium between squamous and columnar cells at the SCJ by damaging the squamous epithelium, in response REC cells. As IM arises in the *Tp63-/-* mouse, they suggest that BO could not develop from a cell previously committed to the squamous lineage.

1.17.6 Transitional cells hypothesis

Studies have demonstrated unique cell population existing at the “transition zone” cell population at the GOJ, which demonstrated features of both squamous and columnar epithelium (Shields, Zwas et al. 1993). Another study again from Frank McKeon’s group investigated the phenotypic changes in *p63-/-* mouse forestomachs.

Unexpectedly lineage tracing experiments using *p63-CreER* mice found that the simple columnar cells and goblet cells that existed in the *p63-/-* forestomachs derived from p63 positive progenitor cells (Jiang, Li et al. 2017). In this study, Jiang and colleagues examined SOX2 (SRY-box 2) overexpressing mice. SOX2 is a squamous transcription factor known to play a role in co-ordinating *P63* expression and the differentiation of squamous epithelium. Mice that over express *Sox2* develop hyperplasia of their squamous epithelium and, in addition hyperplasia in at the transitional zone at the gastric SCJ. The transitional epithelium was found to consist of p63+/ KRT5+ basal cells and KRT8+ luminal cells. These KRT8+ cells stain positively for AB, express intestinal marker AGR2 and KRT7 a gene expressed in BO. Green fluorescent protein (GFP) lineage tracing experiments in *Sox2* over expressing mice showed that these "Transitional cells" expressing KRT8/AGR2/KRT7 derived from SOX2 progenitors at the junction, not from the Claudin18/LGR5 positive GFP negative gastric cardia stem cells. To mimic biliary reflux mice underwent oesophago-jejunal anastomosis surgery, in these mice and expansion of the columnar cell population with IM was seen, linage tracing with Red Tomato revealed that these cells derived from p63 positive cells at in the transitional zone. Critically these metaplastic cells only exist at the junction not in the oesophagus or more distally in the stomach. *In vitro* studies where p63+/ KRT5+/KRT7+ cells were grown out and demonstrated the ability to reconstruct the multi-layered transitional epithelium. In contrast to published work from the McKeon Group, this transitional cell population do express p63. However, there is no evidence that inflammation can drive this P63+/KRT5+/KRT7+ population towards complete IM. Jiang's study and other groups demonstrated that *in vitro* transfection of squamous cells with CDX2 alone does not drive these cells towards columnarisation or MUC2

expression (Kong, Crissey et al. 2011). However, in patients who have undergone an oesophagectomy and gastric pull up to form a conduit, patients often develop severe oesophagitis in their oesophageal remnant, over time they develop a columnar lined oesophagus, which sometimes then develops into IM. As these patients have had their native gastro-oesophageal junction resected, the development of BO post operatively cannot be dependent on a population of cells only present at the native GOJ (Öberg, Johansson et al. 2002, Dunn, Burt et al. 2016).

1.18 Summary

BO is a metaplastic process in the lower oesophagus which increases risk of oesophageal adenocarcinoma. P53 mutations in NDBO predict progression to cancer (Redston, Noffsinger et al. 2022). P53 mutations in oesophageal and gastric adenocarcinoma are associated with intestinal phenotype (Bass, Thorsson et al. 2014). Intestinal metaplasia is a common feature of BO and gastric pre-malignant lesions. Despite a lot of evidence for different sources of the BO cell of origin, no consensus has been made. BO is a human disease and has proven difficult to recapitulate in *in vitro* and *in vivo* models. Improvements in modelling of upper GI pre-malignant lesions may prove new insights into understanding

Aims

The aims of this study are to investigate the cellular origins of Upper GI metaplasia.

Firstly, whether early p53 mutation is associated with intestinal metaplasia at the squamous columnar junction demonstrated by metaplasia as a precursor to gastro-oesophageal cancer development. We will use transgenic mouse models to look at the early role of p53 mutation in the development of upper GI metaplasia cancer. Secondly, we will investigate the cellular heterogeneity of BO using scRNA-sequencing of endoscopic biopsies of the upper GI tract using to define cell types with BO. Thirdly, to investigate the BO progenitor cell niche, develop Barrett's organoid cultures as an *in-vitro* experimental model. Lastly, to examine the embryological development of OSGs.

Chapter 2: Methods

2.1 Materials

2.1.1 Reagents

Alcian Blue

1% final solution of Alcian Blue 8G was prepared in 3% glacial acetic acid. Adjusted to pH2.5.

Citric acid buffer

10mM citric acid solution was prepared in water and the pH adjusted to 6.0 with NaOH.

DAPI staining solution

1000x stock solution of 10mg/ml was prepared by dissolving 4',6 Diamidino-2-phenylindole (DAPI) dihydrochloride hydrate in water and stored at -20°C in 10µl aliquots.

Digestion Solution

Biopsy digestion solution was prepared by mixing 1x phosphate buffered solution (Gibco™), 2mM EDTA, 100U/ml type I collagenase (Worthington Biochemical Company®), sodium phosphate (5.6mM), monopotassium phosphate (8mM), sodium chloride (96mM), potassium chloride (1.6mM), sucrose (44mM), D-Sorbitol (55mM) and Dl-Dithiotreitol (0.5mM).

DNA marker

100bp and 1kb DNA ladders were purchased from Bioline Reagents Ltd. And were used as size standards for agarose gel electrophoresis.

Ethidium Bromide

A 10mg/ml stock solution was prepared by dissolving 0.2g of ethidium bromide in 20ml of distilled water.

Freezing medium

50% FBS;45% DMEM; 5% DMSO; 1% Penicillin- Streptomycin (GIBCO). Stored at 4°C until mixed with cell suspension for freezing.

Lipotransfection reagents

Lipotransfections were performed with Fugene 6 (Roche), following the manufacturers recommendations.

Basal medium for organoid culture

Advanced DMEM/F12 (Invitrogen) + Penicillin/Streptomycin (1X, Invitrogen) + Glutamine (2mM, Invitrogen) + N2 supplement (1X, Invitrogen) + B27 (1X, Invitrogen) + N-acetylcysteine (1X, Sigma-aldrich) + HEPES (10mM, Invitrogen)

Human Organoid Media

Additives to Basal medium (final concentration, supplier):

R-spondin1 (1µg/ml, Peprotech) for duodenal and BO organoids

Noggin (100ng/ml, Peprotech) for duodenal and BO organoids

Wnt3A (100ng/ml, Peprotech) for duodenal and BO organoids

EGF (50ng/ml, Thermofisher PHG0311) for duodenal and BO organoids

Gastrin (10nM, Sigma G9145) for duodenal and BO organoids

Nicotinamide (10mM Sigma Aldrich N0636) for duodenal and BO organoids

A83-01, an ALK 4/5/7 inhibitor (Tocris 2939, 2µM for gastric organoids, 500nM for duodenal organoids)

SB202190, a p38 inhibitor (Sigma-Aldrich, 2µM for gastric organoids, 10µM for duodenal organoids)

FGF-10 (100ng/ml, Peprotech) added to BO organoid culture media alone.

Y-27632, ROCK inhibitor (10mM, Sigma Aldrich) added to medium during organoid culture initiation to avoid anoikis.

CHIR99021 (GSK3β Inhibitor) added to medium only at first passage during organoid culture initiation to support LGR5+ cell population (Sato, Stange et al. 2011, Lindeboom, van Voorthuijsen et al. 2018).

Para-formaldehyde (PFA) fixing solution

4% solution was prepared by first dissolving par-formaldehyde in water in the fume hood. 10X PBS was added until the final concentration of PBS was 1X. The pH was adjusted to 7.0 with 1M HCl and the solution was stored at -20℃.

Permeabilisation Solution for organoid staining

The solution was freshly prepared each time by dissolving 10% FBS and 0.5% Triton-X 100 in PBS. The solution was kept at 4℃ until required.

Phosphate Buffer Saline (PBS)

12mM NaCl

1mM Sodium dihydrogen phosphate (NaH_2PO_4)

1.6mM Disodium Dihydrogen phosphate (Na_2HPO_4)

The pH was adjusted to 7.0 and autoclaved.

Sorting buffer

Sorting buffer for used during FACS was prepared with 1x phosphate buffered solution (Gibco™), 2mM EDTA and heat inactivated 5% foetal bovine serum (Sigma-Aldrich®).

SuperScript® First Strand Synthesis System

Kit for cDNA production from RNA purchased from Invitrogen and stored at -20°C

2.1.2 Cell lines

Name	Tissue Type/ Origin
Caco-2	Human colon adenocarcinoma (mutant p53), Ludwig Institute for Cancer research, Oxford
HCT 116	Human colon adenocarcinoma (mutant RAS), Ludwig Institute for Cancer research, Oxford
LS180	Human colon adenocarcinoma, Wetherill Institute for Molecular Medicine, Oxford
OE33	Human oesophageal adenocarcinoma, ATCC
CP-A	Human Barrett's Oesophagus cell line (H-Tert immortalised), ATCC
MEF	Mouse embryonic fibroblasts, Ludwig Institute for Cancer research, Oxford

2.2 Tissue culture

Basic Media

Dulbecco's Modified Eagle Medium (DMEM) and RPMI 1640 medium was purchased from Gibco-BRL (UK) and stored at 4°C. For Organoid culture DMEM/F12 medium was used as the base medium

Media Supplements

Foetal calf serum (FCS) was purchases from PAA Laboratories and tested for its ability to sustain the growth of cell lines. The FCS was heat treated to inactivate protein activity for 30 minutes at 56℃ and stored at -20℃ in 50ml aliquots. L-Glutamine was purchased from Gibco-BRL at a 200mM concentration and frozen into 2.5ml aliquots for use at final concentration of 2mM. Penicillin / Streptomycin was purchased from Gibco-BRL at 10000 units/ml and again stored in 5ml aliquots at -20℃, used at a final concentration of 200 units/ml.

2.2.1 Culture of cell lines

All immortalised cell lines were cultured in complete medium supplemented with FCS, Penicillin/streptomycin and L-glutamine. Cells were incubated in flasks, dished or plates in an Heraeus® incubator at 37℃ in the presence of 10% CO_2. Culture medium was changed every 2 to 4 days depending on cell confluence and cell line requirements. Once confluent, cells were washed with 1x PBS and incubated with 1-5ml of Trypsin –EDTA (Gibco-BRL) depending on size of plate, dish or flask at 37℃ until cells detached. The trypsin was quenched by adding complete medium, the suspension was then centrifuged at 1200rpm for 5 minutes into a pellet and re-suspended in medium. A small suspension of cells was then added to a new flask with the appropriate amount of medium.

2.2.2 Storage of cells in liquid nitrogen

Cells were frozen once growth had reached 80% confluency. After trypsin treatment, cells were quenched with medium, centrifuged and supernatant discarded. The cell pellet was then re-suspended with freezing medium (described above) and cells were frozen in 1ml aliquots in Corning Cryogenic vials. Once vials were labelled, they were then cooled at a rate of 1℃ per minute, in a Nalgen Cryo 1℃ freezing container

placed in a -80℃ freezer for up to 72 hours before transfer in to a liquid nitrogen tank for long term storage. When freezing organoids/ primary cells organoids, basal culture medium was replaced with basal culture medium containing 5% DMSO. For freezing organoids from 5 wells were mechanically disrupted, centrifuged and re-suspended into 1ml volume and transferred into Cryogenic vials and cooled in a freezing container at 1℃ per minute in a -80℃ freezer for up to 72 hours before transfer to a liquid nitrogen tank for storage for up to 2 years.

To thaw cells from liquid nitrogen stock, vials were placed in a water bath at 37℃ for 2 minutes. Pre-warmed growth medium is then added to the cell suspension and the suspension is centrifuged at 1200rpm for 5 minutes to pellet the cells and remove the freezing medium in the supernatant. Cells are then re-suspended in warm growth-medium and transferred to a new flask and stored in the incubator overnight at 37℃. As routine newly thawed cells were given fresh growth medium 24 hours after thawing, once cells have attached to the flask. For recovery of organoids, vials are rapidly thawed in a 37℃ water bath and the freezing medium is then diluted in warm basal medium. Cells are then pelleted, re-suspended in matrigel and plated into a new dish, once matrigel has set after 15 minutes in a 37℃ incubator and covered in fresh warm basal culture medium.

2.2.3 Organotypic culture

Initially, collagen gels were created on ice by combining: 7 volumes of collagen type 1 (4mg/ml, Corning), 1 volume of 10x concentrated DMEM, 1 volume of FCS, 1 volume of mouse embryonic fibroblasts at a concentration in suspension of $1x10^6$ per ml. The 1ml of this mixture was pipetted into wells of a 24well plate and allowed to polymerise at 37℃ for 30 minutes. Following polymerisation of the collagen, 1ml of DMEM was added to each well to hydrate the collagen and nourish the MEFs

embedded within it. These 24well plates with the MEF containing collagen gels were cultured in the incubator at 37℃ Simultaneously, sterile 1.5 cm diameter nylon discs (100µm pore size; Tetko) were coated in the Type 1 collagen and polymerised at 37℃ in an incubator for 10 minutes, then fixed in glutaraldehyde for 1 hour at room temperature, washed thrice in sterile PBS and stored at 4℃. After 24hours in the incubator, the 24 well plates were removed from the incubator and $5x10^5$ keratinocytes (either primary cells or cell lines) were plated on top of the gels suspended in complete medium and placed back into the incubator. After 24 hours, the gels were removed from the wells, now with the keratinocytes attached to the top of the collagen gels. Each gel was placed on top of a collagen coated nylon disc which, in turn was placed on top of a sterile metal frame. These metal frames were made from stainless steel mesh cut and shaped to form a stand to sit in a 6 well plate and support the nylon discs and gels on. Once assembled, complete medium was pipetted into the bottom of the 6well plate this allowed nourishment of the keratinocytes in the culture to be from underneath rather than cells submerged in medium in traditional cell culture. This enabled cells to grow in an air fluid interface. Medium was changed every 48 hours. Once the 14 day culture had finished. The gels were fixed in paraformaldehyde and processed like pieces of tissue, embedded in wax and cut onto slides for histological analysis (Nyström, Thomas et al. 2005).

2.2.4 Human organoid culture

Biopsy fragments were washed in cold PBS until supernatant became clear. Tissue fragments were then incubated for 30mins on ice, in a dissociation buffer which is the digestion solution as above without the collagenase added. The tissue suspension is then centrifuged, supernatant discarded and tissue fragments are re-suspended in cold chelating buffer, and incubated on a roller at 4℃ for 15 minutes (Sato, Stange et al.

2011). Further mechanical dissociation was carried out by repetitive pipetting with a P1000 pipette with sequential resuspension and centrifugation up to 10 times. Large fragments were removed from the suspension. Isolated crypts were re-suspended in cold chelation buffer and centrifuged at 150-200g for 3 minutes to remove single cells and extracellular matrix fragments. Finally cells were re-suspended in fresh matrigel, plated, placed into a 37℃ incubator for 10 minutes then covered with basal culture medium.

Medium was changed every 48 hours and were passaged to remove dead cells every 7 days. When passaging the culture medium was replaced with fresh basal medium at 5℃. Organoids set within the matrigel droplets are mechanically disrupted using a P1000 micropipette. Further mechanical disruption was carried out by running the suspension in Eddendorf® tubes over a micro centrifuge tube rack causing agitation of the sample. Samples were then transferred into a new micro centrifuge tube. Keeping the sample cool enables liquefaction of the matrigel. Organoid suspensions are then centrifuged and re-suspended in fresh basal medium to wash the organoids. Then, the supernatant is discarded, the organoid/cell pellet is then re-suspended in fresh matrigel. The organoid matrigel mix is then plated onto glass bottom plates, put into a 37℃ incubator for 15 minutes before fresh, warmed medium covering the matrigel droplets, organoids are cultured in an Heraeus® incubator at 37℃ in the presence of 10% CO_2.

2.3 Human tissue

2.3.1 Biobanking

Patients attending routine endoscopic surveillance of BO and patients with mild reflux symptoms undergoing gastroscopy for diagnostic purposes gave informed consent and provided samples (South Central - Oxford C Research Ethics Committee: 09/H0606/5+5). Patient numbers were chosen to provide suitable biological replicates, and cells sequenced to provide balanced sample sizes at sequencing input. Paired quadrantic 2mm biopsies were obtained endoscopically using standard biopsy forceps (Radial Jaw 4 Standard Capacity, Boston Scientific, Natick, USA) from a central region of the BO segment avoiding the neo-SCJ as well as the oesophagogastric junction. Control samples were taken from the second part of the duodenum, the stomach 20mm distal to the gastro-oesophageal junction and the normal oesophageal squamous epithelium at least 20mm clear of the most proximal extent of BO. Samples were used for sequencing, immunohistochemistry or primary cell culture.

2.3.2 Preparation of single cells from endoscopic biopsies

Each sample was fragmented (**Figure 2.3.2**) and then pooled to ensure all sampling sites were represented in each investigative modality. Fragments pools were divided into three groups for histological verification, whole-tissue RNA-seq and scRNA-seq. Patients were selected based on their previously known pathological features Patients without BO described 0-2 reflux episodes per week with normal endoscopic appearances of the upper gastrointestinal tract on endoscopic examination, and no histological evidence of oesophagitis in the processed samples.

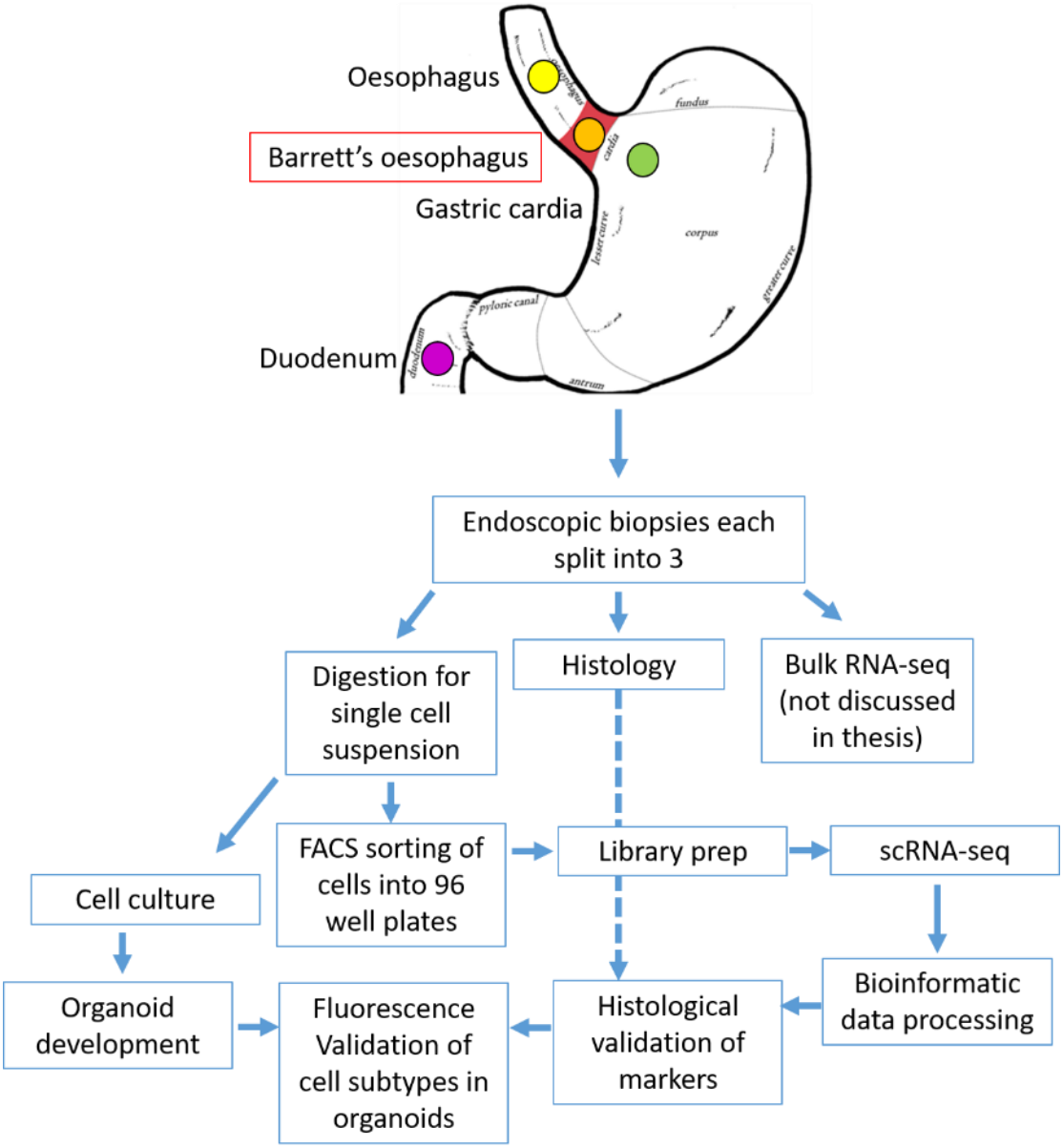


Figure 2.3.2 Diagram to show work flow from endoscopic biopsy to tissue validation.

2.3.3 Cell isolation for flow cytometry

Specimens were placed directly into a digestion solution and mixed at 4°C for 60 minutes on a falcon tube roller. Samples were then further triturated with scissors and a short period of vigorous pipetting. Large tissue pieces were allowed to settle and the cell-containing supernatant filtered (Sysmex Celltrics® 100 micron) into a 15ml Falcon tube. This process was repeated thrice and centrifuged at 1200rpm for 20

minutes at 4°C to create a cell pellet which was re-suspended in sorting buffer. A small amount of each sample was pooled for labelling controls. Pre-conjugated CD45-FITC (1:10, mouse monoclonal, cat. 130-080-202, Miltenyi Biotec) (Kurian, Sancho-Martinez et al. 2013) was used to label cells of haematological lineage and EpCAM-PE (1:10, mouse monoclonal, cat. 130-110-999, Miltenyi Biotec) was used to identifycells from epithelial lineages. Cell suspensions were incubated with antibodies then washed according to manufacturer's advice (Metsuyanim, Harari-Steinberg et al. 2009). DAPI (1:2000, Sigma-Aldrich®) was added to cell suspensions immediately prior to sort. FACS was carried out using a BD Biosciences FACS Aria IIIu platform with 70μm nozzle in the case of the first four patients and the additional squamous samples, and a Sony SH800S Cell Sorter with 100μm chip in the second batch of two patients. Cells were selected based on size and singlet gating to saturate cell output while minimising debris passed to subsequent gates. Size and singlet gating were then adjusted to capture of EpCAM+ cells, on the basis that these would represent a range of epithelial cells and minimise debris selection (Extended Data Figure 10a). Isolated cells were sorted directly into 96 well plates (Life Technologies™ MicroAmp® Optical 96-well Reaction Plate) pre-prepared with 2μl 0.2% Triton™ X-100 (Sigma-Aldrich®) and RNAase inhibitor (Takara Recombinant RNase Inhibitor) at 19:1 and then immediately frozen on dry ice. To confirm spectral accuracy and accuracy of gating, compensation bead controls and pooled cell suspensions were used for fluorescence-minus-one controls where possible. Each plate was re-permuted to avoid batch effects at the next stages of preparation, with no single plate containing cells from only a single patient or tissue type. Variable patterns of six blank wells were also prepared in each plate, 3 of which had a 10pg of brain total RNA (Agilent Technologies) added as a positive control. A single 100 cell pool was also sorted in

experiment using the Sony SH800S Cell Sorter to provide a bulk control as whole tissue RNA-seq was not performed in these patients. To check for bias in cell selection, index sorting was carried out in most experiments to analyse expression of antibodies in relation to tissue type and subsequent data quality.

2.3.4 sc-RNA-seq

Creation of sequencing libraries was outsourced to the Single cell Genomics team at the Wellcome Trust centre for Human Genetics (**Figure 2.3.2**) . Transcriptome libraries were prepared using a Biomek FX liquid handling instrument (Beckman Coulter) with a custom adaptation of the published smart-seq2 method (Picelli, Bjorklund et al. 2013, Picelli, Faridani et al. 2014), with minor modifications, and Nextera XT (Illumina®) methodology with custom, unique index primers after tagmentation and ERCC spike-in at a dilution of 1:100,000. Libraries were sequenced using the Illumina® HiSeq 4000 platform, aiming for $3.5x10^5$ reads per cell at 75bp paired end.

2.3.5 Sequencing data analysis

All sequencing data analysis (**Figure 2.3.2**) was carried out by Dr David Severson and Dr Richard Owen (Owen, White et al. 2018).

2.3.6 Foetal tissue samples

Human foetal upper GI samples samples are derived from two means. Some were part of a collaboration with a gift from Professors Steven Pollard and Richard Anderson at the University of Edinburgh (Lothian NHS health board REC number 08/S1101/1). We also received samples through the Human Developmental Biology Resource (HDBR) project number 200321 (London REC: 08/H0712/34+5 and Newcastle REC:

08/H0906/21+5). Samples were received either fresh frozen or formalin fixed and were processed accordingly.

2.4 Murine studies

2.4.1 Breeding

Mice were bred and housed in individually ventilated cages at the Wellcome Trust Centre for Human Genetics Functional Genomics Facility, University of Oxford. Procedures were carried out under the Home Office Animals for Scientific Procedures Act 1986 (Personal license: I3E51A8F2, Project license: 30/2862). Constitutive $p53^{R172H}$ mutant mice were generated and characterised by Guillermina Lozano (MD Anderson). (Lang, Iwakuma et al. 2004) They were backcrossed for nine generations onto the BALB/C genetic background. Constitutive ASPP2 Δexon3 mutant mice were made by Ingenious targeting laboratories, USA and have been previously characterised (Vives, Su et al. 2006). They have been back crossed for 9 generations onto the BALB/C genetic background. Conditional ASPP2 Δexon3 mutant mice ($ASPP2^{loxP/loxP}$), in which exon 3 is flanked by loxP sites, were crossed with Rosa26cre-ER^{T} mice to induce deletion of exon3 upon 4-hydroxytamoxifen treatment.(Sottocornola, Royer et al. 2010)

2.4.2 Genotyping

Ear biopsies were taken for genetic identification. Biopsies were digested overnight at $55^{O}C$ in 100ul of GNT extraction buffer and 7.8mg/ml of proteinase K (Qiagen). The digested biopsy was then boiled for 10 minutes at $97^{O}C$ and analysed using polymerase chain reaction (PCR). Agarose powder (Gibco BRL, UK) was weighed and dissolved in 1 x TAE buffer at an appropriate weight per volume ratio (w/v). The

mixture was heated in a microwave to dissolve the agarose, and the solution allowed to cool to 40℃. Ethidium bromide was added to a final concentration of 20µg/ml. The agarose solution was then poured into a casting tray with the required number of teeth on the comb for samples, gels were left to set at room temperature

2.4.3 Biliary reflux mouse model

Following weaning at 3 weeks old drinking water was replaced with 0.2% Sodium Deoxycholate at Ph7(Quante, Bhagat et al. 2012). Homozygotes p53r172h mice were treated for 12 weeks and heterozygote p53r172h mice were treated for 12, 24 and 36 weeks. Samples were collected and snap frozen in dry ice for further RNA and protein expression analysis. See results section for further details of method development and optimisation.

2.4.4 Necropsy, dissection, fixation and embedding

The stomachs and oesophagi from mice were dissected and washed in cold PBS to remove gastric contents. The tissue was kept in 10% formalin overnight and processed in ethanol and embedded in paraffin wax using a Leica automated device. Serial 5um tissue sections were cut and put on slides.

2.5 Histological methods

2.5.1 Haematoxylin and eosin staining

Slides were deparaffinised in Histoclear (National Diagnostics) and rehydrated through decreasing concentrations of ethanol to distilled water. Slides were submersed in haematoxylin for 2 minutes, then rinsed in water under a running tap to remove excess stain. Slides were immersed in 1% acid ethanol (1 single dip), then rinsed in tap water. At that point slides are immersed in Scotts' water (for bluing) for 30 seconds before rinsing again in tap water. Immersed in Eosin for 2 minutes, then

washed thoroughly in water bath under running tap for 2 minutes. Slides were dehydrated through increasing concentrations of ethanol and bathed in Histoclear before mounting.

2.5.2 Alcian blue staining

Slides were deparaffinised in Histoclear ™ and rehydrated through decreasing concentrations of ethanol to distilled water. The samples were stained with AB for 30 minutes, then washed under tap water for 2 minutes. Samples were counterstained in nuclear fast red counterstain for 5 minutes and washed for 1 in tap water. Slides were dehydrated through increasing concentrations of ethanol and bathed in Histoclear before mounting. All AB staining data was carried out in with technical and biological triplicates.

2.5.3 Immunohistochemistry

Slides were deparaffinised in Histoclear (National Diagnostics) and rehydrated through decreasing concentrations of ethanol to distilled water. Slides were immersed in 3% hydrogen peroxide in methanol to inactivate any endogenous peroxidases. Antigen retrieval was performed using pH6 buffered Sodium Citrate solution at >100 ^{O}C for 15 minutes. Slides were left to cool in the sodium citrate until they were cool enough to handle. Each section is encircled with wax and blocked with Image-iT® FX Signal Enhancer (Invitrogen) for 1 hour. Next, sections were incubated with primary antibody in Antibody Diluent (Invitrogen) for 16 hours at 4^{O}C. The slides were then washed 3 times for 5 minutes in PBS. Sections were then incubated with a biotinylated secondary antibody in Antibody Diluent for 1 hour at room temperature. Again the slides were washed in PBS, 3 times for 5 minutes in PBS. Sections were then incubated in avidin-biotin perioxidase solution (Vectastain Elite ABC Reagent, Vector Labs) for 15 minutes at room temperature. Slides were washed in PBS, 3 times

for 5 minutes. Each section is then incubated in Horseraddish Peroxidase substrate solution (DAB substrate kit, Vector Labs, 2.5ml ddH_2O with 1 drop of H2O2, 1 drop of buffer and 2 drops of DAB) for 10 minutes at room temperature. Slides were counterstained with haematoxylin for 12 seconds and washed in tap water to remove excess stain. Slides were dehydrated through increasing concentrations of ethanol and bathed in Histoclear before mounting with mounting medium (Vectamount, Vector Labs) and coverslips (22x50mm Cat No. 631-0138). All immunohistochemistry staining was carried out in with technical and biological triplicates unless otherwise stated.

2.5.4 Tissue/ cell immunofluorescence

Once deparaffinised and rehydrated through graded alcohols to water slides were immersed in sodium citrate buffer and boiled for 15 minutes. The rack of slides is then left in the buffer until they are cool enough to handle. Sections were encircled in wax and blocked with Image-iT® FX Signal Enhancer. Sections were incubated with primary antibody (**Table 1.1**) for 16 hours at 4^{O}C. Slides were then washed 3 times for 5 minutes in PBS. Secondary antibody and DAPI (nuclear stain; 1 in 5000) diluted in antibody diluent (Invitrogen) was then added to the sections and incubated at room temperature for 1 hour. Slides were again washed 3 times for 5 minutes each. Finally, slides are mounted using mowiol-glycerol based solution and coverslips. Slides were kept at 4^{O}C and protected from the light prior to imaging. All immunofluorescence staining data was carried out in with technical and biological triplicates.

If cells were being stained, cells were cultured on glass coverslips, then washed with PBS. Following this they were fixed for an hour at room temperature in PFA and washed thrice in PBS. Triton X was then used as antigen retrieval to permeabilised

the cells. The method then merges with the method above with use of Image-iT® FX Signal Enhancer to block non-specific antigen binding.

2.5.5 Table of primary antibodies used for staining

Primary Antibodies			
Antigen	**Source/ Product Code**	**Host**	**Dilution for staining**
iASPP (Notari, Hu et al. 2011)	Xin Lu LX049.3	Mouse	1:1000
ASPP2 (Vives, Su et al. 2006)	Xin Lu LX54.10	Mouse	1:500
β-catenin	Santa Cruz sc47779	Mouse	1:500
CDX2	Santa Cruz sc130716	Rabbit	1:500
Chromogranin A (Chang, Wang et al. 2014)	Abcam ab15160	Rabbit	1:500
COX2 (Hirokawa, Yip et al. 2014)	Santa Cruz sc1747	Goat	1:500
Cytokeratin 5 (Dedeić, Sutendra et al. 2018)	Covance PRB-160P	Mouse	1:1000
Cytokeratin 7 (Fransén-Pettersson, Duarte et al. 2016)	Abcam ab181598	Rabbit	1:4000
Cytokeratin 8 (Xu, Horrell et al. 2017)	Santa Cruz sc-101459	Mouse	1:250
Cytokeratin 14 (Dedeić, Sutendra et al. 2018)	Cambridge bioscience PRB-155P-100	Mouse	1:250
EpCAM	Miltenyi Biotec	Mouse	1:2000

(Sheridan, Kishimoto et al. 2006)	130-110-999		
ITLN1 (Greulich, Chen et al. 2013)	R&D systems AF4254	Sheep	1:500
Ki67 (Montoya, Amaya et al. 2017)	Abcam ab15589		
P63 (Lane and Benchimol 1990)	Santa Cruz sc25039	Goat	1:250
MUC2 (IHC) (Kosinsky, Wegwitz et al. 2015)	Santa Cruz sc15334	Rabbit	1:300
MUC2 (IF) (He, Zhang et al. 2013)	Abcam ab11197	Mouse	1:300
LEFTY1	Cell signalling/ D7E3G	Rabbit	1:1000
pNFκB (Mahoney, Cheung et al. 2008)	Cell signalling/ 3033S	Rabbit	1:500
OLFM4 (Sugimoto, Ohta et al. 2018)	Cell signalling/ 14369	Rabbit	1:200
SPINK4 (Wapenaar, Monsuur et al. 2007)	Sigma Aldrich/ HPA007286	Rabbit	1:500
TFF3 (Perera, Evans et al. 2015)	Sigma Aldrich/ WH0007033MI	Mouse	1:1000

2.5.6 Table of secondary antibodies used for staining

Secondary Antibodies			
Antibody Name	**Source**	**Host**	**Concentration**

Alexa Fluor® 488 Anti-Mouse IgG (H+L)	Invitrogen	Donkey	1:400
Alexa Fluor® 488 Anti-Rabbit IgG (H+L)	Invitrogen	Donkey	1:400
Alexa Fluor® 488 Anti-Goat IgG (H+L)	Invitrogen	Donkey	1:400
Alexa Fluor® 546 Anti-Mouse IgG (H+L)	Invitrogen	Donkey	1:400
Alexa Fluor® 546 Anti-Rabbit IgG (H+L)	Invitrogen	Donkey	1:400
Alexa Fluor® 647 Anti-Mouse IgG (H+L)	Invitrogen	Donkey	1:400
Alexa Fluor® 647 Anti-Rabbit IgG (H+L)	Invitrogen	Donkey	1:400
Biotinylated Anti-Mouse IgG	Vectorlabs	Goat	1:250
Biotinylated Anti-Rabbit IgG	Vectorlabs	Goat	1:250
Biotinylated Anti-Goat IgG	Vectorlabs	Donkey	1:250

2.5.7 Quantification of immunohistochemical staining H-score

For each section stained, three high-power fields (400×) were randomly selected for analysis. Immunoreactivity was quantified using the H-score system, which incorporates both the intensity of the specific staining and the percentage of positive cells. The relative intensity of specific staining was defined as not present (0), weak but detectable above control (1+), distinct (2+) and very strong (3+). The final score was the sum of the relative intensity of specific staining multiplied by the percentage of positive cells (making the highest total out of 300). The H-score analysis was carried out independently by two microscopists who were blinded to the final clinical diagnosis of all cases studied. A third team member would review the score when there was an inconsistency between the two microscopists (Budwit-Novotny, McCarty et al. 1986, Yang, Xiao et al. 2019).

2.5.8 RNA *in situ* hybridisation (RNAscope™)

The RNA probes for *LGR5* (Hs-LGR5-C2, cat no. 311021-C2) and *OLFM4* (HS-OLFM4-C1, cat no. 311041) probes were selected from the ACD RNAscope™ probe catalogue. In order to prepare the slides for RNAscope™ assay slides were baked at 60°C for 1 hour in dry oven. Warm probes in 40°C water bath for 10 minutes then

cool to room temperature (RT). Then deparaffinise sections in Histoclear™ 2x 5 minutes, then 100% Ethanol 2x 2 minutes at RT. Slides were then dried for 5 min in 60°C oven. Antigen retrieval was then carried out with RNAScope™ Hydrogen Peroxide for 10min at RT, then rinsed in distilled water 2x at RT. Slides were then boiled in target retrieval solution for 20 minutes. Slides were carefully removed and washed twice in distilled water, then in 100% ethanol and left to air dry at RT. Once dry, a hydrophoebic barrier was drawn around the tissue sections on each slide with the Immedge™ pen (Vector Laboratories Inc. Burlingame, CA, USA). Then air dried slides were placed in the HybEZ™ slide rack, sections were then just enough "Protease Plus" to cover and returned to the HybEZ™ oven, incubate at 40°C for 30 minutes. The slides were washed in distilled water twice, excess water was then tapped off and slides were returned to the HybEZ™ slide rack and 4-6 drops were added to each section depending of size and incubated at 40°C for 2 hours in the Hybez™ Oven. Slides were then washed twice in Wash Buffer 2 minutes at RT. Six consecutive intubation steps followed to hybridise pre-amplifier and amplify. The first three incubations with AMP 1- AMP 3 were incubated at 40℃. Treatment with AMP 1 was for 30 minutes, followed by AMP 2 for 30 minutes and AMP3 for 15 minutes and with 2 x 2 minute washes in wash buffer between each treatment at RT. Excess liquid was removed then slides were incubated with HRP-C1 for a further 15 minutes at 40℃. Following two 2 minute washes 1:2000 TSA Plus Fluorescein was added for 30min at 40°C. Two further 15 minute incubations at 40 ℃ were carried out with HRP Blocker and HRP-C2 respectively with two washes before, between and after. Next, diluted TSA Plus Cy3 and incubate 30min at 40°C followed by washes and an incubation with HRP blocker for 15 minutes at 40℃. Two further 2 minute washes were carried out with fresh wash buffer each time. Excess wash buffer was removed

from the slides and 1:2000 DAPI was added for a 30 second incubation at RT. Once excess DAPI has been removed Gold Antifade™ mounting medium and cover slips were added before the slides were dried overnight in the dark.

2.6 Molecular methods

2.6.1 Quantitative polymerase chain reaction (PCR)

RNA extracted from tissue following the manufacturer's instructions of the RNeasy Mini Kit with DNase I treatment (Qiagen). cDNA is prepared using SuperScript® III First-Strand Synthesis SuperMix (Life Technologies). RT-PCR was performed using the QuantiTect SYBR Green PCR kit (Qiagen) on the StepOnePlus™ Real-Time PCR System (Applied Biosystems) with the following cycle conditions: 15 min at 95°C, 40 cycles of 95°C for 15 seconds, 55°C for 30 seconds and 72°C for 1 minute. Relative mRNA abundances were normalised to endogenous B2 microglobulin mRNA. Shown qPCR results are analysed by the ΔΔCt-method as previously described with the threshold cycles being determined by the Applied Biosystems software. QPCR primers were all purchased from Qiagen specific to mouse RNA sequences. All graphs and statistical analyses for were conducted using at least three different mice (n=3). Differences were considered significant if $p \leq 0.05$. The T-test was used to calculate the statistical significance between two groups of data. Analysis was carried out in GraphPad Prism 8.

2.6.2 Table of QPCR primers

Gene	**Primer sequence**
IL-1β (mouse)	F 5'-CCTTCCAGGATGAGGACATGA- 3' R 5'-TGAGTCACAGAGGA TGGGCTC- 3'
IL-6 (mouse)	F 5'-TACCACTTCACAAGTCGGAGGC- 3'

	R 5’-CTGCAAGTGCATCATCGTTGTTC- 3’
IL-10 (mouse)	F 5’-AAGGCAGTGGAGCAGGTGAA- 3’ R 5’-CCAGCAGACTCAATACACAC- 3’
B2M (mouse)	F 5’-ACAGTTCCACCCGCCTCACATT- 3’ R 5’-TAGAAAGACCAGTCCTTGCTGAAG-3’
SPINK4 (Human)	F 5’-TGCCAGTGGCAGCAGGAAAGC-3’ R 5’-CCAAGCAGAGCTGGCATTCATTC-3’
ITLN1 (Human)	F 5’-GGACCTGTTCTTCGTCTCCATC-3’ R 5’-GGTCATGTCACAGAAGGTCTGG-3’
MUC2 (Human)	F 5’-ACTCTCCACACCCAGCATCATC-3’ R 5’- GTGTCTCCGTATGTGCCGTTGT-3’
B2M (Human)	F 5’-CCACTGAAAAAGATGAGTATGCCT-3’ R 5’-CCAATCCAAATGCGGCATCTTCA-3’

2.6.3 Expression plasmid transfection

Cell transfection was carried out using Fugene 6 transfection agent as a DNA-lipid carrier and used according to the manufacturer’s protocol. After 24 hours of transfection, cells were used for different experiments. Human SPINK4 Gene ORF cDNA clone expression plasmid (Abclonal, HG11669-UT). Human ITLN1 Gene ORF cDNA clone expression plasmid (Abclonal, HG13038-UT). Human LEFTY1 Gene ORF cDNA clone expression plasmid (Abclonal, HG11877-UT).

Chapter 3: Results – Developing a transgenic/ biliary reflux model to examine Gastric carcinogenesis

3.1 Introduction

In vivo models systems are critical for understanding the development, progression and treatment options for disease. Rodent models particularly murine models are commonly utilised due to their small size, ease of housing, short gestation and generational turnover. However, mouse models of BO, OAC and GOJ junctional cancers require careful interpretation not least because of the absence of OSGs, a key candidate for the potential cell of origin of BO. Additionally the mid-stomach site of the SCJ and inability for rodents to vomit means that refluxate will never bathe the SCJ in a way that mimics human GORD. The forerunning murine model of BO utilises a combined transgenic and environmental strategy. Mice were bred with overexpression of inflammatory cytokine Il-1β in squamous Krt14 expressing epithelium. Once weaned, these mice consume deoxycholic acid (DCA) to induce

IM and histological features of the intestine are common features of BO, OAC and GAC. Interestingly, The Cancer Genome Atlas consortium found a strong correlation between *P53* mutations, chromosomal instability and intestinal histology (Bass, Thorsson et al. 2014). Up to 30% of non-dysplastic BO (NDBO) has been shown to have p53 mutations.(Kastelein, Biermann et al. 2013, Redston, Noffsinger et al. 2022) P53 mutations in NDBO have been shown to help predict progression to cancer. (Redston, Noffsinger et al. 2022) Prevalence of P53 mutations increases in dysplasia and cancer. It is possible that early *P53* mutation may potentiate IM and cancer development by increasing localised inflammation. Mutant *P53* has also been shown to facilitate somatic cell reprogramming both *in vitro* and *in vivo* during

tumorigenesis. Wang et al. have shown that GIM develops in the absence of P63 expression and P63 is critical for the development of all stratified epithelium, particularly squamous epithelium (Yang, Schweitzer et al. 1999, Wang, Ouyang et al. 2011). Since mutant P53 has been shown to bind P63 and abrogate its transcriptional activity, early P53 mutation in squamous oesophagus or gastric glandular epithelium may inhibit P63 activity, drive inflammation and alter P63 driven squamous differentiation initiating IM (Melino 2011).

3.1.1 The P53 family

The P53 family are tumour suppressors, and co-ordinators apoptotic function. The function of P53 varies depending on context; it can act directly as a transcription factor or bind in complexes that initiate signalling cascades (Cheok, Verma et al. 2011). In the cellular stress response to ultra-violet irradiation, hypoxia and DNA damaging events etc. post-translational modifications of P53 are induced, exposing P53's DNA binding domain permitting binding to DNA response elements and allowing transcription of target genes (Renzing, Hansen et al. 1996). Whilst P53 transcription rate is constant in cells, activity is inhibited through interactions with MDM2 (the murine double minute oncogene), which then identifies P53 for polyubiquitination and degradation (BoÈttger, BoÈttger et al. 1999). Other members of the P53 family include P63 and P73. In addition to their tumour suppressive roles they also have important developmental roles with P63 a key player in epithelial development and P73 essential in the developing central nervous system, immune system and germ cell production (Deyoung and Ellisen 2007). Splice variants exist for all three family members. Evading cell death is a critical step in the development of all tumours (Hanahan and Weinberg 2011). Aberrant P53 function has been found in almost all cancers. Mutation rate of P53 varies wisely between tumour types, effecting

approximately 50% of head and neck tumours, 30% of breast tumour and 5% of leukaemias (Muller and Vousden 2013). Gastrointestinal cancers have a particularly high rate with approximately 40% possessing somatic P53 mutations (Dulak, Schumacher et al. 2012). In other tumours with lower mutation rates the P53 pathway is often affected through alterations in P53 regulation.

3.1.2 P53 mutation in upper GI cancer

The importance of IM in the upper GI tract as being a marker of cancer risk is uncertain. IM of the gastric cardia is a phenomenon seen in humans, with endoscopic studies have demonstrating that in many adult humans it occurs and spontaneously resolves, indeed this may be a normal process within the human gastric cardia. IM is a feature of malignancy progression in gastric adenocarcinoma and is closely linked to *H.pylori* infection and associated chronic inflammation. Furthermore, these studies have also demonstrated a link between, *P53* mutations, chromosomal instability and gastric and oesophageal cancers with an intestinal phenotype (Bass, Thorsson et al. 2014). Studies have demonstrated that *P53* mutations may occur early in the development of OAC/GAC (Stachler, Taylor-Weiner et al. 2015). Non-dysplastic segments of BO from patients who do not show any further neoplastic progression display a mutational profile distinct to those of who go on to develop malignancy. 30% of patients with NDBO have *P53* mutations (Redston, Noffsinger et al. 2022). In a recent retrospective examination of NDBO biopsies from these patients who are known to develop dysplasia has shown that 60% had *P53* mutations in their NDBO (Redston, Noffsinger et al. 2022). In some cases, an early *P53* mutation in premalignant metaplasia can lead to a whole genome doubling and a more rapid accumulation of mutational burden and genetic instability predisposing to cancers.

Samples from patients with IM show more frequent copy number alterations in respective cancer genes compared to samples from metaplasia without goblet cells (Stachler, Taylor-Weiner et al. 2015, Stachler, Camarda et al. 2018). **Figure 3.1.2** summarises the *P53* mutations published by the cancer genome atlas research network (Cancer Genome Atlas Research, Analysis Working Group: Asan et al. 2017). Interestingly $P53^{R175H}$ mutation which occurred in 8% of human OACs is analogous to the $p53^{R172H}$ mice studied above, both with point mutations causing an arginine to histidine substitution. In addition to our histological observations, this suggests that the $p53^{R172H}$ mutant mouse model has the potential to be relevant in the development of a murine model of oesophago-gastric cancer.

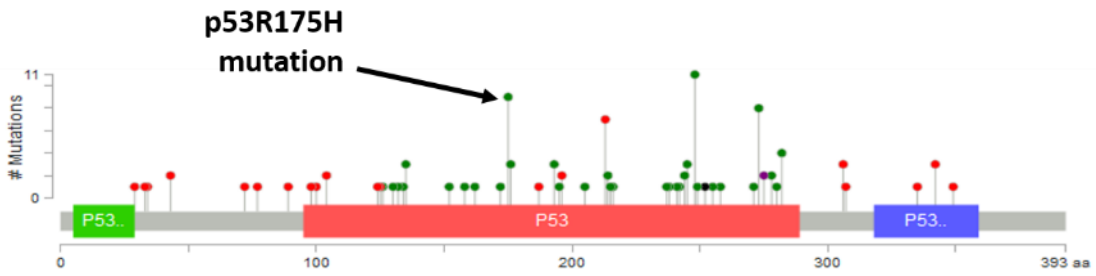


Figure 3.1.2 *P53* mutation pattern in OAC.

A diagram to demonstrate the range P53 mutations seen in TCGA OAC sequencing data (n=72). The black arrow demonstrates R175H mutation occurring in 8% of human OACs. (The Cancer Genome Atlas Research Network, 2017)

The $P53^{R175H}$ mutation in human cancers has been shown to lead to loss of *P53* function as a tumour suppressor but also can have gain of function properties. Gain of function properties of $P53^{R175H}$ include: promoting genomic instability promoting de-differentiation & promoting stemness; modulation of microenvironment signalling; promoting inflammatory signalling (Adorno, Cordenonsi et al. 2009, Liu, Song et al. 2010, Cooks, Pateras et al. 2013, Ubertini, Norelli et al. 2015, Solomon, Dinowitz et

al. 2018). Although *p53*^{R172H} mice are known to have a different tumour profile compared with *p53* null mice (due to them having a higher incidence of carcinomas compared with *p53* null mice) these mice are not known to develop gastrointestinal malignancies.

3.1.3 The ASPP family

The ASPP family of proteins named for their structural similarities with an ankyrin rich region, an SH3 domain and a proline rich region (Sullivan and Lu 2007). The members consist of ASPP1 and ASPP2, which are pro-apoptotic through selectively promoting the binding of p53 to pro-apoptotic gene targets: PUMA, BAX and PIG (Samuels-Lev, O'Connor et al. 2001, Vives, Su et al. 2006). In contrast iASPP, an inhibitory protein, exerts its anti-apoptotic effect by binding p53 and preventing p53 binding to pro-apoptotic promoters. In GAC, *H.pylori* derived oncoprotein cagA has been shown to directly interact with the p53 pathway by targeting the tumour suppressor ASPP2 (Buti, Spooner et al. 2011). Loss of ASPP2 can lead to tumourigenesis through interacting with either p53 or p63 (Vives, Su et al. 2006, Tordella, Koch et al. 2013). Additionally ASPP2 has P53-independent activity; it is required at tight junctions with Par3 to regulate epithelial cell polarity (Sottocornola, Royer et al. 2010). Loss of junctional ASPP2 has been shown to allow activation zeb1 mediated epithelial mesenchymal transformation via β-catenin (Wang, Bu et al. 2014).

Overall, the P53 pathway is highly altered in the development of OAC and GAC. Both P53 and ASPP are known to interact with proteins implicated in the development of upper GI adenocarcinomas. Further examination of the cellular role of P53 and ASPP proteins in this context may lead to a better understanding of P53

biology and may be useful clinically for highlighting patients at risk of malignant progression earlier.

3.2 ASPP expression in the upper GI tract

To investigate the level of expression of iASPP and ASPP2 proteins in the upper GI tract immunohistochemical staining was carried out on bio-banked human samples donated by patients. Five samples were stained from each site: the oesophagus, stomach and OAC specimens from oesophagostomy resection. Additionally, endoscopic biopsies of non-dysplastic BO were stained at the same time. Staining was carried out in technical triplicates were carried out so that an accurate representation of the staining pattern was determined, **Figure 3.2** demonstrates representative images of the iASPP and ASPP2 expression patterns. Staining was conducted on samples from three patients for each tissue type.

In squamous oesophageal epithelium, iASPP and ASPP2 were expressed at low levels in the basal layer of the epithelium in all samples (**Figure 3.2**). In gastric glandular epithelium, iASPP staining was strong in all patient specimens with strongest expression seen in gastric glands, particularly chief cells. ASPP2 was expressed moderately in chief cells and epithelial cells lining the gastric glands (**Figure 3.2**). In BO and OAC tissue, very low level of iASPP expression was detected: no iASPP staining was detected seen in the epithelial or neoplastic cells in BO or OAC, with positive staining in BO and OAC was localised to immune cells beneath the epithelium. There was no evidence of ASPP2 expression in either OAC or BO. Formalin fixed, paraffin-embedded, WT and *iASPP*/ *ASPP2* knock-out murine skin were used as staining controls (**Figure 3.2**).

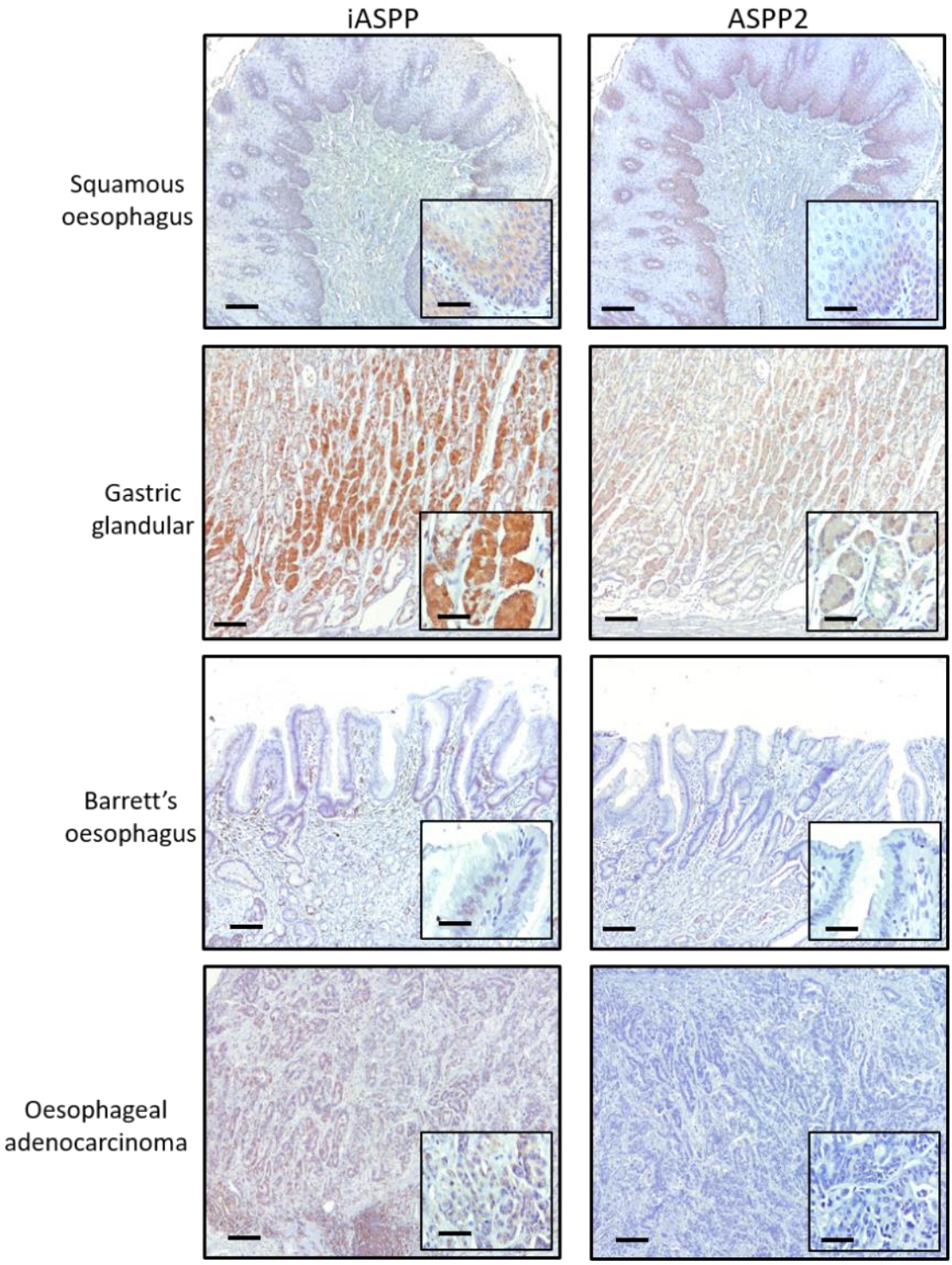


Figure 3.2 Immunohistochemical staining of iASPP and ASPP2 in the human upper GI tract. Immunohistochemical staining for iASPP and ASPP2 in human normal squamous oesophagus, normal gastric mucosa, BO and OAC. Scale bars in the larger zoomed out images are 200um, scale bars of the zoomed in insert images is 25um.

3.3 Investigating an upper GI phenotype of iASPP and ASPP2 transgenic mice

As previously discussed there are key differences in the anatomy and normal histology of the upper GI tract between mice and humans as depicted in the diagram in **Figure 1.1.** Archived stomach specimens of *iASPP* and *ASPP2* transgenic mice (Wild type, constitutively heterozygous or constitutively knocked out) with aged between 40 and 60 weeks were examined for any evidence of a gastric phenotype. Haematoxylin and Eosin staining was carried out on five slides from each stomach with five mice of each genotype were examined. Light microscopy analysis of staining patterns was undertaken with a trained histopathologist, who examine histologically distinguishable cell populations in each stomach looking for any gross changes. In particular, we examined specimens for any evidence of IM or neo-columnarisation of the squamous fore-stomach or evidence of IM within the columnar hind stomach (see **Figure 3.3**). No gross phenotypic differences were demonstrated.

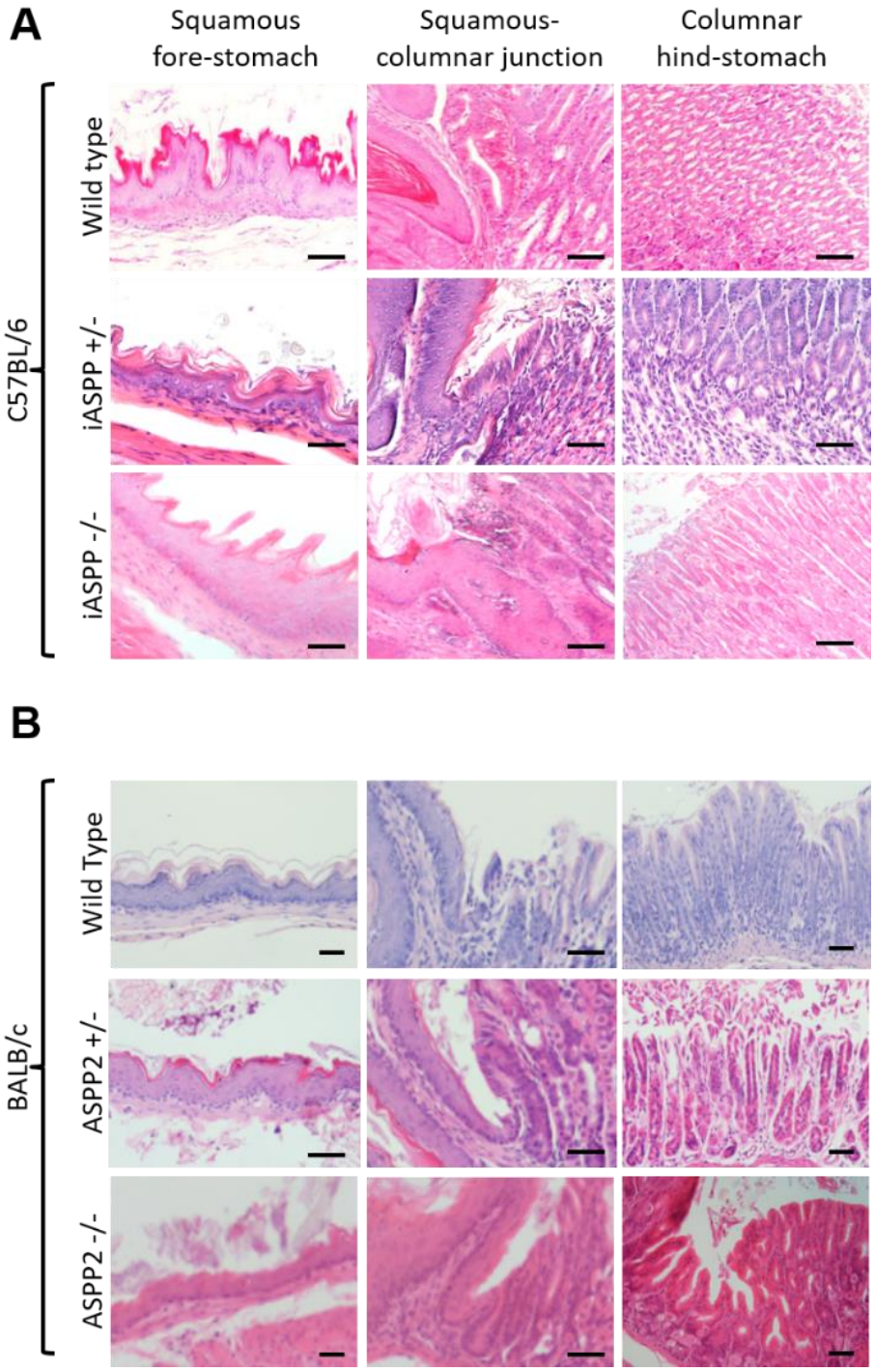


Figure 3.3 Haematoxylin and eosin staining of iASPP and ASPP2 knock out mice.

A) Wild type, *iASPP* heterozygous (+/-) and *iASPP* knock out (-/-) mice on a C57BL/6 background were examined for a gastric phenotype. The squamous fore-stomach, the squamous columnar junction and the columnar hind stomach were examined. Scale bars are 50um

B) Wild type, *ASPP2* heterozygous (+/-) and *ASPP2* knock out (-/-) mice on a BALB/C background were examined for a gastric phenotype. Scale bars are 50um

3.4 Investigating an upper GI phenotype of P53 transgenic mice

Stomach sections of *p53* transgenic mice were also examined (**Figure 3.4**). Whilst wild type and *p53* heterozygous mice were at a similar age to the *iASPP/ASPP2* transgenic mice. *p53* null mice examined however, were by necessity younger ranging from between 16 and 25 weeks old as the majority for *p53* null mice develop malignancy and died before 25 weeks old. As has been previously demonstrated by other groups *p53* heterozygous and null mice were found to have hyperplasia of the gastric glands. However, there was no evidence of aberrant cell differentiation, IM, and no evidence of malignancy (**Figure 3.4**). Staining was carried out on five slides from each stomach five mice of each genotype were examined.

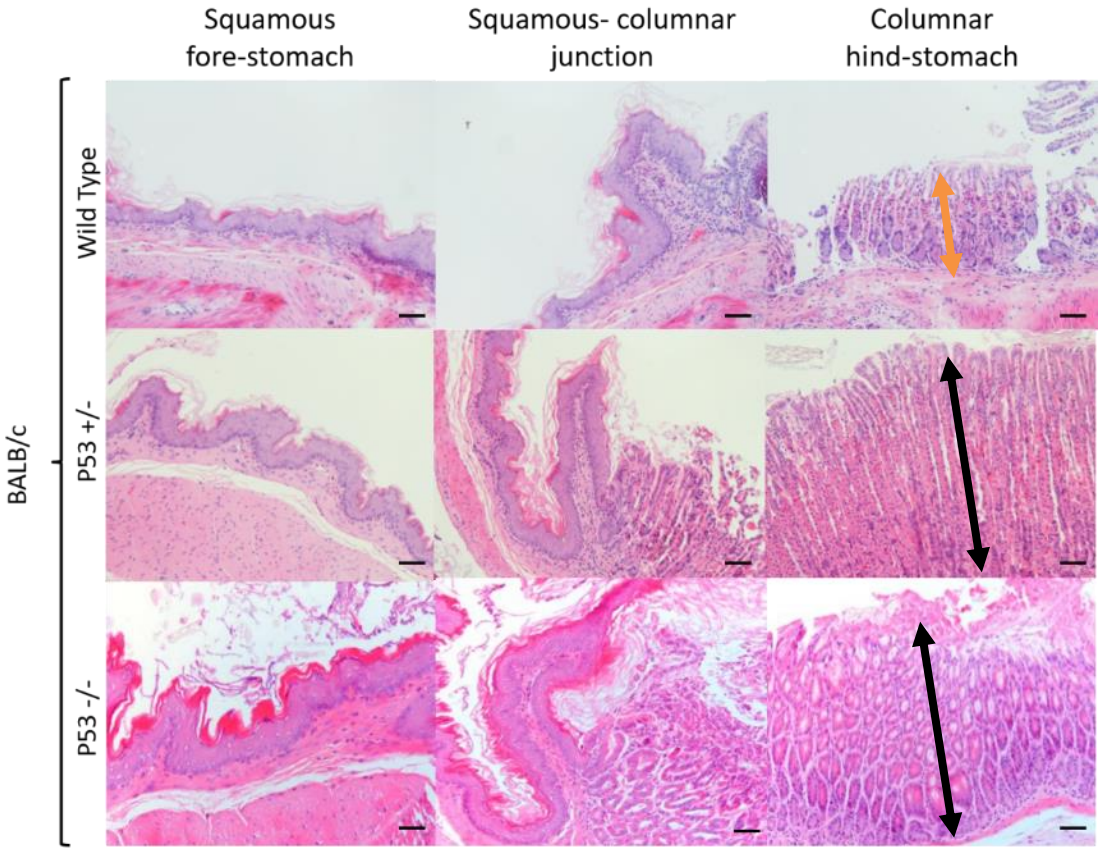


Figure 3.4 Haematoxylin and eosin staining of *p53* transgenic mice.

Wild type, *p53* heterozygous (+/-) and *p53* null (-/-) mice on a C57BL/6 background were examined for a gastric phenotype. The squamous fore-stomach, the squamous columnar junction and the columnar hind stomach were examined. The black arrows demonstrate the depth of gastric glands in the *p53* heterozygous and knock out mice compared to the depth of wild type mice gastric glands as shown by the orange arrow. Scale bars are 30um.

3.5 *p53^{R172H}* mice have increased incidence of carcinomas

Constitutively transgenic *p53^{R172H}* mutant mice had been observed by other laboratory members to have a higher proportion of tumours derived from an epithelial origin (carcinomas) compared with the tumour spectrum seen in *p53* null mice. Both the null and p53R172H mutant mice are used as models of human Li-Fraumeni syndrome, as such the predominant malignancies they develop are lymphomas and sarcomas (Jacks, Remington et al. 1994). **Figure 3.5A** demonstrates the tumour spectrum demonstrated by our cohort of *p53^{R172H}* mice on a BALB/C genetic background. Indeed as demonstrated by the graph approximately 40% of the *p53^{R172H}* heterozygous mice developed carcinomas compared to none observed in the wild type or *p53^{R172H}* homozygous mutant mice. The variation between tumour profiles is likely to be due to difference in survival of the mutant homozygous and heterozygous mice. *p53^{R172H}* homozygous mice have a maximum survival of approximately 26 weeks compared to up to a median of 90 weeks in the *p53^{R172H}* heterozygous mutants. The prolonged survival probably allows more time for carcinomas to develop. Despite the increased incidence of carcinomas these mice have not been reported to have any specific gastrointestinal phenotype. Overall, 16 WT, 22 *p53^{R172H}* Heterozygotes and 20 *p53^{R172H}* homozygotes were included in this analysis.

From the achived murine specimens from the *p53*^{R172H} cohort one gastric adenocarcinoma was found. **Figure 3.5B** Demonstrates a large gastric adenocarcinoma observed in the historical cohort of these mice. The tumour has obliterated the lumen of both the stomach and oesophagus and demonstrates the appearance of a columnar lined epithelium of the oesophagus and fore-stomach shown by H&E staining **(Figure 3.5C & F).** With distinct absence of squamous markers staining for cytokeratin 14 (Krt14; magenta) and p63 (green) and presence of columnar marker cytokeratin 8 (Krt8; yellow) (**Figure 3.5 H & I).** Additionally there is evidence of dysplasia in the gastric fundus (**Figure 3.5D**), dysplasia within the gastric glands (**Figure 3.5E**) and foci of malignant invasion (**Figure 3.5G**).

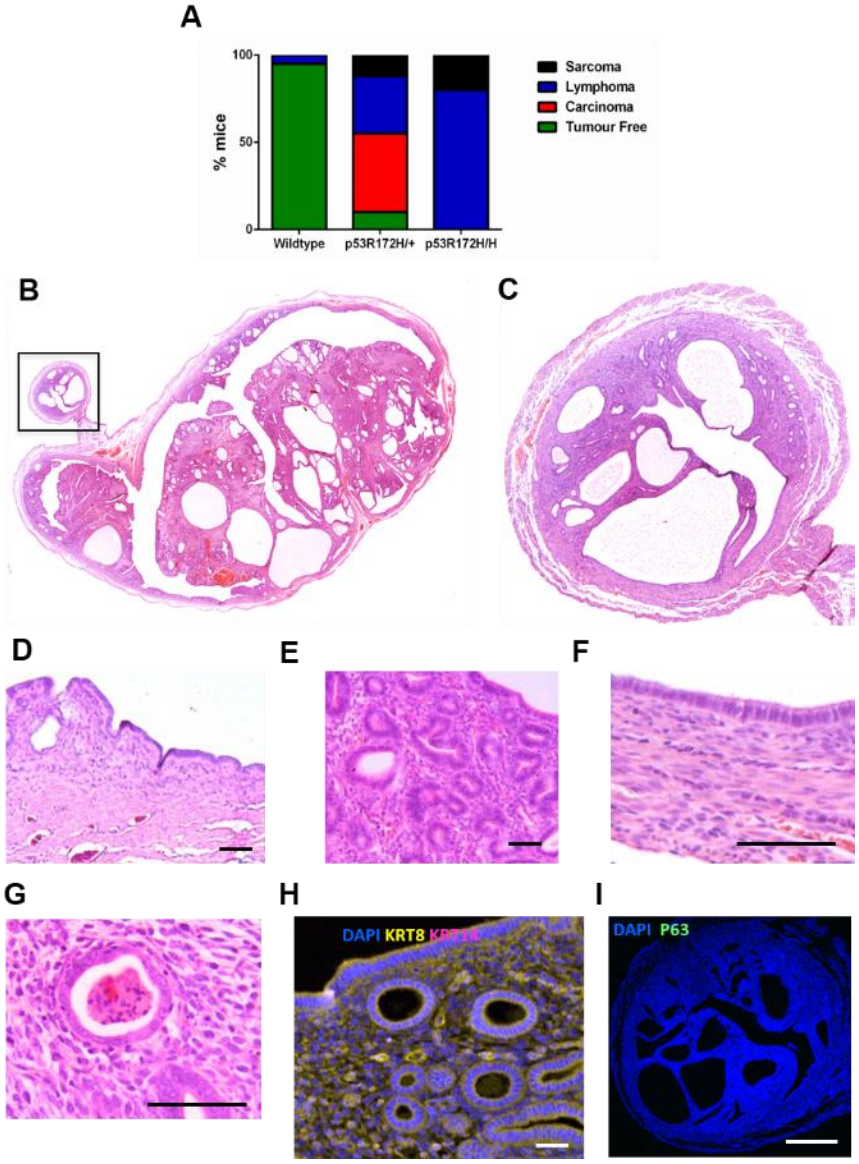


Figure 3.5 Tumour spectrum seen in *p53*^{R172H} mice including one example of a gastric adenocarcinoma.

A) Graph to demonstrate the tumour spectrum observed in *p53*^{R172H} mutant mice using historical lab archive data.

B) H&E stained whole section image of a gastric adenocarcinoma observed in 60-week-old *p53*^{R172H} mouse with extensive disease throughout the stomach and distal oesophagus (delineated by black box) obstructing the gastric and oesophageal lumens.

C) H&E stained magnified image from (**B**) of *p53*^{R172H} mouse oesophagus demonstrating a near completely obliterated oesophageal lumen.

D) H&E staining demonstrating columnarisation and dysplasia at the site of the squamous columnar junction. Scale bar in 50um.

E) H&E Staining demonstrating dysplasia in the gastric glands. Scale bar is 50um.

F) H&E staining demonstrates columnar epithelial lining of the *p53*^{R172H} murine oesophagus. Scale bar 100um.

G) Demonstration of an invasive focus within the murine gastric adenocarcinoma. Scale bar 100um.

H) Immunofluorescence staining of columnar marker Cytokeratin 8 (Krt8; yellow), Cytokeratin 14 (Krt14; magenta) and DAPI (blue) at the gastric fundus demonstrating an absence of Krt14 staining.

I) Immunofluorescence staining of p63 (green) and DAPI (blue) in the mouse oesophagus. Scale bar 500um.

3.6 *p53^{R172H}* mice demonstrate some evidence of IM

In order to examine for more subtle evidence of early of developing gastric malignancy in the *p53^{R172H}* mice five *p53^{R172H}* mice with an aged between 40-60 weeks old underwent necropsy. This identified sarcoma, skin carcinoma, mesothelioma and two with lymphomas. However, the mice they had no overt macroscopic gastrointestinal pathology compared to five age-matched wild type mice. Next we conducted a detailed histological assessment including Alcian blue/ periodic acid schiff staining (AB/PAS), which determines between acidic pH and neutral pH mucins: neutral mucins such as those natively expressed in gastric secretory cells appear magenta, acidic mucins native to goblet cells in colonic epithelium are stained blue. Of the five *p53$^{R172H/+}$* mice examined, three mice had foci suspicious for goblet cell differentiation with postive AB staining. Of those, two mice had positive AB staining in the gastric columnar epithelium adjacent to the SCJ (which will be refered to as gastric cardia) and one had AB staining in the gastric antrum (the black arrows in **Figure 3.6A** demonstrate magenta stained pH neutral mucins; The black arrows in **Figure 3.6B** demonstrate blue stained acid mucins)).

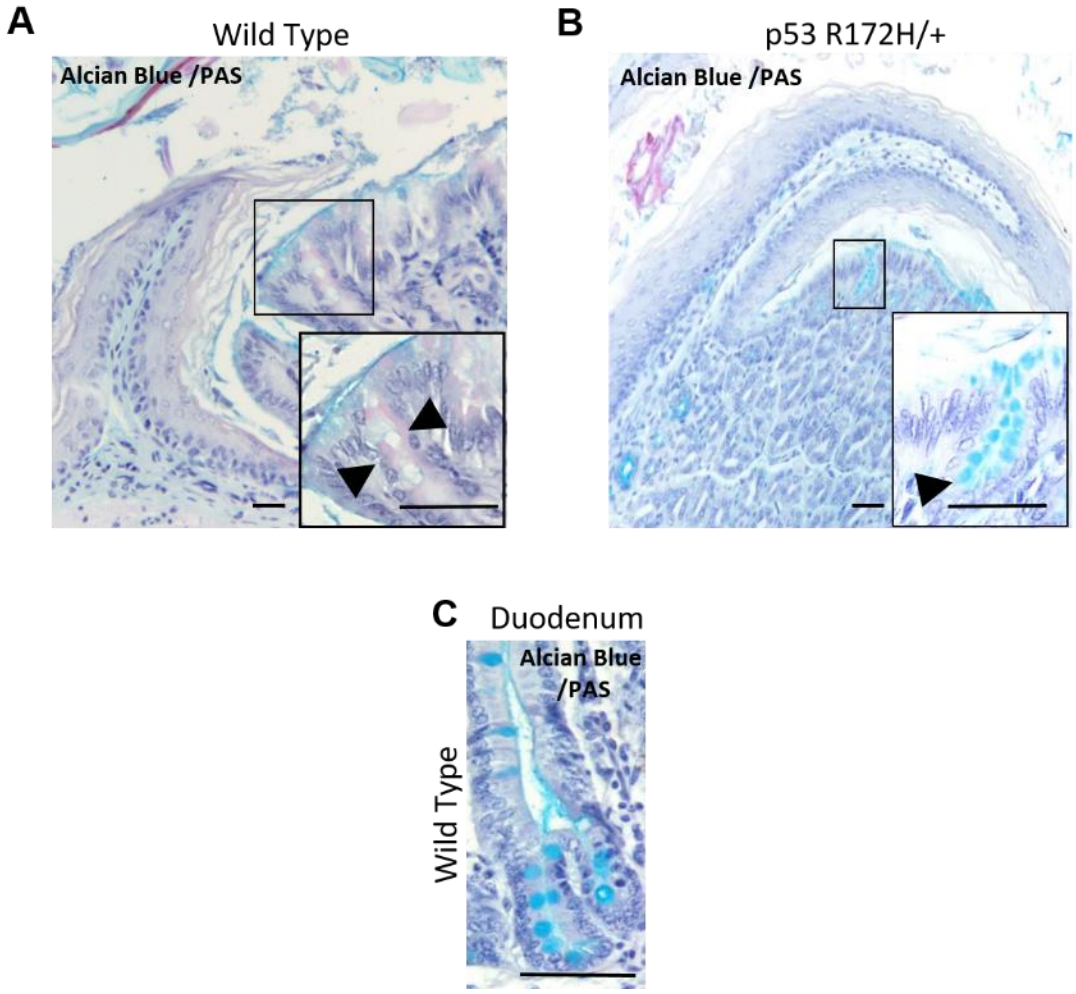


Figure 3.6 AB/ PAS staining of *p53*^{R172H} transgenic mice.

A) Wild type murine squamous-columnar junction on a BALB/C background stained AB/ PAS. The Insert image and arrows demonstrate magenta stain mucin secreting cells stained by PAS, in the absence of AB staining. Scale bars are 50µm.

B) *p53*$^{R172H/+}$ murine SCJ on a BALB/C background stained for H&E and AB/ PAS. Magnified insert image of crypt-like structure with positive AB. Scale bars are 50µm.

C) AB staining of murine duodenum used as a positive control to demonstrate the staining pattern of native goblet cells.

3.7 *p53*$^{R172H/+}$ express Muc2 in their stomachs

Further specific immunohistochemical staining was carried out on these five mice to examine the expression of Mucin 2 (MUC2) and Caudal Homeobox gene 2 (CDX2). Expression of MUC2, an intestinal specific mucin would suggest incomplete IM, whereas CDX2 would suggest complete IM (**Figure 3.7**). BO sections were used as a positive control for the expression of MUC2 and CDX2. Three out of five *p53*^{R172H} mice were found to have foci of Muc2+ staining in their stomachs in the same staining pattern as seen on the positive staining control BO specimen, compared with one mouse out of five wild type mice examined. Studies examining the P53^{R172H} mice have demonstrated that this mutation is linked with a gain of function when directly compared to *p53* null mice. This may therefore suggest a link between *P53* mutation and gastric goblet cell development/ IM.

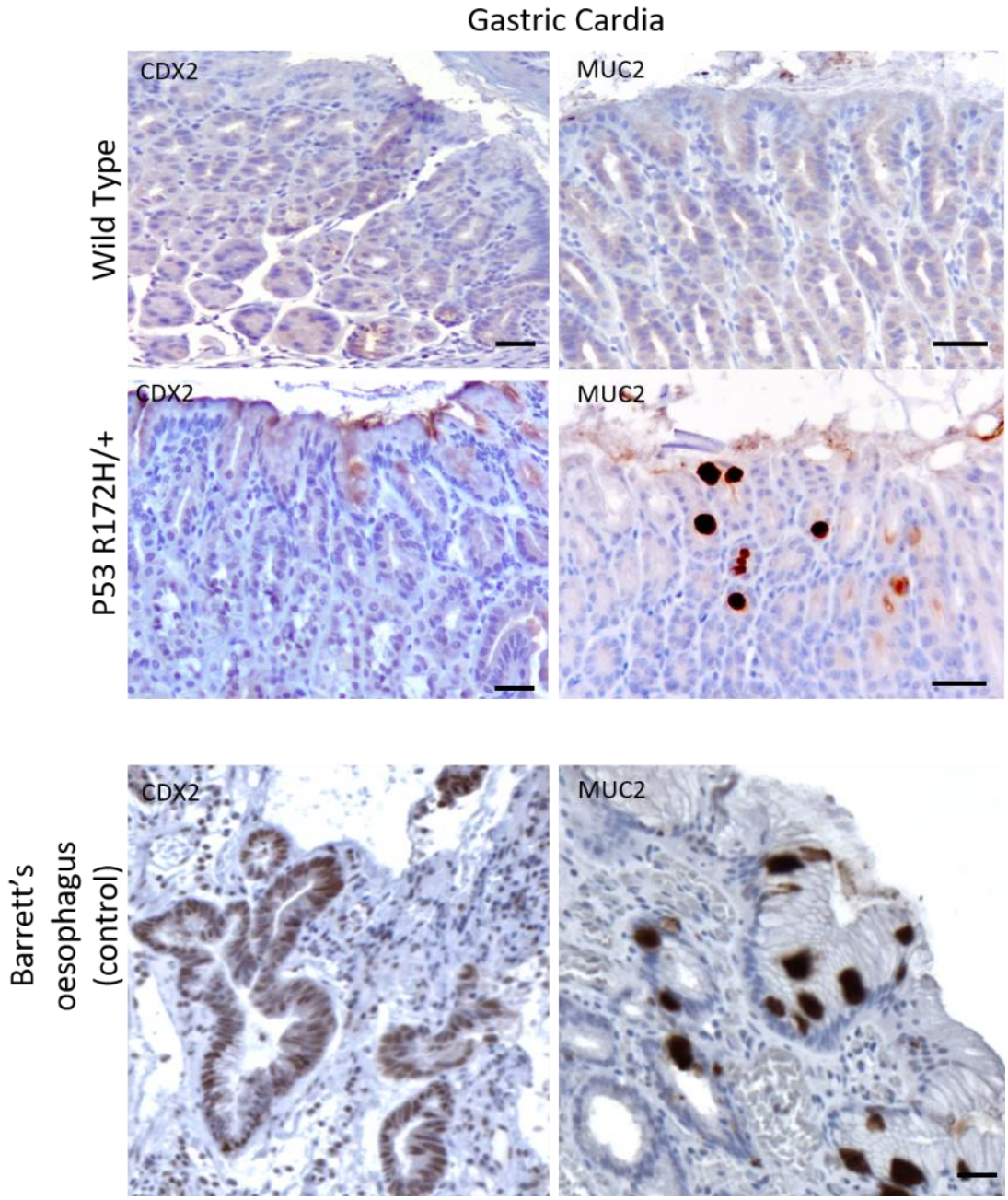


Figure 3.7 Immunohistochemical staining of *p53*^{R172H} transgenic mouse stomachs for MUC2 and CDX2.

Wild type and *p53*^{R172H} mouse stomachs were stained for CDX2 and MUC2. Scale bars 50µm. BO used as positive control for staining, scale bars 50µm

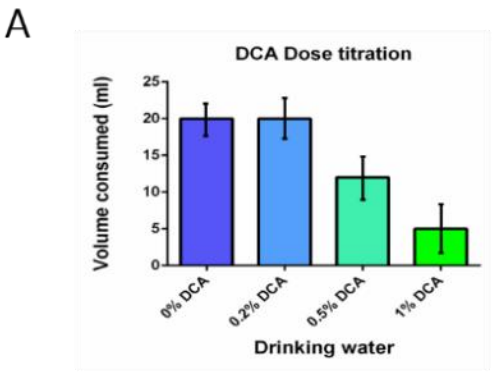
3.8 Examining the potential role for early *p53* mutation in GOJ cancers with biliary reflux model

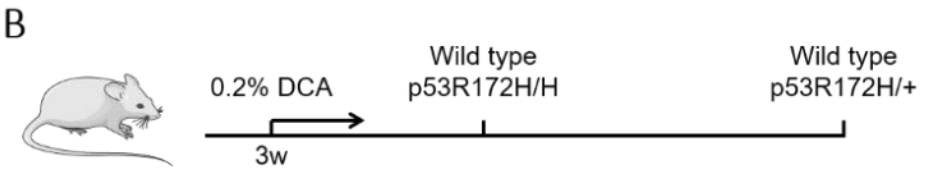
In order to examine if $p53^{R172H}$ mutant mice could develop gastric adenocarcinoma when expose to chronic biliary reflux a model was developed. First, a dose titration of deoxycholic acid in drinking water was carried out to ensure that the dose chosen did not lead to a dehydration or deconditioning of the mice (**Figure 3.8A)**. Mice treated with 0.5% or 1% DCA became acutely unwell within 2 weeks of treatment and therefore sacrificed, whereas those on 0.2% DCA appeared similar to control. This evidence suggested that 0.2% DCA treatment was optimal to create a chronic biliary reflux model as was also used in a previous study that used DCA, but not induce premature illness. Consequently, weaned mice were given 0.2% DCA in drinking water exclusively for the duration of the experiment (summarised in **Figure 3.8B**). After 52 weeks of treatment mice were sacrificed, underwent necropsy examined for epithelial changes to their upper GI tracts. (**Figure 3.8C**). From the overall cohort, 41 $p53^{R172H/+}$ mice underwent necropsy, we found no macroscopic evidence of inflammation or tumours in the stomachs of heterozygous $p53^{R172H/+}$ mice compared to controls. No differences seen when comparing DCA treated (n=20) and untreated (n=21) groups of each genotype.

3.9 Survival of DCA and untreated groups

Figure 3.9 demonstrates Kaplan Meier survival curves of the $p53^{R172H}$ mouse cohort, which were on a pure BALB/C genetic background. BALB/C mice are known to have a stronger adaptive immune response compared with C57BL/6 mice (Trunova,

Makarova et al. 2011). Wild type mice were shown to have a median survival of 60 weeks (**Figure 3.9A**). Heterozygous mice were shown to have a median survival of 39 weeks. $P53^{R172H}$ homozygote mice had a median survival of 16 weeks. No statistical differences were seen between survival of DCA and untreated groups.





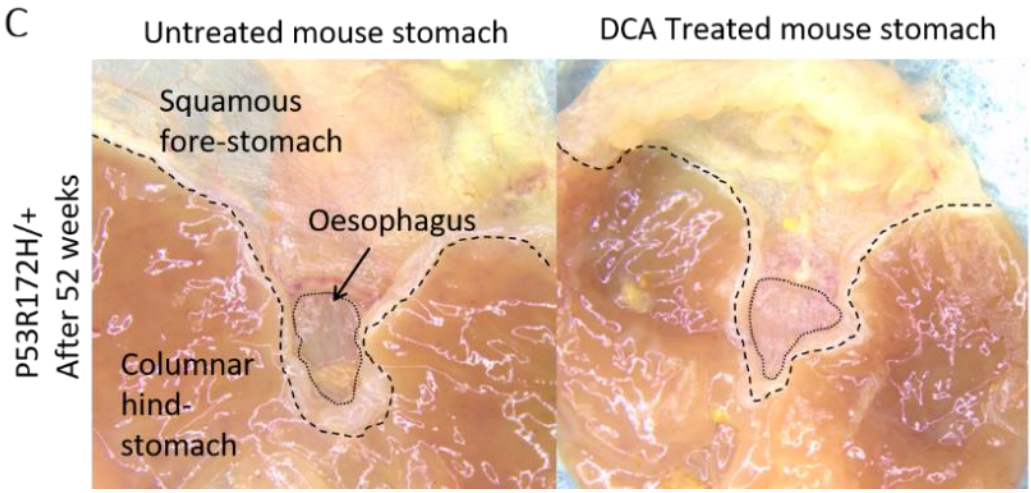


Figure 3.8 Biliary reflux murine model

A) Bar chart demonstrating dose titration of bile acid (deoxycholic acid, DCA) carried out to ensure that mice do not get dehydrated due to too high concentration (n=3)

B) Diagram demonstrating that mice commenced on 0.2% DCA treatment after weaning and genotyped at 3 weeks of age until they were sacrificed.

C) Photographs of the mouse upper GI tract 52 weeks post weaning. No macroscopic evidence of inflammation of gastric tumour development.

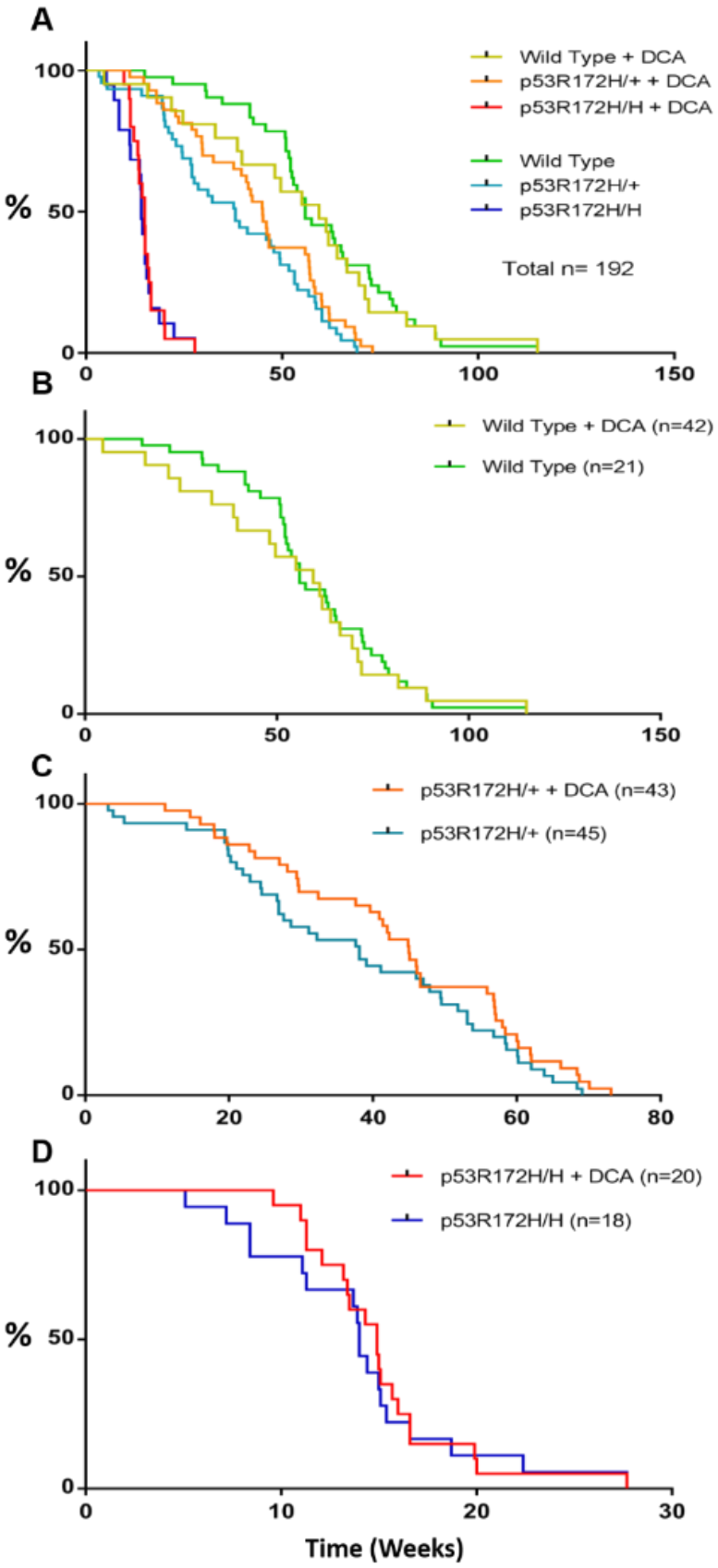

A
100
%
50
0
0
50
100
150
Wild Type + DCA
p53R172H/+ + DCA
p53R172H/H + DCA
Wild Type
p53R172H/+
p53R172H/H
Total n= 192
B
100
%
50
0
0
50
100
150
Wild Type + DCA (n=42)
Wild Type (n=21)
C
100
%
50
0
0
20
40
60
80
p53R172H/+ + DCA (n=43)
p53R172H/+ (n=45)
D
100
%
50
0
0
10
20
30
p53R172H/H + DCA (n=20)
p53R172H/H (n=18)
Time (Weeks)

Figure 3.9 Survival curves of the *p53*^{R172H} mice

A) Kaplan-Meier survival curve of all mice DCA treated and untreated (n=192)

B) Kaplan Meier survival curve demonstrating wild type mice. DCA treated mice (Gold, n=42) versus Untreated mice (green, n=21). No survival difference seen.

C) Kaplan Meier survival curve of *p53*^{R172H} heterozygous mice. DCA treated (orange, n=43) and untreated mice (teal blue, n=45). No survival difference seen.

D) Kaplan Meier survival curve of *p53*^{R172H} homozygous mice. DCA treated (red, n=20) compared with untreated (navy blue, n=18). No survival difference seen.

3.10 Increased expression of inflammatory mediators in mice exposed to high dose bile salts

In order to examine if the DCA treatment led to any evidence of inflammation in the upper GI tract, I further examined the mouse stomachs. Mice undergoing DCA treatment were sacrificed when they showed evidence of physical deterioration. Necropsies were carried out and specimens were inspected macroscopically. As summarised in **Figure 3.10A** the stomachs of three mice from each genotype and each treatment group were retrieved and divided into two longitudinally. One side was formalin fixed and paraffin embedded for histological analysis and the other was sampled for RNA extraction and quantitative PCR analysis. Gastric cardia tissue was used for PCR analysis examining for evidence of increased expression of interleukin genes. As shown in **Figure 3.10B,** I observed a statistically significant increased expression of Il-1β after DCA treatment. Further, the data suggest there may be a trend towards increased expression of Il-8 and Il-10 but this was not statistically significant.

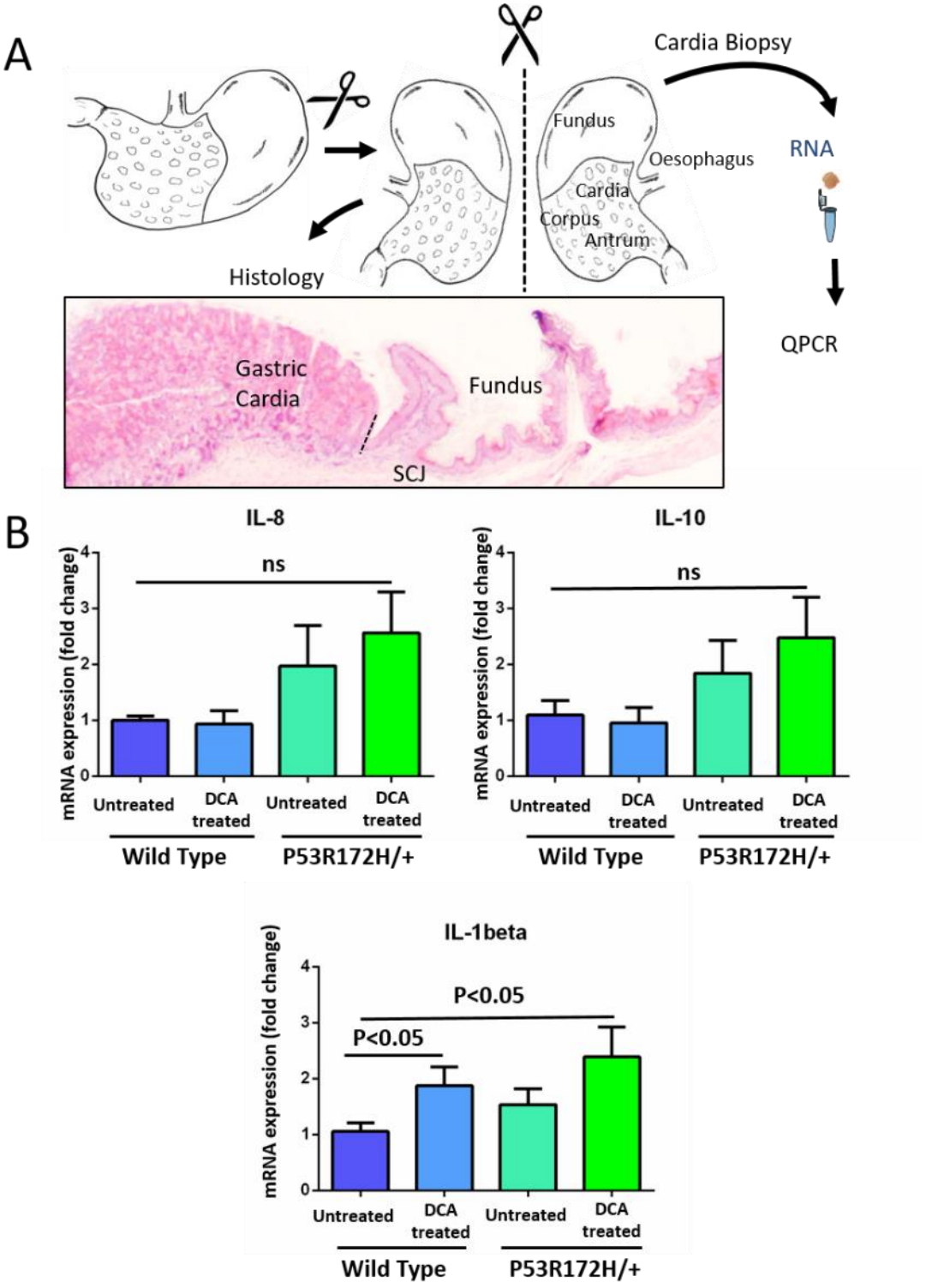


Figure 3.10 Analysis of DCA treated mouse stomachs

A) Diagram to demonstrate processing of mouse samples

B) Bar charts of Quantitative RT-PCR data for inflammatory mediators Il-8, Il-10 and Il-1β of full thickness pieces of mouse gastric cardia (n=3) ΔΔCT for fold change.

3.11 Increased expression of pNfκb in *P53$^{R172H/+}$* DCA treated mice

Next, I conducted immunohistochemical staining for phosphorylated Nfκb, a marker of activated inflammatory signalling. When comparing WT, 52 week DCA treated mice with age matched untreated mice, a trend towards higher nuclear pNfκb expression was seen in DCA treated mouse stomachs. However, this was not statistically significant. Three mice were analysed in each group. (**Figure 3.11A**). This suggests that long term treatment of DCA in mice may induce inflammatory signalling in the murine upper GI tract through the Nfκb pathway. When comparing untreated *p53$^{R172H/+}$* and untreated WT mice, a trend towards higher nuclear expression of pNfκb was seen in *p53$^{R172H/+}$* mice. Again this result was not statistically significant, but suggests that *p53$^{R172H/+}$* may have a role in increasing inflammatory signalling in the upper GI tract independent of reflux. (**Figure 3.11B**).

3.12 Cox2 expression in *p53$^{R172H/+}$* and DCA treated mice

Next, I analysed three mouse gastric specimens from each group for expression of Cox2 in a similar way to pNfκb analysis. Cox2 a well-documented mediator in upper GI reflux-induced inflammation that is thought to have a role in the development of BO (**Figure 3.12).** Overall, there was a general trend towards higher Cox2 staining in *p53$^{R172H/+}$* mice compared to WT, however, these results were not statistically significant due to the large standard deviation in these data. A trend towards increased expression of Cox2 in 52 week, DCA treated mouse stomachs may be suggested by the data when compared with untreated mice, however there is no statistical significance.

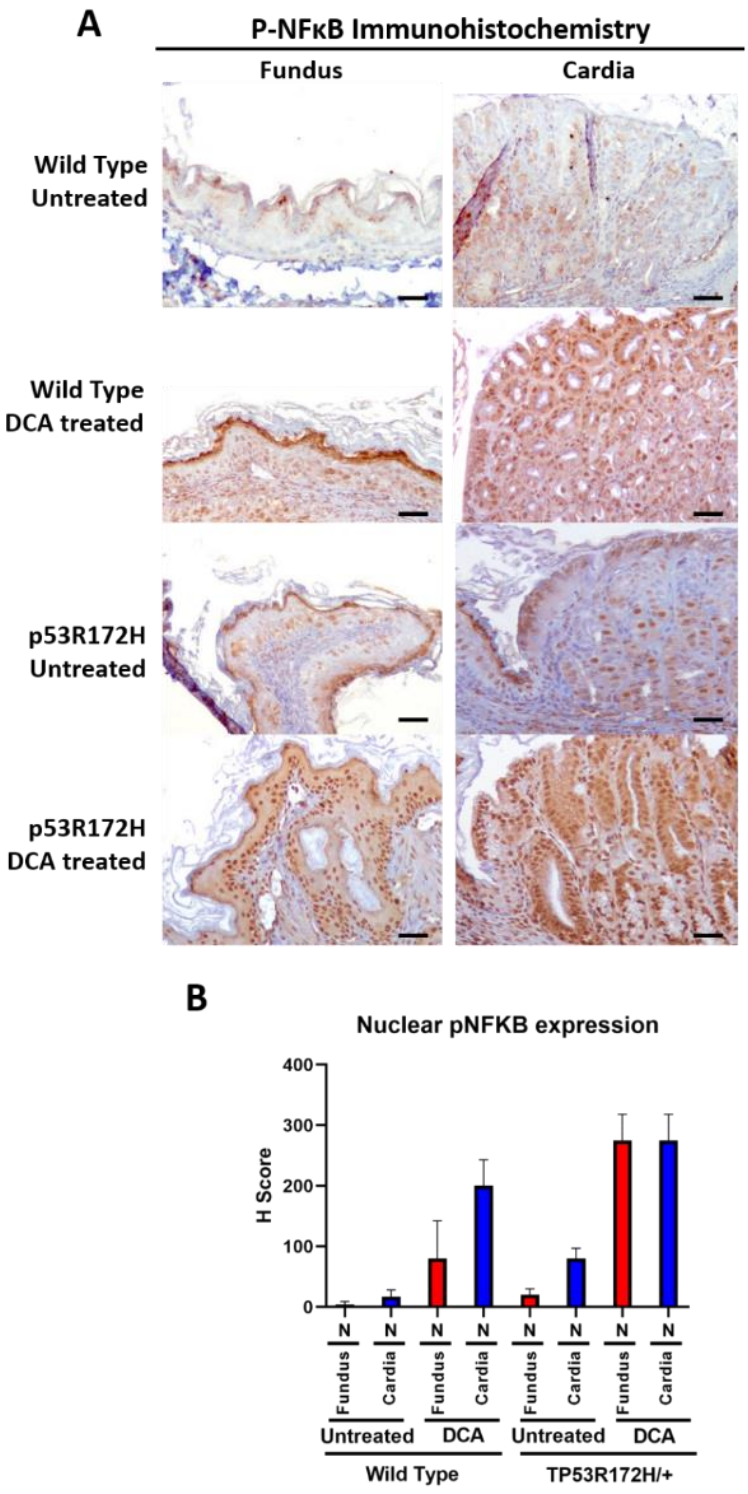


Figure 3.11 Phosphorylated NFκB expression

A) Immunohistochemical staining of phosphorylated Nfκb on wild type and *p53*^{R172H} heterozygous murine stomachs, DCA treated and untreated. Scale bars 50µm.

B) Bar charts to demonstrate H-score calculated for Nuclear staining (N) each specimen analysed (n=3)

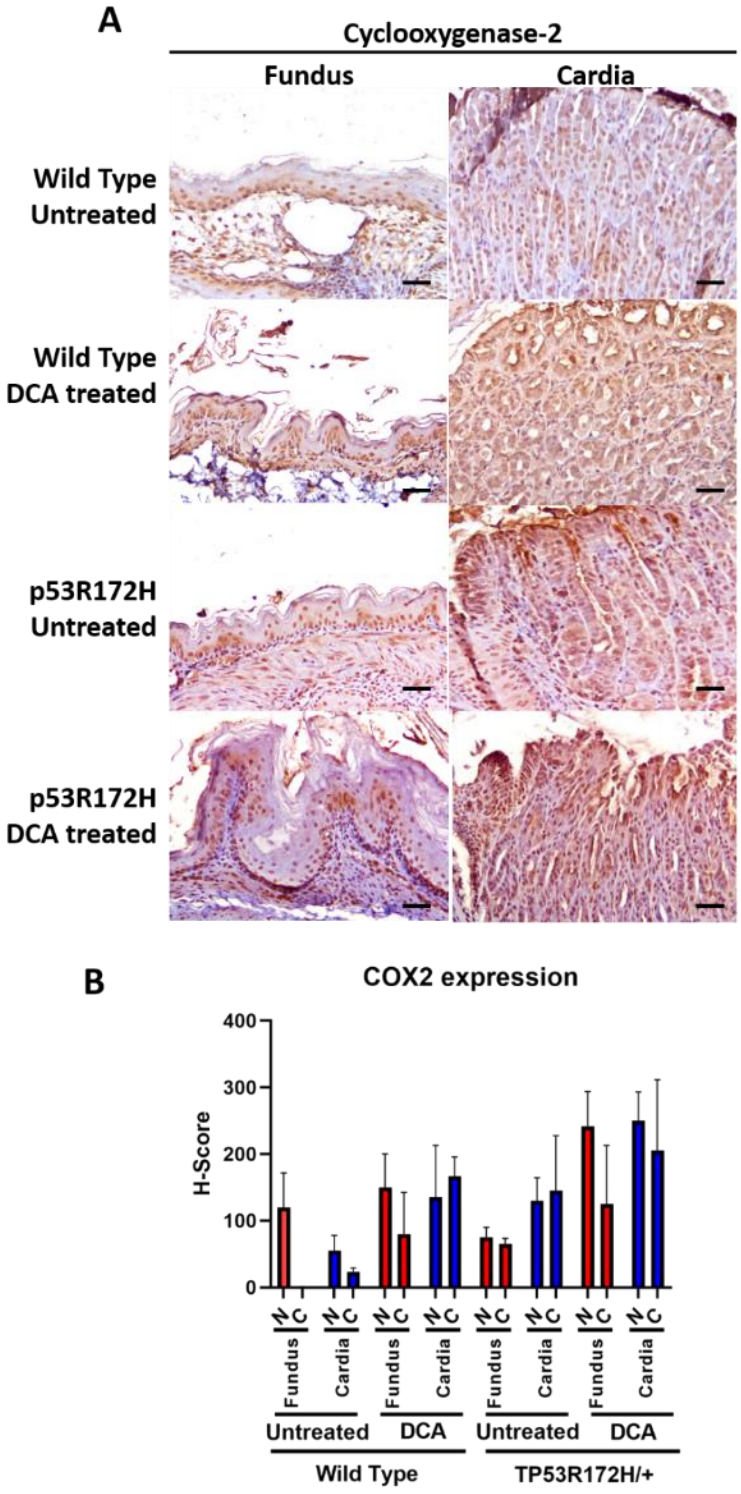


Figure 3.12 Cox2 expression in *p53*^{R172H} DCA treated mice

A) Immunohistochemical staining of Cox2 on wild type and *p53*^{R172H} murine stomachs, DCA treated and untreated. Scale bars 50µm.

B) Bar charts to demonstrate H –Score calculated for Nuclear (N) and Cytoplasmic (C) staining for each specimen analysed (n=3).

3.13 *p53^{R172H}* in a mouse model of biliary reflux does not induce gastric adenocarcinoma development

Overall 114 stomachs of mice underwent detailed histological analysis, in which at least five sections from each mouse were analysed from different areas of the stomach from each individual mouse to determine presence of gastric phenotype. From the DCA treated group: 19 WT, 20 *p53$^{R172H/+}$* mice and 14 *p53$^{R172H/H}$* mice were analysed. From the DCA untreated group: 22 WT, 21 *p53$^{R172H/+}$* mice and 18 *p53$^{R172H/H}$* mice were analysed. As shown in the table in **Figure 3.13A** there were no differences observed between *p53$^{R172H/+}$* treated and untreated mice regarding IM occurrence, with IM occurring in 35% (7/20) of DCA treated mice and 36.4% (8/21) of untreated mice (**Figure 3.13C**). Furthermore, of the mice that exhibited IM there was no evidence of altered distribution within the stomach of DCA treated and untreated mice (**Figure 3.13B**). 15% (3/21) *p53$^{R172H/+}$* DCA treated mice demonstrated evidence of mucinous metaplasia, which is characterised by an increased number of native gastric mucus secreting foveolar cells and is associated with chronic inflammation but not associated with neoplasia (**Figure 3.13G**). As mentioned, homozygous mice (*p53$^{R172H/H}$*) had shorter median survival of 15 weeks, they die of haematological malignancies, and as such they had less time to develop a gastric phenotype. Upon detailed histological analysis of DCA treated *p53$^{R172H/H}$* mice: 14.2% (2/14) demonstrated IM; 7% (1/14) developed gastric hyperplasia; 7% (1/14) developed high grade dysplasia (**Figure 3.13F**), and 1/14 developed gastric adenocarcinoma of the antrum (**Figure 3.13D & E**). In the *p53$^{R172H/H}$* untreated group 3/18 (16.7%) were found to have IM and 3/18 were found to have gastric glandular hyperplasia. Consequently, I concluded that this model did not increase the incidence of GIM and it did not demonstrate a reproducible model for gastric carcinogenesis.

A

Genotype	Intestinal Metplasia	Mucinous Metaplasia	Gastric Glandular hyperplasia	High grade dysplasia	Adenocarcinoma
Wild Type Untreated n=22	5/22 (22.7%)	0/22 (0%)	0/22 (0%)	0/22 (0%)	0/22 (0%)
P53R172H/+ Untreated n=21	8/21(36.4%)	1/21(4.5%)	0/21(0%)	0/21(0%)	0/21(0%)
P53R172H/H Untreated n=18	3/18 (16.7%)	0/18 (0%)	3/18(16.7)	0/18(0%)	0/18 (0%)
Wild Type DCA treated n=19	4/19 (21%)	1/19 (5.2%)	0/19(0%)	0/19(0%)	0/19(0%)
P53R172H/+ DCA treated n=20	7/20 (35%)	3/20(15%)	0/20(0%)	0/20(0%)	0/20(0%)
P53R172H/H DCA Treated n=14	2/14 (14.2)	0/14 (0%)	1/14(7%)	1/14 (7%)	1/14 (7%)

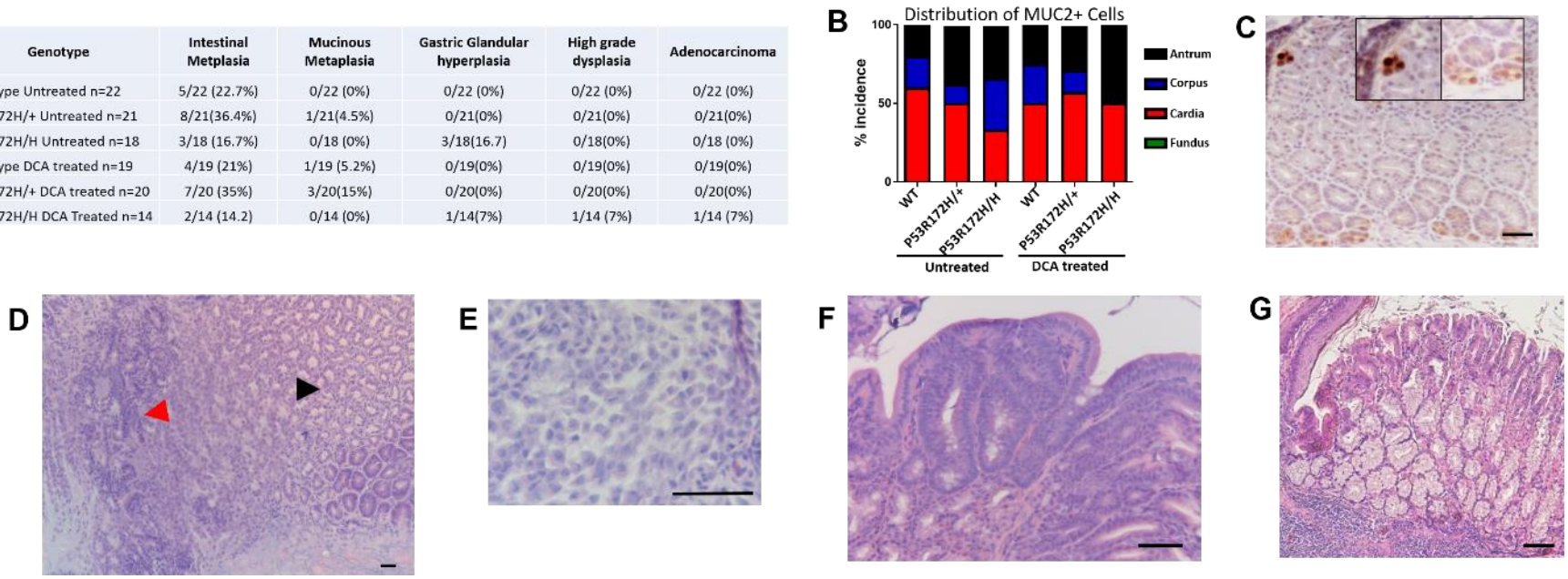


Figure 3.13 Gastric pathology demonstrated within mice
A) A table to demonstrate the gastric pathology observed within the mice examined
B) Graph to demonstrate of the goblet cells observed in mouse stomachs, the distribution of goblet cells within mouse stomachs
C) An example of MUC2+ staining in a *p53*$^{R172H/+}$ mouse cardia. Scale bars 50µm.
D) Zoomed out image of haematoxylin and eosin staining of a mouse gastric adenocarcinoma. Black arrow demonstrates normal gastric gland pattern. Red arrow demonstrates area of adenocarcinoma. Scale bars 50µm.
E) Zoomed in image of loss of gland structure and presence of invasion in gastric adenocarcinoma in DCA treated *p53*$^{R172H/H}$ mouse, same lesion as above in (D). Scale bars 50µm.
F) H&E staining of high grade dysplasia in a DCA treated P53$^{R172H/+}$ murine gastric antrum. Scale bars 50µm.
G) H&E staining of mucinous metaplasia in *p53*$^{R172H/H}$ murine gastric cardia. Scale bars 50µm.

3.14 DCA treated mice developed evidence of hepatitis and liver tumours

Overall, 114 mice were analysed. From the DCA treated cohort all 14 *p53*$^{R172H/H}$ had tumours; all 20 of the *p53*$^{R172H/+}$ mice; and six of the 19 WT DCA treated mice developed tumours (**Figure 3.14**). From the DCA untreated cohort 16 of the 18 *p53*$^{R172H/H}$ had tumours; all 21 of the *p53*$^{R172H/+}$ mice; and three of the 22 WT untreated mice developed tumours (**Figure 3.14**).

Within the *p53*$^{R172H/H}$ DCA treated cohort, only one mouse was seen to have developed a locally invasive gastric adenocarcinoma (**Figure 3.13E**), and one mouse was found to have a colonic tumour. However, although the mice did not reproducibly develop gastric adenocarcinomas as hypothesised, other tumours were seen during necropsy (**Figure 3.14**). Most commonly, mice developed lymphomas, characterised by massive gross splenomegaly, sarcomas within skeletal muscles are large thymus tumours. All mice treated with DCA were observed to have an element of liver inflammation seen on H&E staining confirmed by a consultant histopathologic. Of the 14 DCA treated *p53*$^{R172H/H}$ mice analysed four mice were found to have liver tumours. 20 *p53*$^{R172H/+}$ DCA treated mice analysed 14 mice were found to have liver tumours, 11 of these 14 mice also had evidence of lymphomas and or thymus tumours. This compared to one liver tumour observed in WT DCA treated group. **Figure 3.14B & C** demonstrate liver tumours from a *p53*$^{R172H/+}$ DCA treated mouse.

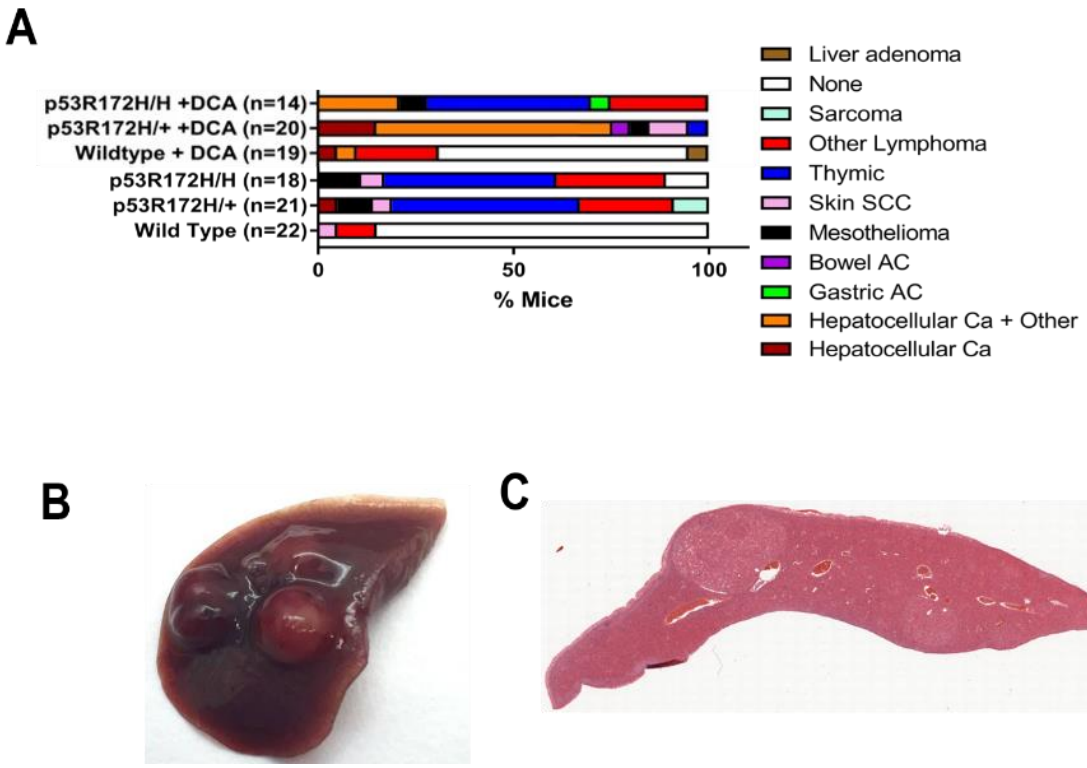


Figure 3.14 DCA treated murine tumour spectrum
A) Graph demonstrating mouse tumour spectrum.
B) Photograph of a murine liver containing tumours
C) Whole section of a Haematoxylin and Eosin stained mouse liver containing a tumours

In addition to tumours in the *p53*^{R172H} mouse cohort incidence of liver tumours in wild type DCA treated mice was also higher than expected. Further histological analysis suggested that independent of genotype, DCA treated mice developed strong nuclear expression of phosphorylated NFκB (**Figure 3.15**). This suggests that DCA was absorbed in the GI tracts of these mice and lead to liver inflammation in these mice.

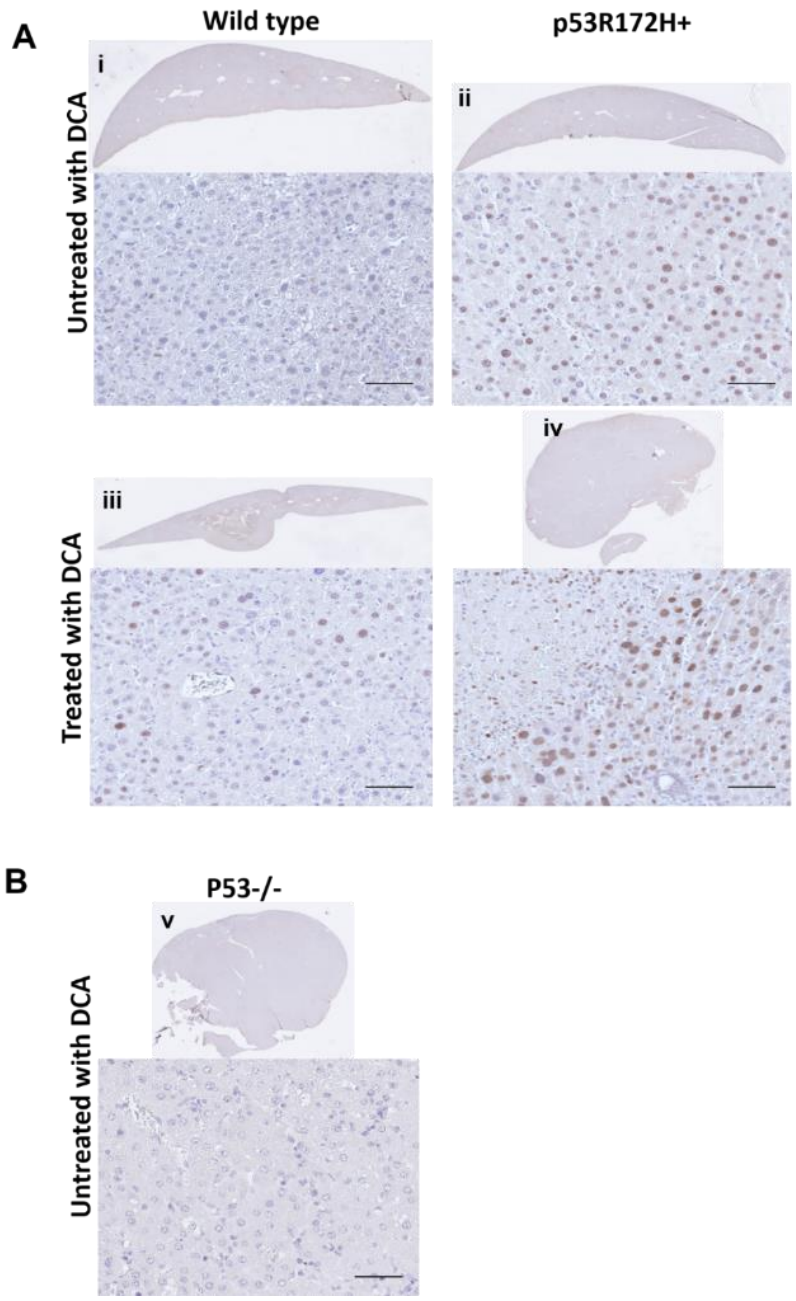


Figure 3.15 Murine liver tumour analysis

A) Photograph of a murine liver containing tumours
B) Whole section of a Haematoxylin and Eosin stained mouse liver containing a tumours
A) Immunohistochemical staining of Phosphorylated NFκB in mouse livers. (i) Wild type untreated liver n=3; (ii) $p53^{R172H}$ untreated liver n=3; (iii) Wild type DCA treated liver with hepatocellular carcinoma n=3; (iv) $p53^{R172H}$ DCA treated liver with lymphoma;
B) Immunohistochemical staining of Phosphorylated NFκB in *p53* null untreated mouse liver containing lymphoma.

3.16 Discussion

Despite the initial observation of presence of goblet cells and by implication IM in *p53*^{R172H} mutant mouse stomachs, challenging *p53*^{R172H} mutant mice with a known biliary reflux model did not result in observable oesophago-gastric carcinogenesis, although a single *p53*^{R172H} mutant DCA-treated mouse developed a gastric adenocarcinoma. These results indicate that the combination of *p53* mutation with a biliary reflux model is not enough to stimulate the development of malignancies of the upper GI tract. This suggests that although *P53* mutations occur frequently and early in OAC and GAC, they are more stable than expected. Other studies have demonstrated that potentially cancer-driving mutations occur in normal epithelium and have a low incidence of malignant transformation (Martincorena, Roshan et al. 2015, Suda, Nakaoka et al. 2018, Fernandez-Antoran, Piedrafita et al. 2019, Yizhak, Aguet et al. 2019). In fact, *P53* mutations have been found in 5-10% of patient's normal oesophageal epithelium (Martincorena, Fowler et al. 2018, Colom, Alcolea et al. 2020). It is important to acknowledge that most gastric cancers are associated with *H.pylori* induced inflammation, however, it was the intention of this study to solely examine the role of chronic reflux associated proximal gastric and GOJ carcinogenesis.

In a recent study, conditional inactivation of *p53* and *Rb1* in Lgr5+ cells over 40 weeks resulted in all mice developing gastric adenocarcinoma at the SCJ (Fu, Wang et al. 2020). This study therefore indicates that P53 mutations can contribute to the initiation of GOJ carcinogenesis, but not without another key cancer-causing mutation. In this case, loss of two key tumour suppressor genes in gastric stem cells was enough to induce carcinogenesis without any further ectopic inflammatory stimulus. They targeted these mutations in Lgr5+ cells within the first pit of gastric

glandular epithelium. Interestingly, they comment that the structure of the first gastric pit more closely resembles the structure of an antral gland than a corpus gland as it lacks secretory parietal cells; this is like gastric cardia epithelium in humans (Fu, Wang et al. 2020).

Cancer genome atlas data demonstrated that proximal gastric and GOJ adenocarcinomas had higher levels of *P53* mutations, chromosomal instability and often demonstrated intestinal type histology. However, our study found no evidence to suggest $p53^{R172H}$ mutant mice developed a higher incidence of goblet cell differentiation after long-term treatment with DCA. In the study by Fu et al. noted no evidence of IM nor intestinal type tumours within mice with $p53^{-/-}$ in Lgr5+ cells. This agrees with our data IM was not seen more frequently in *p53* null mice compared to WT BALB/C mice. However, 36.4% of $p53^{R172H}$ mice demonstrated IM on detailed histological analysis. Previous studies have demonstrated that *Apc* deletion in Lgr5+ cells lead to development of gastric antral adenomas. Inactivation of Smad4 and Pten in Lgr5+ cells has demonstrated the development of intestinal type cancers in the antral and SCJ regions of mice (Li, Yang et al. 2016). This study suggests that the development of intestinal type cancers is driven by the cellular origin of the cancer being Lgr5+ cells; however, it is unclear why *p53* knockout in Lgr5+ cells did not drive this same phenotype. The role of LRG5+ cell in cancer development and metastasis remains controversial (Morgan, Mortensson et al. 2018). Other analyses from Fu et al. suggests that in some cancers induction of initial mutations in Lgr5+ cells leads to an expansion of the naïve cell population in the proximal stomach, beyond this Lgr5 signalling is no longer an essential driver (Fu, Wang et al. 2020).

Despite the absence of increased oesophago-gastric cancer development. A pattern was observed where the DCA treated mice had a high incidence of liver inflammation

and liver tumours than controls. Further histological analysis suggested that independent of genotype, DCA-treated mice developed strong nuclear expression of phosphorylated NFκB. This finding is supported by the literature, DCA is absorbed by the gut and naturally concentrates in the liver. Other studies the oral administration of DCA in mice demonstrated colonic tumour development in wild type C57BL/6 mice, (Flynn, Montrose et al. 2007, Bernstein, Holubec et al. 2011). However, we did not see this in our mice on a BALB/C background. There is therefore a potential that the background of our mice may have confounded this analysis. This is supported by other studies which have demonstrated a difference in the immune response between C57BL/6 mice. BALB/C mice have lower circulating IL-12 and lower levels of natural killer cells compared with C57BL/6 mice (Trunova, Makarova et al. 2011, Fornefett, Krause et al. 2018). In fact, our findings suggest that DCA may have increased phosphorylated Nfκb both in the upper gastro-intestinal epithelium but also in the livers. This is in agreement with previous reports suggesting DCA can induce oxidative stress and has been shown to activate Nfκb signalling (Attili, Angelico et al. 1986, Wu, Chen et al. 2015).

3.17 Limitations

In our study, mice with constitutive mutations were used, this comes with specific limitations, for example $p53^{R172H}$ were vulnerable to other malignancies (lymphoma, sarcomas) with reduced median survival compared to WT mice (Jacks, Remington et al. 1994). All analyses carried out were with age matched WT mice to ensure that no epithelial maturity did not affect results. This innately limited length of time that a chronic reflux model could be used with a *p53* mutant model. Constitutively mutant mice also do not mimic the development of cancer with specific localised mutation in a tissue which then in turn drives a clonal competition in the tissue. The impact of a

p53^{R172H} mutation in all stromal cells in addition to epithelial cells on cell interactions and immune function in our model is poorly understood. This a benefit of conditionally mutant mice where a mutant gene cassette can be inserted downstream of a tissue specific gene triggering mutant expression only in a targeted tissue. Another limitation is the use of tissue pieces including epithelium and stroma to carry out gene expression analysis, gene expression could be looked at in the epithelium and stroma separately using laser capture microdissection to allow for more specific understanding of which cells demonstrated alterations in gene expression. Another key limitation of the study was delays in mouse breeding as conditional mouse strains needed to be inbred for many generations to achieve a pure background which meant that further work using conditional mice could not be bred. Although this could potentially have been anticipated, as I had limited prior experience of mouse breeding. The experiments with constitutive mice were initially seen as preliminary experiments to be followed up by the development of a conditional model. When analysing the murine liver tumours, specific markers for primary liver tumours or lymphomas were not used.

Chapter 4: Dissecting cell populations within BO

4.1 Introduction

At a microscopic level BO has diverse differentiation patterns including intestinal, fundic, cardiac, antral and even pancreatic specialised cells (Griffin and Sweeney 1987, Krishnamurthy and Dayal 1995, Chaves, Cruz et al. 2005). The initiating cell type of BO has been debated. If identified, it is hypothesised that the BO cell of origin would enable improved understanding and surveillance of oesophageal carcinogenesis. Many tissue sequencing studies have been carried out on tissue biopsies, when sequencing highly heterogeneous tissue such as BO deciphering the data can be compromised (Maag, Fisher et al. 2017). Additionally, when examining complex differentiation patterns tissue controls are imperative to enable disentangling pathological and native differentiation. Single cell RNA sequencing (sc-RNA-seq) enables single cell resolution of transcriptional analysis allowing description of cell types by gene expression patterns. When sc-RNA-seq is utilised in tandem with in situ and experimental methods in BO we may gain unique insight into the cellular landscape of BO beyond histological description.

For the purpose of this study, we defined BO as >2cm segment of columnar lined oesophagus proximal to the endoscopic Z-line of the Gastro-oesophageal junction (GOJ) with proven histological presence of goblet cells as this is the most internationally accepted definition.

In this study we aimed to define unbiased markers of upper GI cell populations and to improve on histological description previously used to characterise cellular heterogeneity of BO.

4.2 Creating a biobank of upper GI biopsies

We set up a large biobank of upper gastrointestinal tissues samples accessed through endoscopy and for surgical resection specimens we set up links with the upper GI surgical department. This biobank enabled large scale histological validation of our findings. Once patients were fully informed of the study, its implications, limitations and a formal consent was gained, patients proceeded into the study.

Of the biobank cohort, 13 patients with BO (A-D, I-Q) attending for planned endoscopic surveillance of their oesophagus and donated surplus biopsies for molecular characterisation. Inclusion criteria required patients to be attending to the endoscopy unit at the John Radcliffe hospital for routine follow-up with a proven diagnosis of BO, without any previous diagnosis of dysplasia or OAC.

From each patient, biopsies from BO, adjacent macroscopically normal squamous oesophagus (2cm proximal to the neo-SCJ), proximal gastric epithelium (>2cm distal to the GOJ) and the second part of the duodenum. Samples were taken using standard 2mm endoscopic biopsy forceps. From each location pairs or quadruplets of biopsies, surplus to clinical requirements were taken to ensure that ample tissue was obtained for our multimodal strategy. Upon collection biopsies from all 4 endoscopic sites were divided into 3 pieces to provide tissue for tissue authentication, scRNA-seq, bulk-RNA-seq. (**Chapter 2: Materials and Methods, Bulk RNAseq not shown in thesis but features in Owen & White et al. 2018**). Although the figure only demonstrates images of frozen sections from four (A-D) of the 13 patients, all patients had frozen sections taken with H&E authentication prior to sequencing so that we were able to confirm the epithelium we were sequencing (**Figure 4.2**).

As experimental controls, two patients (patients E & F) attending endoscopy for routine clinical follow up with symptomatic GORD but without BO were recruited to the study. This provided important controls of normal squamous epithelium in patients without BO. These additional GORD controls had no BO, dysplasia or OAC but were taking Proton Pump inhibitor medications to treat their GORD symptoms.

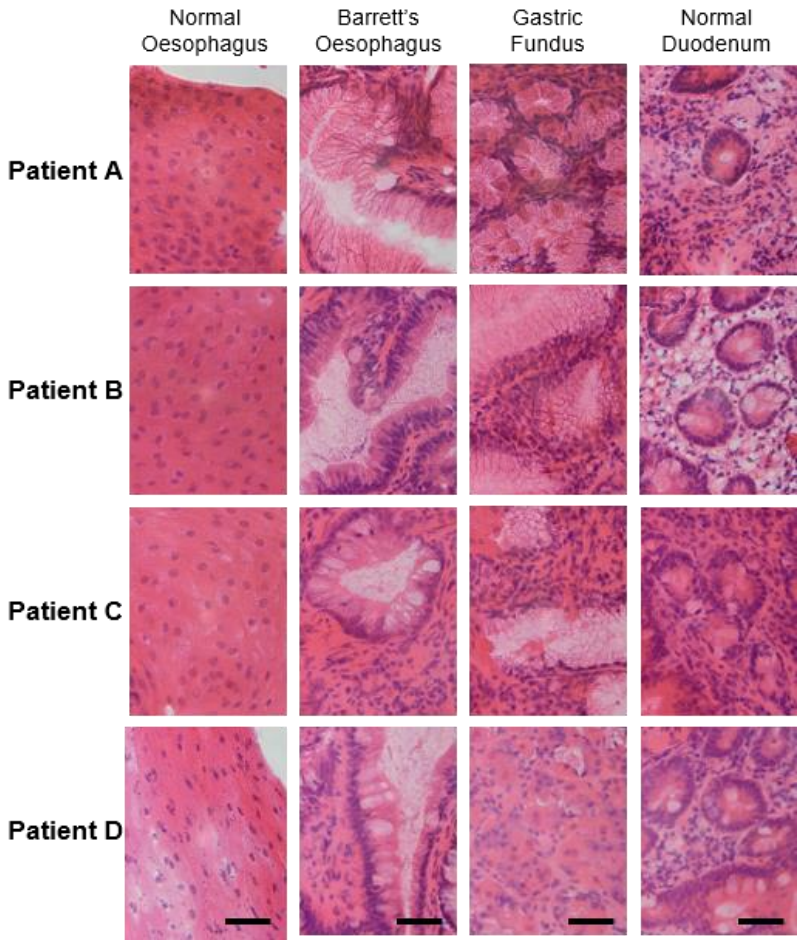


Figure 4.2 Tissue authentication before scRNA-seq.

A panel of images showing H&E staining of frozen sections from Patients A-D endoscopic biopsies before sequencing. All patients had frozen sections of biopsies for tissue authentication. Scale bars represent 100µm. **Figure created by Michael White. Adapted from Owen & White et al. 2018**

4.3 EpCAM high and EpCAM low cell populations were seen in oesophageal cells

In this study, EpCAM was used to help guide cell size gating parameters in forward and side scatter during fluorescence-activated cell sorting (FACS). EpCAM expression was used during sorting to ensure that epithelial cells were captured. Both EpCAM and CD45 antibodies were used to stain cells during FACS, we captured CD45 negative cells and acknowledged whether or not cells expressed EpCAM or not. BO has a higher proportion of EpCAM + cells than other tissues (**Figure 4.3**)

To identify our highly expressing EpCAM populations from FACS of digested biopsies immunohistochemical staining on tissue sections was carried out **(Figure 4.3).** The tissue staining demonstrates oesophageal submucosal glands express high levels of EpCAM, squamous cells did not express high levels of EpCAM.

As we were cautious that unviable cells may have started to demonstrate an altered transcriptome we used DAPI staining to select live cells during FACS.

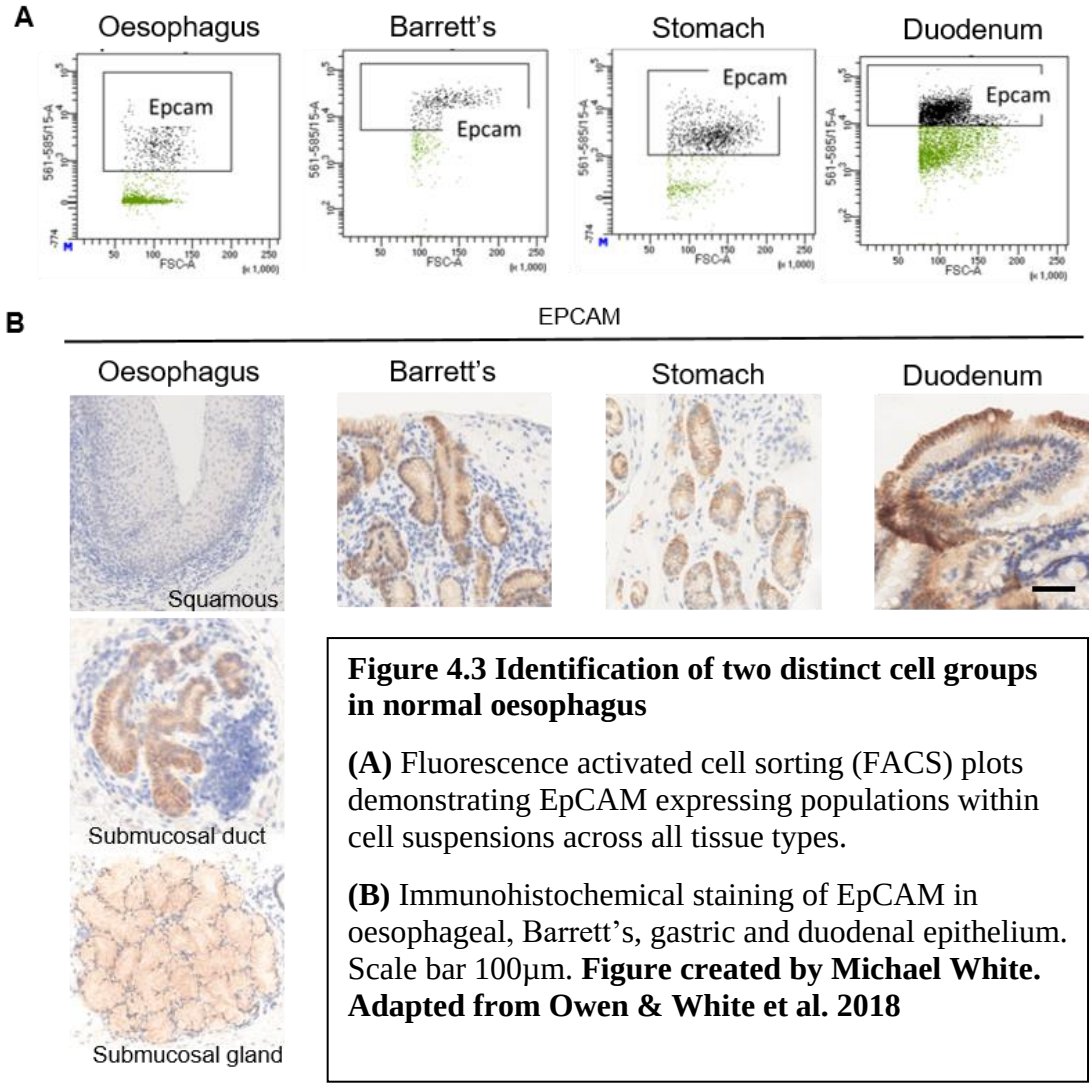


Figure 4.3 Identification of two distinct cell groups in normal oesophagus

(A) Fluorescence activated cell sorting (FACS) plots demonstrating EpCAM expressing populations within cell suspensions across all tissue types.

(B) Immunohistochemical staining of EpCAM in oesophageal, Barrett's, gastric and duodenal epithelium. Scale bar 100µm. **Figure created by Michael White. Adapted from Owen & White et al. 2018**

4.4 Identifying cell populations in normal Upper GI epithelium

4.4.1 Obtaining cells

Dividing samples and processing them into cell suspensions was time intensive. As time went by with each processed cell suspension we noticed that the DAPI stained cell population increased during FACS, suggesting that cell quality could be degrading as the nuclei became permeable. Due to the sensitivity of RNA to degradation and presence of endogenous RNAases within cells we prioritised reducing time between the cells leaving the patient in the biopsy and being snap

frozen in a droplet of lysis buffer in a 96 well plate. To avoid batch effect from processing we permuted the cells from different biopsy sites and from different patients on each of the plates so that batch effects were limited to the best of our ability. Overall, 4237 cells were sequenced from eight patients (A-H) across three batches.

Previous studies using scRNA-seq had published issues with batch effects in experiments. Therefore, analysis of cells from each batch has been kept separate where feasible and cells were permuted across plates and pooled prior to sequencing. Batch 1: 1040 cells (207 duodenum, 227 gastric, 371 BO and 235 oesophagus) suitable for analysis from four patients (A-D). After quality control of the data by Dr David Severson, 214 BO-derived cells were analysed from patient A, 35 from patient B, 66 from patient C and 56 cells from patient D.

Batch 2: 648 cells (derived from normal oesophageal biopsies) from two patients (E-F), which met quality control thresholds for analysis, these patients had with symptoms of GORD but never has any oesophageal pathology diagnosed.

Batch 3: 194 cells (derived from: 29 cells from gastric pylorus, 109 cells from gastric fundus, 32 cells from BO and 24 from normal oesophagus) which met quality control thresholds for analysis from two patients (G-H) with BO and IM.

Overall, there was a mean of $1.2x10^5$ counts per cell and a median of 3978 genes were detected per cell (with at least one read per gene). **Richard Owen and David Severson carried out all sequencing data processing and statistical analysis.**

4.4.2 Analysis of sc-RNA-seq data

Initially, cells from each normal tissue type (normal oesophagus, gastric fundus, duodenum) were clustered by their gene expression across the whole transcriptome (**Figure 4.4**). This created eleven "cell type" clusters, on the basis that cell types with similar characteristics had most similar transcriptional profiles. Of these 11 clusters; four were clusters from oesophageal biopsies (O1-O4); four duodenal cell clusters (D1-D4) and three were clusters with cells of gastric origin.

Interestingly, within the sc-RNA-seq data for normal oesophageal cells four clusters were identified. Cells from two of these clusters expressed the expected squamous markers (KRT5, KRT14, TP63; clusters O1 and O2) and two clusters express the Trefoil factor 3 (TFF3) a gene associated with columnar/ glandular structures (clusters O3 and O4). The two squamous clusters can be distinguished by the presence (O1) or absence (O2) of acute phase response gene, Serum amyloid A1 (SAA1) expression, seemingly representing squamous cells in different states. The detection of TFF3 in O3 and O4 is of great interest and is consistent with these cells being from the columnar epithelium of OSGs as previously seen in the EpCAM staining. In order to ensure we were not identifying TFF3+ cells with intestinal metaplasia as OSGs we analysed the proximal part of five oesophagectomy specimens. These specimens resulted from surgical resection of Siewert type II & III oesophagogastric junctional tumours. H&E staining and analysis confirmed no evidence of metaplasia was present in the tissue before immunohistochemical staining was carried out. This illustrates the structure and expression pattern of OSGs, OSG ducts, squamous epithelium and the corresponding staining pattern for the markers derived from scRNA-seq data (**Figure 4.4B, C, D**).

As expected, the squamous oesophageal epithelium strongly expressed cytokeratin 14 (KRT14, a squamous cell marker) and p63 (a transcription factor critical for squamous cell differentiation) (**Figure 4.4c**). Using the adjacent sections from the same OSG-containing specimen, I observed that the glandular OSG strongly expressed KRT7 and TFF3 markers for transitional epithelium and glandular epithelium respectively (**Figure 4.4d**). Since OSG ducts comprise different cell lineages, including squamous, transitional and glandular epithelium, we detected KRT14, p63 and KRT7-expressing cells at RNA seq level in the OSG duct, demonstrating they are genuine OSG ducts. Interestingly the OSG ducts are P63+KRT14+KRT7+ when triple staining demonstrating protein markers of squamous and columnar/ transitional epithelium at the same time. KRT14 and KRT5 are paired cytokeratins and often simultaneously expressed in squamous epithelium. A recent study has described a candidate for the BO cell of origin to be a "transitional basal cell" that exists at the gastro-oesophageal SCJ which is P63+KRT5+KRT7+ (Jiang, Li et al. 2017). As $p63^{+}$ $KRT7^{+}$ cells have been shown to generate intestinal-like epithelial cells in organoid culture upon CDX2 overexpression, it may be possible that these oesophageal cells could be related to the transitional zone progenitor cells previously observed in humans (Jiang, Li et al. 2017). The most definitive study to date examining BO, OSGs and gastric cardia with multi-omic profiling concluded that BO most likely derives from proximal gastric cells (Nowicki-Osuch, Zhuang et al. 2021). This study has carried out a comprehensive analysis of OSGs and demonstrated no evidence of transcriptional overlap between OSGs and BO cells (Nowicki-Osuch, Zhuang et al. 2021).

Although all samples were histologically authenticated with H&E staining of frozen sections prior to processing for sequencing, no OSG structures were observed within

oesophageal biopsies. Thus, showing that single cell transcriptomic analysis can identify cell subpopulations within endoscopic biopsies from patients which may not have been seen by conventional bulk-RNA-seq. It is possible that the absence of OSGs on histological validation may mean that the sequencing data represents cells undergoing intestinal metaplasia instead OSG cells.

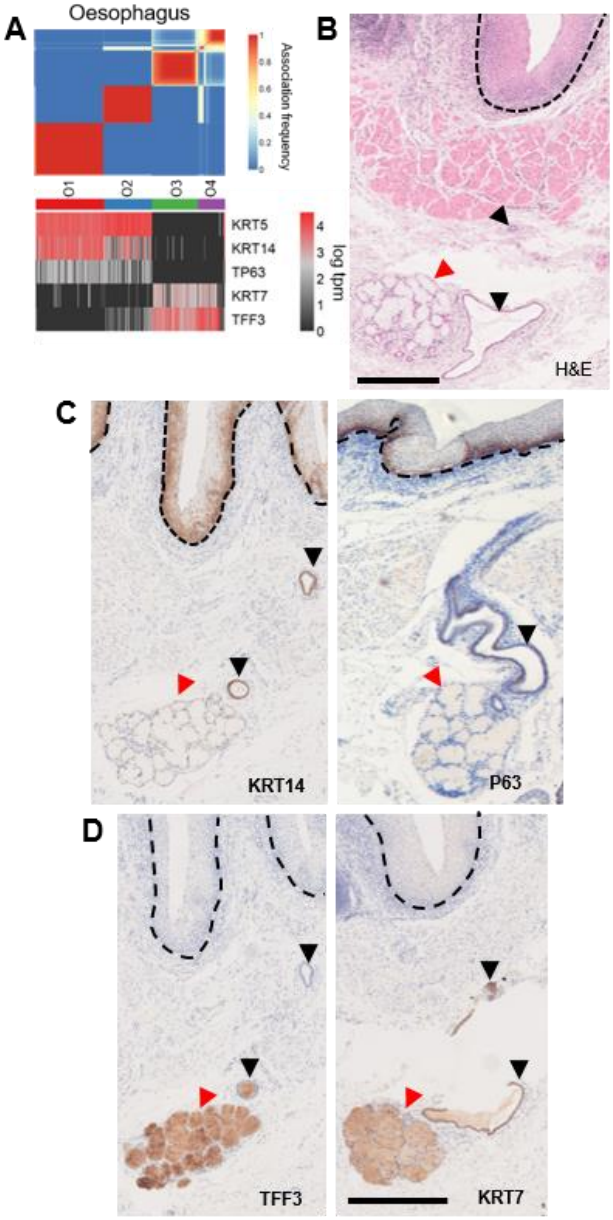


Figure 4.4 Identification of cell groups in normal oesophagus

(A) Upper panel shows the cluster consensus matrices for single cells from normal oesophageal biopsies in four BO patients. Blue-to-red colours denote the frequency with which cells are grouped together in 250 repeat clusterings of simulated technical replicates (see Materials and Methods). Cell clusters are indicated by coloured bars below the matrices. In lower panels, heatmaps show expression of known functionally relevant genes that were differentially expressed between cell clusters (>4 fold change, FDR <1e-5). Heatmaps by Richard Owen

(B) Haematoxylin and eosin staining of normal oesophagus taken from the proximal part of an oesophagectomy specimen resected for Siewert type III junctional tumour in a patient with no BO, showing OSGs (red arrow), OSG ducts (black arrow) and squamous epithelium (marked with dotted black line). Scale bar 500µm. **Figure created by Richard Owen. Adapted from Owen & White et al. 2018**

(C) Immunohistochemical staining of KRT14, TP63 (left and right images, respectively) in adjacent sections from the same specimen as **B,** showing OSG ducts (black arrows) and OSGs (red arrows) and squamous epithelium (marked with dotted black line). Scale bar 500µm. OSG, oesophageal submucosal gland. **Figure created by Michael White. Adapted from Owen & White et al. 2018**

(D) Immunohistochemical staining of TFF3 and KRT7 (left and right images, respectively) in adjacent sections from the same specimen as **B,** showing OSG ducts (black arrows) and OSGs (red arrows) and squamous epithelium (marked with dotted black line). Scale bar 500µm. OSG, oesophageal submucosal gland. **Figure created by Michael White. Adapted from Owen & White et al. 2018**

Cells from gastric and duodenal tissues were also put into clusters based on their transcriptional profile known gene expression for specialised cell types were overlaid to determine which transcriptional profile corresponded to which cell type

Within duodenal biopsies: intestinal alkaline phosphatase (*ALPI*)-expressing enterocytes (D1); mucin 2 (*MUC2*)-expressing goblet cells (D2); olfactomedin 4 (*OLFM4*)-expressing crypt cells (D3); and some uncharacterized cells expressing Joining Chain Of Multimeric IgA And IgM (*JCHAIN*) (D4).

Within gastric biopsies: chromogranin A (*CHGA*)-expressing enteroendocrine cells (G1); gastrokinin (*GKN1*)- and trefoil factor 1 (*TFF1*)-expressing foveolar cells (G2); and mucin 6 (*MUC6*)- and *TFF1*-expressing mucus neck cells (G3). Two parietal cell markers, *ATP4A* and *GIF* undetectable in gastric cells, indicating biopsies were taken from the gastric cardia mucosa (Owen, White et al. 2018).

4.5 High LEFTY1 and KRT7 expression define BO epithelial cells

Next, to examine cellular heterogeneity and characterise distinct BO cell populations we clustered all the BO cells by gene expression (**Figure 4.5A**). The only previously described cell type within BO are goblet cells characterized by MUC2 expression, their presence is required for the definition of IM.

The clusters (B1-B4) can be distinguished by expression of *MUC2* (B1; goblet cells, 19% of BO cells); Left-right determination factor 1 (*LEFTY1)* expression defined (B2 and B3, 71% of BO cells); and *CHGA* (B4; enteroendocrine cells, 9.7% of BO cells). Since all patients had IM on histological authentication, proportion of goblet cells was looked at in patients A to D, they comprised of 22%, 2.9%, 29% and 7.1% of cells

respectively. *KRT7* is expressed similarly across all 4 clusters, consistent with it being a marker of BO (Ormsby, Goldblum et al. 1999).The *LEFTY1*-expressing cells (B2 and B3; **Figure 4.5**) are divided into a larger, low proliferating (*MKI67* (Ki67) negative) cluster (B2) and a smaller, high proliferating (*MKI67* positive) cluster (B3). (LEFTY1), encodes for a secreted protein which is a member of the Nodal signalling pathway and the TGF-β superfamily. LEFTY1 is normally expressed in oesophageal development, where it has roles in left-right asymmetry determination (Sakuma, Ohnishi et al. 2002). Little is known about its potential roles in adult tissues, and it has not previously been associated with BO. Another recent study carrying out scRNA-seq of premalignant gastric lesions demonstrated that LEFTY1 gene and protein expression was high in areas of gastric GIM (Zhang, Yang et al. 2019). This may suggest a common role for LEFTY1 in the development of IM in BO and in the stomach.

To confirm the above finding and to further characterise LEFTY1 expression, we first examined MUC2, LEFTY1 and CHGA expression in tissue sections generated from the same BO endoscopic mucosal resection specimen. These patients had regions of dysplasia within their EMR specimens, where possible we avoided dysplastic regions and focused on marker expression in non-dysplastic BO. LEFTY1 expression was detected in BO cells (**Figure 4.5**). Interestingly, morphologically identifiable goblet cells are positive for MUC2 but not LEFTY1 or CHGA (**Figure 4.5B**).

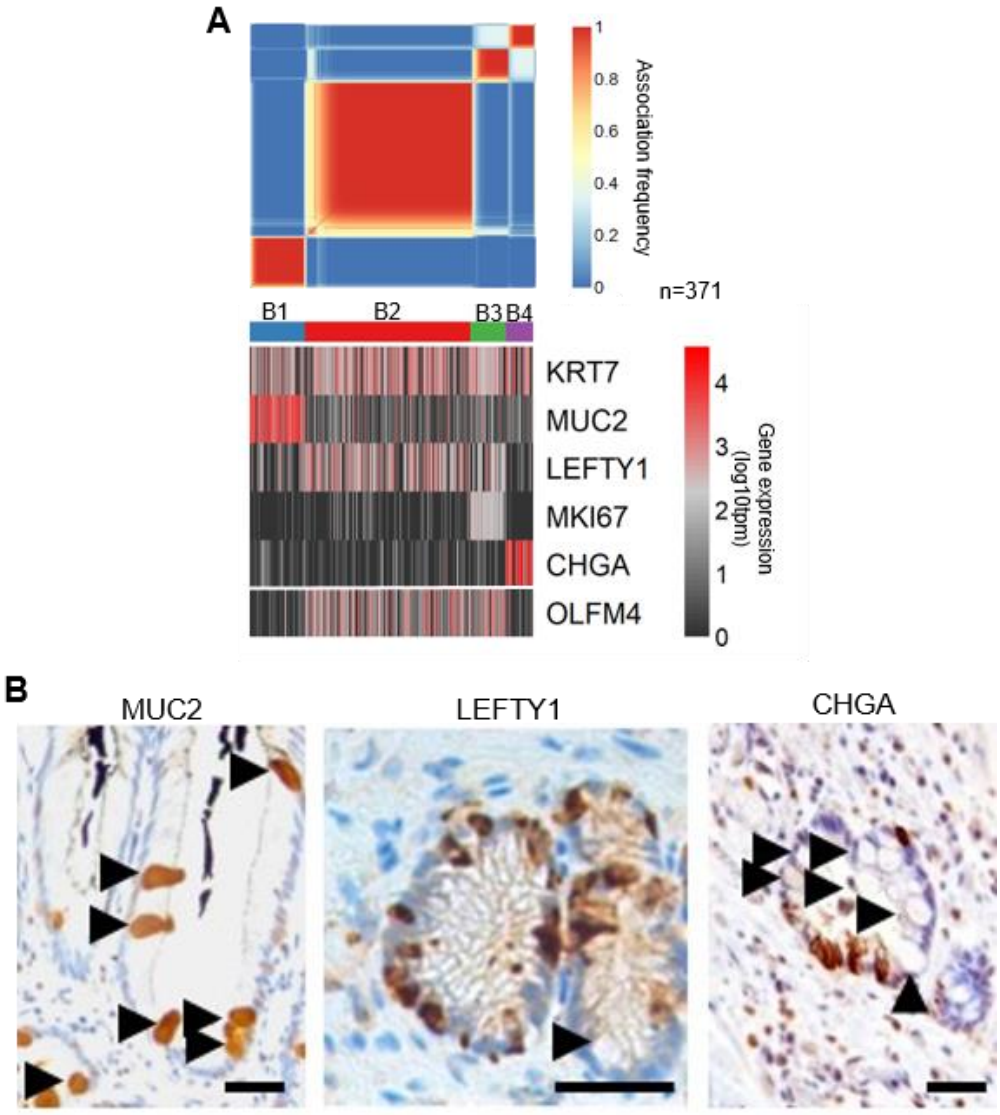
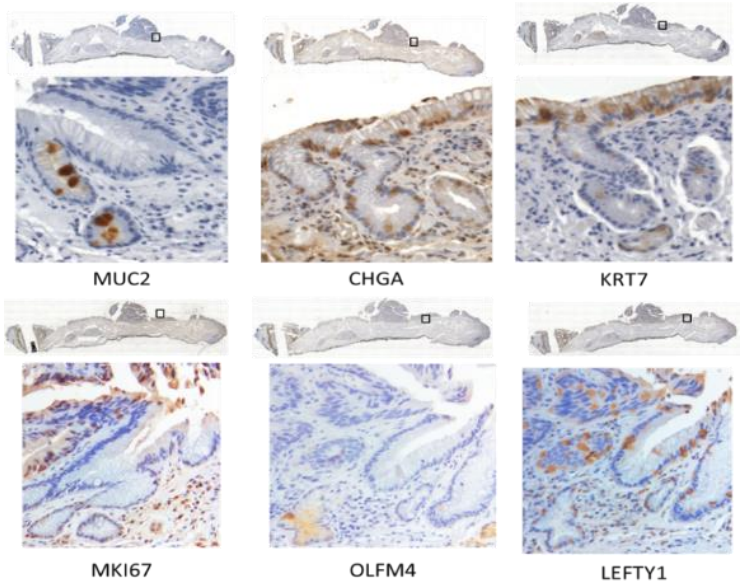


Figure 4.5 LEFTY1 and KRT7 are mainly expressed in BO cells that do not express differentiated secretory cell markers.

(A) Upper panel demonstrates cluster consensus matrix of BO cells from 4 BO patients (n=371cells). Blue-to-red colours denote the frequency with which cells are grouped together in 250 repeat clusterings of simulated technical replicates (see Methods). Clusters (B1-B4) are indicated by the coloured bars below. Lower panel, heatmaps showing expression of selected functionally relevant genes that are differentially expressed between cell clusters (>4 fold change, FDR <1e-5). **Heatmaps by Richard Owen adapted from Owen & White el al. 2018.**
(B) Immunohistochemical staining of MUC2, LEFTY1 and CHGA in adjacent sections from BO resection specimens. Black arrows indicate goblet cells on all sections (positively stained for MUC2; negative for LEFTY1 and CHGA).
(C) Immunohistochemical staining of LEFTY1 in an OSG from a normal squamous endoscopic biopsy obtained from a patient with BO. **Figure created by Michael White. Adapted from Owen & White et al. 2018.**

4.6 Validation cohort to establish expression patterns within BO

Further validation of the expression pattern genes found to depict BO cell populations was carried out on endoscopic mucosal resection (EMR) specimens from 19 patients (**Figure 4.6**). This demonstrates in a larger cohort that cell clusters seen in the scRNA-seq data correspond to cell populations stained in samples of BO. MUC2 expression which localises to goblet cells within BO glands. CHGA expression was seen throughout the epithelium and demonstrates localisation of enteroendocrine cells. KRT7 was shown to be expressed within BO-type epithelial cells. Ki67 expression is seen throughout the stroma and epithelium, Ki67+ epithelial cells expression localise in the lower half of BO glands, suggesting this is where the proliferative cells exist. OLFM4, a known intestinal progenitor cell marker was show to have high levels of expression in cells in the lower parts of the glands, often seen in the same regions of glands with Ki67 (**Figure 4.6**).



Patient sample #	Histological diagnosis	Number of sections stained for each antibody						
		OLFM4	LEFTY	KRT7	CHGA	MUC2	SPINK4	ITLN1
7825	BE with IM	1	1	1	1	1	0	0
5368	BE with IM	1	1	1	1	1	0	0
3104	BE with IM some LGD	2	1	1	1	1	0	0
3612	BE with IM	1	1	1	1	1	0	0
813	BE with IM some LGD	1	0	0	1	0	2	2
8226	BE with IM	1	0	0	2	0	2	2
2318	BE with IM	1	0	0	1	0	1	1
8173	BE with IM some LGD	0	1	0	1	0	3	3
7974	BE with IM	0	2	0	1	1	1	1
282	BE with IM	0	0	0	2	1	1	1
774	BE with IM	0	0	0	1	1	1	1
5519	BE with IM	0	0	0	1	1	1	1
5097	BE with IM dysplastic foci	0	0	0	2	0	2	2
6446	BE with IM some LGD	0	2	0	0	0	0	0
5073	BE with IM	0	2	0	0	0	0	0
9017	BE with IM	0	2	0	0	0	0	0
7836	BE with IM some LGD and HGD	0	2	0	0	0	0	0
6198	BE with IM some LGD	0	1	0	0	0	0	0
6114	BE with some LGD	0	0	0	1	0	0	0

Figure 4.6 Summary of immunohistochemical staining of biobanked endoscopic mucosal resection (EMR) tissue specimens

(A) Representative images of Immunohistochemical staining of 19 patients with BO who underwent EMR. Specimens were immunohistochemically stained for OLFM4, LEFTY1, KRT7, CHGA, MUC2, SPINK4, ITLN1, Ki67.

(**B**) Table summarising histopathology and immunohistochemical staining results of 19 patients with BO who underwent EMR. Staining analysis was carried out on sections of non-dysplastic BO. Specimens were immunohistochemically stained for markers listed above. Figure by Michael White

4.7 Examination of LEFTY1 expression in the GI tract

To further characterise LEFTY1 expression in BO epithelial cells and the GI tract I analysed a validation cohort. The validation cohort comprised of: 140 BO endoscopic biopsy samples from 80 patients; 78 endoscopic biopsies from control sites (normal oesophagus, gastric fundus and duodenum) from 26 BO patients, a further five endoscopic biopsy samples from the pylorus and five resection specimens of normal colon and (**Figure 4.7**).

Although *LEFTY1* gene expression exists in all columnar tissues but the highest levels of expression predominates in BO epithelial cells. Broadly there are two different LEFTY1 expression patterns: intensely positive cytoplasmic staining and moderate cytoplasmic staining. Moderate LEFTY1 expression, was seen in the Brunner's gland of the duodenum and in the lower portion of the glands in the gastric fundus. In the colon there are a few, cells which highly express LEFTY1. Both moderate and intensely expressing LEFTY1 cells are present in the gastric pylorus and BO (**Figure 4.7**). It is possible that more proximal tissues in the gastro-intestinal tract have higher LEFTY1 expression.

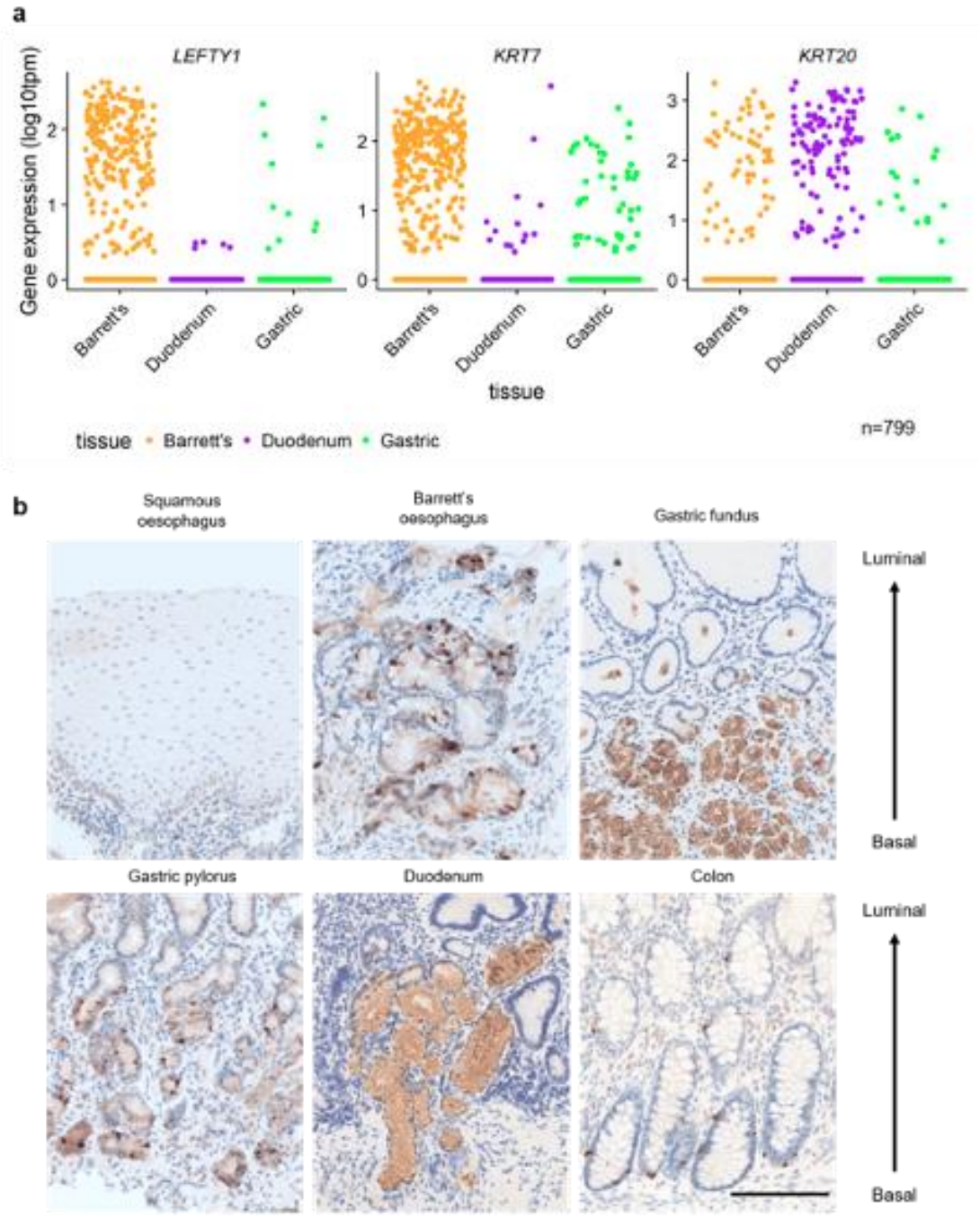


Figure 4.7 Expression of *LEFTY1, KRT7* and *KRT20* in BO, duodenal and gastric cells

(A) Jitter plots showing the expression of *LEFTY1*, *KRT7* and *KRT20* in Barrett's, duodenum and gastric cells. **This plot was created by Richard Owen adapted from (Owen & White et al. 2018)**
(B) Immunohistochemical staining of LEFTY1 in normal tissues and BO as indicated. Scale bar 200µm. **Figure created by Michael White. Adapted from Owen & White et al. 2018**

4.8 OSGs share an expression profile with BO

Data derived from patients A to D were analysed altogether (including BO and the other biopsy sites). Interestingly, expression data derived from the single cells of control sites separates clearly from the BO derived cell data. One exception to this was goblet and enteroendocrine cells. Transcriptomes from these specialised cells appeared transcriptionally indistinguishable from the goblet and enteroendocrine cells from control tissues.

In **Figure 4.8** transcriptome data from single cells derived from biopsies is depicted on a Sankey plot, which then demonstrates cell categorisation into cell types based on all expressed genes in each cell. Highly diluted RNA from brain tissue (with unique expression compared to epithelial cells) was used as a sequencing control in every sequencing batch which allowed to control between batches (**Figure 4.8**). The Sankey plot demonstrates that cell transcriptomes from each biopsy site subscribe to cell type you would expect (for example most cells sequenced from duodenal biopsies fall into the cell category of enterocytes due to their expression profile (**Figure 4.8**). Similarly, the majority of cells derived from gastric biopsies identify as mucus neck cells due to their transcriptional profile (including TFF2 and MUC6).

Fascinatingly, BO derived cells create their own cluster of cell type. In fact, 63% of cells derived from BO samples localise to the ‘Barrett’s-type’ cell category, as they do not fit the expression pattern of any previously characterised cell.

Cells derived from oesophageal biopsies split into several different cell types. A squamous cell type is seen which is driven by high expression of known squamous genes. Some cells from oesophageal biopsies are categorised as non-epithelial, others

as enteroendocrine cells. Some oesophageal cells, BO cells and a few duodenal cells fall into a ‘goblet’ cluster (**Figure 4.8**)

The most notably, a large proportion of cells derived from normal oesophageal biopsies are transcriptionally more similar to BO cells than any other cell type sequenced, and are categorised as Barrett’s type cells. These cells are characterised by high *LEFTY1* and high *TFF3* expression. (**Figure 4.8**). To further examine this LEFTY1 and TFF3 expression was examined in 140 normal oesophageal biopsies from 80 patients and five samples of normal oesophagus taken from the proximal part of an oesophagectomy specimen resected for junctional tumours. Immunohistochemical staining of oesophageal samples showed that no LEFTY1 or TFF3 expression was seen in the squamous epithelium. However, all three OSGs captured in the 140 oesophageal samples showed moderate cytoplasmic expression throughout the OSG similarly, oesophagectomy specimens demonstrated TFF3 and LEFTY1 expression in glands derived from patients who had OAC but no evidence of BO (**Figure 4.8**)**.** The variable presence of *LEFTY1*+ cells in oesophageal biopsies is explained by the fact that OSGs are found sporadically throughout the oesophagus, meaning that only three out of 140 biopsies stained demonstrated these cells in staining.

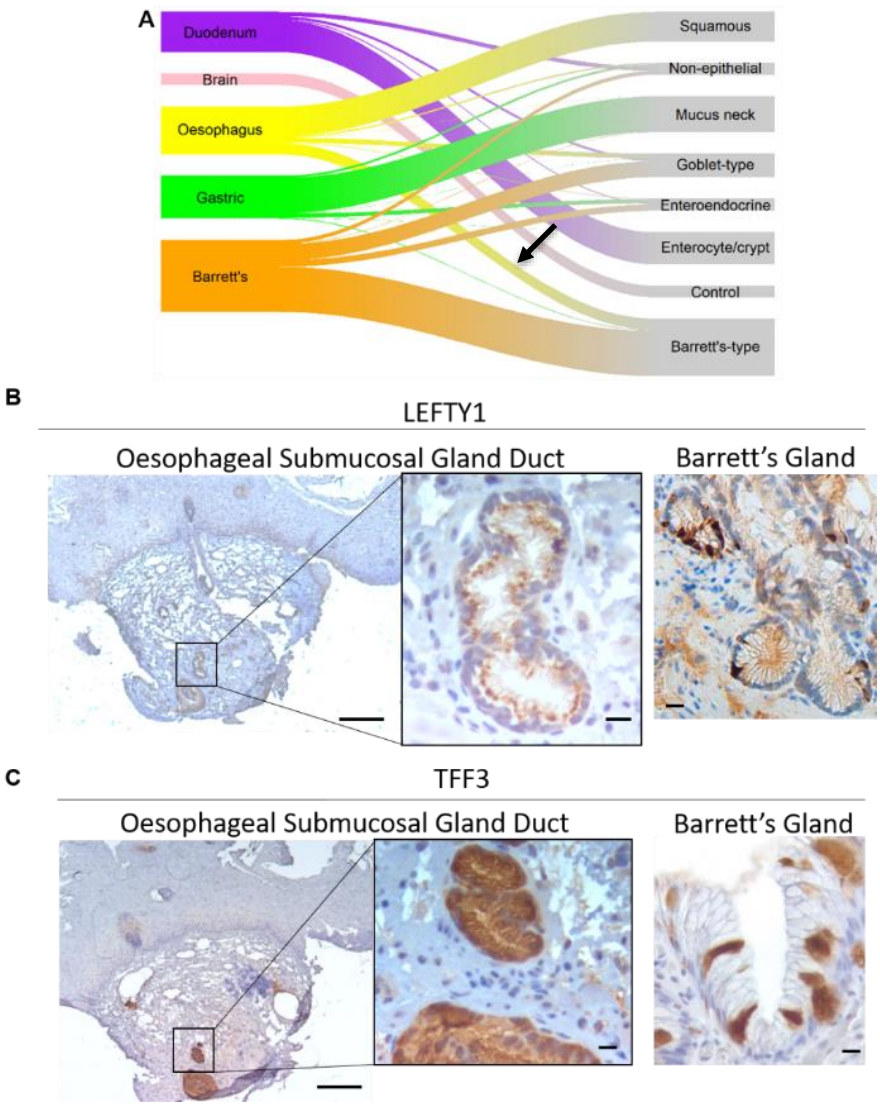


Figure 4.8 Expression profiles of Barrett's type cells and OSG cells are indistinguishable and driven by high LEFTY1 and TFF3 expression.

(A) Sankey diagram demonstrating how each tissue type sampled. Sankey diagram created by Richard Owen. The black arrow demonstrates the sub population of cells from normal oeosphageal biopsies which are transcritionally indistinguishable from Barrett's type cells from biopsies of BO. **This plot was created by Richard Owen adapted from (Owen & White et al. 2018)**

(B) + (C) Immunohistochemical staining of LEFTY1 and TFF3 respectively in normal OSGs and BO as indicated. Scale bar in zoomed out images 200µm. Scale bar in zoomed in images 30µm. **Figure created by Michael White. Adapted from Owen & White et al. 2018**

4.9 SPINK4 and ITLN1 are novel markers of goblet cells in BO

In this study, to satisfy all accepted definitions of BO, biopsies could only progress to sequencing if goblet cells were seen on histological authentication. Of the cells sequenced from BO samples 19% were characterised as goblet cells primarily due to expression of MUC2, ITLN1, SPINK4, TFF3 and other genes. Although goblet cells derived from the duodenal as well as BO tissue the data demonstrated that between tissue types, goblet cell transcriptomes were indistinguishable.

A group analysis of all goblet cells regardless of tissue origin was carried out. *MUC2* mRNA often co-expressed with intelectin 1 (*ITLN1*) and Kazal type 4 serine peptidase inhibitor (*SPINK4*) in 61% of goblet cells from duodenum and BO samples (**Figure 4.9A**). ITLN1 and SPINK4 have been previously shown to mark goblet cells in the normal gut and some non-gastrointestinal tissues (Wapenaar, Monsuur et al. 2007, Kerr, Carrington et al. 2014). In **Figure 4.9B** immunohistochemical staining of BO EMR specimens demonstrates MUC2, SPINK4 and ITLN1 expression patterns. These are representative images from EMR specimens from five patients staining carried out in technical triplicate. I observed that some cells staining strongly positive for SPINK4 were not morphologically in keeping with goblet cells.

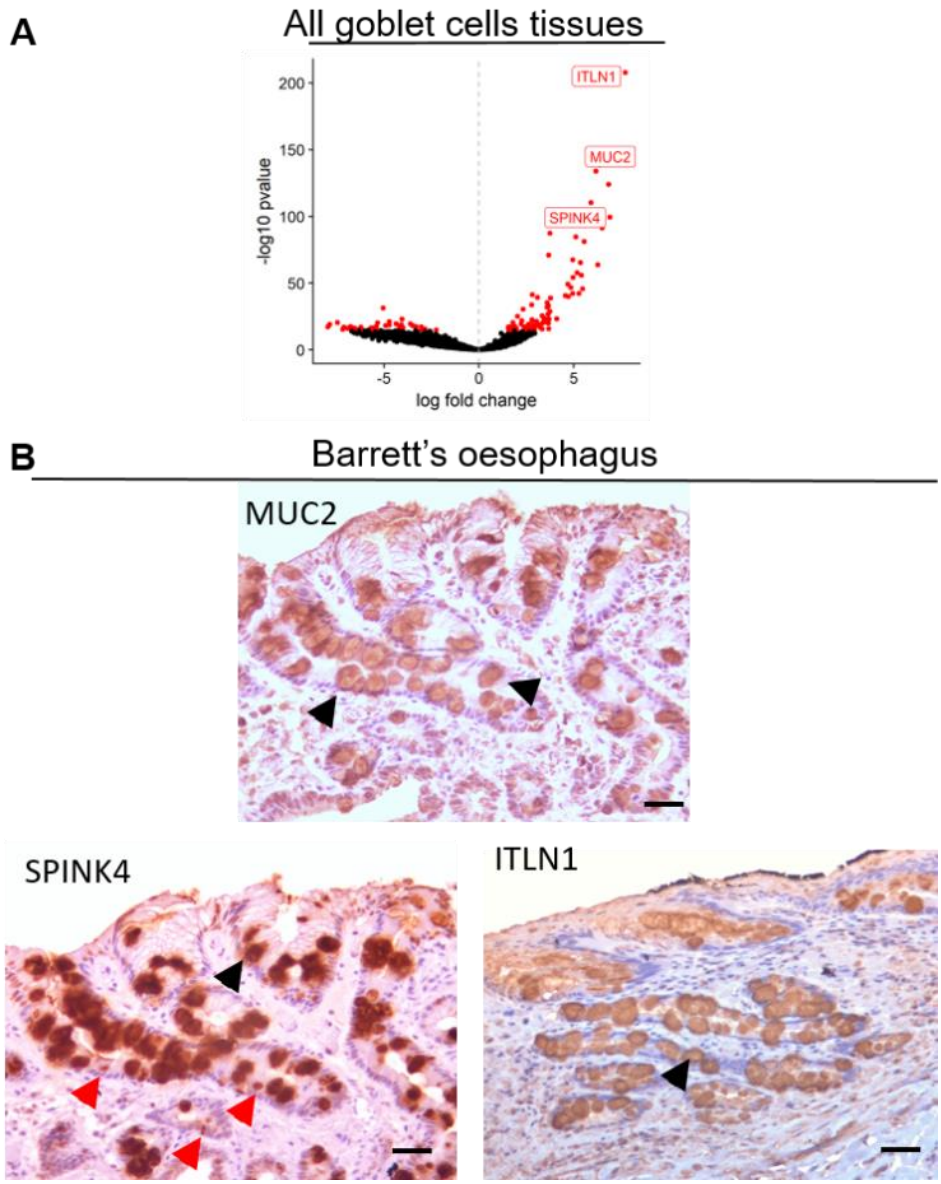


Figure 4.9 Examination of highly expressed genes in goblet cells.

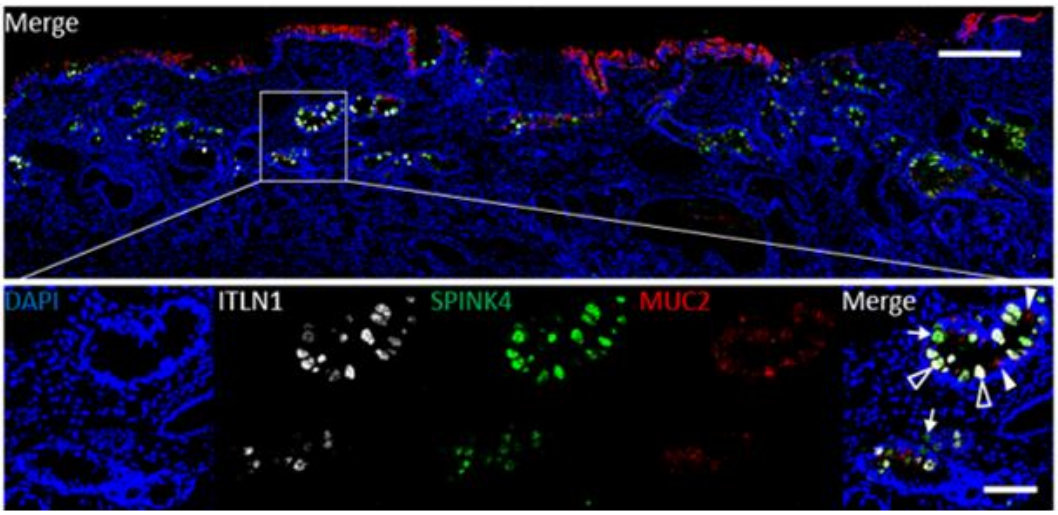
(A) Volcano plot showing fold change and p value of genes differentially expressed in the 'goblet-type' cell cluster as compared to all other cell clusters (see **Figure 3**). To reduce biological noise a threshold was set (at the tenth centile to include 90% of cells) meaning for a cell to be included at least one transcript needed to be detected from each gene of interest. Points coloured red indicate genes significant at 5% permutation test. Selected highly significant genes are labelled. **This plot was created by Richard Owen adapted from (Owen & White et al. 2018)**

(B) Immunohistochemical staining of MUC2, SPINK4 and ITLN1 demonstrating their respective staining in adjacent sections EMR specimens BO. Black arrows mark morphologically typical goblet cells and red arrows mark positively stained cells which do not morphologically resemble goblet cells. Scale bars are 50µm. **Figure by Michael White**

4.10 SPINK4 and ITLN1 mark different cells within a goblet cell population

To examine this further, triple immunofluorescence staining of BO EMR specimens with the same markers was carried out (**Figure 4.10A**). In 30 BO endoscopic mucosal resection (EMR) specimens (from 16 patients) with intestinal metaplasia but no dysplasia present, we also consistently observed cells expressing ITLN1 or SPINK4 without MUC2 (**Figure 4.10A**). I observed that some cells uniquely expressed MUC2, ITLN1 or SPINK4. Specifically, quantification of triple immunofluorescence staining of eight BO EMR specimens with intestinal metaplasia but no dysplasia taken from five patients showed 41% of MUC2 low cells expressed SPINK4 and/or ITLN1, whereas 28% of cells expressed MUC2 alone. Therefore, I hypothesised that their expression pattern may mark stages of goblet cell development *in vivo*.

A



B

Antibody			Patient sample # 8173		8226		5097		6446		5073	
MUC2	SPINK4	ITLN1	n	%	n	%	n	%	n	%	n	%
High	High	High	22	6	34	12	41	16	15	5	2	3
High	High	Low	28	7	26	9	6	2	190	59	4	5
High	Low	High	11	3	17	6	4	2	2	1	3	4
High	Low	Low	150	38	54	18	30	12	55	17	44	55
Low	High	High	40	10	134	45	70	28	26	8	11	14
Low	High	Low	110	28	11	4	7	3	20	6	4	5
Low	Low	High	16	4	7	2	90	36	11	3	7	9
Low	Low	Low	17	4	12	4	5	2	5	2	5	6
		Total cells	394		295		253		324		80	
MUC2 Low, SPINK4 and/or ITLN1 High			166	42	152	52	167	66	57	18	22	28
MUC2 High, SPINK4 and ITLN1 Low			150	38	54	18	30	12	55	17	44	55

Figure 4.10 Examination of the expression pattern of MUC2, SPINK4 and ITLN1 in BO EMR specimens.

(A) Representative triple immunofluorescence staining of Barrett's EMR specimen containing intestinal metaplasia but no dysplasia for MUC2 (red), ITLN1 (white) and SPINK4 (green); nuclei (DAPI) in blue. Scale bars are 400µm and 100µm in enlarged images.

(B) Table summarising MUC2, ITLN1 and SPINK4 immunofluorescence triple-stain expression pattern in sections of BO from 5 patients, sections contained BO with intestinal metaplasia but no dysplasia and no carcinoma. **n** is the number of cells scored as positive for expression of each protein by immunofluorescence. % is the percentage of the total number of scored cells (bottom row) that is positive for the protein(s) listed. See **Methods** for details of the antibodies used. **Figure created by Michael White. Adapted from Owen & White et al. 2018**

4.11 SPINK4 and ITLN1 may be markers of early colonic goblet cell differentiation

To test this, I analysed co- expression of SPINK4, ITLN1 and MUC2 by immunofluorescence staining of five human colon samples (approximately 500 crypts examined in each sample) (**Figure 4.11**). ITLN1 and SPINK4 co-expression was consistently present near the crypt base, whereas MUC2 expression was in cells toward middle or top of the colonic crypts. From previous work on colonic glands we know that the colonic stem cell niche exists at the bottom of the crypt and as cells differentiate they migrate up the gland (Humphries and Wright 2008). This suggests that ITLN1 and SPINK4 expression may identify an earlier stage of goblet cell differentiation in the intestine compared to cells expressing MUC2 (**Figure 4.11**). SPINK4 may be a marker of deep secretory cells in the colon. The staining pattern in BO seemed more disorganised.

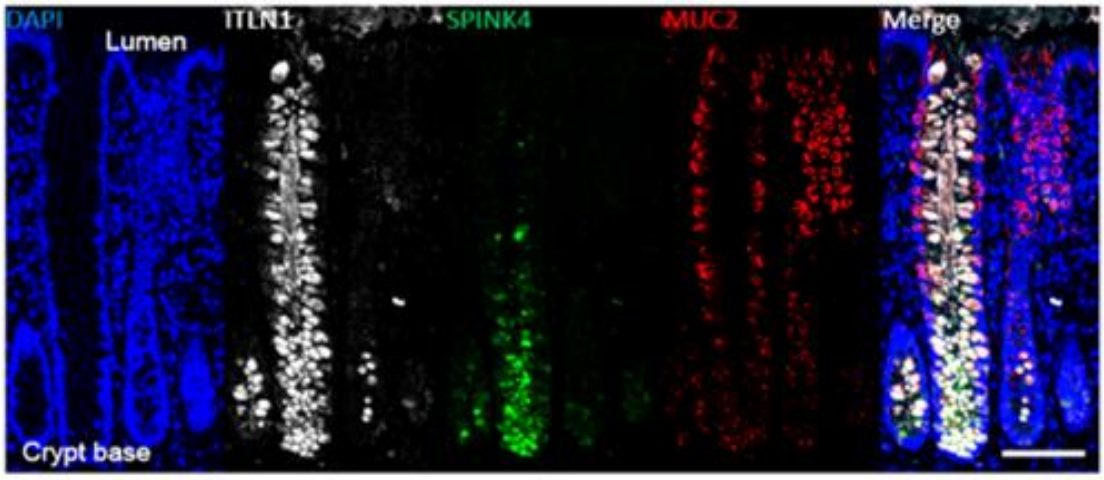


Figure 4.11 Examination of the expression pattern of MUC2, SPINK4 and ITLN1 in colon.
Triple immunofluorescence staining images of MUC2 (red), ITLN1 (white) and SPINK4 (green) in normal colon from a resection specimen (blue stain is DAPI). Scale bar 100μm. **Figure created by Michael White. Adapted from Owen & White et al. 2018**

4.12 OSGs show markers of squamous, transitional and goblet cell differentiation

OSGs are situated deep to the mucosa and are difficult to reliably biopsy. Three oesophageal biopsies containing OSGs were co-stained for SPINK4, ITLN1 and MUC2. I observed that in three out of three OSG specimens from normal oesophageal biopsies in patients with BO, OSG cells consistently co-expressed ITLN1, and MUC2, but not SPINK4. This may be because SPINK4 positive cells are more 'naïve' in goblet cell differentiation and thus they are present lower in the duct or gland and were not captured within these biopsies (**Figure 4.12A**). **Figure 4.12B** shows an OSG duct which expresses KRT14, KRT7 and MUC2 in adjacent cells this suggests a mixed differentiation pattern within OSGs. This is evidence of intestinal metaplasia in an OSG from a squamous oesophageal biopsy >20mm proximal to the BO margin. These data suggest that OSGs and BO may contain cells at different stages towards goblet cell differentiation, as seen in the colon, and that ITLN1 or SPINK4 might mark cells with some goblet cell characteristics that are not yet morphologically identifiable as goblet cells.

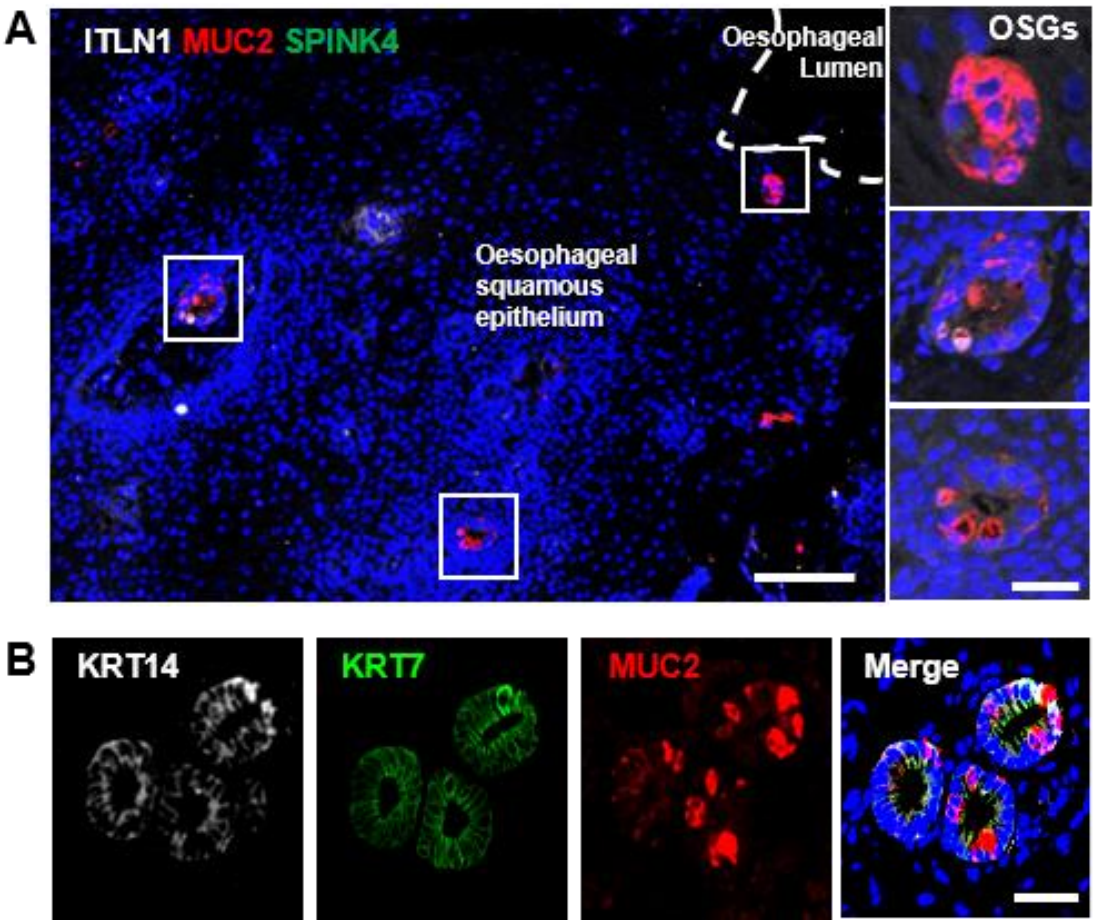


Figure 4.12 Examination of intestinal metaplasia in OSGs.

(**A**) Triple immunofluorescence staining images of MUC2 (red), ITLN1 (white) and SPINK4 (green) in normal oesophageal epithelium obtained by endoscopic biopsy (blue stain is DAPI). OSGs encroaching on the surface epithelium are shown in the enlarged images on the right. Scale bars are 200µm and 50µm in enlarged images.

(**B**) Triple immunofluorescence staining images of KRT14 (white), KRT7 (green) and MUC2 (red) in an OSG beneath normal squamous epithelium from an endoscopic biopsy of normal squamous epithelium from a patient with BO biopsy (blue stain is DAPI). Scale bar 50µm. **Figure created by Michael White. Adapted from Owen & White et al. 2018**

4.13 Goblet cell differentiation in duodenal organoids

In order to examine the difference between SPINK4 high cells and MUC2 high cells functional studies were carried out using human duodenal organoid cultures (Sato, Stange et al. 2011). Organoid cultures from three patients were established and expanded into six wells each. Once the organoid cultures were grown for five days, they were treated with intestinal differentiation media containing 5μm ɣ-secretase inhibitor, DAPT (VanDussen, Marinshaw et al. 2015). DAPT works to block notch cleavage and drive cellular differentiation towards a secretory lineage instead of the absorptive lineage, thus in duodenal cells encouraging the differentiation of goblet cells (Milano, McKay et al. 2004, van Es, van Gijn et al. 2005). Between the different time points (untreated, 24 hours and 48 hours of DAPT treatment) I observed differences in goblet cell differentiation and changes in the expression pattern in organoids when triple-stained for SPINK4, ITLN1 and MUC2. This was carried out in experimental triplicate.

Overall, organoids from nine patients were cultured, treated, fixed and stained. Between five and 10 organoids were analysed for each time-point. Expression was analysed by confocal microscopy. Analysis demonstrated that untreated organoids 44% of cells were SPINK4+ cells compared with 10% MUC2+ cells and 28% in ITLN1+ cells in the untreated organoids. At 24 hours of DAPT treatment 13% of cells were SPINK4+ compared with 24% MUC2+ and 40% in ITLN1+ cells; at 48 hours 36% of cells were MUC2+, 9% SPINK4+ and 20% of ITLN1+ cells. This suggests that ɣ-secretase inhibition, which induces goblet cell differentiation leads to a decrease in SPINK4+ cells and an increase in MUC2+ cells in primary duodenal organoids but no clear difference in ITLN1 expression was seen.

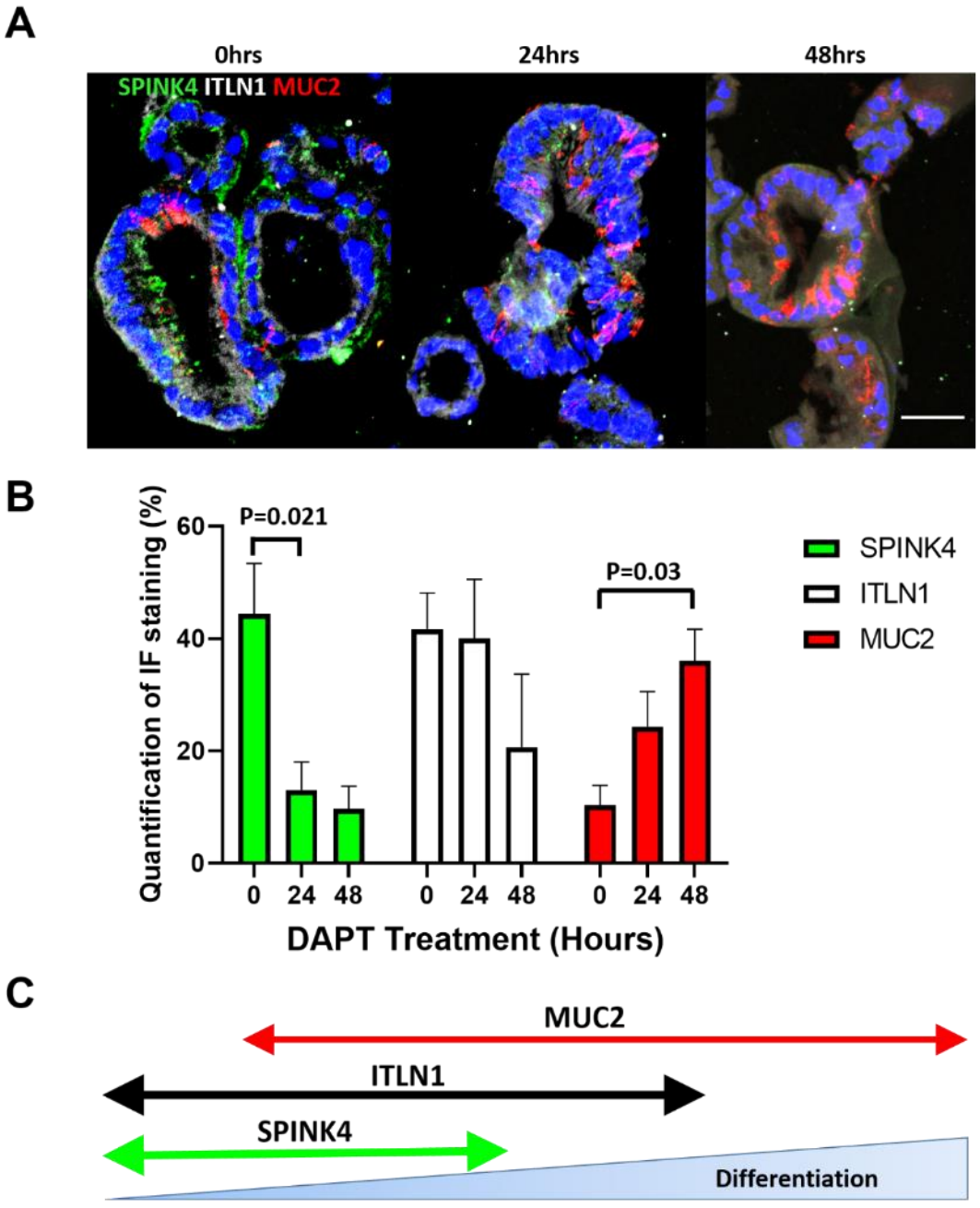


Figure 4.13 Relationship between SPINK4 and MUC2 in duodenal organoids

(**A**) Triple immunofluorescence staining images of MUC2 (red), ITLN1 (white) and SPINK4 (green) of normal duodenal organoids cultured with Notch Inhibitor DAPT for 0 hours, 24 hours or 48 hours (blue stain is DAPI). Scale bar is 20µm.

(**B**) Bar chart demonstrating quantification of the immunofluorescence staining shown above in (**A**)

(**C**) Diagram to demonstrate hypothesis that SPINK4 expression delineates early goblet cells, ITLN1 delineates intermediately differentiated goblet cells and MUC2 expression delineates more terminally differentiated goblet cells. Figure by Michael White

4.14 Effect of ɣ secretase inhibition on *SPINK4*, *ITLN1* and *MUC2* expression in cell lines

To examine the transcriptional effect of ɣ secretase inhibition in cell lines on *SPINK4*, *ITLN1* and *MUC2* expression. LS180 colorectal cancer cell line was chosen as it is known to differentiate into goblet cells *in vitro* (Enss, Cornberg et al. 2000). After 4 hours we see a significant increase in the expression of *MUC2* mRNA alone (**Figure 4.14**). After 8 hours of gamma secretase inhibitor treatment significant increases were seen in *SPINK4*, *ITLN1* and *MUC2* mRNA levels. After 8 hours mRNA expression levels of all 3 genes drops away. At 24, 36 and 48 hours the *MUC*2 mRNA levels again increase. This data suggests that *MUC2* mRNA transcription is more responsive to ɣ secretase inhibition than *SPINK4* and *ITLN1* (**Figure 4.14**). This was carried out in biological triplicate.

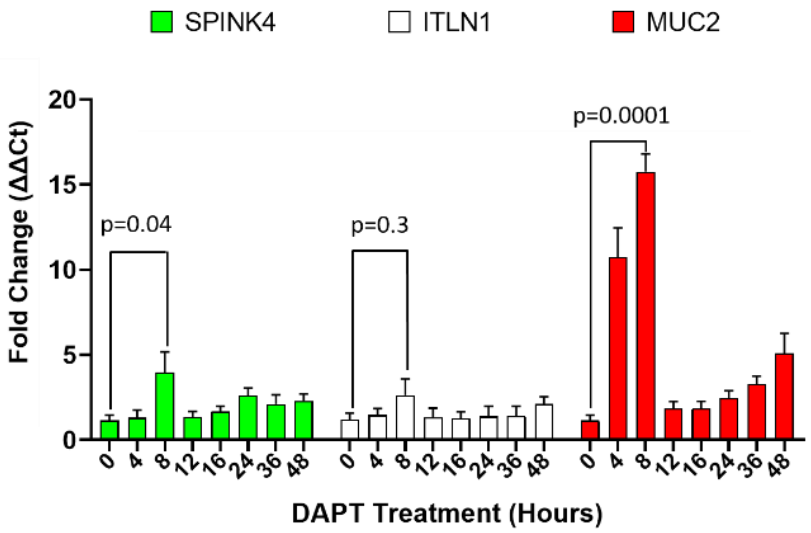


Figure 4.14 Transcriptional response to Notch inhibition to induce Goblet cell differentiation

Relative expression of SPINK4, ITLN1, MUC2 mRNA by quantitative RT-PCR using LS180 colorectal cancer cell line treated at different time points with 5µm DAPT (gamma secretase inhibitor) Treatment in order to induce goblet cell differentiation. Expression relative to β2Microglobulin (B2M). Figure by Michael White

4.15 Inducing *SPINK4* or *ITLN1* expression does not drive goblet cell differentiation in cell lines

Further experiments were carried out to examine if induced expression of SPINK4 and ITLN1 influenced MUC2 protein expression (**Figure 4.16**). Three cell lines Caco2, HCT116 and LS180 were plated and each transfected with a control expression plasmid, a SPINK4 expression plasmid and an ITLN1 expression plasmid. Cells were then triple stained for ITLN1, SPINK4 and MUC2 expression. Whilst transfection of the expression plasmids for SPINK4 and ITLN1 induced their respective protein levels in all three cell types. Neither SPINK4 nor ITLN1 expression induction had any effect on MUC2 expression. Data from **Figure 4.16** suggest there is no evidence of a transcriptional link between SPINK4, ITLN1 and MUC2.

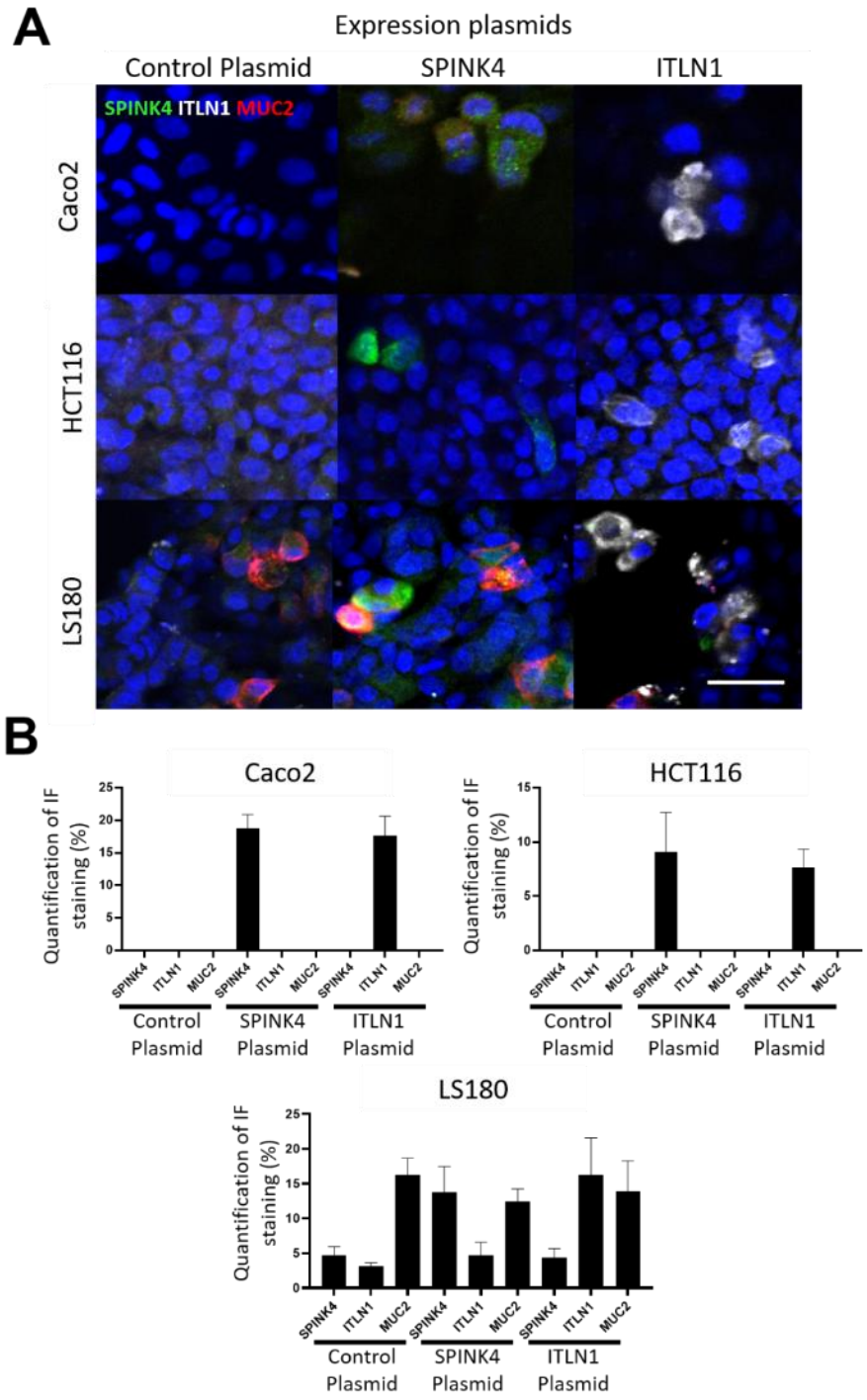


Figure 4.15 Transfection of SPINK4 and ITLN1 plasmid into colorectal cancer cell lines

(**A**) Triple immunofluorescence staining images of MUC2 (red), ITLN1 (white) and SPINK4 (green) of colorectal cancer cell lines Caco2, HCT116 and LS180 following transfected with expression plasmids to SPINK4 and ITLN1. Scale bar is 20µm.

(**B**) Bar charts to demonstrate quantification of immunofluorescence staining above (**C**) in each of the three cell lines. Figure by Michael White

4.17 Discussion

In this study, we used sc-RNA-seq data from human endoscopic biopsies paired with immunohistochemical staining and other experiments to delineate cell sub-populations in BO. These cell populations had never previously been described other than their histological appearance and IHC staining pattern. These data revealed a near identical transcriptional concordance between cells within oesophageal squamous biopsies and BO type cells (Owen, White et al. 2018). The origin of BO has been contested between many groups. Some previous studies have supported a theory that BO may derive from OSGs (Van Nieuwenhove and Willems 1998, Abdulnour-Nakhoul, Nakhoul et al. 2007, Leedham, Preston et al. 2008, Lörinc and Öberg 2012, Garman 2017, von Furstenberg, Li et al. 2017). However, since our study, the most comprehensive study of BO and OSGs to date has been published with much larger numbers of sequenced cells (Nowicki-Osuch, Zhuang et al. 2021) In their study Nowicki Osuch and colleagues revealed that a KRT7+ transitional cell that originates at the GOJ is likely to the cell of origin of BO (Nowicki-Osuch, Zhuang et al. 2021). A key limitation from our study was the low cell numbers, experiments were carried out before higher through-put scRNA-seq methods had been established. Therefore cell numbers did not allow for cell transcription roadmaps which enable mapping of differentiation pathways within OSGs. It is possible that the cells we saw within the sequencing data and labelled as OSGs were not derived from submucosal glands but were instead evidence of early intestinal metaplasia within the squamous oesophagus.

Interestingly, like all other normal gastrointestinal epithelia BO contains cells with specialised differentiation such as entero-endocrine cells expressing chromogranin A. BO is largely made up of a cell type which we have labelled as a BO type cell which is characterised by LEFTY1+, KRT7+ and OLFM4+ expression. Our study also

demonstrated for the first time that *LEFTY1* gene expression is highly expressed in BO and OSG cells. Published literature suggests that LEFTY1 is critical in left-right determination in early embryogenesis (Smith, Noël et al. 2011). Several studies have highlighted the importance of other developmental gene programmes in the development of BO. Many genes previously described in BO pathogenesis have critical roles in development as well as differentiation including but not limited to NOTCH and WNT signalling pathways. It is thus not surprising that the developmental gene *LEFTY1* is expressed in OSGs and that as these structures expand in the development of BO. LEFTY1 has been shown to be part of the Nodal pathway and indirectly regulated by TGF-β and BMP signalling (Miyata, Azuma et al. 2012). Other studies have shown that TGF-β pathway expression is altered in BO (Hyland, Hu et al. 2014). Since our data was published (Owen, White et al. 2018) *LEFTY1* expression in BO has also been highlighted in a recent publication Hans Clever's group who set out to perform a deep molecular characterisation of BO but, rather than only examining non dysplastic BO they also examined LGD, HGD and early adenocarcinoma (Busslinger, Weusten et al. 2021). Although the carried out a comprehensive analysis using whole genome sequencing and scRNA-seq they did not offer further discuss the potential role for LEFTY1 in BO (Busslinger, Weusten et al. 2021). In a further study, epigenetic and transcriptomic analysis was used to determine differentially expressed genes at different stages of normal gastric (NG) and BO differentiation. Direct comparison of undifferentiated cell populations from NG and BO, followed by differential expression between undifferentiated and differentiated cells from BO showed activation of both c-MYC and *HNF4A* drive the transcriptional programs of BO cells (Nowicki-Osuch et al 2021). In this study, normal gastric organoids were grown and transfected with c-MYC and HNF4A

expression plasmids, both were individually shown to significantly increase the expression of *LEFTY1* expression in vitro. This gives *in-vitro* evidence for BO deriving from gastric cells. Since our study was published another study has used single cell RNA sequencing to investigate early gastric cancer development in which they demonstrated candidate gastric cancer stem cells expressed high levels of LEFTY1 and OLFM4 (Zhang, Yang et al. 2019).

Our data suggests a strong overlap with the expression of OSGs. We demonstrate evidence that KRT7+ cells exist within OSGs and KRT7 expression is seen throughout BO. Previous studies have described OSG ducts lined with KRT5+ KRT7+ P63+ cells (Glickman, Chen et al. 2001, Garman, Kruger et al. 2015, Gonzalez, Benezech et al. 2016). Recent studies by Frank McKeon's group have described a hypothesis for a residual embryonic stem cell which is activated by inflammation and also, separately described a KRT5+KRT7+P63+ transitional basal cell which lies at the SCJ and is able to give rise to BO (Wang, Ouyang et al. 2011, Jiang, Li et al. 2017). Indeed these transitional cells at the gastro-oesophageal junction SCJ have a KRT5+KRT7+P63+ profile potentially similar to the OSG ductal cell population described (von Furstenberg, Li et al. 2017). It seems the OSG and GOJ are both sites of squamous columnar junctions and both demonstrate KRT7+ transitional cell populations (Nowicki-Osuch, Zhuang et al. 2021). A recent study by Rebecca Fitzgerald's group carried out an in depth molecular phenotyping of the transitional cell population of the squamous columnar junction of the OSG-oesophageal junction and the squamous columnar junction of the gastro-oesophageal junction (Nowicki-Osuch, Zhuang et al. 2021). They conclude that the $KRT7^{high}$ cell population from the GOJ have the highest similarity to OSG cells. This suggests a possible unification of multiple BO cell of origin hypotheses where the transitional cells, residual embryonic

cells and OSG cells share a rare molecular profile and as such might belong to the same cell lineage and it is possible that they share the same developmental origin. At the same time Nowicki-Osuch and colleagues presented data suggesting very little evidence for BO originating directly from normal squamous oesophageal epithelium and strong data that supports BO deriving from gastric mucosa (Nowicki-Osuch, Zhuang et al. 2021).

Our findings support a potential model in which BO developed from acid and bile reflux-induced damage to the oesophagus activates a 'repair mechanism' through the expansion, differentiation and/or selection of OSGs cells leads to columnarisation of the surface epithelium of the oesophagus. OSG cells have an adaptive advantage when fulfilling is role as they secrete alkaline bicarbonate, which is likely to play a part in protecting the oesophagus from gastro-oesophageal reflux damage. Indeed a substantial body of work has been carried out on the role of OSGs in oesophageal repair (Krüger, Gonzalez et al. 2017)

In order to avoid controversy, we used the most internationally accepted BO definition, which meant in order to be defined as BO the biopsies must contain goblet cells. Classically intestinal goblet cells are labelled with MUC2. scRNA-seq enabled more detailed transcriptional analysis of BO cell populations than had ever been previously published at the time. In fact, goblet cells comprised of 19% of BO cells sequenced, which if separated from their tissue of origin had a strong transcriptional overlap with goblet cells within the duodenum control cells. Using the well-understood crypt-differentiation pattern of the intestine, we examined the expression patterns of SPINK4, ITLN1 and MUC2 expression. Intestinal stem cells exist within a niche at the bottom of the crypt and as they divide asymmetrically, cells progress up the sides of the crypt and become more terminally differentiated at the top of the

crypt. Interestingly ITLN1 and SPINK4 were expressed lower in intestinal crypts compared with MUC2, which demonstrated higher expression at the top of the crypts on the luminal surface. This finding was further investigated in the *in-vitro* setting using ɣ secretase inhibitor treatment on human duodenal organoids in order to drive differentiation down the secretory lineage. We found SPINK4 expression to occur early in the differentiation of goblet cells.

Similarly, we also observed that SPINK4 and ITLN1 were often expressed deeper down the BO crypt and less often at the luminal surface where MUC2 expression was strongest. ITLN1 expression but not SPINK4 expression was observed in oesophageal biopsies containing OSGs taken from BO patients, which further supports our hypothesis that BO may originate from a cell type that exists in OSGs. Our results suggest that intestinal goblet cell characteristics exist in BO even without the presence of morphologically identifiable goblet cells, supporting the view that clinical diagnosis of BO should not require the detection of goblet cells. In a recent study, sc-RNA-seq was used to examine role of Paneth cells in the colonic crypt, SPINK4 was identified as a marker expression in Paneth cells, and this suggests that SPINK4 may be expressed in other cells within the secretory differentiation lineage (Van es et al. 2019). The morphological presence of Paneth cells in BO is not a common feature but it is sometimes noted. This data further still suggests that SPINK4 is an early differentiation marker in goblet cells and the secretory lineage generally

4.18 Limitations

A significant limitation of our sc-RNA-seq data is that the majority of the TFF3+ OSG type cells derived from patient A. All of patient C's oesophageal cells failed

sequencing quality control. Sequencing data from patient B and D's oesophageal biopsies consisted of a majority of squamous cells by did not demonstrate any OSGs. This is an effect of endoscopic biopsying, OSGs are not visible endoscopically and our ethical approval limited the number of normal squamous biopsies biobanked. In our validation immunohistochemical staining I demonstrated only 3 of 140 biopsies from 80 patients had evidence of OSGs within the biopsy. The density of OSGs varies throughout the oesophagus with more towards the lower oesophagus.

It is highly likely that our FACS selection of cells during cell processing has a tendency towards more vital cells and reduced number of terminally differentiated cells. This has been demonstrated in quality control figures by Dr Richard Owen, not in this thesis (Owen, White et al. 2018).

Patient number and cell number are a limitation to this study. In another recent study, sc-RNA-seq was used in BO where cells from oxyntic and antral gastric biopsies were used as control sites. This study identified that the strongest transcriptional overlap was between BO and antral cells (Busslinger, de Barbanson et al. 2021). Examining the data it can be seen that they did not detect any OSG cells profiles within their normal oesophageal biopsies, thus illustrating the difficulty examining OSGs using endoscopic biopsies when their distribution is unpredictable and deep to the surface epithelium.

Together, our findings help characterize BO in humans. In addition, this study demonstrates the power of single cell analysis of clinical samples to uncover biological relationships among cell types and cellular heterogeneity in healthy and diseased tissues. In order to make more progress in identifying the cell of origin in BO further experimental tools are required. An animal model of BO which demonstrated

disease similar to human BO and also demonstrated OSGs would be an important model. Given that rodents lack OSGs, and the lack of an *in vitro* model of human oesophageal glands, analysis of human biopsies currently provides the most reliable approach to dissect the cell relationships of BO (Kabir, Karami et al. 2022).

At present porcine models are used, however they have limitations such as animal size and space required for environmental enrichment. Within this model lineage tracing experiments could be carried out to track the development of BO.

There are limitations to experiments examining early goblet cell differentiation. Use of human duodenal organoids is hampered by the atypical physiology of the organoid culture environment, lack of stroma, which are difficult to improve on when using in vitro culture systems.

Future improvements in single cell sequencing techniques may enable more systematic genetic confirmation of the cellular origin of BO through DNA analysis and allow higher throughput, to reduce the selection bias inherent in the methodology we have used. Also, it is important to note that our study has not investigated potential origins of OAC. Future studies are needed to address the cell relationships of BO and OAC and how this relates to recent work suggesting that OAC is highly similar to a sub-set of gastric cancers.

Chapter 5: Results – Identification of stem-like cells in BO and OSGs

Identification of stem cells or progenitor cells has long been the goal of many studies into epithelial development and carcinogenesis. The oesophagus is a complex organ with potentially more than one niche containing multipotent cells. Through understanding the progenitor cell for BO better, we aim to improve understanding of why patients develop BO.

5.1 sc-RNA-seq identifies candidate progenitor markers

We used sc-RNA-seq data to investigate a potential progenitor population within BO. Other groups have tried carrying out similar work. StemID is a published workflow designed to find cells with stem-like properties in scRNA-seq data by calculating a 'stem-ness' score based on the entropy of cell clusters and the number of links between clusters (Grun et al., 2015, 2016). Progenitor cell markers and populations are better understood in some epithelial populations that others. In the upper Gastro-intestinal tract duodenal progenitors are the best described. As a control, we analysed duodenal cells from endoscopic biopsies of BO patients (A-D) from D2 of the duodenum. Using the StemID algorithm we found the highest scoring cluster was enriched for *LGR5* expression, consistent with *LGR5* being a known marker of intestinal stem cells (Barker, van Es et al. 2007, Sato, Vries et al. 2009). However, applying StemID to isolated, sequence cell data from other individual tissues biopsies from the same patients did not identify any well-known stem cell markers (**Figure 5.1**), even though a small number of LGR5 positive cells are present in all tissues sequenced (**Figure 5.1**). Stem ID is not specific or biased towards LGR5+ cells and has been shown to identify known stem cell populations in several data sets including

haematopoietic stem cells (Grun, Muraro et al. 2016). The algorithm is limited when an incomplete data set is used where there is not full representation of the cell types within the tissues or when the progenitor cell is not present in the data.

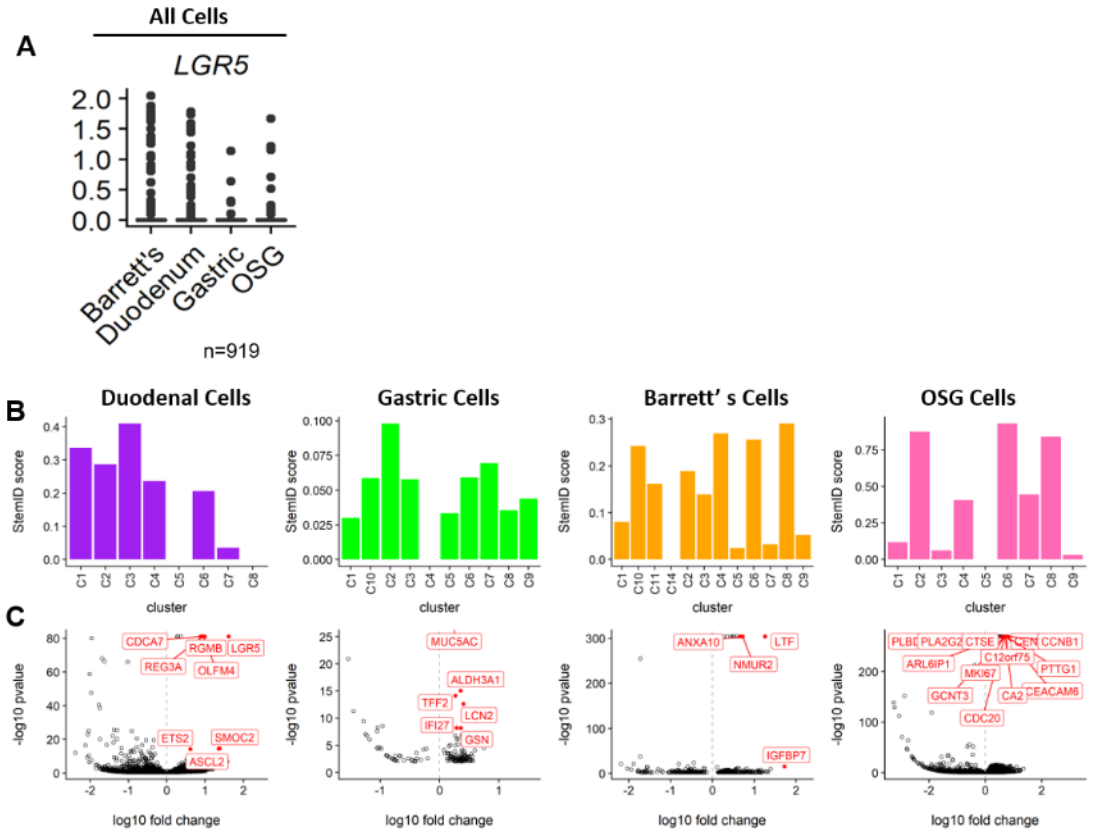


Figure 5.1 Using StemID to identify candidate progenitor cell markers.

Differentially expressed genes in candidate stem cell-like clusters in upper gastrointestinal tissues. (**A**) A boxplot showing the expression of stem cell marker LGR5 across all cells isolated from biopsies across all tissue types. Including (207 duodenal cells, 221 gastric cells, 371 Barrett's cells and 120 Oesophageal submucosal gland cells due to their derivation for biopsies of normal oesophagus but expression of TFF3, in total 919 cells. (**B**) StemID scores across all clusters computed for duodenum (purple), gastric (green), BO (orange) and oesophageal submucosal gland cells (pink) in bar plots from top to bottom. Scores are calculated from multiplication of the entropy (spread from the cluster mean) and the number of cluster links arising from a given cluster. Oesophageal submucosal gland cells were deduced by removing squamous (KRT14+) cells from all normal oesophagus cells from patients A-D (cells from patients E and F were removed to avoid comparing cells between batches). (C) Volcano plots showing significantly expressed genes in the highest scoring cluster corresponding the adjacent plot in A, from top to bottom these are duodenum, gastric, BO and oesophageal submucosal gland cells. **(This figure was created by Richard Owen and David Severson and features in Owen & White et al. 2018.)**

5.2 Combined analysis of BO and OSGs suggests *OLFM4* as a possible progenitor cell marker

Since a recent study showed that BO contains pluripotent cells (Yamamoto, Wang et al. 2016), and in view of the striking transcript profile overlap between OSG and BO cells, we therefore analysed all BO and OSG cells together using StemID (patients A-F). Interestingly, the highest scoring cluster was enriched for the stem-cell associated gene *OLFM4* (**Figure 5.2A**, blue asterisk). BO cells from all four patients with BO (A-D) contributed to this cluster, and oesophageal cells from two patients with BO (A and B) (**Figure 5.1**). The second highest scoring cell cluster (**Figure 5.2A**, red asterisk) was enriched for *LYZ*, a marker of Paneth cells, which are long-lived secretory cells found adjacent to the stem cell niche in the intestinal crypt base.

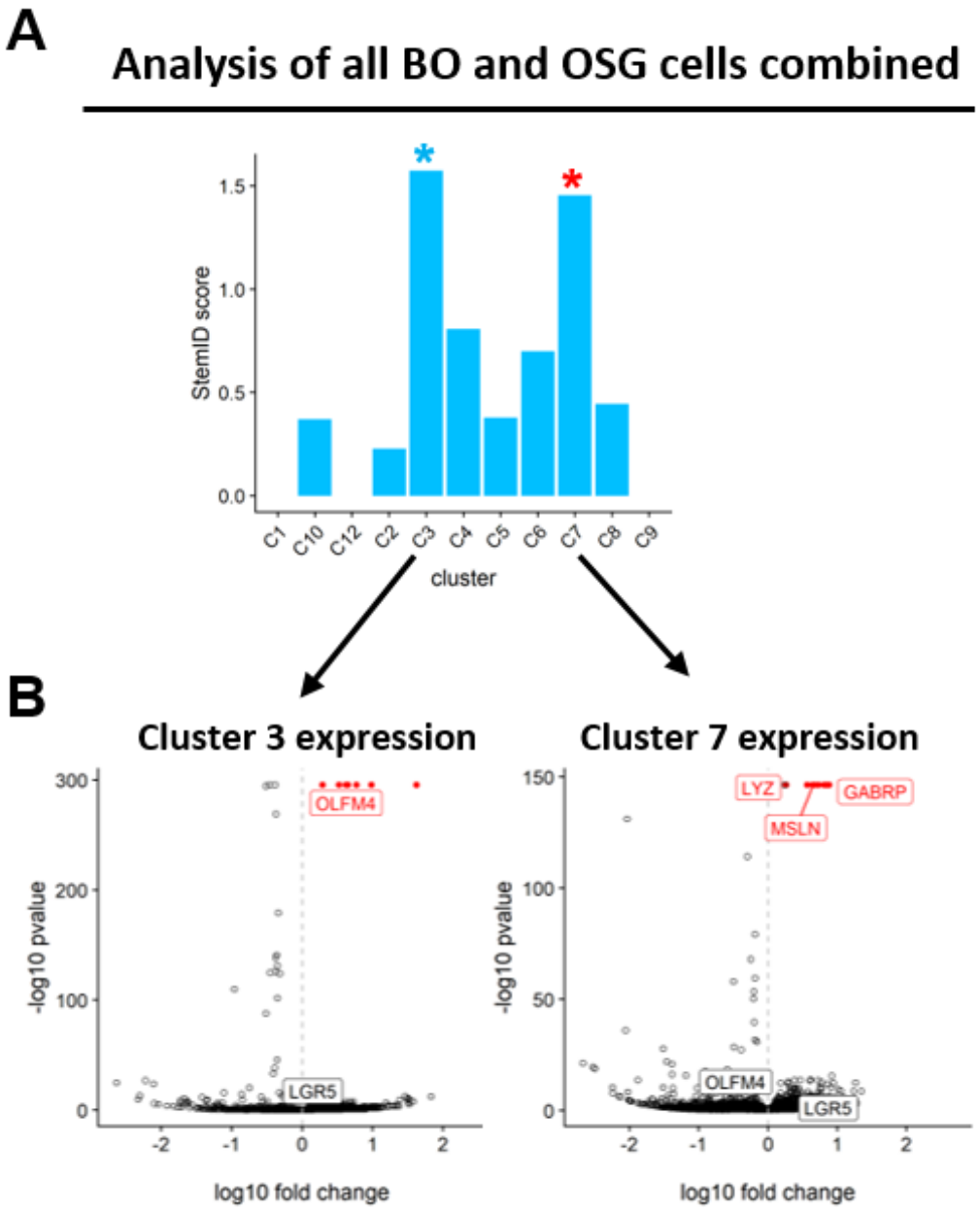


Figure 5.2: Combined analysis of BO and OSG cells demonstrate candidate progenitor populations from highly expressed genes. (A) Bar plot shows StemID scores across all RaceID2 clusters applied to all non-squamous oesophageal cells (BO and oesophageal cells with <5 KRT14 counts to exclude squamous cells, n=533). Scores are calculated from multiplication of the entropy (spread from the cluster mean) and the number of cluster links arising from a given cluster. (B) Bar plot showing the number of BO and OSG cells isolated from each patient and represented in the highest scoring StemID cluster in A (cluster 3). (C) Volcano plots showing differentially expressed genes in the highest scoring cluster (C3, blue asterisk, left side) and second highest scoring cluster (C7, red asterisk, right side). Points coloured red indicate the most significant genes with a fold change > 2. Selected highly significant genes are labelled. **(This figure was created by Richard Owen and David Severson and features in Owen & White et al. 2018)**

5.3 Examining OLFM4 expression in the gastro-intestinal tract

OLFM4 has been shown to associate with *LGR5* expression and marks stem cells in intestinal tissue in normal and metaplastic contexts (van der Flier et al., 2009; Jang et al., 2015). Consistent with this, immunohistochemical staining of samples from 5 patients detected OLFM4 expression in human colon crypt bases, where stem cells are known to be located (**Figure 5.3A**). In 8 BO sections from 7 patients, we observed that OLFM4 protein expression was less restricted to the crypt base (**Figure 5.3B**), similar to previous observations of LGR5 expression patterns in BO (Lavery, Nicholson et al. 2014) and in contrast to the expression of OLFM4 in control tissues, samples from 3 patients were stained for each tissue type to ensure that a representative staining pattern was obtained (**Figure 5.3C**).

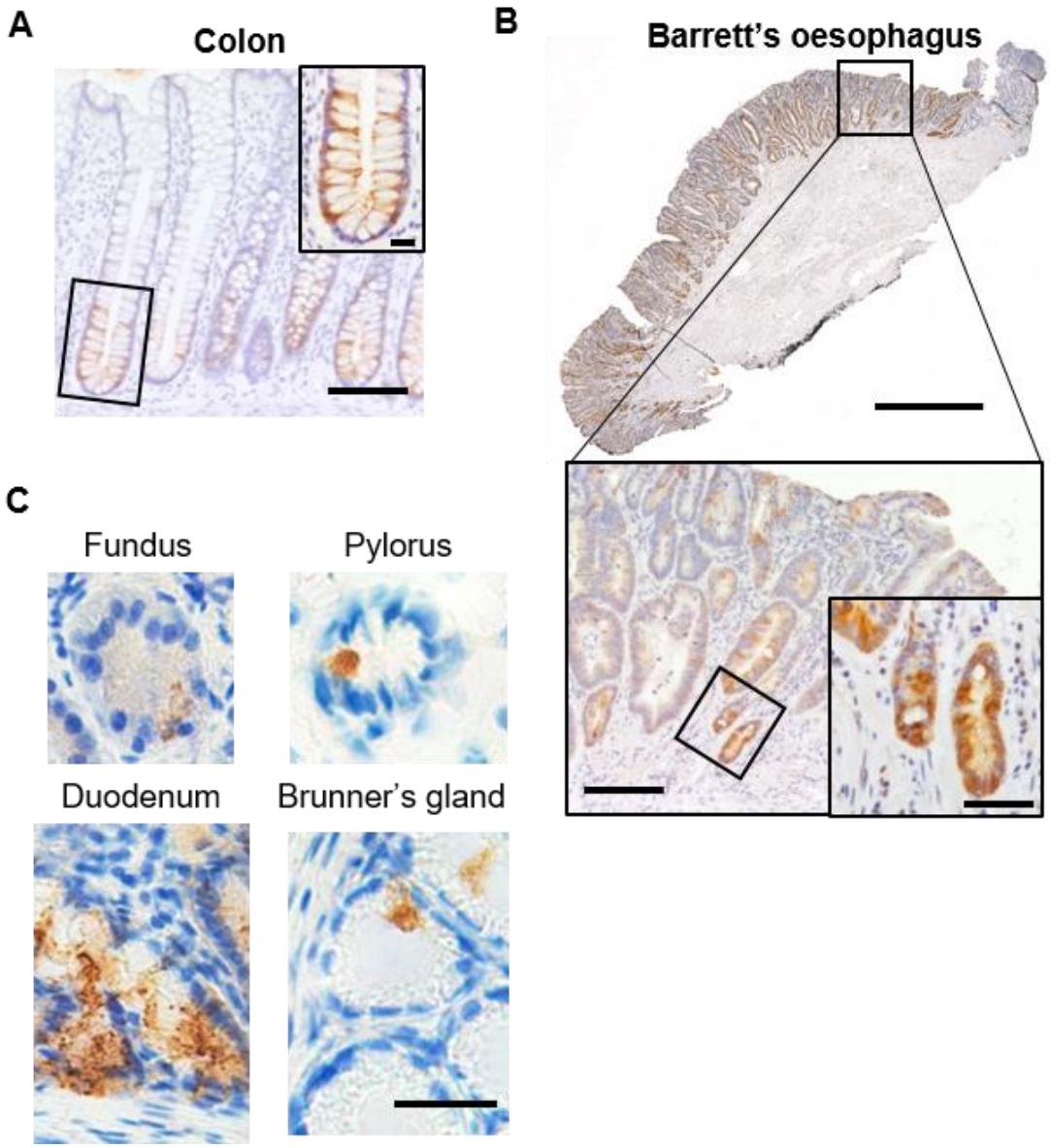


Figure 5.3: Immunohistochemical staining of OLFM4 in upper gastrointestinal tissues.

(A) Immunohistochemical staining of OLFM4 in human colon (close-up of base of crypt inset). Scale bars are 100 µm and 20 µm in inset.

(B) Immunohistochemical staining of OLFM4 in BO mucosal resection containing intestinal metaplasia but no dysplasia, with enlarged image. Scale bars are 1000 µm, 200 µm in enlarged image and 50 µm in inset.

(C) Immunohistochemical staining of OLFM4 in glandular structures in the upper GI tract and structures as indicated. Scale bars are 50µm. **Figure created by Michael White. Adapted from Owen & White et al. 2018**

5.4 Examining OLFM4 expression in oesophageal epithelium

In OSGs beneath normal squamous epithelium, OLFM4 positive cells were seen within the gland structures (**Figure 5.4**). Interestingly, OLFM4 staining in OSGs from patients without BO was much more restricted than seen in OSGs taken from patients with BO (**Figure 5.4**), although the number of cases examined is limited this staining pattern was observed in 5 patient's oesophagostomy resection specimens. This seems to suggest that OLFM4+ cell population is expanded in OSGs of patients with BO. This may be why other studies of OSGs have not seen OLFM4+ cells as OSGs under BO seem to have a higher expression of OLFM4.

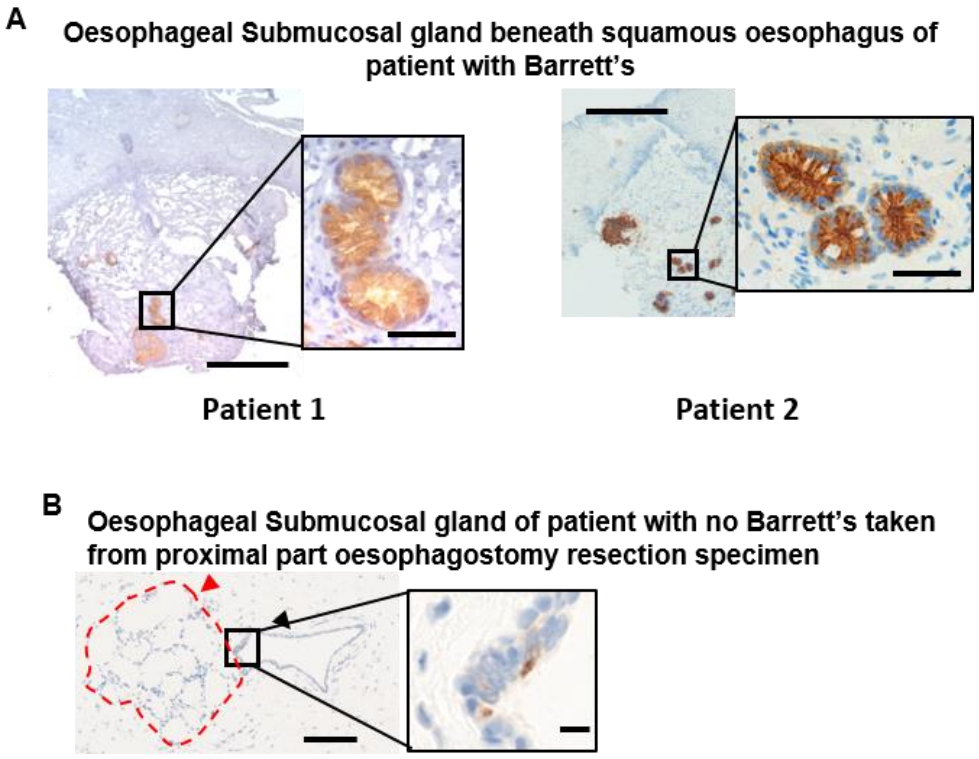


Figure 5.4: Immunohistochemical staining of OLFM4 in OSGs associated with BO and normal oesophageal epithelium.

(A) Two separate examples of immunohistochemistry in OSGs from endoscopic biopsies of normal squamous oesophagus in patients with BO. Scale bars are 300 µm and 50 µm in enlarged image.

(B) Immunohistochemical staining of OLFM4 in OSG under normal oesophagus taken from the proximal part of an oesophagectomy specimen resected for Siewert type III junctional tumour in a patient with no BO. Red dashed area and arrow indicates OSG, black arrow indicates OSG duct. Scale bars are 300 µm and 20 µm in enlarged image. **Figure created by Michael White. Adapted from Owen & White et al. 2018**

5.5 Examining co-expression in OLFM4+ cells

Most notably from the scRNA-seq data, *OLFM4* has a higher mean expression in the *LEFTY1*-positive clusters (B2/B3) compared to the clusters expressing known markers of the differentiated goblet (*MUC2*) and enteroendocrine (*CHGA*) lineages (**Figure 4.5a**, B1 and B4, respectively). To examine co-expression of *OLFM4*, *LEFTY1*, *MUC2* and *CHGA* in individual cells, we applied a threshold at the tenth centile to include 90% of cells in which at least one transcript was detected from each

gene of interest. Using this threshold, half of the BO cells express *LEFTY1* and *OLFM4*, alone or in combination (29% *OLFM4* and *LEFTY1*; 13% *OLFM4* only; 11% *LEFTY1* only). *LEFTY1* and *OLFM4* positive BO cells rarely co-expressed markers of terminal differentiation (*MUC2* or *CHGA)* (**Figure 5.5)**. Together, these data suggest that B2/B3 represent a cell population that harbours BO progenitor cells.

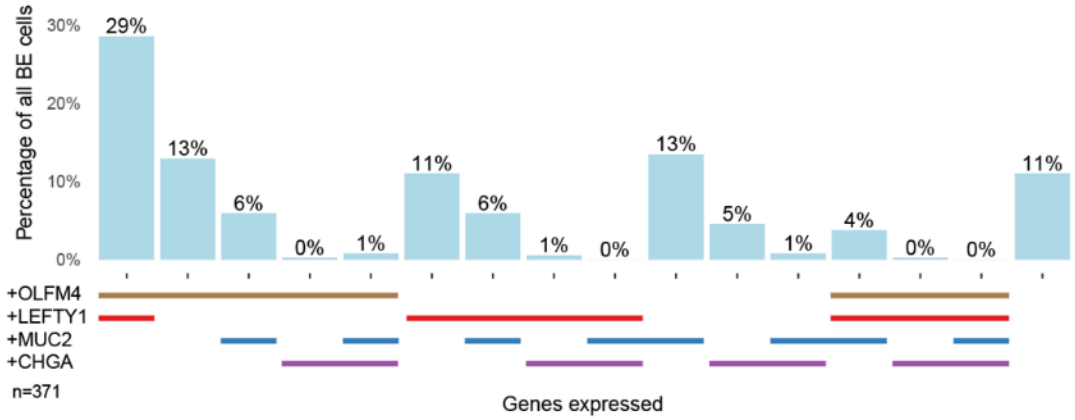


Figure 5.5 Bar plot showing OLFM4, LEFTY1, MUC2 and CHGA gene expression in BO cells. Single cell RNA-seq data showing percentage of BO cells from patients A-D expressing OLFM4, LEFTY1, MUC2 or CHGA alone and in all combinations (thresholds for calling a gene 'expressed' were set at the tenth centile to include 90% of cells in which at least one transcript was detected from each gene). **Figure created by Richard Owen, adapted from Owen & White et al 2018**.

5.6 RNA *in situ* hybridisation suggests *OLFM4/ LGR5* co-expression in OSGs

OLFM4 and *LGR5* have been shown to co-express in multiple cell populations (van der Flier, Haegebarth et al. 2009). In our hands, it was difficult to get LGR5 antibodies for staining to reliably stain positive control tissues such as duodenal crypts (Barker 2014, Dame, Huang et al. 2020). Therefore, to examine co-expression in situ

in tissues we carried out RNA *in situ* hybridisation in order to localise RNA species in normal tissues such as duodenum, normal oesophageal epithelium from an oesophagostomy resection specimen; and OSGs. **Figure 5.6** and **Figure 5.7** are representative images of *in situ* hybridisation experiments carried out with >3 biological replicates and three experimental replicates As expected, the duodenal crypt contains *LGR5* and *OLFM4* positively stained cells. This demonstrates that there is a concordance with the localisation of the RNA species within the tissue but there is also mutual exclusivity as well. The white arrow in **Figure 5.6A** demonstrates an *LGR5*+ve *OLFM4*-ve cell in the bottom of a duodenal crypt. The *in situ* hybridisation assay demonstrated no staining in squamous epithelium throughout all 5 samples stained. Some staining of *OLFM4* and *LGR5* is also seen in the OSGs where fewer positive cells exist than in the duodenum, but the staining pattern matches the *OLFM4* immunohistochemical staining pattern of OSGs from **Figure 5.4B.**

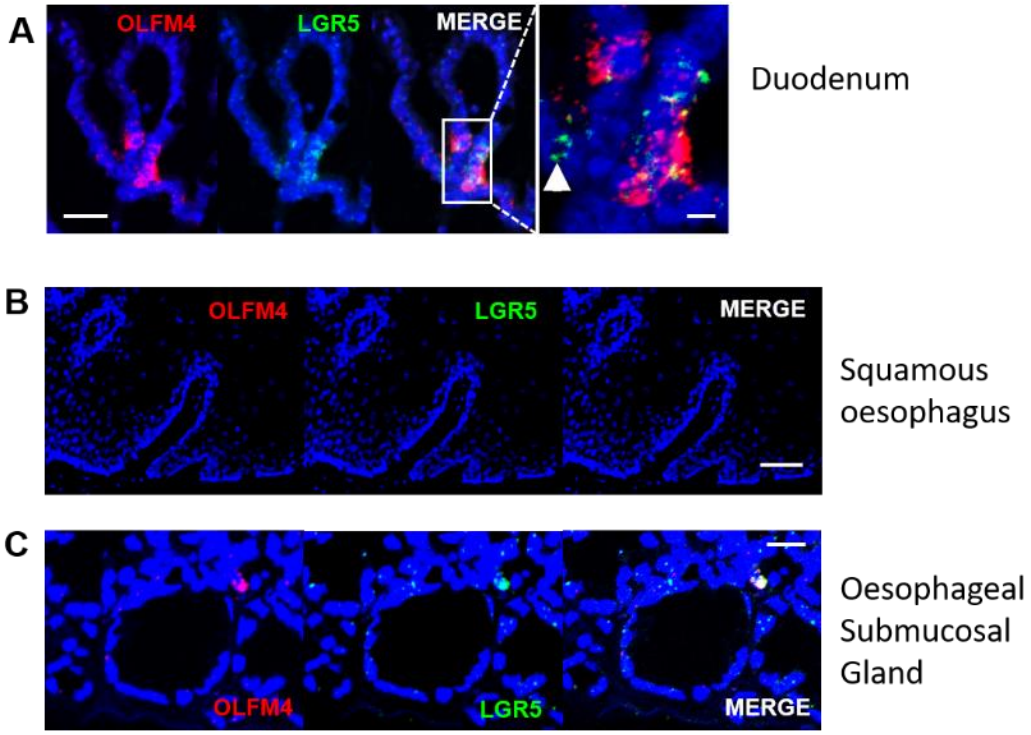


Figure 5.6: Multiplexed RNA ISH with OLFM4 and LGR5 probes. (**A**) Multiplexed RNA-ISH fluorescence imaging of OLFM4 (Red) and LGR5 (Green) in an endoscopic biopsy specimen of duodenum, scale bar 50µm. The right most image is an inset zoomed in image of duodenum crypt bases showing cellular localisation of probes; white arrow demonstrates a cell with green but no red fluorescence. Scale bar 10µm.

(**B**) Multiplexed RNA-ISH fluorescence imaging of squamous oesophagus taken from the proximal part of an oesophagectomy specimen resected for Siewert type III junctional tumour in a patient with no BO scale bar 100µm

(**C**) Multiplexed RNA-ISH fluorescence imaging of OSGs. The blue stain is DAPI. The scale bar is 30µm.

5.7 RNA *in situ* hybridisation to examine *OLFM4* and *LGR5* expression in BO

Examination of BO EMR specimens with multiplexed RNA *in situ* hybridisation demonstrated that tissue distribution of *LGR5* reactivity was similar to that demonstrated in other recent studies (Neyaz, Odze et al. 2021). It demonstrates an overlapping cell population expressing *OLFM4* and *LGR5* mRNA which is

demonstrated by the yellow appearance in the merged image, however these populations were evidently not the same identical population. This *in situ* hybridisation was carried out using duodenum as the positive control and squamous epithelium as the negative control during each experimental replicate.

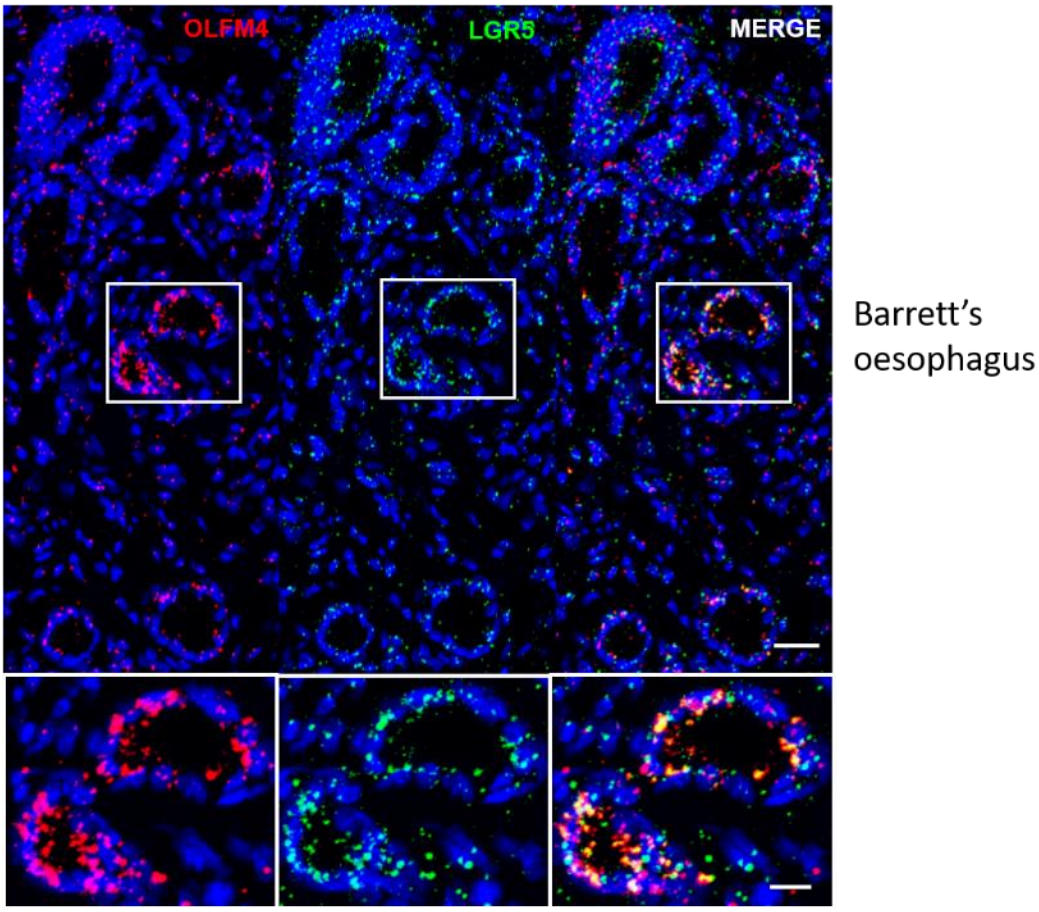


Figure 5.7: Multiplexed RNA ISH hybridisation with OLFM4 and LGR5 probes in BO.

Multiplexed RNA-ISH fluorescence imaging of OLFM4 (Red) and LGR5 (Green) in an endoscopic mucosal resection specimen of BO, scale bar in top panel is 80µm. The lower row of magnified images are an inset zoomed in image of cells in the middle of the Barrett's crypt showing tissue localisation of probes. Scale bar 20µm.

5.8 Using organotypic models to examine cell differentiation in BO

In order to demonstrate cellular differentiation and recreate the progenitor cell niche in vitro, we developed in vitro models in order to demonstrate the cell types present in

BO (Nyström, Thomas et al. 2005). Several different versions of *in vitro* models for carcinogenesis and epithelial/ co-culture exist in the literature, each with their own benefits and draw backs. The importance of air fluid interface in epithelial cell differentiation has been stated in several groups (Zhang, Bailey et al. 2021). In these experiments due to lack of availability of human fibroblasts we used mouse embryonic fibroblasts, which itself due to variation in species may have had an impact on epithelial cell differentiation. Similar to the duodenum, BO has a crypt glandular structure with differentiation most easily demonstrated by cell morphology on H&E staining. This experimental model has particular limitations. Primary cells require growth factors and other additives to the media to support cell differentiation. Using this organotypic culture there are several millimetres of matrigel and nylon sheet that the media additives have to diffuse across, which gives a potential reason why the BO cells, although retained their columnar phenotype did not develop a crypt-villus structure, nor did the cells exhibit any evidence of goblet cell differentiation. **Figure 5.8** includes representative images of organotypic cultures carried out in experimental triplicate.

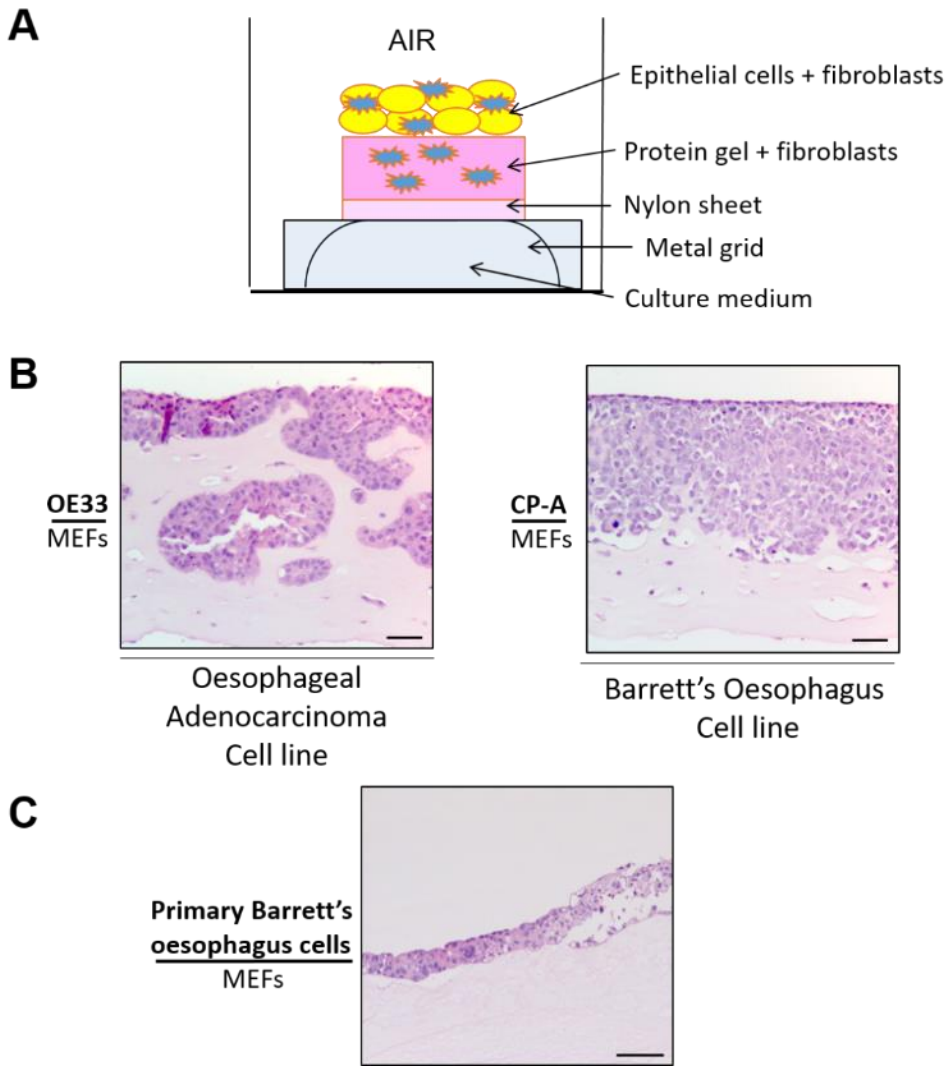


Figure 5.8: Organotypic cultures of oesophageal cell lines and Primary cells from BO

(A) A diagram to demonstrate the structure of the organotypic cultures Organotypic cultures were processed embedded and cut onto slides like histological tissue specimens.

(B) Haematoxylin and eosin stained organotypic cultures from published cell lines OE33 (human OAC cell line); CPA (hTERT immortalised human BO cell line.

(C) Primary cells cultured from BO derived from endoscopic biopsies

5.9 Organoid models developed to support LGR5+ populations

In order to develop an experimental model for examining cell subtypes seen in scRNA-seq, I established BO organoid cultures. This would enable future manipulation of BO differentiation and support *in vitro* experiments. Other groups such as Hans Clever's group have been developing organoid models of BO had already (Sato et al. 2011). Using the same method they used for the dissociation and proliferation of duodenal crypts, based on a specific growth factor mix which supports LGR5+ cell populations and gland culture. I recreated BO organoids so that we could demonstrate differentiated cell populations found from sc-RNA-seq in an *in vitro* model.

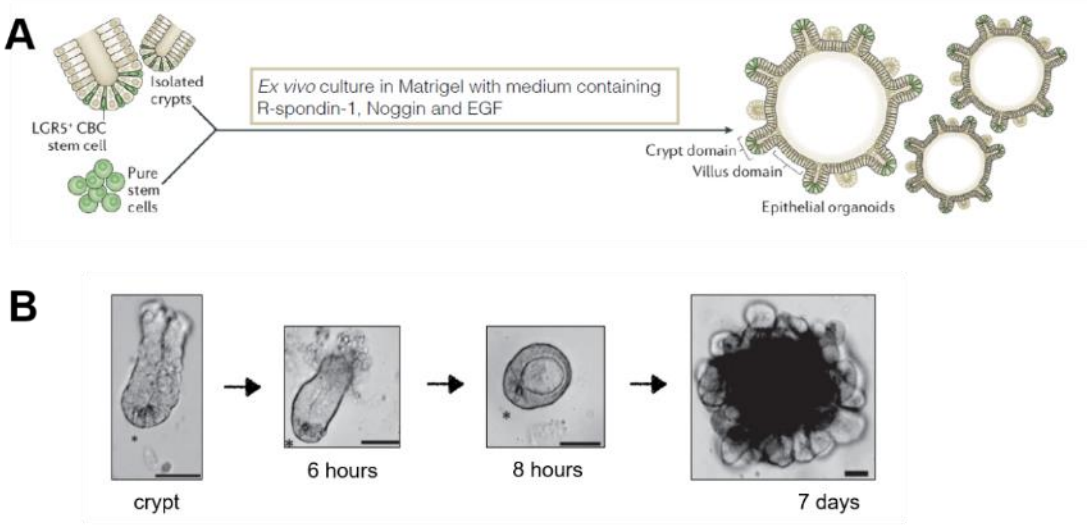


Figure 5.9: Schematic diagram to show organoid culture method used to develop organoids from endoscopic biopsies

(A) Diagram to demonstrate that this method is optimised to support the growth and proliferation of LGR5+ve cells from the duodenum to develop into three-dimensional luminal structures with a crypt-villus architecture.

(B) Diagram demonstrating development of duodenal organoids from dissociated crypts to complex differentiated crypt-villus organoids.

This figure is from (Sato, Stange et al. 2011)

5.10 BO organoids recapitulate crypt/gland structure seen *in vivo*

Using this previously published method we established routine isolation and culture of BO organoids. We were often able to isolate duodenal organoids from the same patients too. Times we were not able to isolate duodenal organoids were due to; the duodenum not being intubated during the procedure, meaning, no ability to get the duodenal biopsy; poor cell yield from the biopsies or infection of the culture before organoid growth and passaging was established. **Figure 5.10A** is a table to demonstrate the extent of our primary organoid growth from endoscopic biopsies, this featured part of the wider INGEN, upper GI tissue collection from both endoscopic and surgical resection specimens, which were bio-banked for use in multiple work streams. **Figure 5.10B** is an H&E stained organoid, which, demonstrates a glandular architecture close to that of a histological tissue specimen of BO. Black arrows demonstrate the presence and location of goblet cells within the organoids demonstrating that they can differentiate *in vitro*. We were able to passage these organoids up to six passages. These images in **Figures 5.10**, **5.11** and **5.12** are of organoids, which have been passaged two or three times. CDX2 immunohistochemical staining of the BO organoids as seen in **Figure 5.10C** demonstrates that the cells isolated and cultured have indeed undergone intestinal metaplasia. CDX2 positive staining along with direct visualisation of the site of endoscopic biopsy ensures that the culture contains BO cells. A different pair of biopsy forceps were used for the duodenal biopsies to ensure that there was no cross contamination of cells from the other biopsy sites.

A

Ingen	Barretts	Duodenum
1214	Y	
1228	Y	
1372	Y	
2022		Y
2043	Y	Y
2455	Y	Y
2513	Y	
2519		
2520	Y	Y
2522	Y	
2523	Y	
2662	Y	Y
2668	Y	Y
2671	Y	Y
2180	Y	Y
1801	Y	Y
2668	Y	Y
2482	Y	Y
2364	Y	Y
2754	Y	Y
2049	Y	Y
2830	Y	Y

B



C

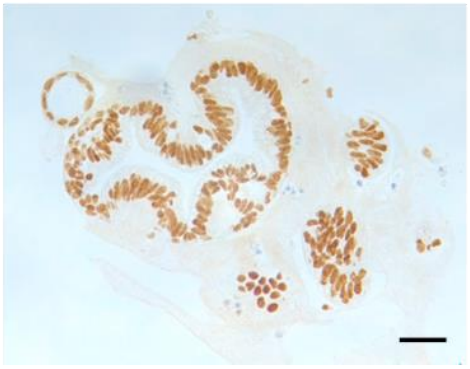


Figure 5.10: Development of BO and duodenal organoids from endoscopic biopsies

(A) Table demonstrates tissue collection and organoid cultures developed from different patients.

(B) Haematoxylin and Eosin staining of BO organoid cultured from an endoscopic biopsies from patient INGEN1372. Scale bars 50µm.

(C) Immunohistochemical staining of BO organoids with CDX2 from the same patient INGEN1372. Scale bars 50µm.

5.11 BO organoids show differentiation of all cell types seen in sc-RNA-seq data

In order to demonstrate cell populations seen in the sc-RNA-seq data, BO organoids were developed and immunofluorescence staining was carried out. Antibodies used for staining were for proteins correlated with specific RNA species, which derived from the RNA-seq data to depict cell subpopulations within BO. A panel of immunofluorescence images of BO organoids in **Figure 5.11** demonstrates different cell sub-populations, which defined by the RNA sequencing data are also represented within the BO organoids. The distribution of the respective staining patterns is close to what we would expect from staining of BO tissue samples. These images are representative images from organoids cultured and stained from 5 different patients. MUC2 demonstrates goblet cell differentiation, demonstrated by white arrows. OLFM4 stains positive in a small subset of cells although there is no defined crypt glandular structure in this image of an organoid in **Figure 5.11**, it demonstrates that OLFM4 positive cells are present in white. The staining demonstrates that all cells are strongly positive with cytoplasmic staining for KRT7 (yellow), LEFTY1 (green). OLFM4 (magenta). A small subset of cells stained positive for Chromogranin A (CHGA, green), depicting the enteroendocrine cell population.

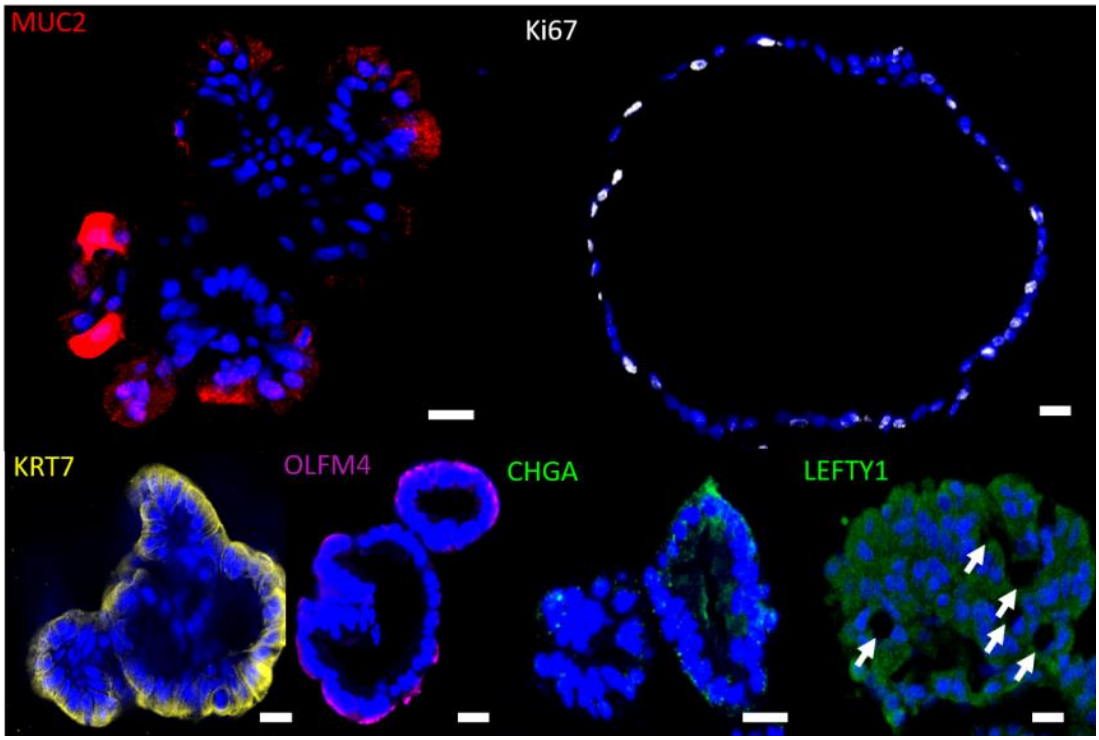


Figure 5.11: Immunofluorescence staining of BO organoids

A panel of immunofluorescence images of BO organoids grown in vitro from dissociated endoscopic biopsies of BO. The staining is of MUC2 (red), Ki67 (white), Cytokeratin 7 (yellow), OLFM4 (magenta), Chromogranin A (green) and LEFTY1 (green) respectively. White arrows demonstrate goblet cells that remain unstained with anti-LEFTY1 antibody. Scale bars are 20µm.

5.12 RNA *in situ* hybridisation in BO organoids

In order to examine the co-localisation of OLFM4 and LGR5, a previously characterised progenitor marker in BO, RNA in-situ hybridisation was carried out on cultured BO organoids. As you can see from the images panel in **Figure 5.12** despite multiple attempts to optimise the RNA-ISH of organoid cultures it did not demonstrate reliable staining patterns in the BO organoids or the duodenal organoids, however the BO and duodenal tissues sections did demonstrate the expected staining patterns when processed in the same batch. RNA-ISH was carried out on organoids from 6 patients with experimental triplicate.

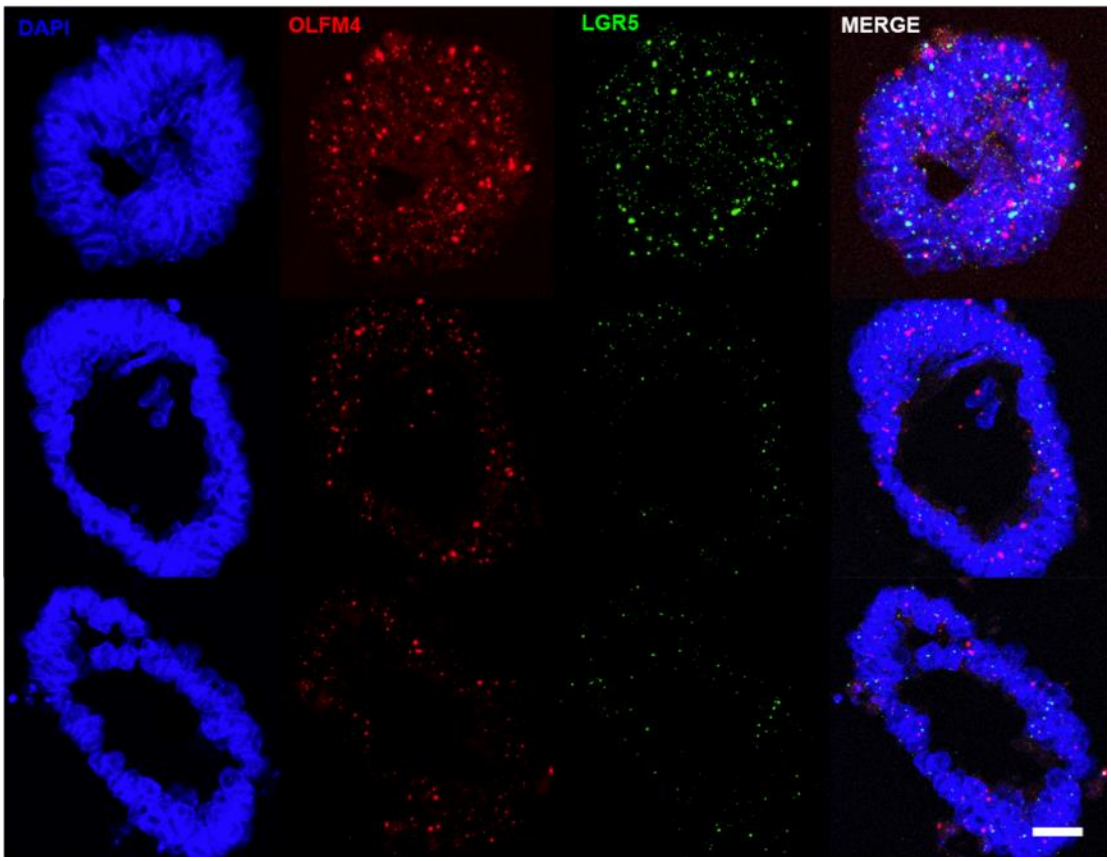


Figure 5.12: RNA *in-situ* hybridisation of BO organoids

A panel of ISH fluorescence images of BO organoids grown in vitro from dissociated endoscopic biopsies of BO. Multiplexed RNA-ISH fluorescence imaging of OLFM4 (Red) and LGR5 (Green). Scale bars are 20µm.

Further optimisation needs to be carried out to determine if a different antigen retrieval method should be used when processing formalin fixed paraffin embedded (FFPE) organoid cultures for RNA ISH instead of the same method used from FFPE tissue sections. I hypothesise that a similar expression pattern to the RNA-ISH pattern of BO *in vivo* there is co-localisation of *OLFM4* and *LGR5* gene expression in a similar cell population. OLFM4 expression has been shown to increase in chronic inflammation such as in inflammatory bowel disease (Kuno, Ito et al. 2021, Liu and Rodgers 2022). OLFM4+ cells may represent a regenerative stem cell population. Further work is required to further characterise this population of OLFM4+ cells and examine their role as a progenitor cell in BO. If OLFM4+ cells possessed a progenitor

function in BO it should be possible to culture an organoid from one OLFM4+ cell, which then leads to differentiation down all epithelial cell type lineages demonstrate in the single cell sequencing.

5.13 Culture of EpCAM+ cells from oesophageal biopsies

Further to understanding the progenitor population of BO, as the scRNA sequencing data suggested that the transcriptional profile of BO cells is indistinguishable from the transcriptional profile of the OSGs. One of the limitations for characterising these cells is the low number of OSGs; that they are not visible on endoscopy and they therefore cannot be sampled on purpose endoscopically their presence endoscopic biopsies is unpredictable. I therefore attempted to characterise these cells better but culturing them to have a higher cell number and utilise these primary cells for further in depth experimental characterised. The staining in **Figure 4.4** where upon FACS sorting with EpCAM antibody labelling native oesophageal cells dissociated from biopsies fell into two categories, a high and low EpCAM staining populations. Immunohistochemical staining of proximal normal epithelium from oesophagectomy specimens with the same antibody demonstrated that the normal stratified squamous epithelium of the oesophagus has a low expression level whereas the staining demonstrates that the OSGs stained strongly for EpCAM through all throughout all five patient samples examined. As EpCAM is a cell surface protein, we were able to sort by EpCAM high expressing cells from oesophageal biopsies using flow cytometry. In order that we might be able to isolate OSG cells, develop them into organoids and with larger populations of cultured cell populations potentially develop a model for the early development of BO. The images in **Figure 5.13** demonstrates phase contrast light microscope images of organoids cultured EpCAM high expressing cells sorted from endoscopic biopsies of normal oesophagi. The cells

isolated did not survive passage and were therefore not usable in further experiments. Nowici-Osuch and colleagues have carried out a comprehensive characterisation of OSG cells (Nowicki-Osuch, Zhuang et al. 2021). Further work could be carried out to culture OSG organoids in order that they can be used as an experimental model.

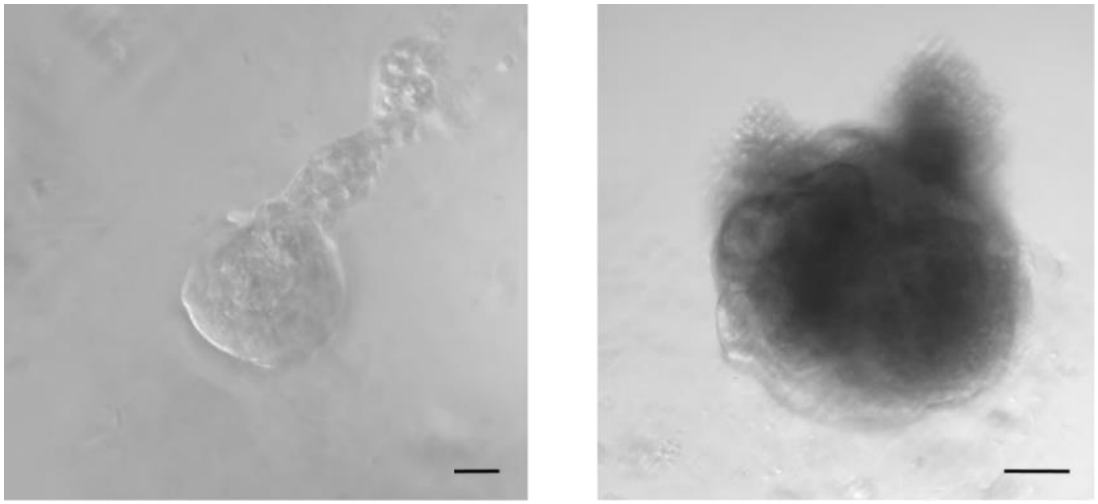


Figure 5.13: Phase contrast images of organoids normal oesophageal biopsies. Endoscopic biopsies were taken of normal oesophagus, dissociated into a cell suspension and sorted on a Flow cytometer to isolate cells highly expressing EPCAM. These organoids developed from the EPCAM+ cell population. Scale bars are 20µm.

5.14 Discussion

In this study, we interrogated our scRNA-seq data using 'StemID', a published bioinformatic pipeline that organises cell populations by their transcriptional profile using entropy (Grun, Muraro et al. 2016). As expected, analysis of duodenal control cells demonstrated that LGR5+ve cells are the likely stem cell marker for the duodenum, which reinforces published data (Barker, van Es et al. 2007). Combined analysis of OSG and BO cells using StemID suggest OLFM4+ cells as the most likely progenitor cell population. OLFM4 is a target of Notch signalling and a robust marker of human and mouse intestinal stem cells in its own right (Pellegrinet, Rodilla et al. 2011). OLFM4 is strongly expressed in the small intestine, colon and prostate, with

lower expression levels in the gastric epithelium and bone marrow. The intracellular expression pattern varies with membranous, cytoplasmic, nuclear and mitochondrial staining in epithelial cells. Up-regulation of OLFM4 expression has been documented in gastrointestinal cancers, *H. pylori* infection and inflammatory bowel disease (van der Flier, Haegebarth et al. 2009, Pellegrinet, Rodilla et al. 2011). Several studies have demonstrate that OLFM4 expression is regulated by NFκB driven inflammation in chronic *H. pylori* gastric infection (Liu, Yan et al. 2010). Other studies have drawn associations between the expression of LRG5 and OLFM4 expressing stem cells (Itzkovitz, Lyubimova et al. 2012).

It may be that this is limited by number of stem cells sequenced within the dissociated cell population or the low levels of expression of LGR5 within these cells. Indeed, it may well be effected by the lysis buffers we used to dissociate the tissues, either by in advertently selecting the cell populations due to the stresses of the tissue dissociation process. It is not inconceivable that gene transcription was altered during the processing, however we managed to get a median time of 4 hours between receiving the endoscopic biopsy from the patient, dissociated, sorting the cells, and freezing the dissociated single cells frozen in 96 well plates. To mitigate time taken to process samples they were kept ice during the process in order to slow down biological processes, including gene transcription.

We examine the expression pattern of OLFM4+ cells, a known progenitor cell marker which has links with LGR5+ cell populations. Resident gastro-intestinal stem cell populations are themselves a widely researched field, with wide implications in carcinogenesis. LGR5+ cells are the most widely researched stem cell candidate, recognised as a stem cell marker in expressed by proliferating adult stem cells in the intestine. An accumulating body of evidence indicated that LGR5 is essential for

normal embryological development of many organ systems; indeed Lgr5 knockout is embryologically lethal in mice (Morita, Mazerbourg et al. 2004). Through R-spondin, the LGR5 ligand, the Wnt/B-catenin signalling pathway has a crucial role in embryonic development, tissue regeneration and morphology. In adults, canonical Wnt/B-catenin signalling is essential for regulating stemness, proliferation, and differentiation within stem cell niches. This pathway has been shown to be critical in tissues including but not limited to hair follicles in the skin, ovaries, the intestinal crypt, the mammary gland and gastric glands (Garcia et al 2008; Jaks et al.2008; Barker et al. 2010; Barker et al. 2010; Plaks et al. 2013; Huch et al. 2013; Ng et al. 2014).

This is supported by our observation that this sub-population of BO cells and OSGs expresses the stem cell-associated gene *OLFM4*, consistent with the hypothesis that these populations might contain similar progenitor cells. Importantly, a separate recently published study looking at the early development of gastric adenocarcinomas used sc-RNA-seq to demonstrate that OLFM4 is also highly expressed in GIM (Zhang, Yang et al. 2019). In this study, they concluded that OLFM4 expression is important in the development of intestinal phenotype that is seen in a high proportional of proximal gastric and junctional adenocarcinomas.

5.15 Limitations

Number of cells sequenced was a significant limitation to this study. We sort to develop a better understanding of the BO progenitor cell population. Owing to the transcriptional overlap of the two cell groups and limited of number of BO cells sequenced, data from OSGs and BO cells were combined for the analysis. As single

cell sequencing technology develops new platforms will allow for higher numbers of cells to be sequenced.

Data from RNA-ISH suggests that there is often co-expression of *LGR5+* and *OLFM4+*, it is not clear why this is not born out in the sequencing data. Representation of LGR5+ cell populations within the sc-RNA-seq data may well have been impacted by the way in which single cells were dissociated and sorted. There are limitations of carrying out RNA-ISH on FFPE tissue although the method used, RNAscope®, is optimised for use in FFPE tissue during the tissue fixation process RNAases are likely to lead to breakdown of mRNA species.

In this study, our attempts to label a cell as the progenitor cell for BO are limited. StemID Tissue specific stem cells are defined as multipotent and self-renewing cells, which possess endogenous functions for tissue renewal and repair (van der Kooy, Weiss et al. 2000). Therefore, in order to demonstrate a BO progenitor cell, a single 'progenitor' cell should be isolated, cultured and be able to demonstrate self-replication and differentiation into all lineages seen within the scRNA-seq data.

In vitro models are useful to understand differentiation within BO. Organotypic cultures have been demonstrated to be a useful model of modelling epithelial- stromal interactions, however organoids have been demonstrated to recapitulate the glandular structure of BO. Any *in vitro* model will have limitations, as it is difficult to model in-vivo physiology. In order to isolate OSGs to attempt to develop OSG organoids we attempted to isolate EPCAM+ cells for culture. I was unable to culture EPCAM+ cells reproducibly, further work needs to be carried to isolate OSGs and understand cell lineages within OSGs can be better understood.

Chapter 6: Results – Linking BO with columnar lined oesophagus of developmental origins

In previous chapters, we have looked at the cellular heterogeneity of BO and demonstrated some evidence complete transcriptional similarity between non-specialised BO cells and a columnar population within normal squamous biopsies that we have concluded are OSGs. There are at least two other occasions where columnar lined oesophagus exists. One such instance is the foetal columnar oesophageal epithelium which transiently lines the oesophagus *in utero* and the other is Cervical oesophageal inlet patches (OIPs) which are an under researched phenomenon described in the proximal oesophagus of adults.

6.1 Morphology of the human foetal oesophagus

Detailed histological analysis was carried out on 12 foetal oesophagi at varying ages. **Figure 6.1** demonstrates a range of ages of these specimens. All sections were taken from the middle of the oesophagus. Using H&E staining we examined the cellular morphology of the epithelium, including examination for glandular structures, which demonstrated any secretory morphology or for any evidence of developing OSG structures. At 9-10 weeks gestation the oesophageal epithelium seems to be lined with a simple columnar epithelium with nuclei located in the apical position demonstrated by the green arrows in **Figure 6.1**. At this time, we notice the human foetal oesophageal epithelium is divided into large longitudinal primary folds as demonstrated by the zoomed-out image from the 11+3 week foetal oesophagus image in **Figure 6.1**. From 11+3 weeks we see cilia development on the epithelial surface delineated by the blue arrows in **Figure 6.1**. By 11 to 13 weeks gestation the epithelium becomes a stratified cuboidal epithelium. We see the transition of the

nuclei to the basal position within the basal layer of the epithelium by 12+6 weeks. Gradually from 9 weeks to 18 weeks of development, the epithelium develops from one cell thick to up to five cells thick in places. We do not see any evidence of squamous cell morphology.

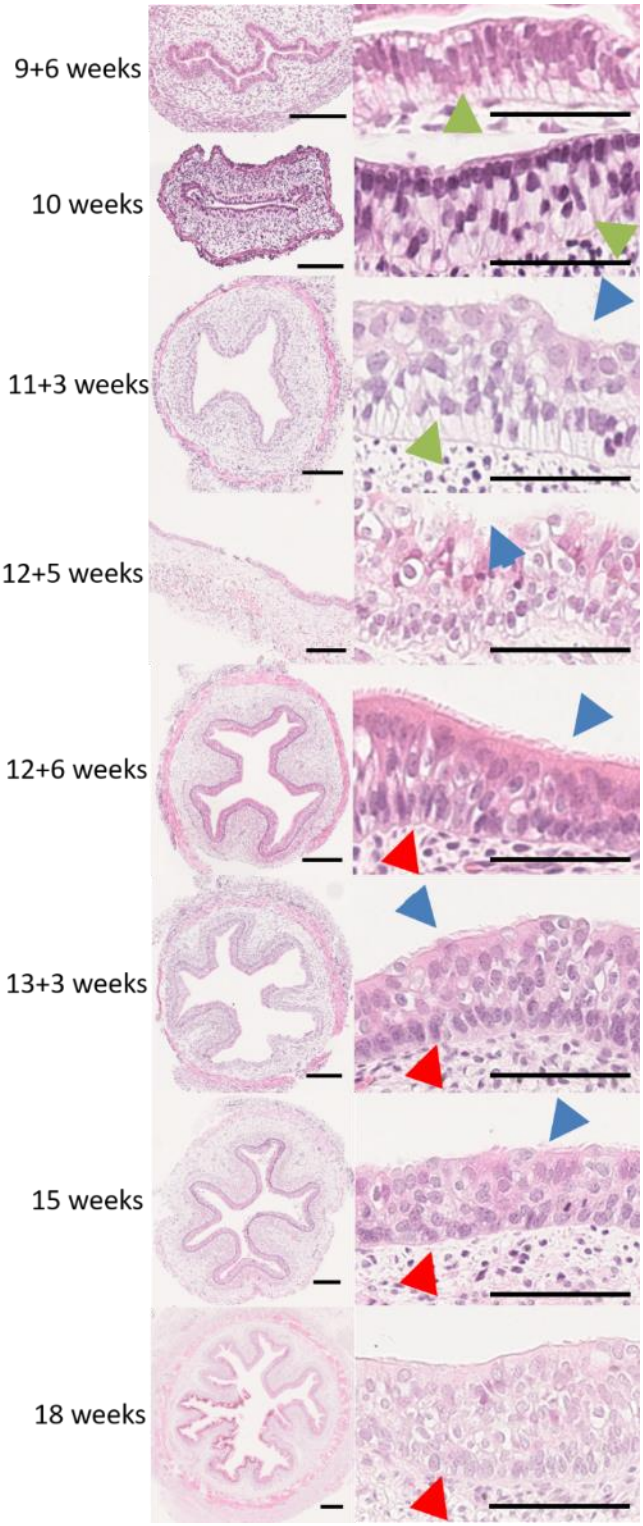


Figure 6.1: Haematoxylin and Eosin staining of foetal oesophagus samples.

The column of images on the left are zoomed out images of transverse sections of the foetal oesophagi at different ages (except for the specimen at 12+5 weeks, which is a longitudinal section; scale bars are 300um). The column on the right are magnified images of the same specimens. Green arrows demonstrate apical positioning of nuclei. Blue arrows delineate ciliated epithelium. Red arrows demonstrate basal position of nuclei. Scale bars on the right column are 60um.

6.2 Expression of BO markers in the foetal oesophagus

Our data from **Results: Chapter 4** demonstrated a significant transcriptional overlap between BO cells and OSG cells. This conclusion is derived from demonstrated the potential role for OSGs in the development of BO. In a recent study it has been suggested that BO derives from a transitional epithelium seen at the SCJ with the distinctive expression pattern with KRT7, KRT5 and P63 expressed in the same cells (Jiang, Li et al. 2017). In **Figure 4.3,** we demonstrated that a very similar cell population occurs within the OSG duct. Indeed, the main duct of an OSG has a transitional epithelium that connects the glandular submucosal gland to the stratified squamous epithelium of the surface of the oesophagus. We carried out immunohistochemical staining of these same markers KRT7, KRT5 and P63 in the human foetal oesophagus to examine differentiation in the naïve cells lining the foetal oesophagus. **Figure 6.3** shows single staining KRT7, KRT5 and P63 in a 15-week-old human foetal oesophagus. This staining shows reliable p63 nuclear staining in the majority of cells in the basal layer. Some cells in the suprabasal layer also demonstrate nuclear P63 staining. KRT7 staining stains strongly in the suprabasal cells, but not at all in the basal layer. KRT5 stains throughout the epithelium with some nonspecific staining in the stromal layer.

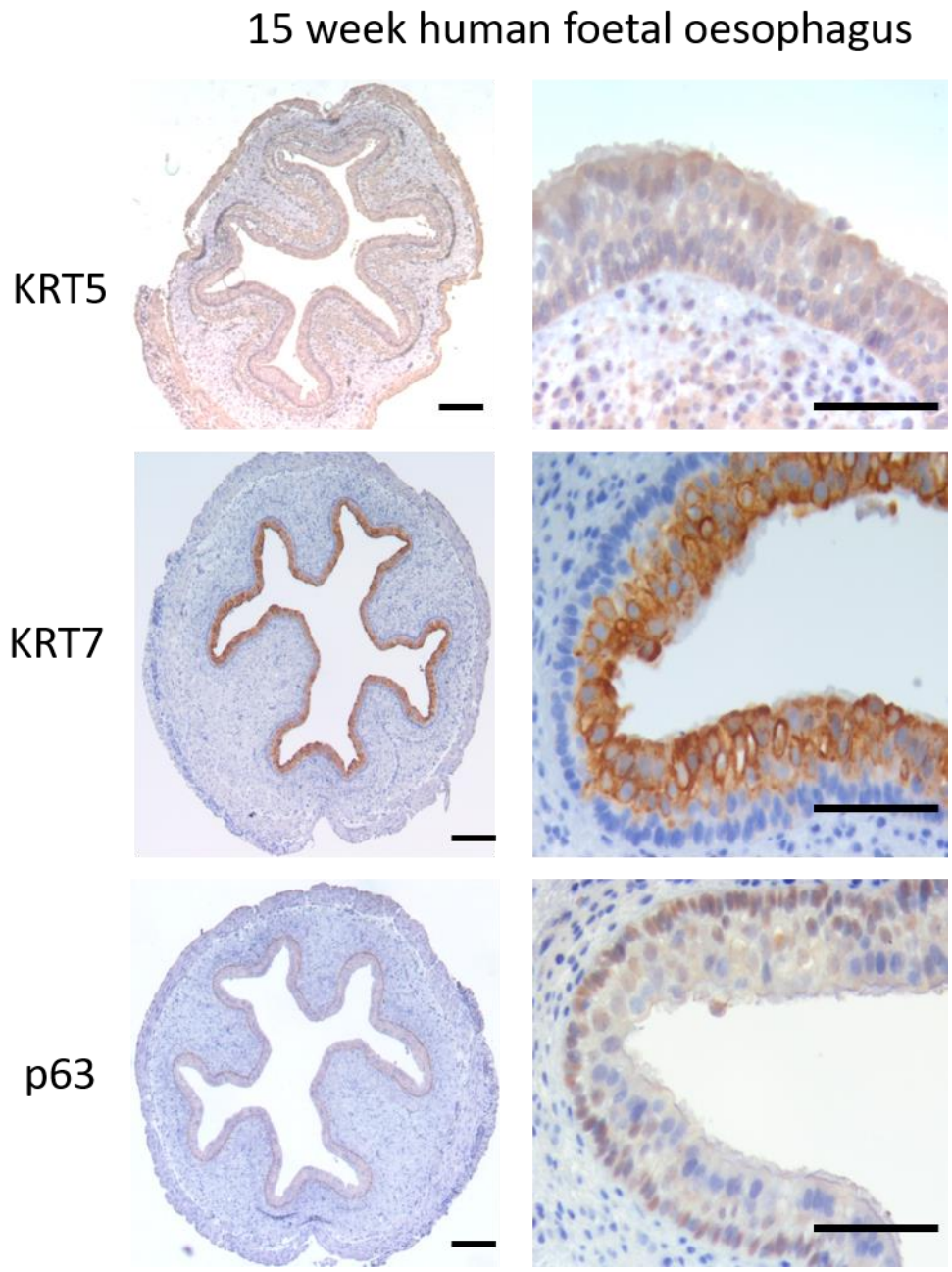


Figure 6.2: Immunohistochemical staining of KRT5, KRT7 and p63 in human foetal.

The column of images on the left demonstrates consecutive transverse sections of the IHC stained 15-week-old foetal oesophagi. Scale bars are 300µm. The column of images on the right demonstrates magnified images of the same samples. Scale bars are 50µm.

6.3 Immunofluorescence co-staining of P63, KRT5 and KRT7 in the early foetal oesophagus

In order to understand the P63, KRT5, KRT7 staining pattern triple staining immunofluorescence was carried out to examine for co-expression seen in the Wang et al study. **Figure 6.3** shows staining of foetal oesophageal specimens from various ages. In specimens aged 11+3, 12+5 and 13+3-weeks (each age n=1) p63 staining is localised to the basal layer of the epithelium; KRT7 stains throughout the epithelium; these is no evidence of specific KRT5 staining. However, in the 13+3-week specimen there is a focus of KRT5 staining in the suprabasal epithelium, which is depicted by the white arrows. In the 15-week specimen there is weak evidence of triple staining, the KRT5 (yellow staining) may be nonspecific staining in the basal epithelium as demonstrated by **Figure 6.3E** zoomed in images from **Figure 6.3D**. It is clear that further work needs to be carried out to assess evidence of the P63+, KRT5+, and KRT7+ triple expressing cells, which are described by Wang et al. as the transitional epithelium that are the source of BO progenitor cells.

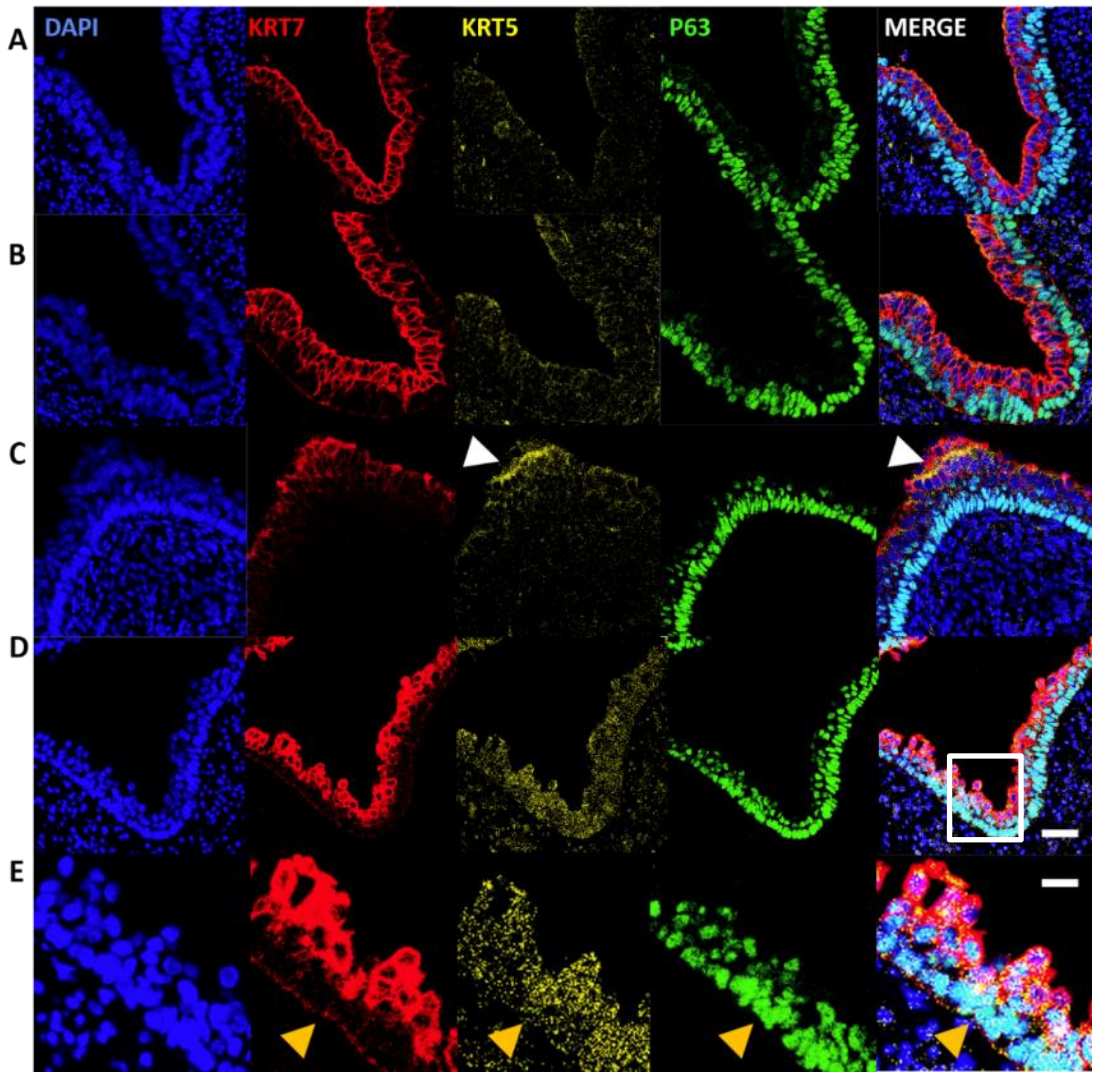


Figure 6.3 Immunofluorescence staining of KRT7, KRT5 and p63 of transverse sections of human foetal oesophagus samples

Triple immunofluorescence staining images of KRT7 (red), KRT5 (yellow) and p63 (green) in human foetal oesophageal samples of different ages throughout development (blue stain is DAPI).The white arrow demonstrates a focal area of high KRT5 expression. (A) 11+3 weeks (B) 12+5 weeks (C) 13+3 weeks (D) 15 weeks. Scale bars are 30µm. (E) Zoom in of the 15-week-old sample staining. Orange arrow shows cells with triple staining present. Scale bar 10µm

6.4 Immunofluorescence co-staining of, KRT7, KRT5 and P63 in the 18 week foetal oesophagus

The same triple immunofluorescence staining was used to examine the expression pattern of in the 18-week (n=1) human foetal specimen, here we see a different expression pattern. There still is not evidence of a stratified squamous epithelium morphologically. We see areas where there is thickening of the p63 positive basal layer up to six cells deep as seen in **Figure 6.4B**. Conversely, there are areas of loss of p63 staining within the basal layer. As seen in **Figure 6.4C** & **Figure 6.4D**.

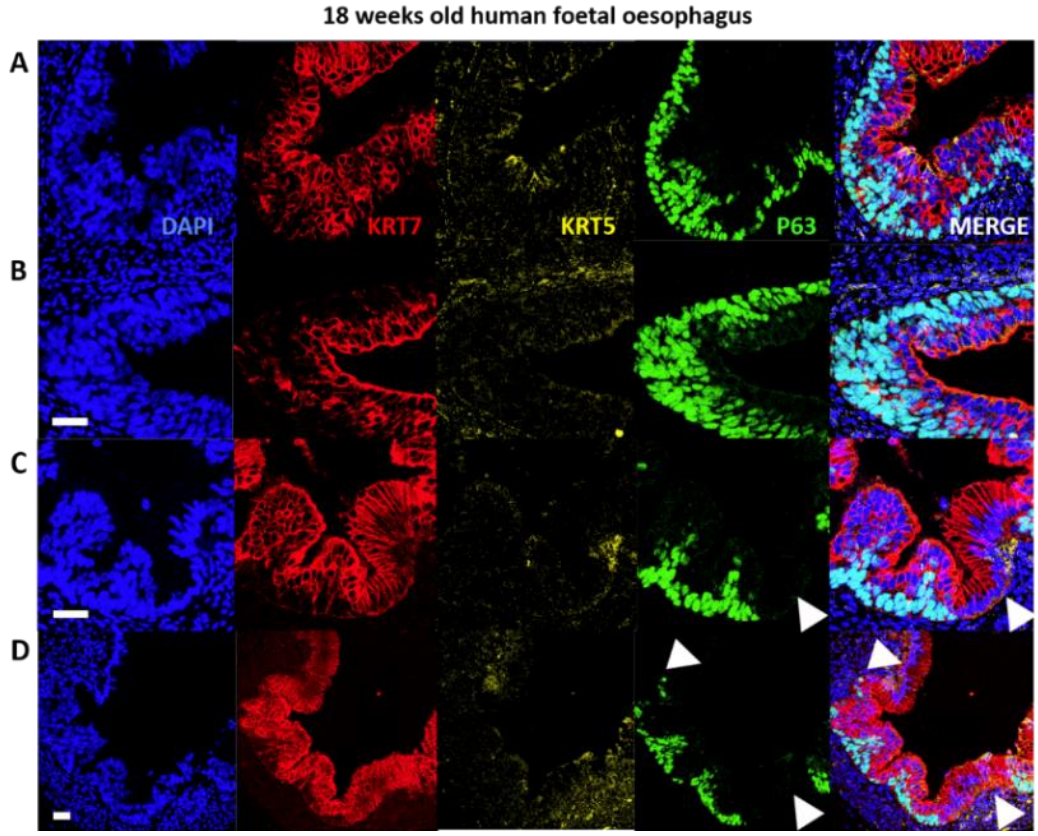


Figure 6.4: Immunofluorescence staining of KRT7, KRT5 and p63 of transverse sections of human foetal oesophagus samples at 18 weeks of development

Images A-D Demonstrate triple immunofluorescence staining images of KRT7 (red), KRT5 (yellow) and p63 (green) in human foetal oesophageal samples at 18 weeks of development in utero (blue stain is DAPI).The white arrow demonstrates focal areas of loss of p63 expression in the basal layer of the epithelium. Scale bars are 30µm.

6.5 LEFTY1 and TFF3 expression in the foetal oesophagus

To further examine the expression pattern of the embryological oesophageal epithelium we looked at OSG/BO cell markers from the scRNA-sequencing data in **Results: Chapter 4**. **Figure 6.5** shows LEFTY1 and TFF3 immunohistochemical staining of the 10 week old and the 15-week-old foetal oesophagus. The 18-week-old foetal oesophageal specimen was not included in this analysis as it was received after the staining was carried out. At 10-weeks old there is some, but limited staining of TFF3 and LEFTY1 however by 15 weeks old there is more specific and defined staining of both LEFTY1 and TFF3 in the epithelium. This staining suggests similarities between the expression pattern of the foetal oesophagus and BO cells. OLFM4 immunohistochemical staining was carried out on the foetal oesophageal samples, but no staining was seen.

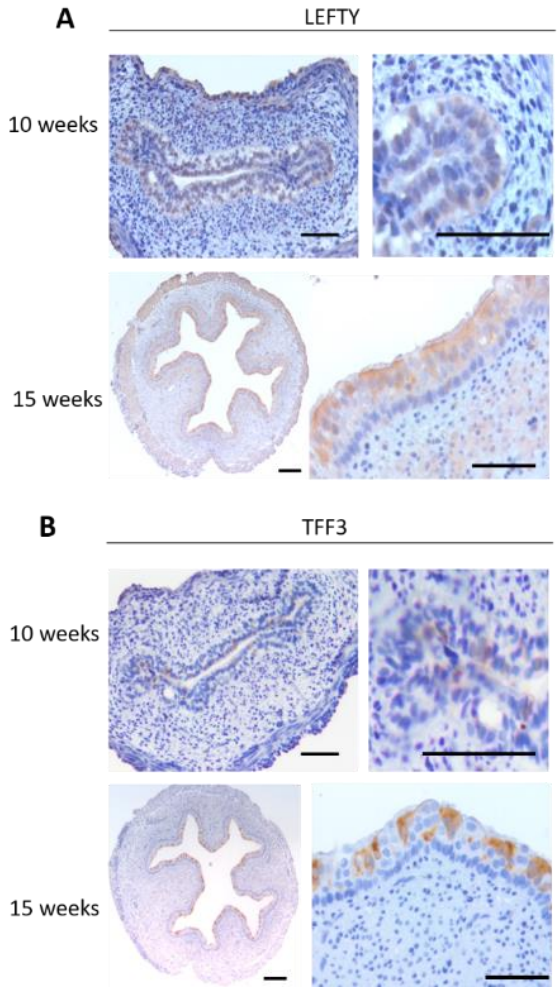


Figure 6.5: Immunohistochemical staining of BO markers LEFTY and TFF3 in the human foetal oesophagus

A) Immunohistochemical staining of Lefty1 in a 10-week-old (scale bar 100um) and 15-week-old human foetal oesophagus (scale bar 200um. Images on the left are zoomed out transverse sections. On the right of the panel are zoomed images of the LEFTY1 staining demonstrating the staining pattern within the epithelium.

B) Immunohistochemical staining of TFF3 in a 10-week-old (scale bar 100um) and 15-week-old human foetal oesophagus (scale bar 200um. Images on the left are zoomed out transverse sections. On the right of the panel are zoomed images of the TFF3 staining demonstrating the staining pattern within the epithelium.

6.6 *LGR5* and *OLFM4* localisation in the foetal duodenum

To further understand the expression pattern of the progenitor cell markers RNA in situ hybridisation was carried out for LGR5 and OLFM4 expression was carried out in the foetal oesophagus (**Figure 6.7**) and the foetal duodenum (**Figure 6.6**) as a control. **Figure 6.6** shows that LGR5 RNA expression (green) in the crypt base of the foetal duodenum depicted by the yellow arrows. OLFM4 expression is predominantly at the neck of the crypt in a 19+6-week-old foetal oesophagus. LRG5 RNA expression is also seen in the crypt neck adjacent to the OLFM4 expressing cells.

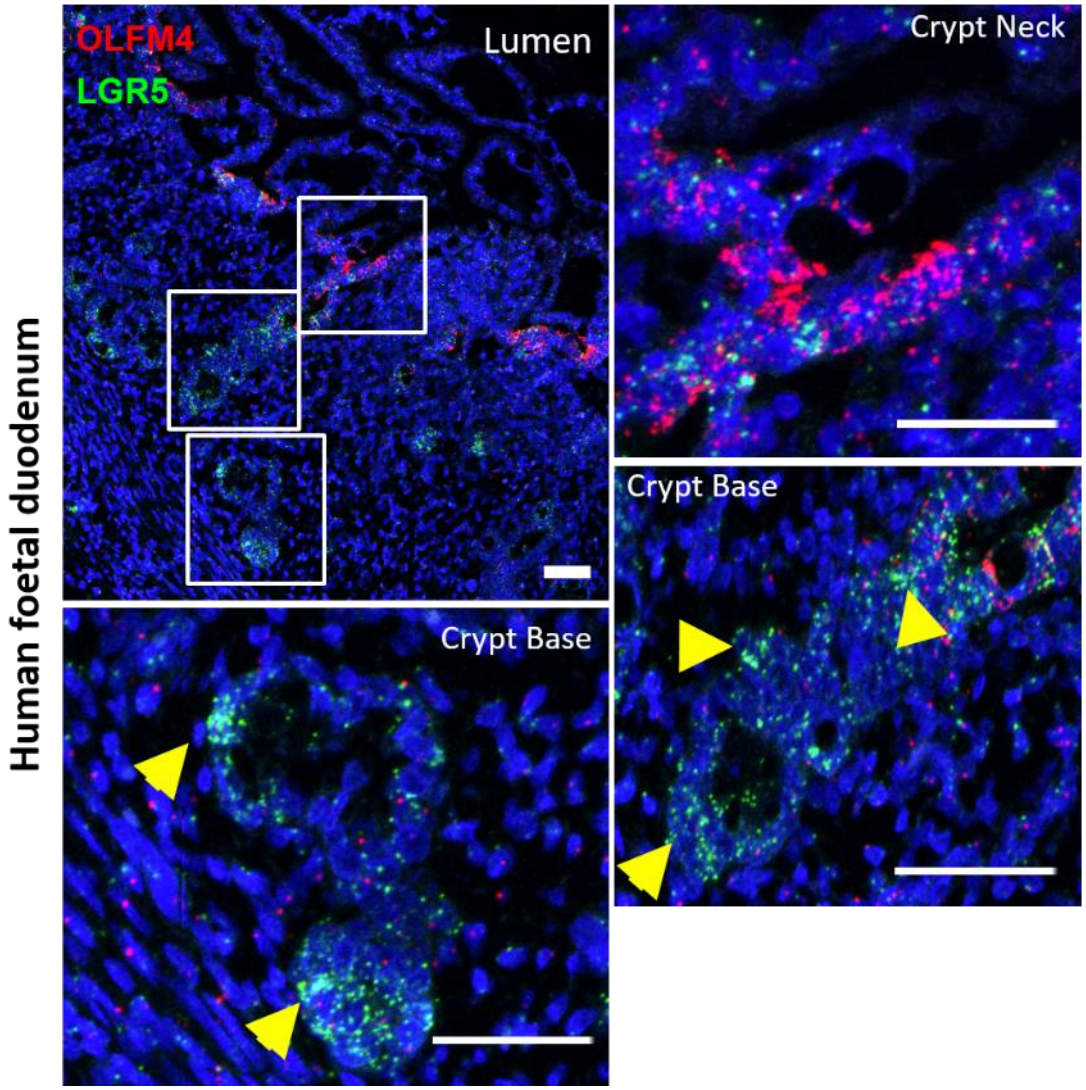


Figure 6.6: Multiplexed RNA *in-situ* hybridisation with OLFM4 and LGR5 probes on human foetal duodenal samples.

Multiplexed RNA-ISH fluorescence imaging of OLFM4 (Red) and LGR5 (Green) human foetal specimen of duodenum from 19+6-week foetus. The zoomed out image demonstrates a human foetal duodenal gland. To the right is a magnified image of red staining demonstrating olfm4 expression at the neck of the crypt. Beneath and to the right of the zoomed out image are magnified images of crypt bases demonstrating green LRG5 expression at the crypt base. Yellow arrows demonstrate LRG5 expressing cells. Scale bars are 50um.

6.7 Expression of *LGR5* and *OLFM4* in the foetal oesophagus

In the adult oesophagus, LGR5 expression only exists in the OSGs. There has been no evidence of squamous epithelium expressing LGR5 within the literature. In order to examine further expression of LGR5 and OLFM4 within the foetal oesophagus and to examine potential areas of early "pre-budding" foetal OSG cells RNA ISH was carried out in the foetal oesophagus. 12 human foetal oesophagus samples were stained. No positive staining for LGR5 or OLFM4 was seen in any of the foetal oesophagus samples up to 18-weeks-old. In the 18+5 week old specimen we saw clustered areas of LRG5 RNA expression. This same pattern was seen in all three of the technical replicates. This expression was always in cells at the base of a longitudinal fold. It may be that BMP and SHH signalling is active in the embryological oesophagus as it has been shown to function in the embryological intestine. Studies have shown that when embryological epithelium bends it changes the gradient of signalling molecules encouraging stem cells to cluster at the bottom of crypts (Shyer, Huycke et al. 2015). In these foci of staining no high level OLFM4 RNA ISH fluorescence was seen co-expressed in these cells. If any OLFM4 hybridisation is present it is difficult to determine from the background staining, see **figure 6.7.**

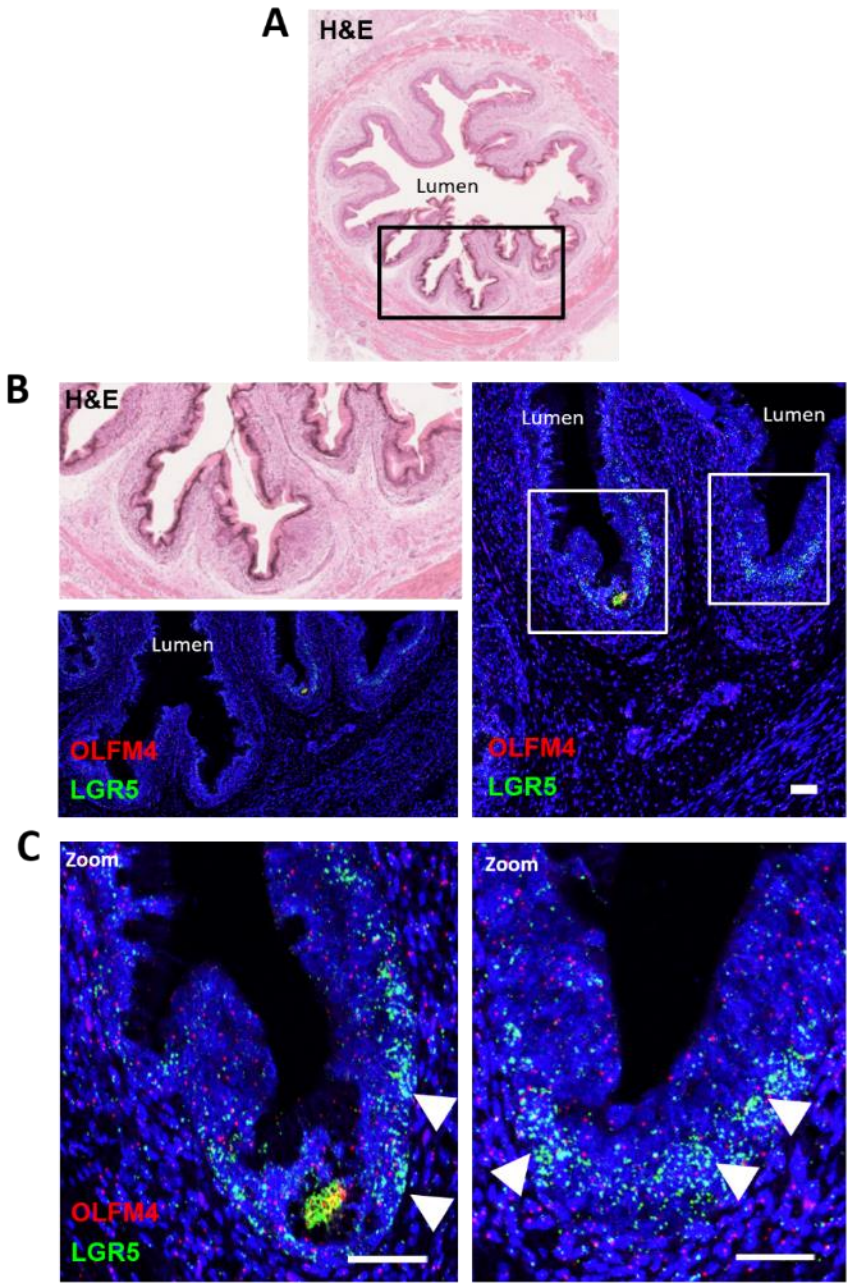


Figure 6.7: OLFM4 and LGR5 expression using RNA *in situ* hybridisation in foetal oesophagus

A) Haematoxylin and Eosin staining of transverse section of 18 week old human foetal oesophagus

B) H&E stained magnified image of an 18-week-old human foetal oesophagus. Beneath is an adjacent section from the same specimen with multiplexed RNA *in-situ* hybridisation using probes designed for OLFM4 (red) and LGR5 (green). To the right is an intermediate magnified image demonstrating an area of positive staining. Scale bars are 50um.

C) Magnified images of the same staining as above (B), demonstrating multiplexed RNA-ISH for OLFM4 and LGR5. White arrows demonstrate green, LRG5 expressing cells. Scale bars are 50um.

6.8 KRT7 and P63 expression in oesophageal inlet patches

Another instance of a columnar-lined oesophagus in an adult is the cervical oesophageal inlet patch (OIPs). We have carried out a panel of immunohistochemical staining on tissue from three patients with OIPs in order that we might be able to better understand the expression pattern of OIP in comparison with BO and the foetal oesophagus. **Figure 6.8** demonstrates representative images of the staining. The H&E staining shows strong eosin (pink) staining demonstrating parietal cells. Morphologically the OIP mucosa is most similar to the structure of gastric epithelium and does not appear to be similar to BO with no evidence of goblet cell differentiation. OIPs also test positive for KRT7 and MUC6 but not p63 (**Figure 6.8)**.

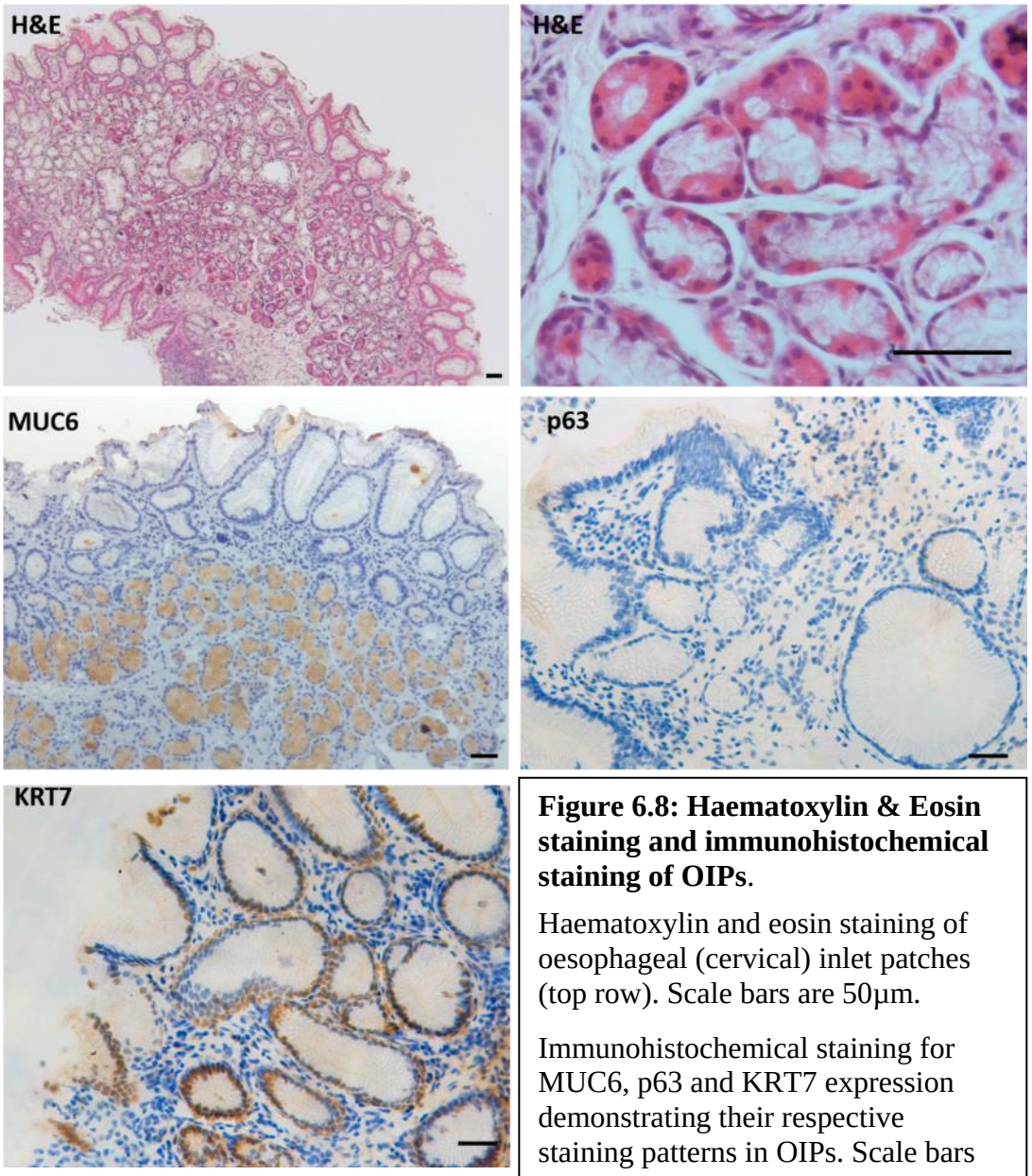


Figure 6.8: Haematoxylin & Eosin staining and immunohistochemical staining of OIPs.

Haematoxylin and eosin staining of oesophageal (cervical) inlet patches (top row). Scale bars are 50µm.

Immunohistochemical staining for MUC6, p63 and KRT7 expression demonstrating their respective staining patterns in OIPs. Scale bars are 50µm.

6.9 Expression of BO markers in oesophageal inlet patches

Further immunohistochemistry staining was carried out on the same three OIP specimens for specific BO/ OSG markers. TFF3 and LEFTY expression where both demonstrated in the OIP tissues. Similarly, OLFM4 (indicated by the red arrows) and CDX2 (indicated by the orange arrows) expression were seen at very low levels in specific cells. These three samples where histological archive specimens, their fixation and storage was not optimised for molecular analysis. Although RNA ISH

was carried out on this tissue, there was a lot of background noise, but no specific ISH observed.

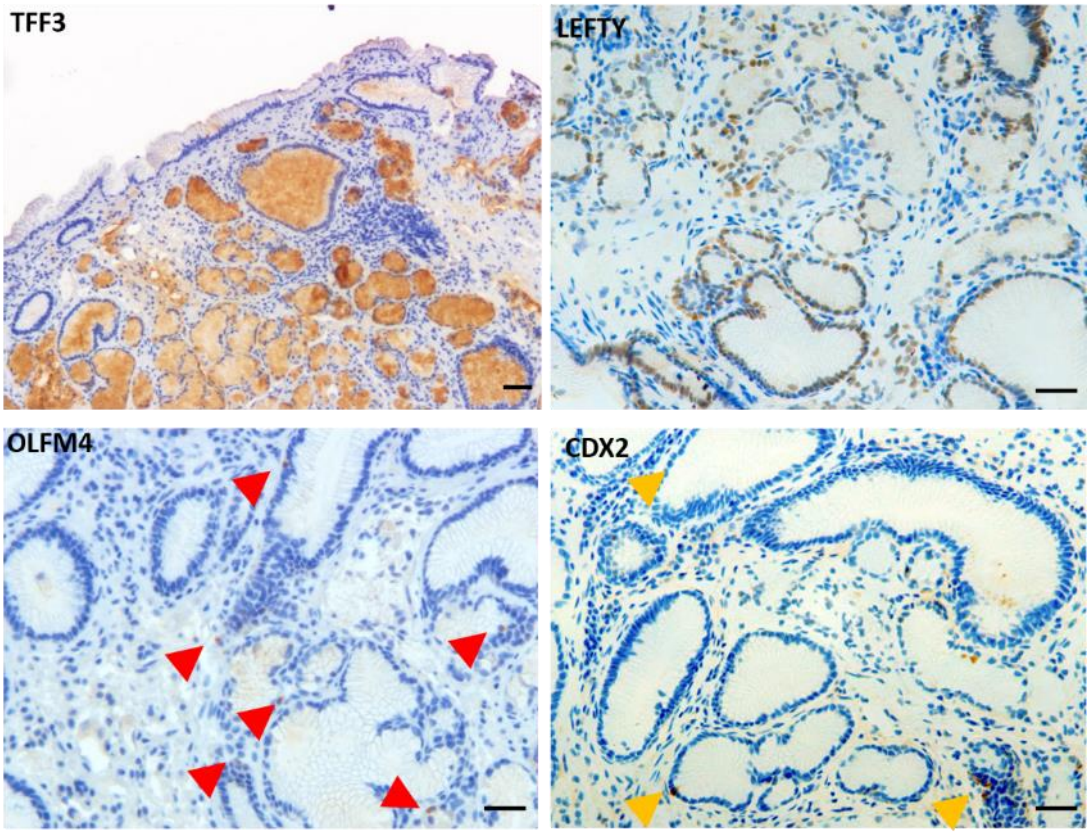


Figure 6.9: Immunohistochemical staining of OIPs.
Immunohistochemical staining for TFF3, LEFTY1, OLFM4 and CDX2 expression demonstrating their respective staining patterns in OIPs

6.10 Discussion

In this chapter, I investigated the morphology and expression patterns in the foetal oesophagus and OIPs, two instances of columnar lined oesophagus separate to BO. I investigated the morphology of the human foetal oesophagus with H&E staining of specimens, ranging from nine to 18 weeks. These specimens are too young to demonstrate when squamation of the oesophagus or OSGs develop in the foetal oesophagus, as suggested by a previous study (Johns 1952). P63, KRT5 and KRT7 staining in the foetal oesophagus has demonstrated p63 expression basal layer and

KRT7 expression suprabasal layer, KRT5 staining appears generally less reliable and consistent. Staining was carried out in a series of twelve foetal oesophageal samples spanning from 9-18 weeks gestation. This staining demonstrated expression of P63, KRT5 and KRT7 in different cell populations, some cells were seen to co-expression KRT7 and p63. However, there was no definitive evidence of triple staining and there was no evidence of squamous differentiation of the oesophagus from 16-weeks as demonstrated in previous studies (Rishniw, Rodriguez et al. 2011). There was no evidence of the P63+KRT5+KRT7+ TBC population in the foetal oesophagus from our staining (Jiang, Li et al. 2017). Indeed in a recent study Nowiki-Osuch suggested that the KRT7+ population seen in OSGs, the KRT7+ population (described by Jiang and colleagues) seen in the transitional zone at the GOJ may well have the same developmental origins (Nowicki-Osuch, Zhuang et al. 2021). These KRT7+ cell populations may well be a remnant cell population from the embryological oesophagus.

Interestingly, TFF3 expression is seen in the human foetal oesophagus demonstrates that the surface epithelium expresses a marker of secretory epithelium, which is a known marker of OSGs and BO. LEFTY1 expression is also noted in the foetal oesophageal samples, this is harder to interpret as LEFTY1 expression has been demonstrated throughout the GI tract. Together with previous staining this suggests that this series of human foetal oesophagi exhibit a mixed differentiation pattern of squamous, transitional and secretory markers, similar to the OSGs stained in **Chapter 4.**

Examination of *LGR5* and *OLFM4* expression in the foetal samples using RNA-ISH showed that both are expressed in the human foetal duodenum. Data should be interpreted carefully as only one sample of human duodenum has been stained. The

LGR5+ expression is seen at the crypt base as demonstrated in other studies of murine and adult human duodenum (Barker, van Es et al. 2007). However, RNA-ISH co-staining of *OLFM4* and *LGR5* did not demonstrate co-localisation which has been demonstrated in adult intestinal studies. RNA ISH shows *OLFM4*+ expressing cells at the neck of the foetal intestinal crypt whereas in adult small intestine OLFM4 expression localises at the base of the crypts with LGR5+ cells.

LRG5 RNA ISH of the 18-week-old foetal oesophagus suggested that LGR5 expression in the oesophagus localised to the base of the longitudinal folds, however No OLFM4 expression was seen in the foetal oesophagus at all (**Figure 6.7**). This again needs to be interpreted carefully as this staining pattern was seen in one sample. This may suggest that OLFM4 expression is not a marker for progenitor cells in the foetal GI tract. In the adult oesophagus, the only expression of LGR5 or OLFM4 is seen in submucosal gland ducts. Previous studies have described the way that OSGs form in the developing oesophagus as persisting islands of columnar cells surrounded by the differentiating stratified squamous epithelium (Rishniw, Rodriguez et al. 2011). LGR5 localisation in the foetal human oesophagus at 18 weeks might demonstrate early development of the OSG.

Further preliminary work has been carried out examining the histological appearance and expression profile of OIPs. H&E staining suggested that OIP histology resembles that of the human gastric fundus. OIPs also demonstrate an expression profile similar to that of BO with expression of KRT7, TFF3 and CDX2, none of which are usually expressed in normal gastric epithelium, it is clear that there are some similarities between OIPs and BO expression. This data is supported by previous studies which demonstrated expression of BO markers in OIPs (Lauwers, Mino et al. 2005)

6.11 Limitations

There are a limited number of foetal samples assessed in this study. These specimens are highly sensitive and donated at a particularly challenging time during the parent's life. As such donation of the samples is un predictable. Twelve specimens were donated to our study over 18 months of collection. Foetal specimens from later gestations are harder to come by and may be associated with less likelihood of parents donating specimens. Continued collection over a longer time will allow for more specimens to be collected particularly specimens of later gestation.

This study was also limited by the number of OIPs biopsies that have been biobanked. As OIP is a non-pathological phenomenon they are often not biopsied by endoscopists. In order to increase biobanking numbers ethical approval would be needed so that a larger OIP tissue bank can be developed. This would allow optimally fixed and preserved specimens for more sensitive molecular testing.

Chapter 7: Discussion

7.1 Investigating the role of early p53 mutation in GOJ carcinogenesis

7.1.1 Discussion

In this study, a potential role for early P53 mutation was investigated in the development of GOJ adenocarcinomas. Previous studies have demonstrated that up to 40% of non-dysplastic BO epithelium harbour significant P53 mutations; this is at a higher level than the rate of P53 mutations found in the native squamous oesophageal epithelium (Martincorena, Fowler et al. 2018). An initial finding suggested that IM was present in $P53^{R172H}$ mice more frequently than wild type mice. IM has been previously documented as being an important part of the internationally accepted diagnostic criteria for BO diagnosis. Additionally GIM induced by *H.pylori* infection is a premalignant lesion in the development of gastric cancers. The importance of IM in malignant transformation is itself highly contentious, one study has demonstrated that the presence of IM in BO is linked with increased cancer risk (Spechler and Goyal 1996, Spechler 2002). However, other studies have demonstrated that presence or absence of IM in inconsequential on the underlying pathological progression and should, instead be seen as a bystander effect on the normal differentiation of the tissue (Kelty, Gough et al. 2007) (Barbera, di Pietro et al. 2015). $P53^{R172H}$ transgenic mice were utilised with a biliary reflux model as a potential means to develop a reliable model of murine GOJ adenocarcinoma. Although the $P53^{R172H}$ mutation (analogous to the $p53^{R175H}$ hot spot mutation seen in human malignancies) is a potent tumour suppressor, in this study a constitutive p53 mutation and high dietary intake of bile salt, deoxycholic acid (DCA) was not enough to induce GOJ carcinogenesis

reproducibly. Quante and colleagues used a biliary reflux model in transgenic mice which overexpressed IL-1β upon activation of the Krt14 promoter (Quante, Bhagat et al. 2012). We were unable to demonstrate significant evidence that $P53^{R172H}$ induced increased levels of inflammation in the upper GI tract compared with wild type treated mice. Examination of the DCA treated mouse livers showed tumour development and suggested liver inflammation, likely to be due to DCA absorption and storage in the murine livers (Flynn, Montrose et al. 2007, Yang, Yao et al. 2021).

7.1.2 Future directions

Further analysis of the liver specimens from these mice could confirm the mechanism of their inflammation. With the focus on trying to develop a model of GAC, further murine experiments could be carried out to examine the role of P53 combined with other cancer-causing mutations in LGR5 expressing stem cells and other gastric cell populations in order to understand the initiation of gastric tumours. Animal models are critical in the simulation of human disease but, all *in vivo* models have drawbacks. Some groups have used mice and rats to attempt to model BO, however, rodents do not possess OSGs, which are implicated in the development of BO. A recent study suggests that the first gastric crypt distal to the SCJ has a unique cell population as it is the only crypt in the proximal murine stomach that contains LGR5+ cells. The authors suggest that this crypt is akin to an OSG at the SCJ, however this is contentious (Fu, Wang et al. 2020, Kabir, Karami et al. 2022). Further work should be carried out to isolate and characterise this cell population. Murine models may be useful models of gastric and GOJ tumours, but there is scant evidence that they can recapitulate surface columnarisation of the luminal surface epithelium as seen in human BO. Further developments in animal models trying to model BO and oesophago-gastric cancers should utilise animals with OSGs (avian and porcine

species) as they are increasingly understood to be important in BO development (Krüger, Gonzalez et al. 2017, von Furstenberg, Li et al. 2017, Saxena and Klimbacher 2019).

7.2 Identification of cell populations within BO

7.2.1 Discussion

In this study, we carried out sc-RNA-seq to examine cellular heterogeneity of BO. We then compared differentiated cells in BO with the gene expression profiles of control cell populations in the oesophagus, stomach and duodenum. This identified a similarity of the expression between BO cells and OSG cells at the gene and protein level. This could be due to a convergent phenotype of columnar cells and secretory, goblet-like cells. In another more recent study a comprehensive analysis of BO and OSGs has determined that BO is most likely to be derived from gastric cardia epithelium (Nowicki-Osuch, Zhuang et al. 2021). In this study they identify KRT7+ cells which are a transitional cell type at the GOJ which are responsible for the development of BO. However, it doesn't completely explain endoscopic studies of patients with BO demonstrate islands of BO proximal to the SCJ. Conversely islands of squamous epithelium also occur inside segments of BO (Nakanishi, Saka et al. 2007, Epstein, Cosby et al. 2017). It may be that the same KRT7+ population exist in the OSG ducts at the transition zone between the stratified squamous epithelium and the glandular OSG. In other studies, OSGs have been found to be in continuity with squamous islands and BO segments (Coad, Woodman et al. 2005, Paulson, Xu et al. 2006, Leedham, Preston et al. 2008, Nicholson, Graham et al. 2012). OSG cells have been shown to respond to inflammatory stimuli and oesophageal injury by

proliferating and replacing damaged surface epithelium (Abdulnour-Nakhoul, Nakhoul et al. 2007). It may be that the transitional epithelia retain some regenerative capacity. Porcine and canine models of oesophageal injury and biliary reflux respectively recapitulate human data showing induction of OSG proliferation. They also show that OSG cells can differentiate into both squamous and columnar epithelial lineages (Krüger, Gonzalez et al. 2017, von Furstenberg, Li et al. 2017). In an early canine study, OSGs were found to be the source of epithelial columnarisation after iatrogenic endoscopic mucosal stripping and reflux treatment (Hennessy, Edlich et al. 1968). The lack of an intuitive small animal model and the challenges of biopsying submucosal structures has held back research in OSGs. LEFTY1 and TFF3 the most highly expressed markers unique to BO and OSGs. The biological function of LEFTY1 expression in this context is not understood, as part of the TGF-β family it may have a direct effect on morphogenesis. TFF3 is the marker used in the Barrett's Oesophagus Trial (BEST) studies with the cytosponge to development a screening too for BO (Offman, Muldrew et al. 2018). In fact we find TFF3 expression to be as abundant in BO as OSGs.

In this study demonstrate the presence of MUC2+ expression in OSGs demonstrating intestinal differentiation. Although this does not prove the cell of origin of BO, this is correlative data to support the body of evidence in the literature, which suggests that OSGs are a potential source of BO. Taken together, these studies suggest that OSGs possess plastic progenitor cells capable of differentiating into both squamous and columnar epithelium and that OSGs and BO possess strong similarities.

There is a significant body of evidence that suggests BO could have a gastric origin. Another single cell genomics study used sc-RNA-seq and sc-DNA-seq to compare transcriptional and mutational overlap between BO, LGD, HGD and control cells

from the upper GI tract (Busslinger, de Barbanson et al. 2021). They concluded that BO had most significant overlap with gastric epithelium, however, they saw only squamous cells in their normal oesophageal biopsies with no evidence of OSGs. Interestingly they noted a higher mutational burden in BO cells compared with gastric cells. Further evidence of a possible gastric BO origin are from histological studies which have characterised BO crypts and demonstrated that often BO adopts the phenotype of gastric glands (oxyntic, antral and pyloric) (Lavery, Nicholson et al. 2014, McDonald, Lavery et al. 2015). These again are correlative data and do not rule out other cell of origin theories. Given the acidic environment BO develops within, it is possible that this environment informs differentiation during BO development and plastic cells may likely differentiate into a gland structure with ability to defend against a low pH setting. Therefore making a gastric phenotype advantageous. Two front running studies identify residual embryonic cells (RECs) and separately transitional basal cells (TBCs) at the gastro-oesophageal SCJ (Wang, Ouyang et al. 2011, Jiang, Li et al. 2017). Both studies have highlighted KRT7 expression as a key marker. In a separate recent study, Nowicki-Osuch and colleagues identify a $KRT7^{high}$ population at the SCJ (Nowicki-Osuch, Zhuang et al. 2021). In keeping with our findings, they also commented that OSG cells have been shown to have a $KRT7^{high}$ expression profile. In this study, they suggest that OSGs, RECs and TBCs, which are all associated with SCJs, may have the same embryological origin and therefore these studies may separately describe similar cell populations.

SPINK4 and ITLN1 have also been found to be markers of goblet cells independent of MUC2 expression. Due to the expression pattern seen in colonic crypts we saw that SPINK4 expression was seen towards the bottom of crypts, whereas MUC2 expression towards the top of crypts. Utilisation of differentiated duodenal organoids

suggested that SPINK4 expression may increase before MUC2 expression at the protein level, however this data was not recapitulated in cell lines treated with the same ɣ-secretase inhibitor. Previous studies have demonstrated the importance of ATOH1 in co-ordinating the secretory lineage and SPDEF in goblet cell differentiation. We do not understand if this known signalling has a role in regulating SPINK4 expression.

7.2.2 Future directions

In order to investigate a potential link between these cell types we would like to carry out targeted biopsies of the oesophago-gastric SCJ and OSGs. Using positive selection through cell sorting to grow up the cell populations of the OSGs, TBCs and RECs so that larger populations can be analysed through sc-RNA-seq and *in vitro* cell differentiation assays. Additionally we suggest SPINK4 as a potential marker of early goblet cell differentiation. Further work to understand the relationship between SPINK4 and MUC2 expression in goblet cells is needed.

Additional further work could also be carried out to address the loss of the spatial context of the single cells when sequenced. This issue could be addressed either by carrying out further RNA-ISH for all cell populations identified in BO in addition to antibody-based protein staining or by micro-dissecting out regions of BO specimens and carrying out sequencing to determine the localisation of cells within BO and OSGs.

OAC remains a diagnosis with poor outcomes and future work should be directed towards early diagnosis and defining which BO patients should be followed up and how intensively. Further longitudinal studies could also be carried out on dysplastic

tissue to understand which cell populations predominate in early cancers and identify a cell signature of early tumours.

7.3 OLFM4 and LGR5 expression in the adult oesophagus

7.3.1 Discussion

The progenitor cell of BO remains elusive. In this study, we examined expression patterns of candidate BO progenitor cell markers. LGR5 was highlighted as a likely stem cell marker our duodenal cell population (Grun, Lyubimova et al. 2015, Grun, Muraro et al. 2016). Next a combined analysis of BO and OSG cells using StemID demonstrated OLFM4 as a likely marker of the progenitor population, but not LGR5. Previous descriptive histological studies have demonstrated LGR5 cells in BO, suggesting that LGR5 expressing cells are likely to be the BO progenitor (Lavery, Nicholson et al. 2014). Localisation of this population was carried out using RNA ISH which consistently showed co-localisation of LGR5 and OLFM4 expression within the same cells in BO and OSGs, with no evidence of an OLFM4+ LGR5- population. In light of this it is not clear why LGR5 expression was not highlighted by StemID as a potential marker in BO/OSG cells. LGR5 expression was at a very low low level in the BO data, it was therefore unlikely to reach statistical significance even if present in the same cluster as OLFM4.

Previous studies have suggested that a TBC population expressing KRT7+/ KRT5+/p63+ are the progenitors to BO (Jiang, Li et al. 2017). As supportive evidence of progenitor cell properties the KRT7+/p63+ cells were isolated and developed organoids, which upon transfection with CDX2 expression plasmids organoids exhibited intestinal differentiation. The TBCs may be an analogous population to the

KRT7+/KRT14+/p63+ population seen within OSGs. KRT14, pairs with KRT5, in many studies of squamous epithelium KRT5 and KRT14 are interchangeable as markers of stratified squamous differentiation (Moll, Franke et al. 1982, Schweizer, Bowden et al. 2006). RNA ISH suggests that OLFM4+ LGR5+ cells exist within the OSG ducts as do the TBC cells. These two cell populations: KRT7+/KRT5+/p63+ cells and OLFM4+/ LGR5+ cells may indeed be the same population which exist both at the gastro-oesophageal SCJ and in OSGs.

7.3.2 Future directions

Further work should be carried out to isolate and culture the proposed BO progenitor cells, one challenge of this will be to identify a unique cell surface marker that could be used to positively select these cells. Once cultured and expanded if they are able to demonstrate all cell populations within BO biopsies it would demonstrate a BO progenitor cell. Further work could also be carried out to examine the expression of these progenitor cell markers in LGD, HGD and OAC. Further culture of human OSGs could help the understanding of oesophageal repair adding to previous work suggesting that OSGs contain a progenitor cell population that has a role in squamous repair in response to oesophageal injury as well as a role in the development of BO (Krüger, Gonzalez et al. 2017). Little is known about the developmental origins of the OSGs of the role of this LGR5+ cell population in the foetal oesophagus. Further work could be carried out to understand the role of LGR5+ cells in oesophageal development.

7.4 Human foetal oesophagus and OIPs may have links to BO

7.4.1 Discussion

Many studies have implicated increased expression of developmental signalling pathways in BO compared to normal tissues. In the foetal oesophagus the transition of columnar to squamous epithelium is co-ordinated by changes in DNA methylation changing gene expression (Yu, Slack et al. 2005). Previous studies have hypothesised that this process could be reversed in the development of BO. This study has implicated the developmentally important gene LEFTY1 expression in BO, which is part of the Nodal pathway first described with its role in left-right determination during development *in utero* (Smith, Noël et al. 2011). In this study we saw expression of BO markers LEFTY1 and TFF3 in the early foetal oesophagus. Individually KRT7+/ KRT5+/p63+ expression is seen in the early foetal oesophagus, but definitive co-localisation is not seen. This suggests that within the foetal epithelium a there is a mixed differentiation pattern where multiple differentiation lineages are present at the same time. This has similarities to the multi-lineage differentiation pattern seen in OSGs.

Little is known about the foetal development of OSGs, but we know that some OSGs form during the late stages of foetal development and continue to develop post-natally (Johns 1952). RNA ISH analysis was carried out to examine LGR5 and OLFM4 expression. In adults OLFM4 and LGR5 co-express. In foetal oesophagus samples 9 to 16-weeks no LRG5 or OLFM4 was detected. However, in the one 18-week-old foetal oesophagus sample LGR5 but not OLFM4 expression was observed at the bottom of epithelial fold (**Figure 7.0A**). The only LGR5+ cell population that has been observed in the adult human oesophagus is in OSGs (**Figure 7.0B**). More

characterisation needs to be carried out, this data may suggest that the LGR5+ cells in the foetal oesophagus could be the site of early budding of OSGs.

In this study we show that OIPs and BO share expression of LEFTY1 and TFF3. OIPs are foci of columnar cells in the proximal oesophagus thought to be a developmental remnant (Dziadkowiec, Szu et al. 2019). Expression of KRT7 and CDX2 is seen within OIPs suggesting that they are not simply islands of heterotopic gastric epithelium as other studies have described, but demonstrate transitional and intestinal differentiation (Ciocalteu, Popa et al. 2019). We are unable draw strong comparisons between the expression pattern of OIP and the foetal oesophagus although other studies have drawn comparisons between the two (Feurle, Helmstaedter et al. 1990). Further understand of OIPs may help understand why progression of OIPs to dysplasia and adenocarcinoma is extremely rare (Von Rahden, Stein et al. 2004).

7.4.2 Future directions

We were unable to clearly demonstrate the timing of the squamous development of the oesophagus as it is likely to be after 18-weeks gestation. Our main limitation of this study was the availability of tissue. For understandable reasons it is particularly difficult to get human foetal specimens after 18-weeks of gestation. It may be possible to apply for ethical approval for post-mortem analysis of early post-natal oesophagi. Otherwise, utilisation of animal models such as porcine or guinea pig models to track the foetal development of OSG cells and identify cell oesophageal progenitor populations that exist within OSGs. Further work could be carried out to examine foetal porcine samples later in gestation and early neonatal samples which could be used to understand the early development of OSGs in pigs. Understanding this potential progenitor population in the oesophagus could shed more light on oesophageal repair mechanisms.

OIPs demonstrate stable columnar epithelium in the oesophagus, it is unclear why malignant progression from OIPs is a rare event whereas development of BO to OAC is more frequent. It may be that better understanding of OIPs could help guide molecular assessment of low or high risk for malignant transformation in BO. Further analysis should be carried out to investigate differentiation within OIPs.

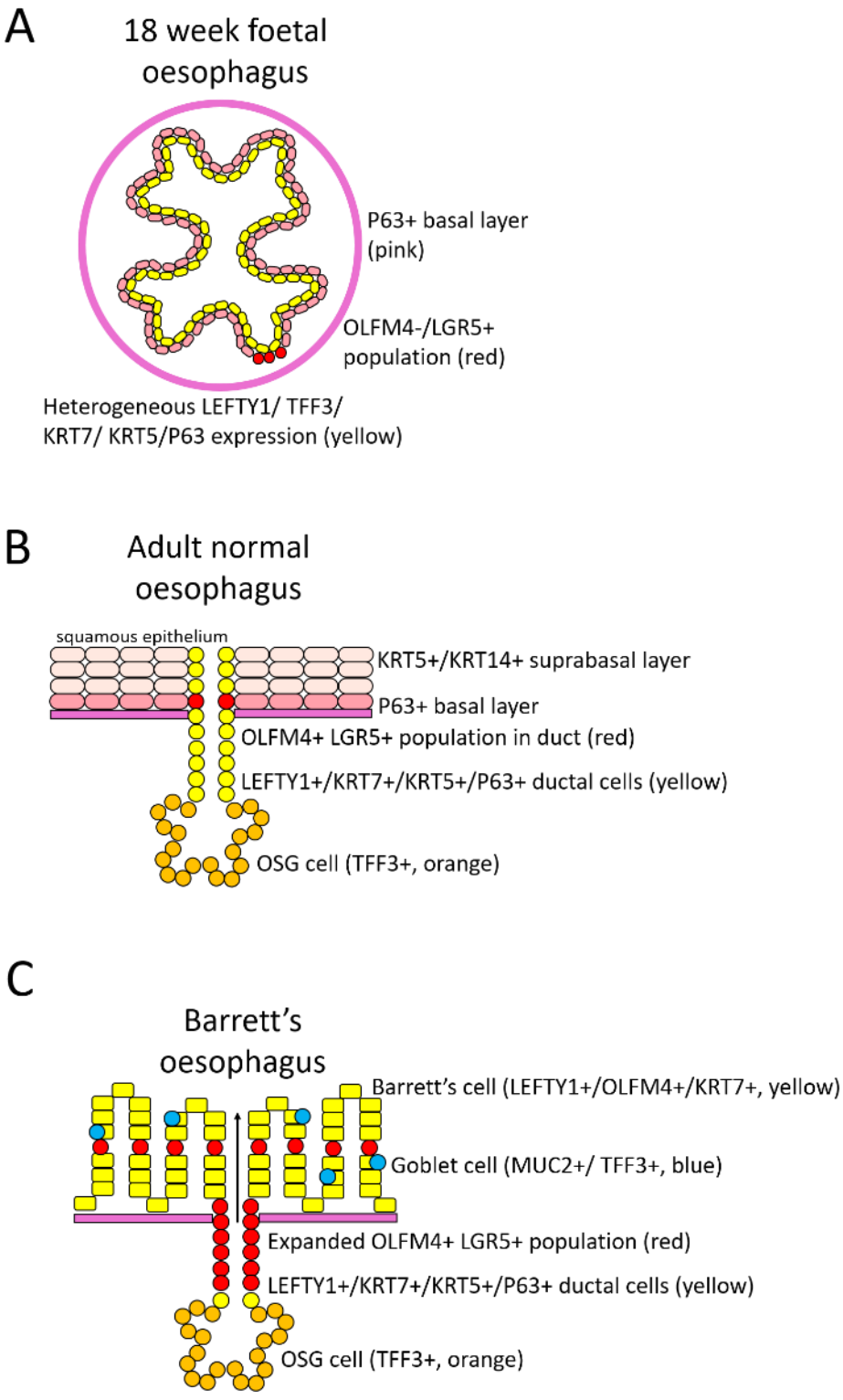


Figure 7.0: Summary diagram of findings

A Diagram of cell expression in the 18 week gestation human foetal oesophagus

B Diagram of submucosal gland in adult oesophagus

C Diagram of submucosal gland in a patient with Barrett's oesophagus

Chapter 8: Conclusion

In this study, I used a biliary reflux murine model to examine the role of early p53 mutation in the development of proximal gastric cancers. P53 mutation did not significantly increase incidence of gastric adenocarcinoma development. These mice did however develop liver inflammation and some developed liver tumours, we suggest this is due to chronic exposure of bile salt (DCA), which other studies have also demonstrated causes cancer and increase inflammatory signalling.

I have described the cellular heterogeneity of BO. I have demonstrated that the expression pattern of BO most strongly overlaps with a sub-population within squamous oesophageal biopsies, which we have shown to be OSG cells, but not in gastric or duodenal cells. This alludes to but does not demonstrate that OSG cells may be a cell of origin for BO. Although not uniquely expressed in BO or OSG cells, I demonstrate that high LEFTY1 and OLFM4 expression is found in BO and OSG cells. I have demonstrated experimentally that SPINK4 may be an early markers of goblet cell differentiation.

I examined the expression pattern of candidate BO stem cell marker OLFM4. OLFM4 is highly expressed with LEFTY1 in BO cells, which do not exhibit other specialised differentiation. In patients without BO, OLFM4+ cells are sparse in the OSG ducts; however, in patients with BO, OLFM4 expression is higher and demonstrated throughout the OSG ducts. BO organoids demonstrate all the differentiated cell types that have been seen within the sc-RNA-seq data. RNA ISH analysis has shown that in BO, OSGs and duodenal controls LGR5 and OLFM4 expression co-localises in the same cells.

Finally, I investigated human foetal oesophageal samples and oesophageal inlet patches for expression of specific BO markers I examined expression patterns of progenitor markers, OLFM4 and LGR5 in human foetal specimens. Based on limited data, the expression pattern suggests that OLFM4 does not routinely co-express with LGR5 in the foetus, suggesting OLFM4 may not be an important marker of progenitor cells in the foetus.

Bibliography

Abdalla, S. I., P. Lao-Sirieix, M. R. Novelli, L. B. Lovat, I. R. Sanderson and R. C. Fitzgerald (2004). "Gastrin-induced cyclooxygenase-2 expression in Barrett's carcinogenesis." Clinical cancer research **10**(14): 4784-4792.

Abdulnour-Nakhoul, S., N. L. Nakhoul, S. A. Wheeler, S. Haque, P. Wang, K. Brown, G. Orlando and R. C. Orlando (2007). "Characterization of esophageal submucosal glands in pig tissue and cultures." Digestive diseases and sciences **52**(11): 3054-3065.

Abela, J.-E., J. J. Going, J. F. Mackenzie, M. McKernan, S. O'mahoney and R. C. Stuart (2008). "Systematic four-quadrant biopsy detects Barrett's dysplasia in more patients than nonsystematic biopsy." Official journal of the American College of Gastroenterology| ACG **103**(4): 850-855.

Adorno, M., M. Cordenonsi, M. Montagner, S. Dupont, C. Wong, B. Hann, A. Solari, S. Bobisse, M. B. Rondina and V. Guzzardo (2009). "A mutant-p53/Smad complex opposes p63 to empower TGFβ-induced metastasis." Cell **137**(1): 87-98.

Agoston, A. T., T. H. Pham, R. D. Odze, D. H. Wang, K. M. Das, S. J. Spechler and R. F. Souza (2018). "Columnar-Lined Esophagus Develops via Wound Repair in a Surgical Model of Reflux Esophagitis." Cell Mol Gastroenterol Hepatol **6**(4): 389-404.

Agrawal, N., Y. Jiao, C. Bettegowda, S. M. Hutfless, Y. Wang, S. David, Y. Cheng, W. S. Twaddell, N. L. Latt and E. J. Shin (2012). "Comparative genomic analysis of esophageal adenocarcinoma and squamous cell carcinoma." Cancer discovery **2**(10): 899-905.

Aikou, S., J. Aida, K. Takubo, Y. Yamagata, Y. Seto, M. Kaminishi and S. Nomura (2013). "Columnar metaplasia in a surgical mouse model of gastro-esophageal reflux disease is not derived from bone marrow-derived cell." Cancer Science **104**(9): 1154-1161.

Al Yassin, T. M. and P. G. Toner (1977). "Fine structure of squamous epitheilum and submucosal glands of human oesophagus." Journal of Anatomy **123**(Pt 3): 705.

Alexandrov, L. B., S. Nik-Zainal, D. C. Wedge, S. A. Aparicio, S. Behjati, A. V. Biankin, G. R. Bignell, N. Bolli, A. Borg and A.-L. Børresen-Dale (2013). "Signatures of mutational processes in human cancer." Nature **500**(7463): 415-421.

Attili, A., M. Angelico, A. Cantafora, D. Alvaro and L. Capocaccia (1986). "Bile acid-induced liver toxicity: relation to the hydrophobic-hydrophilic balance of bile acids." Medical hypotheses **19**(1): 57-69.

Aubin, J., U. Déry, M. Lemieux, P. Chailler and L. Jeannotte (2002). "Stomach regional specification requires Hoxa5-driven mesenchymal-epithelial signaling."

Babu, A., X. Meng, A. M. Banerjee, F. Gamboni-Robertson, J. C. Cleveland, S. Damle, D. A. Fullerton and M. J. Weyant (2008). "Secretory phospholipase A2 is required to produce histologic changes associated with gastroduodenal reflux in a murine model." The Journal of Thoracic and Cardiovascular Surgery **135**(6): 1220-1227.

Ban, S. (2013). "The Normal Stomach: Anatomy, Specimen Dissection and Histology Relevant to Pathological Practice." Morson and Dawson's Gastrointestinal Pathology: 87-103.

Barbera, M., M. di Pietro, E. Walker, C. Brierley, S. MacRae, B. D. Simons, P. H. Jones, J. Stingl and R. C. Fitzgerald (2015). "The human squamous oesophagus has widespread capacity for clonal expansion from cells at diverse stages of differentiation." Gut **64**(1): 11-19.

Barker, N. (2014). "Adult intestinal stem cells: critical drivers of epithelial homeostasis and regeneration." Nature reviews Molecular cell biology **15**(1): 19-33.

Barker, N., M. Huch, P. Kujala, M. van de Wetering, H. J. Snippert, J. H. van Es, T. Sato, D. E. Stange, H. Begthel and M. van den Born (2010). "Lgr5+ ve stem cells drive self-renewal in the stomach and build long-lived gastric units in vitro." Cell stem cell **6**(1): 25-36.

Barker, N., M. B. Rookmaaker, P. Kujala, A. Ng, M. Leushacke, H. Snippert, M. van de Wetering, S. Tan, J. H. Van Es, M. Huch, R. Poulsom, M. C. Verhaar, P. J. Peters and H. Clevers (2012). "Lgr5(+ve) stem/progenitor cells contribute to nephron formation during kidney development." Cell Rep **2**(3): 540-552.

Barker, N., J. H. van Es, J. Kuipers, P. Kujala, M. van den Born, M. Cozijnsen, A. Haegebarth, J. Korving, H. Begthel, P. J. Peters and H. Clevers (2007). "Identification of stem cells in small intestine and colon by marker gene Lgr5." Nature **449**(7165): 1003-1007.

Barrett, N. (1957). "The lower esophagus lined by columnar epithelium." Surgery **41**(6): 881-894.

Barrett, N. R. (1950). "Chronic peptic ulcer of the oesophagus and 'oesophagitis'." Br J Surg **38**(150): 175-182.

Bass, A. J., V. Thorsson, I. Shmulevich, S. M. Reynolds, M. Miller, B. Bernard, T. Hinoue, P. W. Laird, C. Curtis, H. Shen, D. J. Weisenberger, N. Schultz, R. L. Shen, N. Weinhold, D. P. Keiser, R. Bowlby, P. Sipahimalani, A. D. Cherniack, G. Getz, Y. C. Liu, M. S. Noble, C. Pedamallu, C. Sougnez, A. Taylor-Weiner, R. Akbani, J. S. Lee, W. B. Liu, G. B. Mills, D. Yang, W. Zhang, A. Pantazi, M. Parfenov, M. Gulley, M. B. Piazuelo, B. G. Schneider, J. Kim, A. Boussioutas, M. Sheth, J. A. Demchok, C. S. Rabkin, J. E. Willis, S. Ng, K. Garman, D. G. Beer, A. Pennathur, B. J. Raphael, H. T. Wu, R. Odze, H. K. Kim, J. Bowen, K. M. Leraas, T. M. Lichtenberg, L. Weaver, M. McLellan, M. Wiznerowicz, R. Sakai, G. Getz, C. Sougnez, M. S. Lawrence, K. Cibulskis, L. Lichtenstein, S. Fisher, S. B. Gabriel, E. S. Lander, L. Ding, B. F. Niu, A. Ally, M. Balasundaram, I. Birol, R. Bowlby, D. Brooks, Y. S. N. Butterfield, R. Carlsen, A. Chu, J. Chu, E. Chuah, H. J. E. Chun, A. Clarke, N. Dhalla, R. Guin, R. A. Holt, S. J. M. Jones, K. Kasaian, D. Lee, H. Y. A. Li, E. Lim, Y. Ma, M. A. Marra, M. Mayo, R. A. Moore, A. J. Mungall, K. L. Mungall, K. M. Nip, A. G. Robertson, J. E. Schein, P. Sipahimalani, A. Tam, N. Thiessen, R. Beroukhim, S. L. Carter, A. D. Cherniack, J. Cho, K. Cibulskis, D. DiCara, S. Frazer, S. Fisher, S. B. Gabriel, N. Gehlenborg, D. I. Heiman, J. Jung, J. Kim, E. S. Lander, M. S. Lawrence, L. Lichtenstein, P. Lin, M. Meyerson, A. I. Ojesina, C. S. Pedamallu, G. Saksena, S. E. Schumacher, C. Sougnez, P. Stojanov, B. Tabak, A. Taylor-Weiner, D. Voet, M. Rosenberg, T. I. Zack, H. L. Zhang, L. H. Zou, A. Protopopov, N. Santoso, M. Parfenov, S. Lee, J. Zhang, H. S. Mahadeshwar, J. B. Tang, X. J. Ren, S. Seth, L. X. Yang, A. W. Xu, X. Z. Song, A. Pantazi, R. B. Xi, C. A. Bristow, A. Hadjipanayis, J. Seidman, L. Chin, P. J. Park, R. Kucherlapati, R. Akbani, S. Y. Ling, W. B. Liu, A. Rao, J. N. Weinstein, S. B. Kim, J. S. Lee, Y. L. Lu, G. Mills, T. Hinoue, D. J. Weisenberger, M. S. Bootwalla, P. H. Lai, H. Shen, T. Triche, D. J. Van Den Berg, S. B. Baylin, J. G. Herman, G. Getz, L. Chin, Y. C. Liu, B. A. Murray, M. S. Noble, B. A. Askoy, G. Ciriello, G. Dresdner, J. J. Gao, B. Gross, A. Jacobsen, W. Lee, R. Ramirez, C. Sander, N. Schultz, Y. Senbabaoglu, R. Sinha, S. O. Sumer, Y. C. Sun, N. Weinhold, V. Thorsson, B. Bernard, L. Iype, R. W. Kramer, R. Kreisberg, M. Miller, S. M. Reynolds, H. Rovira, N. Tasman, I. Shmulevich, S. Ng, D. Haussler, J. M. Stuart, R. Akbani, S. Y. Ling, W. B. Liu, A. Rao, J. N. Weinstein, R. G. W. Verhaak, G. B. Mills, M. D. M. Leiserson, B. J. Raphael, H. T. Wu, B. S. Taylor, A. D. Black, J. Bowen, J. A. Carney, J. M. Gastier-Foster, C. Helsel, K. M. Leraas, T. M. Lichtenberg, C. McAllister, N. C. Ramirez, T. R. Tabler, L. Wise, E. Zmuda, R. Penny, D. Crain, J. Gardner, K. Lau, E. Curely, D. Mallery, S. Morris, J. Paulauskis, T. Shelton, C. Shelton, M. Sherman, C. Benz, J. H. Lee, K. Fedosenko, G. Manikhas, O. Voronina, D. Belyaev, O. Dolzhansky, W. K. Rathmell, J. Brzezinski, M. Ibbs, K. Korski, W. Kycler, R. Lazniak, E. Leporowska, A. Mackiewicz, D. Murawa, P. Murawa, A. Spychala, W. M. Suchorska, H. Tatka, M. Teresiak, M. Wiznerowicz, R. Abdel-Misih, J. Bennett, J. Brown, M. Iacocca, B. Rabeno, S. Y. Kwon, R. Penny, J. Gardner, A. Kemkes, D. Mallery, S. Morris, T. Shelton, C. Shelton, E. Curley, I. Alexopoulou, J. Engel, J. Bartlett, M. Albert, D. Y. Park, R. Dhir, J. Luketich, R. Landreneau, Y. Y. Janjigian, D. P. Kelsen, E. Cho, M. Ladanyi, L. Tang, S. J. McCall, Y. S. Park, J. H. Cheong, J. Ajani, M. C. Camargo, S. Alonso, B. Ayala, M. A. Jensen, T. Pihl, R. Raman, J. Walton, Y. H. Wan, J. A. Demchok, G. Eley, K. R. M. Shaw, M. Sheth, R. Tarnuzzer, Z. N. Wang, L. M. Yang, J. C. Zenklusen, T. Davidsen, C. M. Hutter, H. J. Sofia, R. Burton, S. Chudamani, J. Liu and C. G. A. R. Network (2014). "Comprehensive molecular characterization of gastric adenocarcinoma." Nature **513**(7517): 202-209.

Baxter, A. G., M. A. Jordan, P. A. Silveira, W. E. Wilson and I. R. Van Driel (2005). "Genetic control of susceptibility to autoimmune gastritis." International reviews of immunology **24**(1-2): 55-62.

Bennett, C., P. Moayyedi, D. A. Corley, J. DeCaestecker, Y. Falck-Ytter, G. Falk, N. Vakil, S. Sanders, M. Vieth and J. Inadomi (2015). "BOB CAT: a large-scale review and Delphi consensus for management of Barrett's esophagus with no dysplasia, indefinite for, or low-grade dysplasia." The American journal of gastroenterology **110**(5): 662.

Beresford, W. A. (1990). "Direct transdifferentiation: can cells change their phenotype without dividing?" Cell Differ Dev **29**(2): 81-93.

Bernstein, C., H. Holubec, A. K. Bhattacharyya, H. Nguyen, C. M. Payne, B. Zaitlin and H. Bernstein (2011). "Carcinogenicity of deoxycholate, a secondary bile acid." Archives of toxicology **85**(8): 863-871.

Bhat, S., H. G. Coleman, F. Yousef, B. T. Johnston, D. T. McManus, A. T. Gavin and L. J. Murray (2011). "Risk of malignant progression in Barrett's esophagus patients: results from a large population-based study." Journal of the National Cancer Institute **103**(13): 1049-1057.

Bitgood, M. J. and A. P. McMahon (1995). "HedgehogandBmpGenes are coexpressed at many diverse sites of cell–cell interaction in the mouse embryo." Developmental biology **172**(1): 126-138.

Boch, J., H. Shields, D. Antonioli, F. Zwas, R. Sawhney and J. Trier (1997). "Distribution of cytokeratin markers in Barrett's specialized columnar epithelium." Gastroenterology **112**(3): 760-765.

BoÈttger, V., A. BoÈttger, C. Garcia-Echeverria, Y. F. Ramos, A. J. van der Eb, A. G. Jochemsen and D. P. Lane (1999). "Comparative study of the p53-mdm2 and p53-MDMX interfaces." Oncogene **18**(1): 189-199.

Böhmer, A. C., J. Hecker, J. Schröder, P. Gharahkhani, A. May, C. Gerges, M. Anders, J. Becker, T. Hess and N. Kreuser (2020). "Shared genetic etiology of obesity-related traits and Barrett's esophagus/adenocarcinoma: insights from genome-wide association studies." Cancer Epidemiology and Prevention Biomarkers **29**(2): 427-433.

Boivin, G. P., B. A. O'Toole, I. E. Orsmby, R. J. Diebold, M. J. Eis, T. Doetschman and A. B. Kier (1995). "Onset and progression of pathological lesions in transforming growth factor-beta 1-deficient mice." The American journal of pathology **146**(1): 276.

Bornschein, J., M. Quante and M. Jansen (2021). "The complexity of cancer origins at the gastro-oesophageal junction." Best Practice & Research Clinical Gastroenterology **50**: 101729.

Bremner, C. G., V. P. Lynch and F. H. Ellis, Jr. (1970). "Barrett's esophagus: congenital or acquired? An experimental study of esophageal mucosal regeneration in the dog." Surgery **68**(1): 209-216.

Broda, T. R., K. W. McCracken and J. M. Wells (2019). "Generation of human antral and fundic gastric organoids from pluripotent stem cells." Nature protocols **14**(1): 28-50.

Buas, M. F., D. M. Levine, K. W. Makar, H. Utsugi, L. Onstad, X. Li, P. C. Galipeau, N. J. Shaheen, L. J. Hardie and Y. Romero (2014). "Integrative post-genome-wide association analysis of CDKN2A and TP53 SNPs and risk of esophageal adenocarcinoma." Carcinogenesis **35**(12): 2740-2747.

Buas, M. F., L. Onstad, D. M. Levine, H. A. Risch, W.-H. Chow, G. Liu, R. C. Fitzgerald, L. Bernstein, W. Ye and N. C. Bird (2015). "MiRNA-related SNPs and risk of esophageal adenocarcinoma and Barrett's esophagus: post genome-wide association analysis in the BEACON consortium." PLoS one **10**(6): e0128617.

Budwit-Novotny, D. A., K. S. McCarty, E. B. Cox, J. T. Soper, D. G. Mutch, W. T. Creasman and J. L. Flowers (1986). "Immunohistochemical analyses of estrogen receptor in endometrial adenocarcinoma using a monoclonal antibody." Cancer research **46**(10): 5419-5425.

Busslinger, G. A., B. de Barbanson, R. Oka, B. L. Weusten, M. de Maat, R. van Hillegersberg, L. A. Brosens, R. van Boxtel, A. van Oudenaarden and H. Clevers (2021). "Molecular characterization of Barrett's esophagus at single-cell resolution." Proceedings of the National Academy of Sciences **118**(47).

Busslinger, G. A., B. L. Weusten, A. Bogte, H. Begthel, L. A. Brosens and H. Clevers (2021). "Human gastrointestinal epithelia of the esophagus, stomach, and duodenum resolved at single-cell resolution." Cell Reports **34**(10): 108819.

Busuttil, R. A. and A. Boussioutas (2009). "Intestinal metaplasia: a premalignant lesion involved in gastric carcinogenesis." J Gastroenterol Hepatol **24**(2): 193-201.

Buti, L., E. Spooner, A. G. Van der Veen, R. Rappuoli, A. Covacci and H. L. Ploegh (2011). "Helicobacter pylori cytotoxin-associated gene A (CagA) subverts the apoptosis-stimulating protein of p53 (ASPP2) tumor suppressor pathway of the host." Proceedings of the National Academy of Sciences **108**(22): 9238-9243.

Calvert, R. and P. Pothier (1990). "Migration of fetal intestinal intervillous cells in neonatal mice." Anat Rec **227**(2): 199-206.

Cancer Genome Atlas Research, N., U. Analysis Working Group: Asan, B. C. C. Agency, Brigham, H. Women's, I. Broad, U. Brown, U. Case Western Reserve, I. Dana-Farber Cancer, U. Duke, C. Greater Poland Cancer, S. Harvard Medical, B. Institute for Systems, K. U. Leuven, C. Mayo, C. Memorial Sloan Kettering Cancer, I. National Cancer, H. Nationwide Children's, U. Stanford, A. University of, M. University of, C. University of North, P. University of, R. University of, C. University of Southern, M. D. A. C. C. University of Texas, W. University of, I. Van Andel Research, U. Vanderbilt, U. Washington, I. Genome Sequencing Center: Broad, L. Washington University in St, B. C. C. A. Genome Characterization Centers, I. Broad, S. Harvard Medical, U. Sidney Kimmel Comprehensive Cancer Center at Johns Hopkins, C. University of North, C. University of Southern California Epigenome, M. D. A. C. C. University of Texas, I. Van Andel Research, I. Genome Data Analysis Centers: Broad, U. Brown, S. Harvard Medical, B. Institute for Systems, C. Memorial Sloan Kettering Cancer, C. University of California Santa, M. D. A. C. C. University of Texas, C. Biospecimen Core Resource: International Genomics, H. Research Institute at Nationwide Children's, S. Tissue Source Sites: Analytic Biologic, C. Asan Medical, B. Asterand, H. Barretos Cancer, BioreclamationIvt, C. Botkin Municipal, S. Chonnam National University Medical, S. Christiana Care Health, Cureline, U. Duke, U. Emory, U. Erasmus, M. Indiana University School of, M. Institute of Oncology of, C. International Genomics, Invidumed, H. Israelitisches Krankenhaus, M. Keimyung University School of, C. Memorial Sloan Kettering Cancer, G. National Cancer Center, B. Ontario Tumour, C. Peter MacCallum Cancer, S. Pusan National University Medical, S. Ribeirao Preto Medical, H. St. Joseph's, C. Medical, U. St. Petersburg Academic, B. Tayside Tissue, D. University of, C. University of Kansas Medical, M. University of, H. University of North Carolina at Chapel, M. University of Pittsburgh School of, M. D. A. C. C. University of Texas, U. Disease Working Group: Duke, C. Memorial Sloan Kettering Cancer, I. National Cancer, M. D. A. C. C. University of Texas, M. Yonsei University College of, C. I. Data Coordination Center and H. Project Team: National Institutes of (2017). "Integrated genomic characterization of oesophageal carcinoma." Nature **541**(7636): 169-175.

Cervantes, S., T. P. Yamaguchi and M. Hebrok (2009). "Wnt5a is essential for intestinal elongation in mice." Developmental biology **326**(2): 285-294.

Chandrasoma, P. (1997). Pathophysiology of Barrett's esophagus. Seminars in thoracic and cardiovascular surgery, Philadelphia, PA: WB Saunders,[1989-.

Chandrasoma, P. T., D. M. Lokuhetty, T. R. Demeester, C. G. Bremner, J. H. Peters, S. Oberg and S. Groshen (2000). "Definition of histopathologic changes in gastroesophageal reflux disease." The American journal of surgical pathology **24**(3): 344-351.

Chang, P.-C., T.-Y. Wang, Y.-T. Chang, C.-Y. Chu, C.-L. Lee, H.-W. Hsu, T.-A. Zhou, Z. Wu, R. H. Kim and S. J. Desai (2014). "Autophagy pathway is required for IL-6

induced neuroendocrine differentiation and chemoresistance of prostate cancer LNCaP cells." PloS one **9**(2): e88556.

Chaves, P., C. Cruz, A. Dias Pereira, A. Suspiro, J. C. de Almeida, C. N. Leitao and J. Soares (2005). "Gastric and intestinal differentiation in Barrett's metaplasia and associated adenocarcinoma." Dis Esophagus **18**(6): 383-387.

Chawengsaksophak, K., R. James, V. Hammond, F. Köntgen and F. Beck (1997). "Homeosis and intestinal tumours in Cdx2 mutant mice." Nature **386**(6620): 84-87.

Chen, X., R. Qin, B. Liu, Y. Ma, Y. Su, C. S. Yang, J. N. Glickman, R. D. Odze and N. J. Shaheen (2008). "Multilayered epithelium in a rat model and human Barrett's esophagus: similar expression patterns of transcription factors and differentiation markers." BMC gastroenterology **8**(1): 1-9.

Cheok, C. F., C. S. Verma, J. Baselga and D. P. Lane (2011). "Translating p53 into the clinic." Nature reviews Clinical oncology **8**(1): 25-37.

Choi, M. Y., A. I. Romer, Y. Wang, M. P. Wu, S. Ito, A. B. Leiter and R. A. Shivdasani (2008). "Requirement of the tissue-restricted homeodomain transcription factor Nkx6. 3 in differentiation of gastrin-producing G cells in the stomach antrum." Molecular and Cellular Biology **28**(10): 3208-3218.

Ciocalteu, A., P. Popa, M. Ionescu and D. I. Gheonea (2019). "Issues and controversies in esophageal inlet patch." World Journal of Gastroenterology **25**(30): 4061.

Coad, R. A., A. C. Woodman, P. J. Warner, H. Barr, N. A. Wright and N. A. Shepherd (2005). "On the histogenesis of Barrett's oesophagus and its associated squamous islands: a three-dimensional study of their morphological relationship with native oesophageal gland ducts." J Pathol **206**(4): 388-394.

Colom, B., M. P. Alcolea, G. Piedrafita, M. W. Hall, A. Wabik, S. C. Dentro, J. C. Fowler, A. Herms, C. King and S. H. Ong (2020). "Spatial competition shapes the dynamic mutational landscape of normal esophageal epithelium." Nature genetics **52**(6): 604-614.

Cooks, T., I. S. Pateras, O. Tarcic, H. Solomon, A. J. Schetter, S. Wilder, G. Lozano, E. Pikarsky, T. Forshew and N. Rozenfeld (2013). "Mutant p53 prolongs NF-κB activation and promotes chronic inflammation and inflammation-associated colorectal cancer." Cancer cell **23**(5): 634-646.

Correa, P., M. B. Piazuelo and K. T. Wilson (2010). "Pathology of gastric intestinal metaplasia: clinical implications." Am J Gastroenterol **105**(3): 493-498.

Coste, I., J. N. Freund, S. Spaderna, T. Brabletz and T. Renno (2007). "Precancerous lesions upon sporadic activation of β-catenin in mice." Gastroenterology **132**(4): 1299-1308.

Curtius, K., J. H. Rubenstein, A. Chak and J. M. Inadomi (2020). "Computational modelling suggests that Barrett's oesophagus may be the precursor of all oesophageal adenocarcinomas." Gut.

Dai, J. Y., J. de Dieu Tapsoba, M. F. Buas, L. E. Onstad, D. M. Levine, H. A. Risch, W.-H. Chow, L. Bernstein, W. Ye and J. Lagergren (2015). "A newly identified susceptibility locus near FOXP1 modifies the association of gastroesophageal reflux with Barrett's esophagus." Cancer Epidemiology and Prevention Biomarkers **24**(11): 1739-1747.

Dame, M. K., S. Huang, D. Attili, J. R. Spence and J. A. Colacino (2020). Identification and Isolation of Human LGR5+ Cells Using an Antibody-Based Strategy. Intestinal Stem Cells, Springer**:** 3-23.

Dedeić, Z., G. Sutendra, Y. Hu, K. Chung, E. A. Slee, M. J. White, F. Y. Zhou, R. D. Goldin, D. J. Ferguson and D. McAndrew (2018). "Cell autonomous role of iASPP deficiency in causing cardiocutaneous disorders." Cell Death & Differentiation **25**(7): 1289-1303.

Derdoy, J. J., A. Bergwerk, H. Cohen, M. Kline, H. L. Monforte and D. W. Thomas (2003). "The gastric cardia: to be or not to be?" The American journal of surgical pathology **27**(4): 499-504.

Derynck, R., R. J. Akhurst and A. Balmain (2001). "TGF-β signaling in tumor suppression and cancer progression." Nature genetics **29**(2): 117-129.

Desai, T. J., S. Malpel, G. R. Flentke, S. M. Smith and W. V. Cardoso (2004). "Retinoic acid selectively regulates Fgf10 expression and maintains cell identity in the prospective lung field of the developing foregut." Developmental biology **273**(2): 402-415.

Deyoung, M. and L. Ellisen (2007). "p63 and p73 in human cancer: defining the network." Oncogene **26**(36): 5169-5183.

Domyan, E. T., E. Ferretti, K. Throckmorton, Y. Mishina, S. K. Nicolis and X. Sun (2011). "Signaling through BMP receptors promotes respiratory identity in the foregut via repression of Sox2." Development **138**(5): 971-981.

Dong, J., M. F. Buas, P. Gharahkhani, B. J. Kendall, L. Onstad, S. Zhao, L. A. Anderson, A. H. Wu, W. Ye and N. C. Bird (2018). "Determining risk of Barrett's esophagus and esophageal adenocarcinoma based on epidemiologic factors and genetic variants." Gastroenterology **154**(5): 1273-1281. e1273.

Dong, J., D. M. Levine, M. F. Buas, R. Zhang, L. Onstad, R. C. Fitzgerald, D. A. Corley, N. J. Shaheen, J. Lagergren and L. J. Hardie (2018). "Interactions between genetic variants and environmental factors affect risk of esophageal adenocarcinoma and Barrett's esophagus." Clinical Gastroenterology and Hepatology **16**(10): 1598-1606. e1594.

Doupé, D. P., M. P. Alcolea, A. Roshan, G. Zhang, A. M. Klein, B. D. Simons and P. H. Jones (2012). "A single progenitor population switches behavior to maintain and repair esophageal epithelium." Science **337**(6098): 1091-1093.

Drubbel, A. V., S. Pirard, S. Kin, B. Dassy, A. Lefort, F. Libert, S. Nomura and B. Beck (2021). "Reactivation of the Hedgehog pathway in esophageal progenitors turns on an embryonic-like program to initiate columnar metaplasia." Cell Stem Cell **28**(8): 1411-1427. e1417.

Duits, L. C., M. J. van der Wel, C. C. Cotton, K. N. Phoa, F. J. Ten Kate, C. A. Seldenrijk, G. J. A. Offerhaus, M. Visser, S. L. Meijer and R. C. Mallant-Hent (2017). "Patients with Barrett's esophagus and confirmed persistent low-grade dysplasia are at increased risk for progression to neoplasia." Gastroenterology **152**(5): 993-1001. e1001.

Dulak, A. M., S. E. Schumacher, J. Van Lieshout, Y. Imamura, C. Fox, B. Shim, A. H. Ramos, G. Saksena, S. C. Baca and J. Baselga (2012). "Gastrointestinal adenocarcinomas of the esophagus, stomach, and colon exhibit distinct patterns of genome instability and oncogenesis." Cancer research **72**(17): 4383-4393.

Dulak, A. M., P. Stojanov, S. Peng, M. S. Lawrence, C. Fox, C. Stewart, S. Bandla, Y. Imamura, S. E. Schumacher and E. Shefler (2013). "Exome and whole-genome sequencing of esophageal adenocarcinoma identifies recurrent driver events and mutational complexity." Nature genetics **45**(5): 478-486.

Dunn, L. J., A. D. Burt, N. Hayes and S. M. Griffin (2016). "Columnar metaplasia in the esophageal remnant after esophagectomy: a common occurrence and a valuable insight into the development of Barrett esophagus." Annals of Surgery **264**(6): 1016-1021.

Dvorak, K., C. M. Payne, M. Chavarria, L. Ramsey, B. Dvorakova, H. Bernstein, H. Holubec, R. E. Sampliner, N. Guy, A. Condon, C. Bernstein, S. B. Green, A. Prasad and H. S. Garewal (2007). "Bile acids in combination with low pH induce oxidative stress and oxidative DNA damage: relevance to the pathogenesis of Barrett's oesophagus." Gut **56**(6): 763-771.

Dziadkowiec, K. N., E. Szu, E. Delaflor-Weiss and J. Proenza (2019). "1832 Adenocarcinoma arising from a cervical esophageal inlet Patch: the malignant potential of a small lesion." Official journal of the American College of Gastroenterology| ACG **114**: S1027-S1028.

Eda, A., H. Osawa, I. Yanaka, K. Satoh, H. Mutoh, K. Kihira and K. Sugano (2002). "Expression of homeobox gene CDX2 precedes that of CDX1 during the progression of intestinal metaplasia." J Gastroenterol **37**(2): 94-100.

Ek, W. E., D. M. Levine, M. D'Amato, N. L. Pedersen, P. K. Magnusson, F. Bresso, L. E. Onstad, P. T. Schmidt, H. Törnblom and H. Nordenstedt (2013). "Germline genetic contributions to risk for esophageal adenocarcinoma, Barrett's esophagus, and gastroesophageal reflux." Journal of the National Cancer Institute **105**(22): 1711-1718.

El-Serag, H. B., A. Sonnenberg, M. M. Jamal, D. Kunkel, L. Crooks and R. M. Feddersen (1999). "Characteristics of intestinal metaplasia in the gastric cardia." Am J Gastroenterol **94**(3): 622-627.

El-Serag, H. B., S. Sweet, C. C. Winchester and J. Dent (2014). "Update on the epidemiology of gastro-oesophageal reflux disease: a systematic review." Gut **63**(6): 871-880.

Ellis Jr, F. H., X. Xu, M. H. Kulke, J. LoCicero III and M. Loda (2001). "Malignant transformation of the esophageal mucosa is enhanced in p27 knockout mice." The Journal of Thoracic and Cardiovascular Surgery **122**(4): 809-814.

Elsheaita, A., M. A. El-Bially, M. M. Shamseya, S. S. Ahmed, M. A. Madkour, A. M. Shamseya and H. H. Nouh (2020). "Seattle protocol vs narrow band imaging guided biopsy in screening of Barrett's esophagus in gastroesophageal reflux disease patients." Medicine **99**(8).

Enss, M.-L., M. Cornberg, S. Wagner, A. Gebert, M. Henrichs, R. Eisenblätter, W. Beil, R. Kownatzki and H. Hedrich (2000). "Proinflammatory cytokines trigger MUC gene expression and mucin release in the intestinal cancer cell line LS180." Inflammation Research **49**(4): 162-169.

Epperly, M. W., H. Guo, H. Shen, Y. Niu, X. Zhang, M. Jefferson, C. A. Sikora and J. S. Greenberger (2004). "Bone marrow origin of cells with capacity for homing and differentiation to esophageal squamous epithelium." Radiation research **162**(3): 233-240.

Epstein, J. A., H. Cosby, G. W. Falk, M. A. Khashab, R. Kiesslich, E. A. Montgomery, J. S. Wang and M. I. Canto (2017). "Columnar islands in Barrett's esophagus: Do they impact Prague C&M criteria and dysplasia grade?" Journal of Gastroenterology and Hepatology **32**(9): 1598-1603.

Farinati, F., R. Cardin, P. Degan, M. Rugge, F. D. Mario, P. Bonvicini and R. Naccarato (1998). "Oxidative DNA damage accumulation in gastric carcinogenesis." Gut **42**(3): 351-356.

Fein, M., J. H. Peters, N. Baril, M. McGarvey, P. Chandrasoma, D. Shibata, P. W. Laird and K. A. Skinner (1999). "Loss of Function ofTrp53, but NotApc, Leads to the Development of Esophageal Adenocarcinoma in Mice with Jejunoesophageal Reflux." Journal of Surgical Research **83**(1): 48-55.

Fernandez-Antoran, D., G. Piedrafita, K. Murai, S. H. Ong, A. Herms, C. Frezza and P. H. Jones (2019). "Outcompeting p53-mutant cells in the normal esophagus by redox manipulation." Cell stem cell **25**(3): 329-341. e326.

Feurle, G., V. Helmstaedter, A. Buehring, U. Bettendorf and V. Eckardt (1990). "Distinct immunohistochemical findings in columnar epithelium of esophageal inlet patch and of Barrett's esophagus." Digestive diseases and sciences **35**(1): 86-92.

Fitzgerald, R. C., M. di Pietro, K. Ragunath, Y. Ang, J. Y. Kang, P. Watson, N. Trudgill, P. Patel, P. V. Kaye, S. Sanders, M. O'Donovan, E. Bird-Lieberman, P. Bhandari, J. A. Jankowski, S. Attwood, S. L. Parsons, D. Loft, J. Lagergren, P. Moayyedi, G. Lyratzopoulos, J. de Caestecker and G. British Society of (2014). "British Society of Gastroenterology guidelines on the diagnosis and management of Barrett's oesophagus." Gut **63**(1): 7-42.

Fitzgerald, R. C., I. T. Saeed, D. Khoo, M. J. Farthing and W. R. Burnham (2001). "Rigorous surveillance protocol increases detection of curable cancers associated with Barrett's esophagus." Digestive diseases and sciences **46**(9): 1892-1898.

Flynn, C., D. C. Montrose, D. L. Swank, M. Nakanishi, J. N. Ilsley and D. W. Rosenberg (2007). "Deoxycholic acid promotes the growth of colonic aberrant crypt foci." Molecular Carcinogenesis: Published in cooperation with the University of Texas MD Anderson Cancer Center **46**(1): 60-70.

Fornefett, J., J. Krause, K. Klose, F. Fingas, R. Hassert, L. Benga, T. Grunwald, U. Müller, W. Schrödl and C. G. Baums (2018). "Comparative analysis of humoral immune responses and pathologies of BALB/c and C57BL/6 wildtype mice experimentally infected with a highly virulent Rodentibacter pneumotropicus (Pasteurella pneumotropica) strain." BMC microbiology **18**(1): 1-11.

Fox, J. G., C. A. Dangler, M. T. Whary, W. Edelman, R. Kucherlapati and T. C. Wang (1997). "Mice carrying a truncated Apc gene have diminished gastric epithelial proliferation, gastric inflammation, and humoral immunity in response to Helicobacter felis infection." Cancer research **57**(18): 3972-3978.

Fox, J. G., X. Li, R. J. Cahill, K. Andrutis, A. K. Rustgi, R. Odze and T. C. Wang (1996). "Hypertrophic gastropathy in Helicobacter felis-infected wild-type C57BL/6 mice and p53 hemizygous transgenic mice." Gastroenterology **110**(1): 155-166.

Frankell, A. M., S. Jammula, X. Li, G. Contino, S. Killcoyne, S. Abbas, J. Perner, L. Bower, G. Devonshire and E. Ococks (2019). "The landscape of selection in 551

esophageal adenocarcinomas defines genomic biomarkers for the clinic." Nature genetics **51**(3): 506-516.

Fransén-Pettersson, N., N. Duarte, J. Nilsson, M. Lundholm, S. Mayans, Å. Larefalk, T. D. Hannibal, L. Hansen, A. Schmidt-Christensen and F. Ivars (2016). "A new mouse model that spontaneously develops chronic liver inflammation and fibrosis." PLoS One **11**(7): e0159850.

Fu, D. J., L. Wang, F. K. Chouairi, I. M. Rose, D. A. Abetov, A. D. Miller, R. J. Yamulla, J. C. Schimenti, A. Flesken-Nikitin and A. Y. Nikitin (2020). "Gastric squamous-columnar junction contains a large pool of cancer-prone immature osteopontin responsive Lgr5(-)CD44(+) cells." Nat Commun **11**(1): 84.

Fujitani, Y., S. Fujitani, D. F. Boyer, M. Gannon, Y. Kawaguchi, M. Ray, M. Shiota, R. W. Stein, M. A. Magnuson and C. V. Wright (2006). "Targeted deletion of a cis-regulatory region reveals differential gene dosage requirements for Pdx1 in foregut organ differentiation and pancreas formation." Genes & development **20**(2): 253-266.

Fukuda, K. and S. Yasugi (2005). "The molecular mechanisms of stomach development in vertebrates." Development, growth & differentiation **47**(6): 375-382.

Gao, N., P. White and K. H. Kaestner (2009). "Establishment of intestinal identity and epithelial-mesenchymal signaling by Cdx2." Developmental cell **16**(4): 588-599.

Garman, K. S. (2017). "Origin of Barrett's epithelium: esophageal submucosal glands." Cellular and Molecular Gastroenterology and Hepatology **4**(1): 153-156.

Garman, K. S., L. Kruger, S. Thomas, M. Swiderska-Syn, B. K. Moser, A. M. Diehl and S. J. McCall (2015). "Ductal metaplasia in oesophageal submucosal glands is associated with inflammation and oesophageal adenocarcinoma." Histopathology **67**(6): 771-782.

Gawenis, L. R., J. M. Greeb, V. Prasad, C. Grisham, L. P. Sanford, T. Doetschman, A. Andringa, M. L. Miller and G. E. Shull (2005). "Impaired gastric acid secretion in mice with a targeted disruption of the NHE4 Na+/H+ exchanger." Journal of Biological Chemistry **280**(13): 12781-12789.

Gharahkhani, P., R. C. Fitzgerald, T. L. Vaughan, C. Palles, I. Gockel, I. Tomlinson, M. F. Buas, A. May, C. Gerges and M. Anders (2016). "Genome-wide association studies in oesophageal adenocarcinoma and Barrett's oesophagus: a large-scale meta-analysis." The lancet oncology **17**(10): 1363-1373.

Gillen, P., P. Keeling, P. J. Byrne, M. Healy, R. R. O'Moore and T. P. Hennessy (1988). "Implication of duodenogastric reflux in the pathogenesis of Barrett's oesophagus." Br J Surg **75**(6): 540-543.

Giroux, V. and A. K. Rustgi (2017). "Metaplasia: tissue injury adaptation and a precursor to the dysplasia-cancer sequence." Nat Rev Cancer **17**(10): 594-604.

Glickman, J. N., Y.-Y. Chen, H. H. Wang, D. A. Antonioli and R. D. Odze (2001). "Phenotypic characteristics of a distinctive multilayered epithelium suggests that it is a precursor in the development of Barrett's esophagus." The American journal of surgical pathology **25**(5): 569-578.

Goldenring, J. R. and J. C. Mills (2021). "Cellular Plasticity, Reprogramming, and Regeneration: Metaplasia in the Stomach and Beyond." Gastroenterology.

Goldenring, J. R. and K. T. Nam (2010). "Oxyntic atrophy, metaplasia, and gastric cancer." Progress in molecular biology and translational science **96**: 117-131.

Goldenring, J. R., K. T. Nam and J. C. Mills (2011). "The origin of pre-neoplastic metaplasia in the stomach: chief cells emerge from the Mist." Experimental cell research **317**(19): 2759-2764.

Gonzalez, J.-M., A. Benezech and M. Barthet (2016). "Complications of submucosal endoscopy." Best Practice & Research Clinical Gastroenterology **30**(5): 783-791.

Goss, A. M., Y. Tian, T. Tsukiyama, E. D. Cohen, D. Zhou, M. M. Lu, T. P. Yamaguchi and E. E. Morrisey (2009). "Wnt2/2b and β-catenin signaling are necessary and sufficient to specify lung progenitors in the foregut." Developmental cell **17**(2): 290-298.

Gotley, D., A. Morgan and M. Cooper (1988). "Bile acid concentrations in the refluxate of patients with reflux oesophagitis." Journal of British Surgery **75**(6): 587-590.

Grainger, S., J. G. Savory and D. Lohnes (2010). "Cdx2 regulates patterning of the intestinal epithelium." Developmental biology **339**(1): 155-165.

Greenberg, A. K., H. Yee and W. N. Rom (2002). "Preneoplastic lesions of the lung." Respiratory research **3**(1): 1-10.

Gregorieff, A., D. E. Stange, P. Kujala, H. Begthel, M. van den Born, J. Korving, P. J. Peters and H. Clevers (2009). "The ets-domain transcription factor Spdef promotes maturation of goblet and paneth cells in the intestinal epithelium." Gastroenterology **137**(4): 1333-1345 e1331-1333.

Greulich, S., W. J. Chen, B. Maxhera, L. J. Rijzewijk, R. W. van der Meer, J. T. Jonker, H. Mueller, D. H. de Wiza, R.-R. Floerke and K. Smiris (2013). "Cardioprotective properties of omentin-1 in type 2 diabetes: evidence from clinical and in vitro studies." PloS one **8**(3): e59697.

Griffin, M. and E. C. Sweeney (1987). "The relationship of endocrine cells, dysplasia and carcinoembryonic antigen in Barrett's mucosa to adenocarcinoma of the oesophagus." Histopathology **11**(1): 53-62.

Grun, D., A. Lyubimova, L. Kester, K. Wiebrands, O. Basak, N. Sasaki, H. Clevers and A. van Oudenaarden (2015). "Single-cell messenger RNA sequencing reveals rare intestinal cell types." Nature **525**(7568): 251-255.

Grun, D., M. J. Muraro, J. C. Boisset, K. Wiebrands, A. Lyubimova, G. Dharmadhikari, M. van den Born, J. van Es, E. Jansen, H. Clevers, E. J. de Koning and A. van Oudenaarden (2016). "De Novo Prediction of Stem Cell Identity using Single-Cell Transcriptome Data." Cell Stem Cell **19**(2): 266-277.

Gutierrez-Gonzalez, L. and N. A. Wright (2008). "Biology of intestinal metaplasia in 2008: more than a simple phenotypic alteration." Dig Liver Dis **40**(7): 510-522.

Hadjinicolaou, A. V., S. N. van Munster, A. Achilleos, J. S. Garcia, S. Killcoyne, K. Ragunath, J. J. Bergman, R. C. Fitzgerald and M. Di Pietro (2020). "Aneuploidy in targeted endoscopic biopsies outperforms other tissue biomarkers in the prediction of histologic progression of Barrett's oesophagus: A multi-centre prospective cohort study." EBioMedicine **56**: 102765.

Hahm, K. B., K. Lee, Y. Kim, W. Hong, W. Lee, S. Han, M. Kim, B. Ahn, T. Oh and M. Lee (2002). "Conditional loss of TGF-β signalling leads to increased susceptibility to gastrointestinal carcinogenesis in mice." Alimentary pharmacology & therapeutics **16**: 115-127.

Hamade, N., S. Vennelaganti, S. Parasa, P. Vennalaganti, S. Gaddam, M. C. Spaander, S. H. van Olphen, P. N. Thota, K. F. Kennedy and M. J. Bruno (2019). "Lower annual rate of progression of short-segment vs long-segment Barrett's esophagus to esophageal adenocarcinoma." Clinical Gastroenterology and Hepatology **17**(5): 864-868.

Hamelin, R., J.-F. Fléjou, F. Muzeau, F. Potet, P. Laurent-Puig, F. Fékété and G. Thomas (1994). "TP53 gene mutations and p53 protein immunoreactivity in malignant and premalignant Barrett's esophagus." Gastroenterology **107**(4): 1012-1018.

Hanahan, D. and R. A. Weinberg (2011). "Hallmarks of cancer: the next generation." cell **144**(5): 646-674.

Hao, J., B. Liu, C. S. Yang and X. Chen (2009). "Gastroesophageal reflux leads to esophageal cancer in a surgical model with mice." BMC gastroenterology **9**(1): 1-7.

Harris-Johnson, K. S., E. T. Domyan, C. M. Vezina and X. Sun (2009). "β-Catenin promotes respiratory progenitor identity in mouse foregut." Proceedings of the National Academy of Sciences **106**(38): 16287-16292.

Harrison, R., I. Perry, W. Haddadin, S. McDonald, R. Bryan, K. Abrams, R. Sampliner, N. J. Talley, P. Moayyedi and J. A. Jankowski (2007). "Detection of intestinal metaplasia in Barrett's esophagus: an observational comparator study suggests the need for a minimum of eight biopsies." Official journal of the American College of Gastroenterology| ACG **102**(6): 1154-1161.

He, Y.-f., M.-y. Zhang, X. Wu, X.-j. Sun, T. Xu, Q.-z. He and W. Di (2013). "High MUC2 expression in ovarian cancer is inversely associated with the M1/M2 ratio of tumor-associated macrophages and patient survival time." PloS one **8**(12): e79769.

Heitzmann, D., F. Grahammer, T. von Hahn, A. Schmitt-Gräff, E. Romeo, R. Nitschke, U. Gerlach, H. J. Lang, F. Verrey and J. Barhanin (2004). "Heteromeric KCNE2/KCNQ1 potassium channels in the luminal membrane of gastric parietal cells." The Journal of physiology **561**(2): 547-557.

Hennessy, T. P., R. F. Edlich, R. J. Buchin, M. S. Tsung, M. Prevost and O. H. Wangensteen (1968). "Influence of Gastroesophageal Incompetence: On Regeneration of Esophageal Mucosa." Archives of Surgery **97**(1): 105-107.

Hirokawa, Y., K. H. Y. Yip, C. W. Tan and A. W. Burgess (2014). "Colonic myofibroblast cell line stimulates colonoid formation." American Journal of Physiology-Gastrointestinal and Liver Physiology.

Hirota, W. K., T. M. Loughney, D. J. Lazas, C. L. Maydonovitch, V. Rholl and R. K. Wong (1999). "Specialized intestinal metaplasia, dysplasia, and cancer of the esophagus and esophagogastric junction: prevalence and clinical data." Gastroenterology **116**(2): 277-285.

Hosokawa, Y., T. Kinoshita, M. Konishi, S. Takahashi, N. Gotohda, Y. Kato, H. Daiko, M. Nishimura, K. Katsumata and Y. Sugiyama (2012). "Clinicopathological features and prognostic factors of adenocarcinoma of the esophagogastric junction according to Siewert classification: experiences at a single institution in Japan." Annals of Surgical Oncology **19**(2): 677-683.

Hou, P., X. Ma, Q. Zhang, C.-J. Wu, W. Liao, J. Li, H. Wang, J. Zhao, X. Zhou and C. Guan (2019). "USP21 deubiquitinase promotes pancreas cancer cell stemness via Wnt pathway activation." Genes & development **33**(19-20): 1361-1366.

Huang, R. J., A. R. Ende, A. Singla, J. T. Higa, A. Y. Choi, A. B. Lee, S. G. Whang, K. Gravelle, S. D'Andrea, S. J. Bang, R. A. Schmidt, M. M. Yeh and J. H. Hwang (2020). "Prevalence, risk factors, and surveillance patterns for gastric intestinal metaplasia among patients undergoing upper endoscopy with biopsy." Gastrointest Endosc **91**(1): 70-77 e71.

Humphries, A. and N. A. Wright (2008). "Colonic crypt organization and tumorigenesis." Nature Reviews Cancer **8**(6): 415-424.

Hutchinson, L., B. Stenstrom, D. Chen, B. Piperdi, S. Levey, S. Lyle, T. C. Wang and J. Houghton (2011). "Human Barrett's adenocarcinoma of the esophagus, associated myofibroblasts, and endothelium can arise from bone marrow-derived cells after allogeneic stem cell transplant." Stem cells and development **20**(1): 11-17.

Hvid-Jensen, F., L. Pedersen, A. M. Drewes, H. T. Sørensen and P. Funch-Jensen (2011). "Incidence of adenocarcinoma among patients with Barrett's esophagus." New England Journal of Medicine **365**(15): 1375-1383.

Hyland, P. L., N. Hu, M. Rotunno, H. Su, C. Y. Wang, L. M. Wang, R. M. Pfeiffer, B. Gherman, C. Giffen, C. Dykes, S. M. Dawsey, C. C. Abnet, K. M. Johnson, R. D. Acosta, P. E. Young, B. D. Cash and P. R. Taylor (2014). "Global Changes in Gene Expression of Barrett's Esophagus Compared to Normal Squamous Esophagus and Gastric Cardia Tissues." Plos One **9**(4).

Itzkovitz, S., A. Lyubimova, I. C. Blat, M. Maynard, J. Van Es, J. Lees, T. Jacks, H. Clevers and A. Van Oudenaarden (2012). "Single-molecule transcript counting of stem-cell markers in the mouse intestine." Nature cell biology **14**(1): 106-114.

Jacks, T., L. Remington, B. O. Williams, E. M. Schmitt, S. Halachmi, R. T. Bronson and R. A. Weinberg (1994). "Tumor spectrum analysis in p53-mutant mice." Current biology **4**(1): 1-7.

Jacobsen, C. M., S. Mannisto, S. Porter-Tinge, E. Genova, H. Parviainen, M. Heikinheimo, I. I. Adameyko, S. G. Tevosian and D. B. Wilson (2005). "GATA-4: FOG interactions regulate gastric epithelial development in the mouse." Developmental dynamics: an official publication of the American Association of Anatomists **234**(2): 355-362.

Jacobsen, C. M., N. Narita, M. Bielinska, A. J. Syder, J. I. Gordon and D. B. Wilson (2002). "Genetic mosaic analysis reveals that GATA-4 is required for proper differentiation of mouse gastric epithelium." Developmental biology **241**(1): 34-46.

Jankowski, J., D. Hopwood, R. Pringle and K. G. Wormsley (1993). "Increased expression of epidermal growth factor receptors in Barrett's esophagus

associated with alkaline reflux: a putative model for carcinogenesis." Am J Gastroenterol **88**(3): 402-408.

Jankowski, J. A., N. A. Wright, S. J. Meltzer, G. Triadafilopoulos, K. Geboes, A. G. Casson, D. Kerr and L. S. Young (1999). "Molecular evolution of the metaplasia-dysplasia-adenocarcinoma sequence in the esophagus." The American journal of pathology **154**(4): 965-973.

Janmaat, V. T., K. Nesteruk, M. C. Spaander, A. P. Verhaar, B. Yu, R. A. Silva, W. A. Phillips, M. Magierowski, A. van de Winkel and H. S. Stadler (2021). "HOXA13 in etiology and oncogenic potential of Barrett's esophagus." Nature communications **12**(1): 1-17.

Jayewickreme, C. D. and R. A. Shivdasani (2015). "Control of stomach smooth muscle development and intestinal rotation by transcription factor BARX1." Developmental biology **405**(1): 21-32.

Jiang, M., H. Li, Y. Zhang, Y. Yang, R. Lu, K. Liu, S. Lin, X. Lan, H. Wang, H. Wu, J. Zhu, Z. Zhou, J. Xu, D. K. Lee, L. Zhang, Y. C. Lee, J. Yuan, J. A. Abrams, T. C. Wang, A. R. Sepulveda, Q. Wu, H. Chen, X. Sun, J. She, X. Chen and J. Que (2017). "Transitional basal cells at the squamous-columnar junction generate Barrett's oesophagus." Nature **550**(7677): 529-533.

Jin, R. U. and J. C. Mills (2018). "Are gastric and esophageal metaplasia relatives? The case for Barrett's stemming from SPEM." Digestive diseases and sciences **63**(8): 2028-2041.

Johns, B. (1952). "Developmental changes in the oesophageal epithelium in man." Journal of anatomy **86**(Pt 4): 431.

Jovov, B., C. M. Van Itallie, N. J. Shaheen, J. L. Carson, T. M. Gambling, J. M. Anderson and R. C. Orlando (2007). "Claudin-18: a dominant tight junction protein in Barrett's esophagus and likely contributor to its acid resistance." American Journal of Physiology-Gastrointestinal and Liver Physiology.

Judd, L. M., B. M. Alderman, M. Howlett, A. Shulkes, C. Dow, J. Moverley, D. Grail, B. J. Jenkins, M. Ernst and A. S. Giraud (2004). "Gastric cancer development in mice lacking the SHP2 binding site on the IL-6 family co-receptor gp130." Gastroenterology **126**(1): 196-207.

Jung, K. W., N. J. Talley, Y. Romero, D. A. Katzka, C. D. Schleck, A. R. Zinsmeister, K. T. Dunagan, L. S. Lutzke, T.-T. Wu and K. K. Wang (2011). "Epidemiology and natural history of intestinal metaplasia of the gastroesophageal junction and Barrett's esophagus: a population-based study." The American journal of gastroenterology **106**(8): 1447.

Kabir, M. F., A. L. Karami, R. Cruz-Acuña, A. Klochkova, R. Saxena, A. Mu, M. G. Murray, J. Cruz, A. D. Fuller and M. H. Clevenger (2022). "Single cell transcriptomic analysis reveals cellular diversity of murine esophageal epithelium." Nature communications **13**(1): 1-15.

Kararli, T. T. (1995). "Comparison of the gastrointestinal anatomy, physiology, and biochemistry of humans and commonly used laboratory animals." Biopharmaceutics & drug disposition **16**(5): 351-380.

Kastelein, F., K. Biermann, E. W. Steyerberg, J. Verheij, M. Kalisvaart, L. H. Looijenga, H. A. Stoop, L. Walter, E. J. Kuipers and M. C. Spaander (2013). "Aberrant p53 protein expression is associated with an increased risk of neoplastic progression in patients with Barrett's oesophagus." Gut **62**(12): 1676-1683.

Kastelein, F., S. Van Olphen, E. Steyerberg, M. Spaander and M. Bruno (2016). "Impact of surveillance for Barrett's oesophagus on tumour stage and survival of patients with neoplastic progression." Gut **65**(4): 548-554.

Katz-Summercorn, A., S. Jammula, A. Frangou, I. Peneva, M. O'Donovan, M. Tripathi, S. Malhotra, M. di Pietro, S. Abbas and G. Devonshire (2022). "Multi-omic cross-sectional cohort study of pre-malignant Barrett's esophagus reveals early structural variation and retrotransposon activity." Nature Communications **13**(1): 1-17.

Katz, J. P., N. Perreault, B. G. Goldstein, L. Actman, S. R. McNally, D. G. Silberg, E. E. Furth and K. H. Kaestner (2005). "Loss of Klf4 in mice causes altered proliferation and differentiation and precancerous changes in the adult stomach." Gastroenterology **128**(4): 935-945.

Kaur, B. S., R. Ouatu-Lascar, M. B. Omary and G. Triadafilopoulos (2000). "Bile salts induce or blunt cell proliferation in Barrett's esophagus in an acid-dependent fashion." Am J Physiol Gastrointest Liver Physiol **278**(6): G1000-1009.

Kawaguchi, H., K. Haruma, K. Komoto, M. Yoshihara, K. Sumii and G. Kajiyama (1996). "Helicobacter pylori infection is the major risk factor for atrophic gastritis." Am J Gastroenterol **91**(5): 959-962.

Kelty, C. J., R. Ackroyd, N. J. Brown, T. J. Stephenson, C. J. Stoddard and M. W. Reed (2004). "Endoscopic ablation of Barrett's oesophagus: a randomized-controlled trial of photodynamic therapy vs. argon plasma coagulation." Aliment Pharmacol Ther **20**(11-12): 1289-1296.

Kelty, C. J., M. D. Gough, Q. Van Wyk, T. J. Stephenson and R. Ackroyd (2007). "Barrett's oesophagus: intestinal metaplasia is not essential for cancer risk." Scand J Gastroenterol **42**(11): 1271-1274.

Kerr, S. C., S. D. Carrington, S. Oscarson, M. E. Gallagher, M. Solon, S. Yuan, J. N. Ahn, R. H. Dougherty, W. E. Finkbeiner and M. C. Peters (2014). "Intelectin-1 is a prominent protein constituent of pathologic mucus associated with eosinophilic airway inflammation in asthma." American Journal of Respiratory and Critical Care Medicine **189**(8): 1005-1007.

Kilgore, S. P., A. H. Ormsby, T. L. Gramlich, T. W. Rice, J. E. Richter, G. W. Falk and J. R. Goldblum (2000). "The gastric cardia: fact or fiction?" The American journal of gastroenterology **95**(4): 921-924.

Kim, B.-G., C. Li, W. Qiao, M. Mamura, B. Kasperczak, M. Anver, L. Wolfraim, S. Hong, E. Mushinski and M. Potter (2006). "Smad4 signalling in T cells is required for suppression of gastrointestinal cancer." Nature **441**(7096): 1015-1019.

Kim, B.-M., G. Buchner, I. Miletich, P. T. Sharpe and R. A. Shivdasani (2005). "The stomach mesenchymal transcription factor Barx1 specifies gastric epithelial identity through inhibition of transient Wnt signaling." Developmental cell **8**(4): 611-622.

Kim, B. M., J. Mao, M. M. Taketo and R. A. Shivdasani (2007). "Phases of canonical Wnt signaling during the development of mouse intestinal epithelium." Gastroenterology **133**(2): 529-538.

Kim, T.-H. and R. A. Shivdasani (2016). "Stomach development, stem cells and disease." Development **143**(4): 554-565.

Kivilaakso, E., D. Fromm and W. Silen (1980). "Effect of bile salts and related compounds on isolated esophageal mucosa." Surgery **87**(3): 280-285.

Kong, J., M. A. Crissey, S. Funakoshi, J. L. Kreindler and J. P. Lynch (2011). "Ectopic Cdx2 expression in murine esophagus models an intermediate stage in the emergence of Barrett's esophagus." PloS one **6**(4): e18280.

Kosinsky, R. L., F. Wegwitz, N. Hellbach, M. Dobbelstein, A. Mansouri, T. Vogel, Y. Begus-Nahrmann and S. A. Johnsen (2015). "Usp22 deficiency impairs intestinal epithelial lineage specification in vivo." Oncotarget **6**(35): 37906.

Krishnamurthy, S. and Y. Dayal (1995). "Pancreatic metaplasia in Barrett's esophagus. An immunohistochemical study." Am J Surg Pathol **19**(10): 1172-1180.

Krüger, L., L. M. Gonzalez, T. A. Pridgen, S. J. McCall, R. J. von Furstenberg, I. Harnden, G. E. Carnighan, A. M. Cox, A. T. Blikslager and K. S. Garman (2017). "Ductular and proliferative response of esophageal submucosal glands in a porcine model of esophageal injury and repair." American Journal of Physiology-Gastrointestinal and Liver Physiology **313**(3): G180-G191.

Kuno, R., G. Ito, A. Kawamoto, Y. Hiraguri, H. Y. Sugihara, S. Takeoka, S. Nagata, J. Takahashi, M. Tsuchiya and S. Anzai (2021). "Notch and TNF-α signaling promote cytoplasmic accumulation of OLFM4 in intestinal epithelium cells and exhibit a cell protective role in the inflamed mucosa of IBD patients." Biochemistry and biophysics reports **25**: 100906.

Kurian, L., I. Sancho-Martinez, E. Nivet, A. Aguirre, K. Moon, C. Pendaries, C. Volle-Challier, F. Bono, J. M. Herbert, J. Pulecio, Y. Xia, M. Li, N. Montserrat, S. Ruiz, I. Dubova, C. Rodriguez, A. M. Denli, F. S. Boscolo, R. D. Thiagarajan, F. H. Gage, J. F. Loring, L. C. Laurent and J. C. I. Belmonte (2013). "Conversion of human fibroblasts to angioblast-like progenitor cells." Nature Methods **10**(1): 77-U116.

Lagergren, J., R. Bergstrom, A. Lindgren and O. Nyren (1999). "Symptomatic gastroesophageal reflux as a risk factor for esophageal adenocarcinoma." N Engl J Med **340**(11): 825-831.

Lane, D. P. and S. Benchimol (1990). "p53: oncogene or anti-oncogene." Genes Dev **4**(1): 1-8.

Lang, G. A., T. Iwakuma, Y. A. Suh, G. Liu, V. A. Rao, J. M. Parant, Y. A. Valentin-Vega, T. Terzian, L. C. Caldwell, L. C. Strong, A. K. El-Naggar and G. Lozano (2004). "Gain of function of a p53 hot spot mutation in a mouse model of Li-Fraumeni syndrome." Cell **119**(6): 861-872.

Langner, C., E.-M. Wolf, W. Plieschnegger, M. Geppert, B. Wigginghaus, G. M. Höss, A. Eherer, N. I. Schneider, P. Rehak and M. Vieth (2014). "Multilayered epithelium at the gastroesophageal junction is a marker of gastroesophageal reflux disease: data from a prospective Central European multicenter study (histoGERD trial)." Virchows Archiv **464**(4): 409-417.

Lauwers, G. Y., M. Mino, S. Ban, D. Forcione, D. E. Eatherton, M. Shimizu and H. Sevestre (2005). "Cytokeratins 7 and 20 and mucin core protein expression in esophageal cervical inlet patch." The American journal of surgical pathology **29**(4): 437-442.

Lavery, D. L., A. M. Nicholson, R. Poulsom, R. Jeffery, A. Hussain, L. J. Gay, J. A. Jankowski, S. S. Zeki, H. Barr, R. Harrison, J. Going, S. Kadirkamanathan, P. Davis, T. Underwood, M. R. Novelli, M. Rodriguez-Justo, N. Shepherd, M. Jansen, N. A. Wright and S. A. McDonald (2014). "The stem cell organisation, and the proliferative and gene expression profile of Barrett's epithelium, replicates pyloric-type gastric glands." Gut **63**(12): 1854-1863.

Leedham, S. J., S. L. Preston, S. A. C. McDonald, G. Elia, P. Bhandari, D. Poller, R. Harrison, M. R. Novelli, J. A. Jankowski and N. A. Wright (2008). "Individual crypt genetic heterogeneity and the origin of metaplastic glandular epithelium in human Barrett's oesophagus." Gut **57**(8): 1041-1048.

Leung, W. K. and J. J. Sung (2002). "Review article: intestinal metaplasia and gastric carcinogenesis." Aliment Pharmacol Ther **16**(7): 1209-1216.

Li, D., M. C. Bautista, S. F. Jiang, P. Daryani, M. Brackett, M. A. Armstrong, Y. Y. Hung, D. Postlethwaite and U. Ladabaum (2016). "Risks and Predictors of Gastric Adenocarcinoma in Patients with Gastric Intestinal Metaplasia and Dysplasia: A Population-Based Study." Am J Gastroenterol **111**(8): 1104-1113.

Li, X.-B., G. Yang, L. Zhu, Y.-L. Tang, C. Zhang, Z. Ju, X. Yang and Y. Teng (2016). "Gastric Lgr5+ stem cells are the cellular origin of invasive intestinal-type gastric cancer in mice." Cell research **26**(7): 838-849.

Li, X., P. C. Galipeau, T. G. Paulson, C. A. Sanchez, J. Arnaudo, K. Liu, C. L. Sather, R. L. Kostadinov, R. D. Odze and M. K. Kuhner (2014). "Temporal and spatial evolution of somatic chromosomal alterations: a case-cohort study of Barrett's esophagus." Cancer prevention research **7**(1): 114-127.

Li, Y., J. Gordon, N. R. Manley, Y. Litingtung and C. Chiang (2008). "Bmp4 is required for tracheal formation: a novel mouse model for tracheal agenesis." Developmental biology **322**(1): 145-155.

Li, Y., Y. Litingtung, P. Ten Dijke and C. Chiang (2007). "Aberrant Bmp signaling and notochord delamination in the pathogenesis of esophageal atresia." Developmental dynamics: an official publication of the American Association of Anatomists **236**(3): 746-754.

Lindeboom, R. G., L. van Voorthuijsen, K. C. Oost, M. J. Rodríguez-Colman, M. V. Luna-Velez, C. Furlan, F. Baraille, P. W. Jansen, A. Ribeiro and B. M. Burgering (2018). "Integrative multi-omics analysis of intestinal organoid differentiation." Molecular systems biology **14**(6): e8227.

Litingtung, Y., L. Lei, H. Westphal and C. Chiang (1998). "Sonic hedgehog is essential to foregut development." Nature genetics **20**(1): 58-61.

Liu, D., H. Song and Y. Xu (2010). "A common gain of function of p53 cancer mutants in inducing genetic instability." Oncogene **29**(7): 949-956.

Liu, W. and G. P. Rodgers (2022). "Olfactomedin 4 is not a precise marker for human intestinal stem cells, but is involved in intestinal carcinogenesis." Gastroenterology **162**(4): 1001-1004.

Liu, W., M. Yan, Y. Liu, R. Wang, C. Li, C. Deng, A. Singh, W. G. Coleman and G. P. Rodgers (2010). "Olfactomedin 4 down-regulates innate immunity against Helicobacter pylori infection." Proceedings of the National Academy of Sciences **107**(24): 11056-11061.

Long, J. D. and R. C. Orlando (1999). "Esophageal submucosal glands: structure and function." Am J Gastroenterol **94**(10): 2818-2824.

Lord, R. V., K. Wickramasinghe, J. J. Johansson, S. R. DeMeester, J. Brabender and T. R. DeMeester (2004). "Cardiac mucosa in the remnant esophagus after esophagectomy is an acquired epithelium with Barrett's-like features." Surgery **136**(3): 633-640.

Lorinc, E., L. Mellblom and S. Oberg (2015). "The immunophenotypic relationship between the submucosal gland unit, columnar metaplasia and squamous islands in the columnar-lined oesophagus." Histopathology **67**(6): 792-798.

Lorinc, E. and S. Oberg (2015). "Hyperplasia of the submucosal glands of the columnar-lined oesophagus." Histopathology **66**(5): 726-731.

Lörinc, E. and S. Öberg (2012). "Submucosal glands in the columnar-lined oesophagus: evidence of an association with metaplasia and neosquamous epithelium." Histopathology **61**(1): 53-58.

Maag, J. L., O. M. Fisher, A. Levert-Mignon, D. C. Kaczorowski, M. L. Thomas, D. J. Hussey, D. I. Watson, A. Wettstein, Y. V. Bobryshev and M. Edwards (2017). "Novel aberrations uncovered in Barrett's esophagus and esophageal adenocarcinoma using whole transcriptome sequencing." Molecular Cancer Research **15**(11): 1558-1569.

Mahlapuu, M., M. Pelto-Huikko, M. Aitola, S. Enerbäck and P. Carlsson (1998). "FREAC-1 contains a cell-type-specific transcriptional activation domain and is expressed in epithelial–mesenchymal interfaces." Developmental biology **202**(2): 183-195.

Mahoney, D., H. Cheung, R. L. Mrad, S. Plenchette, C. Simard, E. Enwere, V. Arora, T. Mak, E. Lacasse and J. Waring (2008). "Both cIAP1 and cIAP2 regulate TNFα-mediated NF-κB activation." Proceedings of the National Academy of Sciences **105**(33): 11778-11783.

Maley, C. C., P. C. Galipeau, X. Li, C. A. Sanchez, T. G. Paulson and B. J. Reid (2004). "Selectively advantageous mutations and hitchhikers in neoplasms: p16 lesions are selected in Barrett's esophagus." Cancer research **64**(10): 3414-3427.

Malhotra, G. K., U. Yanala, A. Ravipati, M. Follet, M. Vijayakumar and C. Are (2017). "Global trends in esophageal cancer." Journal of surgical oncology **115**(5): 564-579.

Marques-Pereira, J. and C. Leblond (1965). "Mitosis and differentiation in the stratified squamous epithelium of the rat esophagus." American Journal of Anatomy **117**(1): 73-87.

Martincorena, I., J. C. Fowler, A. Wabik, A. R. Lawson, F. Abascal, M. W. Hall, A. Cagan, K. Murai, K. Mahbubani and M. R. Stratton (2018). "Somatic mutant clones colonize the human esophagus with age." Science **362**(6417): 911-917.

Martincorena, I., A. Roshan, M. Gerstung, P. Ellis, P. Van Loo, S. McLaren, D. C. Wedge, A. Fullam, L. B. Alexandrov and J. M. Tubio (2015). "High burden and pervasive positive selection of somatic mutations in normal human skin." Science **348**(6237): 880-886.

Martinez, P., M. R. Timmer, C. T. Lau, S. Calpe, M. d. C. Sancho-Serra, D. Straub, A.-M. Baker, S. L. Meijer, F. J. Ten Kate and R. C. Mallant-Hent (2016). "Dynamic clonal equilibrium and predetermined cancer risk in Barrett's oesophagus." Nature communications **7**(1): 1-10.

Matsuyama, M., S. Aizawa and A. Shimono (2009). "Sfrp controls apicobasal polarity and oriented cell division in developing gut epithelium." PLoS genetics **5**(3): e1000427.

McCracken, K. W., E. Aihara, B. Martin, C. M. Crawford, T. Broda, J. Treguier, X. Zhang, J. M. Shannon, M. H. Montrose and J. M. Wells (2017). "Wnt/β-catenin promotes gastric fundus specification in mice and humans." Nature **541**(7636): 182-187.

McCracken, K. W. and J. M. Wells (2017). Mechanisms of embryonic stomach development. Seminars in cell & developmental biology, Elsevier.

McDonald, S. A., D. Lavery, N. A. Wright and M. Jansen (2015). "Barrett oesophagus: lessons on its origins from the lesion itself." Nat Rev Gastroenterol Hepatol **12**(1): 50-60.

Melino, G. (2011). "p63 is a suppressor of tumorigenesis and metastasis interacting with mutant p53." Cell Death & Differentiation **18**(9): 1487-1499.

Metsuyanim, S., O. Harari-Steinberg, E. Buzhor, D. Omer, N. Pode-Shakked, H. Ben-Hur, R. Halperin, D. Schneider and B. Dekel (2009). "Expression of Stem Cell Markers in the Human Fetal Kidney." Plos One **4**(8).

Milano, J., J. McKay, C. Dagenais, L. Foster-Brown, F. Pognan, R. Gadient, R. T. Jacobs, A. Zacco, B. Greenberg and P. J. Ciaccio (2004). "Modulation of notch processing by γ-secretase inhibitors causes intestinal goblet cell metaplasia and induction of genes known to specify gut secretory lineage differentiation." Toxicological Sciences **82**(1): 341-358.

Mills, J. C. and O. J. Sansom (2015). "Reserve stem cells: differentiated cells reprogram to fuel repair, metaplasia, and neoplasia in the adult gastrointestinal tract." Science signaling **8**(385): re8-re8.

Mills, J. C. and R. A. Shivdasani (2011). "Gastric epithelial stem cells." Gastroenterology **140**(2): 412-424.

Minacapelli, C. D., M. Bajpai, X. Geng, C. L. Cheng, A. A. Chouthai, R. Souza, S. J. Spechler and K. M. Das (2017). "Barrett's metaplasia develops from cellular reprograming of esophageal squamous epithelium due to gastroesophageal reflux." Am J Physiol Gastrointest Liver Physiol **312**(6): G615-G622.

Miwa, K., H. Sahara, M. Segawa, S. Kinami, T. Sato, I. Miyazaki and T. Hattori (1996). "Reflux of duodenal or gastro-duodenal contents induces esophageal carcinoma in rats." Int J Cancer **67**(2): 269-274.

Miwa, K., M. Segawa, Y. Takano, H. Matsumoto, H. Sahara, M. Yagi, I. Miyazaki and T. Hattori (1994). "Induction of oesophageal and forestomach carcinomas in rats by reflux of duodenal contents." Br J Cancer **70**(2): 185-189.

Miyagi, S., H. Kato and A. Okuda (2009). "Role of SoxB1 transcription factors in development." Cellular and molecular life sciences **66**(23): 3675-3684.

Miyashita, T., K. Miwa, T. Fujimura, I. Ninomiya, S. Fushida, F. A. Shah, J. W. Harmon, T. Hattori and T. Ohta (2013). "The severity of duodeno-esophageal reflux influences the development of different histological types of esophageal cancer in a rat model." International journal of cancer **132**(7): 1496-1504.

Miyashita, T., F. A. Shah, G. P. Marti, J. Wang, P. Bonde, M. K. Gibson, T. Ohta, E. A. Montgomery, M. Duncan and J. W. Harmon (2011). "Rabeprazole impedes the development of reflux-induced esophageal cancer in a surgical rat model." Digestive diseases and sciences **56**(5): 1309-1314.

Miyashita, T., F. A. Shah, K. Miwa, S. Sasaki, K. Nishijima, K. Oyama, I. Ninomiya, S. Fushida, T. Fujimura and T. Hattori (2013). "Impact of inflammation-metaplasia-adenocarcinoma sequence and prevention in surgical rat models." Digestion **87**(1): 6-11.

Miyata, N., T. Azuma, S. Hozawa, H. Higuchi, A. Yokoyama, A. Kabashima, T. Igarashi, K. Saeki and T. Hibi (2012). "Transforming growth factor β and Ras/MEK/ERK signaling regulate the expression level of a novel tumor suppressor Lefty." Pancreas **41**(5): 745-752.

Moll, R., W. W. Franke, D. L. Schiller, B. Geiger and R. Krepler (1982). "The catalog of human cytokeratins: patterns of expression in normal epithelia, tumors and cultured cells." Cell **31**(1): 11-24.

Montoya, A., C. N. Amaya, A. Belmont, N. Diab, R. Trevino, G. Villanueva, S. Rains, L. A. Sanchez, N. Badri and S. Otoukesh (2017). "Use of non-selective β-blockers

is associated with decreased tumor proliferative indices in early stage breast cancer." Oncotarget **8**(4): 6446.

Morgan, R. G., E. Mortensson, D. N. Legge, B. Gupta, T. J. Collard, A. Greenhough and A. C. Williams (2018). "LGR5 expression is regulated by EGF in early colorectal adenomas and governs EGFR inhibitor sensitivity." British journal of cancer **118**(4): 558-565.

Morita, H., S. Mazerbourg, D. M. Bouley, C.-W. Luo, K. Kawamura, Y. Kuwabara, H. Baribault, H. Tian and A. J. Hsueh (2004). "Neonatal lethality of LGR5 null mice is associated with ankyloglossia and gastrointestinal distension." Molecular and cellular biology **24**(22): 9736-9743.

Motoyama, J., J. Liu, R. Mo, Q. Ding, M. Post and C.-c. Hui (1998). "Essential function of Gli2 and Gli3 in the formation of lung, trachea and oesophagus." Nature genetics **20**(1): 54-57.

Muller, P. A. and K. H. Vousden (2013). "p53 mutations in cancer." Nature cell biology **15**(1): 2-8.

Murphy, A. J., Y. Li, J. B. Pietsch, C. Chiang and H. N. Lovvorn (2012). "Mutational analysis of NOG in esophageal atresia and tracheoesophageal fistula patients." Pediatric surgery international **28**(4): 335-340.

Mutoh, H., Y. Hakamata, K. Sato, A. Eda, I. Yanaka, S. Honda, H. Osawa, Y. Kaneko and K. Sugano (2002). "Conversion of gastric mucosa to intestinal metaplasia in Cdx2-expressing transgenic mice." Biochemical and biophysical research communications **294**(2): 470-479.

Nakamura, T., K. Tsuchiya and M. Watanabe (2007). "Crosstalk between Wnt and Notch signaling in intestinal epithelial cell fate decision." J Gastroenterol **42**(9): 705-710.

Nakanishi, Y., M. Saka, T. Eguchi, S. Sekine, H. Taniguchi and T. Shimoda (2007). "Distribution and significance of the oesophageal and gastric cardiac mucosae: a study of 131 operation specimens." Histopathology **51**(4): 515-519.

Neyaz, A., R. D. Odze, S. Rickelt, L. T. Nieman, J. R. Bledsoe, K. K. Mahadevan, K. Arora, W. R. Jeck, M. S. Taylor and M. Gala (2021). "LGR5 in Barrett's Esophagus and its Utility in Predicting Patients at Increased Risk of Advanced Neoplasia." Clinical and Translational Gastroenterology **12**(1).

Nicholson, A. M., T. A. Graham, A. Simpson, A. Humphries, N. Burch, M. Rodriguez-Justo, M. Novelli, R. Harrison, N. A. Wright and S. A. McDonald (2012). "Barrett's metaplasia glands are clonal, contain multiple stem cells and share a common squamous progenitor." Gut **61**(10): 1380-1389.

Nielsen, C., L. C. Murtaugh, J. C. Chyung, A. Lassar and D. J. Roberts (2001). "Gizzard formation and the role of Bapx1." Developmental Biology **231**(1): 164-174.

Nirwan, J. S., S. S. Hasan, Z. U. Babar, B. R. Conway and M. U. Ghori (2020). "Global Prevalence and Risk Factors of Gastro-oesophageal Reflux Disease (GORD): Systematic Review with Meta-analysis." Sci Rep **10**(1): 5814.

Noah, T. K., A. Kazanjian, J. Whitsett and N. F. Shroyer (2010). "SAM pointed domain ETS factor (SPDEF) regulates terminal differentiation and maturation of intestinal goblet cells." Experimental Cell Research **316**(3): 452-465.

Nomura, S., S. H. Settle, C. M. Leys, A. L. Means, R. M. Peek Jr, S. D. Leach, C. V. Wright, R. J. Coffey and J. R. Goldenring (2005). "Evidence for repatterning of the gastric fundic epithelium associated with Ménétrier's disease and TGFα overexpression." Gastroenterology **128**(5): 1292-1305.

Nones, K., N. Waddell, N. Wayte, A.-M. Patch, P. Bailey, F. Newell, O. Holmes, J. L. Fink, M. C. Quinn and Y. H. Tang (2014). "Genomic catastrophes frequently arise in esophageal adenocarcinoma and drive tumorigenesis." Nature communications **5**(1): 1-9.

Noorani, A., X. Li, M. Goddard, J. Crawte, L. B. Alexandrov, M. Secrier, M. D. Eldridge, L. Bower, J. Weaver and P. Lao-Sirieix (2020). "Genomic evidence supports a clonal diaspora model for metastases of esophageal adenocarcinoma." Nature genetics **52**(1): 74-83.

Notari, M., Y. Hu, S. Koch, M. Lu, I. Ratnayaka, S. Zhong, C. Baer, A. Pagotto, R. Goldin and V. Salter (2011). "Inhibitor of apoptosis-stimulating protein of p53 (iASPP) prevents senescence and is required for epithelial stratification." Proceedings of the National Academy of Sciences **108**(40): 16645-16650.

Nowicki-Osuch, K., L. Zhuang, S. Jammula, C. W. Bleaney, K. T. Mahbubani, G. Devonshire, A. Katz-Summercorn, N. Eling, A. Wilbrey-Clark and E. Madissoon (2021). "Molecular phenotyping reveals the identity of Barrett's esophagus and its malignant transition." Science **373**(6556): 760-767.

Nucci, M. R. and C. P. Crum (2007). "Redefining early cervical neoplasia: recent progress." Advances in anatomic pathology **14**(1): 1-10.

Nyström, M., G. Thomas, M. Stone, I. Mackenzie, I. Hart and J. Marshall (2005). "Development of a quantitative method to analyse tumour cell invasion in organotypic culture." The Journal of Pathology: A Journal of the Pathological Society of Great Britain and Ireland **205**(4): 468-475.

O'riordan, J., O. Tucker, P. Byrne, G. McDonald, N. Ravi, P. Keeling and J. Reynolds (2004). Factors influencing the development of Barrett's epithelium in the esophageal remnant postesophagectomy, LWW. **99:** 205-211.

Öberg, S., J. Johansson, J. Wenner and B. Walther (2002). "Metaplastic columnar mucosa in the cervical esophagus after esophagectomy." Annals of surgery **235**(3): 338.

Oberg, S., J. H. Peters, T. R. DeMeester, P. Chandrasoma, J. A. Hagen, A. P. Ireland, M. P. Ritter, R. J. Mason, P. Crookes and C. G. Bremner (1997). "Inflammation and specialized intestinal metaplasia of cardiac mucosa is a manifestation of gastroesophageal reflux disease." Annals of surgery **226**(4): 522.

Odze, R. D. (2005). "Pathology of the gastroesophageal junction." Semin Diagn Pathol **22**(4): 256-265.

Oezcelik, A. and S. R. DeMeester (2011). "General anatomy of the esophagus." Thorac Surg Clin **21**(2): 289-297, x.

Offman, J., B. Muldrew, M. O'Donovan, I. Debiram-Beecham, F. Pesola, I. Kaimi, S. G. Smith, A. Wilson, Z. Khan and P. Lao-Sirieix (2018). "Barrett's oESophagus trial 3 (BEST3): study protocol for a randomised controlled trial comparing the Cytosponge-TFF3 test with usual care to facilitate the diagnosis of oesophageal pre-cancer in primary care patients with chronic acid reflux." BMC cancer **18**(1): 1-16.

Ong, J.-S., J. An, X. Han, M. H. Law, P. Nandakumar, J. Schumacher, I. Gockel, A. Bohmer, J. Jankowski and C. Palles (2021). "Multitrait genetic association analysis identifies 50 new risk loci for gastro-oesophageal reflux, seven new loci for Barrett's oesophagus and provides insights into clinical heterogeneity in reflux diagnosis." Gut.

Ormsby, A. H., J. R. Goldblum, T. W. Rice, J. E. Richter, G. W. Falk, M. F. Vaezi and T. L. Gramlich (1999). "Cytokeratin subsets can reliably distinguish Barrett's esophagus from intestinal metaplasia of the stomach." Human pathology **30**(3): 288-294.

Oshima, H., A. Matsunaga, T. Fujimura, T. Tsukamoto, M. M. Taketo and M. Oshima (2006). "Carcinogenesis in mouse stomach by simultaneous activation of the Wnt signaling and prostaglandin E2 pathway." Gastroenterology **131**(4): 1086-1095.

Oue, N., K. Sentani, N. Sakamoto, N. Uraoka and W. Yasui (2019). "Molecular carcinogenesis of gastric cancer: Lauren classification, mucin phenotype expression, and cancer stem cells." International Journal of Clinical Oncology **24**(7): 771-778.

Owen, R. P., M. J. White, D. T. Severson, B. Braden, A. Bailey, R. Goldin, L. M. Wang, C. Ruiz-Puig, N. D. Maynard and A. Green (2018). "Single cell RNA-seq reveals profound transcriptional similarity between Barrett's oesophagus and oesophageal submucosal glands." Nature communications **9**(1): 1-12.

Pan, Q., A. M. Nicholson, H. Barr, L. A. Harrison, G. D. Wilson, J. Burkert, R. Jeffery, M. R. Alison, L. Looijenga and W. R. Lin (2013). "Identification of lineage-uncommitted, long-lived, label-retaining cells in healthy human esophagus and stomach, and in metaplastic esophagus." Gastroenterology **144**(4): 761-770.

Parsonnet, J. (1995). "The incidence of Helicobacter pylori infection." Aliment Pharmacol Ther **9 Suppl 2**: 45-51.

Paulson, T. G., L. Xu, C. Sanchez, P. L. Blount, K. Ayub, R. D. Odze and B. J. Reid (2006). "Neosquamous epithelium does not typically arise from Barrett's epithelium." Clinical Cancer Research **12**(6): 1701-1706.

Peck-Radosavljevic, M., A. Püspök, R. Pötzi and G. Oberhuber (1999). "Histological findings after routine biopsy at the gastro-oesophageal junction." European journal of gastroenterology & hepatology **11**(11): 1265-1270.

Peignon, G., A. Durand, W. Cacheux, O. Ayrault, B. Terris, P. Laurent-Puig, N. F. Shroyer, I. Van Seuningen, T. Honjo, C. Perret and B. Romagnolo (2011). "Complex interplay between beta-catenin signalling and Notch effectors in intestinal tumorigenesis." Gut **60**(2): 166-176.

Pellegrinet, L., V. Rodilla, Z. Liu, S. Chen, U. Koch, L. Espinosa, K. H. Kaestner, R. Kopan, J. Lewis and F. Radtke (2011). "Dll1- and dll4-mediated notch signaling are required for homeostasis of intestinal stem cells." Gastroenterology **140**(4): 1230-1240 e1231-1237.

Pepicelli, C. V., P. M. Lewis and A. P. McMahon (1998). "Sonic hedgehog regulates branching morphogenesis in the mammalian lung." Current biology **8**(19): 1083-1086.

Pera, M., M. J. Brito, R. Poulsom, E. Riera, L. Grande, A. Hanby and N. A. Wright (2000). "Duodenal-content reflux esophagitis induces the development of glandular metaplasia and adenosquamous carcinoma in rats." Carcinogenesis **21**(8): 1587-1591.

Perera, O., A. Evans, M. Pertziger, C. MacDonald, H. Chen, D. X. Liu, P. E. Lobie and J. K. Perry (2015). "Trefoil factor 3 (TFF3) enhances the oncogenic characteristics of prostate carcinoma cells and reduces sensitivity to ionising radiation." Cancer Letters **361**(1): 104-111.

Perreault, N., J. P. Katz and K. H. Kaestner (2000). "The mesenchymal transcription factor Fkh6 affects the Wnt/b-catenin pathway by modulating the expression of proteoglycans in the gut epithelium." Gastroenterology **4**(118): A294.

Pham, T. H., R. M. Genta, S. J. Spechler, R. F. Souza and D. H. Wang (2014). "Development and characterization of a surgical mouse model of reflux esophagitis and Barrett's esophagus." Journal of Gastrointestinal Surgery **18**(2): 234-241.

Picelli, S., A. K. Bjorklund, O. R. Faridani, S. Sagasser, G. Winberg and R. Sandberg (2013). "Smart-seq2 for sensitive full-length transcriptome profiling in single cells." Nat Methods **10**(11): 1096-1098.

Picelli, S., O. R. Faridani, A. K. Bjorklund, G. Winberg, S. Sagasser and R. Sandberg (2014). "Full-length RNA-seq from single cells using Smart-seq2." Nat Protoc **9**(1): 171-181.

Pohl, H., O. Pech, H. Arash, M. Stolte, H. Manner, A. May, K. Kraywinkel, A. Sonnenberg and C. Ell (2016). "Length of Barrett's oesophagus and cancer risk: implications from a large sample of patients with early oesophageal adenocarcinoma." Gut **65**(2): 196-201.

Qiao, Y., A. Hyder, S. J. Bae, W. Zarin, T. J. O'neill, N. E. Marcon, L. Stein and H.-H. Thein (2015). "Surveillance in patients with Barrett's esophagus for early detection of esophageal adenocarcinoma: a systematic review and meta-analysis." Clinical and translational gastroenterology **6**(12): e131.

Quante, M., G. Bhagat, J. A. Abrams, F. Marache, P. Good, M. D. Lee, Y. Lee, R. Friedman, S. Asfaha, Z. Dubeykovskaya, U. Mahmood, J. L. Figueiredo, J. Kitajewski, C. Shawber, C. J. Lightdale, A. K. Rustgi and T. C. Wang (2012). "Bile acid and inflammation activate gastric cardia stem cells in a mouse model of Barrett-like metaplasia." Cancer Cell **21**(1): 36-51.

Quante, M., T. C. Wang and A. J. Bass (2022). "Adenocarcinoma of the oesophagus: is it gastric cancer?" Gut.

Que, J., M. Choi, J. W. Ziel, J. Klingensmith and B. L. Hogan (2006). "Morphogenesis of the trachea and esophagus: current players and new roles for noggin and Bmps." Differentiation **74**(7): 422-437.

Que, J., K. S. Garman, R. F. Souza and S. J. Spechler (2019). "Pathogenesis and cells of origin of Barrett's esophagus." Gastroenterology **157**(2): 349-364. e341.

Que, J., X. Luo, R. J. Schwartz and B. L. Hogan (2009). "Multiple roles for Sox2 in the developing and adult mouse trachea."

Que, J., T. Okubo, J. R. Goldenring, K.-T. Nam, R. Kurotani, E. E. Morrisey, O. Taranova, L. H. Pevny and B. L. Hogan (2007). "Multiple dose-dependent roles for Sox2 in the patterning and differentiation of anterior foregut endoderm." Development **134**(13): 2521-2531.

Radyk, M. D., J. Burclaff, S. G. Willet and J. C. Mills (2018). "Metaplastic cells in the stomach arise, independently of stem cells, via dedifferentiation or transdifferentiation of chief cells." Gastroenterology **154**(4): 839-843. e832.

Raggi, M., R. Langer, M. Feith, H. Friess, M. Schauer and J. Theisen (2010). "Successful evaluation of a new animal model using mice for esophageal adenocarcinoma." Langenbeck's archives of surgery **395**(4): 347-350.

Raghoebir, L., E. R. Bakker, J. C. Mills, S. Swagemakers, M. B.-v. Kempen, A. B.-d. Munck, S. Driegen, D. Meijer, F. Grosveld and D. Tibboel (2012). "SOX2 redirects the developmental fate of the intestinal epithelium toward a premature gastric phenotype." Journal of molecular cell biology **4**(6): 377-385.

Ramalho-Santos, M., D. A. Melton and A. P. McMahon (2000). "Hedgehog signals regulate multiple aspects of gastrointestinal development." Development **127**(12): 2763-2772.

Ramus, J. R., C. P. Caygill, P. A. Gatenby and A. Watson (2008). "Current United Kingdom practice in the diagnosis and management of columnar-lined oesophagus: results of the United Kingdom National Barrett's Oesophagus Registry endoscopist questionnaire." Eur J Cancer Prev **17**(5): 422-425.

Rankin, S. A., L. Han, K. W. McCracken, A. P. Kenny, C. T. Anglin, E. A. Grigg, C. M. Crawford, J. M. Wells, J. M. Shannon and A. M. Zorn (2016). "A retinoic acid-hedgehog cascade coordinates mesoderm-inducing signals and endoderm competence during lung specification." Cell reports **16**(1): 66-78.

Redston, M., A. Noffsinger, A. Kim, F. G. Akarca, M. Rara, D. Stapleton, L. Nowden, R. Lash, A. J. Bass and M. D. Stachler (2022). "Abnormal TP53 predicts risk of progression in patients with Barrett's esophagus regardless of a diagnosis of dysplasia." Gastroenterology **162**(2): 468-481.

Reid, B. J., P. L. Blount, Z. Feng and D. S. Levine (2000). "Optimizing endoscopic biopsy detection of early cancers in Barrett's high-grade dysplasia." The American journal of gastroenterology **95**(11): 3089-3096.

Renzing, J., S. Hansen and D. P. Lane (1996). "Oxidative stress is involved in the UV activation of p53." Journal of cell science **109**(5): 1105-1112.

Riddell, R. H. and R. D. Odze (2009). "Definition of Barrett's esophagus: time for a rethink—is intestinal metaplasia dead?" Official journal of the American College of Gastroenterology| ACG **104**(10): 2588-2594.

Rishniw, M., P. Rodriguez, J. W. Que, Z. D. Burke, D. Tosh, H. Chen and X. X. Chen (2011). "Molecular aspects of esophageal development." Barrett's Esophagus: The 10th Oeso World Congress Proceedings **1232**: 309-315.

Robertson, E. V., M. H. Derakhshan, A. A. Wirz, Y. Y. Lee, J. P. Seenan, S. A. Ballantyne, S. L. Hanvey, A. W. Kelman, J. J. Going and K. E. McColl (2013). "Central obesity in asymptomatic volunteers is associated with increased intrasphincteric acid reflux and lengthening of the cardiac mucosa." Gastroenterology **145**(4): 730-739.

Robertson, E. V., M. H. Derakhshan, A. A. Wirz, D. R. Mitchell, J. J. Going, A. W. Kelman, S. A. Ballantyne and K. E. McColl (2017). "Hiatus hernia in healthy volunteers is associated with intrasphincteric reflux and cardiac mucosal lengthening without traditional reflux." Gut **66**(7): 1208-1215.

Rodriguez, P., S. Da Silva, L. Oxburgh, F. Wang, B. L. Hogan and J. Que (2010). "BMP signaling in the development of the mouse esophagus and forestomach." Development **137**(24): 4171-4176.

Ross-Innes, C. S., J. Becq, A. Warren, R. K. Cheetham, H. Northen, M. O'Donovan, S. Malhotra, M. Di Pietro, S. Ivakhno and M. He (2015). "Whole-genome sequencing provides new insights into the clonal architecture of Barrett's esophagus and esophageal adenocarcinoma." Nature genetics **47**(9): 1038-1046.

Rubio, C., T. Hirota, M. Itabashi, K. Mandai, A. Yanagisawa, T. Kitagawa, H. Sugano and Y. Kato (2004). "Extended intestinal metaplasia. A survey of 1392 gastrectomies from dwellers of the Pacific basin." Anticancer research **24**(5B): 3185-3192.

Sakuma, R., Y. i. Ohnishi, C. Meno, H. Fujii, H. Juan, J. Takeuchi, T. Ogura, E. Li, K. Miyazono and H. Hamada (2002). "Inhibition of Nodal signalling by Lefty mediated through interaction with common receptors and efficient diffusion." Genes to Cells **7**(4): 401-412.

Samuels-Lev, Y., D. J. O'Connor, D. Bergamaschi, G. Trigiante, J.-K. Hsieh, S. Zhong, I. Campargue, L. Naumovski, T. Crook and X. Lu (2001). "ASPP proteins specifically stimulate the apoptotic function of p53." Molecular cell **8**(4): 781-794.

Sancho, E., E. Batlle and H. Clevers (2004). "Signaling pathways in intestinal development and cancer." Annu. Rev. Cell Dev. Biol. **20**: 695-723.

Sarosi, G., G. Brown, K. Jaiswal, L. Feagins, E. Lee, T. Crook, R. Souza, Y. Zou, J. Shay and S. J. Spechler (2008). "Bone marrow progenitor cells contribute to esophageal regeneration and metaplasia in a rat model of Barrett's esophagus." Diseases of the Esophagus **21**(1): 43-50.

Sato, T., D. E. Stange, M. Ferrante, R. G. Vries, J. H. Van Es, S. Van Den Brink, W. J. Van Houdt, A. Pronk, J. Van Gorp and P. D. Siersema (2011). "Long-term expansion of epithelial organoids from human colon, adenoma, adenocarcinoma, and Barrett's epithelium." Gastroenterology **141**(5): 1762-1772.

Sato, T., J. H. van Es, H. J. Snippert, D. E. Stange, R. G. Vries, M. van den Born, N. Barker, N. F. Shroyer, M. van de Wetering and H. Clevers (2011). "Paneth cells constitute the niche for Lgr5 stem cells in intestinal crypts." Nature **469**(7330): 415-418.

Saukkonen, K., C. Tomasetto, K. Narko, M.-C. Rio and A. Ristimäki (2003). "Cyclooxygenase-2 expression and effect of celecoxib in gastric adenomas of trefoil factor 1-deficient mice." Cancer research **63**(12): 3032-3036.

Savory, J. G., N. Pilon, S. Grainger, J.-R. Sylvestre, M. Béland, M. Houle, K. Oh and D. Lohnes (2009). "Cdx1 and Cdx2 are functionally equivalent in vertebral patterning." Developmental biology **330**(1): 114-122.

Saxena, A. K. and G. Klimbacher (2019). "Comparison of esophageal submucosal glands in experimental models for esophagus tissue engineering applications." Esophagus **16**(1): 77-84.

Schottenfeld, D. and J. Beebe-Dimmer (2006). "Chronic inflammation: a common and important factor in the pathogenesis of neoplasia." CA: a cancer journal for clinicians **56**(2): 69-83.

Schuijers, J. and H. Clevers (2012). "Adult mammalian stem cells: the role of Wnt, Lgr5 and R-spondins." EMBO J **31**(12): 2685-2696.

Schultheis, P. J., L. L. Clarke, P. Meneton, M. Harline, G. P. Boivin, G. Stemmermann, J. J. Duffy, T. Doetschman, M. L. Miller and G. E. Shull (1998). "Targeted disruption of the murine Na+/H+ exchanger isoform 2 gene causes reduced viability of gastric parietal cells and loss of net acid secretion." The Journal of clinical investigation **101**(6): 1243-1253.

Schweizer, J., P. E. Bowden, P. A. Coulombe, L. Langbein, E. B. Lane, T. M. Magin, L. Maltais, M. B. Omary, D. A. Parry and M. A. Rogers (2006). "New consensus nomenclature for mammalian keratins." The Journal of cell biology **174**(2): 169-174.

Secrier, M., X. Li, N. De Silva, M. D. Eldridge, G. Contino, J. Bornschein, S. MacRae, N. Grehan, M. O'Donovan and A. Miremadi (2016). "Mutational signatures in esophageal adenocarcinoma define etiologically distinct subgroups with therapeutic relevance." Nature genetics **48**(10): 1131-1141.

Shah, S. C., A. J. Gawron, R. A. Mustafa and M. B. Piazuelo (2020). "Histologic Subtyping of Gastric Intestinal Metaplasia: Overview and Considerations for Clinical Practice." Gastroenterology **158**(3): 745-750.

Shaheen, N. J., M. A. Crosby, E. M. Bozymski and R. S. Sandler (2000). "Is there publication bias in the reporting of cancer risk in Barrett's esophagus?" Gastroenterology **119**(2): 333-338.

Shames, B. (2019). Anatomy and physiology of the duodenum. Shackelford's Surgery of the Alimentary Tract, 2 Volume Set, Elsevier**:** 786-803.

Sharma, P., J. Dent, D. Armstrong, J. J. Bergman, L. Gossner, Y. Hoshihara, J. A. Jankowski, O. Junghard, L. Lundell, G. N. Tytgat and M. Vieth (2006). "The development and validation of an endoscopic grading system for Barrett's esophagus: the Prague C & M criteria." Gastroenterology **131**(5): 1392-1399.

Sharma, P., T. G. Morales, A. Bhattacharyya, H. S. Garewal and R. E. Sampliner (1998). "Squamous islands in Barrett's esophagus: what lies underneath?" Am J Gastroenterol **93**(3): 332-335.

Sheikh, M., H. Poustchi, A. Pourshams, A. Etemadi, F. Islami, M. Khoshnia, A. Gharavi, M. Hashemian, G. Roshandel and H. Khademi (2019). "Individual and combined effects of environmental risk factors for esophageal cancer based on results from the Golestan Cohort Study." Gastroenterology **156**(5): 1416-1427.

Sheridan, C., H. Kishimoto, R. K. Fuchs, S. Mehrotra, P. Bhat-Nakshatri, C. H. Turner, R. Goulet, S. Badve and H. Nakshatri (2006). "CD44+/CD24-breast cancer cells exhibit enhanced invasive properties: an early step necessary for metastasis." Breast Cancer Research **8**(5): 1-13.

Shields, H. M., F. Zwas, D. A. Antonioli, W. G. Doos, S. Kim and S. J. Spechler (1993). "Detection by scanning electron microscopy of a distinctive esophageal surface cell at the junction of squamous and Barrett's epithelium." Digestive diseases and sciences **38**(1): 97-108.

Shull, M. M., I. Ormsby, A. B. Kier, S. Pawlowski, R. J. Diebold, M. Yin, R. Allen, C. Sidman, G. Proetzel and D. Calvin (1992). "Targeted disruption of the mouse transforming growth factor-β1 gene results in multifocal inflammatory disease." Nature **359**(6397): 693-699.

Shyer, A. E., T. R. Huycke, C. Lee, L. Mahadevan and C. J. Tabin (2015). "Bending gradients: how the intestinal stem cell gets its home." Cell **161**(3): 569-580.

Siewert, J. and H. Stein (1996). "Carcinoma of the gastroesophageal junction-classification, pathology and extent of resection." Diseases of the Esophagus **9**(3): 173-182.

Sihvo, E. I., J. T. Salminen, T. K. Rantanen, O. J. Ramo, M. Ahotupa, M. Farkkila, M. I. Auvinen and J. A. Salo (2002). "Oxidative stress has a role in malignant transformation in Barrett's oesophagus." Int J Cancer **102**(6): 551-555.

Silberg, D. G., J. Sullivan, E. Kang, G. P. Swain, J. Moffett, N. J. Sund, S. D. Sackett and K. H. Kaestner (2002). "Cdx2 ectopic expression induces gastric intestinal metaplasia in transgenic mice." Gastroenterology **122**(3): 689-696.

Singh, H., K. Ha, J. L. Hornick, S. Madha, P. Cejas, K. Jajoo, P. Singh, P. Polak, H. Lee and R. A. Shivdasani (2021). "Hybrid stomach-intestinal chromatin states underlie human Barrett's metaplasia." Gastroenterology **161**(3): 924-939. e911.

Singh, V., A. P. Singh, I. Sharma, L. C. Singh, J. Sharma, B. B. Borthakar, A. K. Rai, A. C. Kataki, S. Kapur and S. Saxena (2019). "Epigenetic deregulations of Wnt/β-catenin and transforming growth factor beta-Smad pathways in esophageal cancer: Outcome of DNA methylation." Journal of cancer research and therapeutics **15**(1): 192.

Slack, J. M. (1985). "Homoeotic transformations in man: implications for the mechanism of embryonic development and for the organization of epithelia." J Theor Biol **114**(3): 463-490.

Slack, J. M. and D. Tosh (2001). "Transdifferentiation and metaplasia—switching cell types." Current opinion in genetics & development **11**(5): 581-586.

Smith, K. A., E. Noël, I. Thurlings, H. Rehmann, S. Chocron and J. Bakkers (2011). "Bmp and nodal independently regulate lefty1 expression to maintain unilateral nodal activity during left-right axis specification in zebrafish." PLoS genetics **7**(9): e1002289.

Snyder, P., K. Dunbar, D. J. Cipher, R. F. Souza, S. J. Spechler and V. J. Konda (2019). "Aberrant p53 immunostaining in Barrett's esophagus predicts neoplastic progression: systematic review and meta-analyses." Digestive diseases and sciences **64**(5): 1089-1097.

Solomon, H., N. Dinowitz, I. S. Pateras, T. Cooks, Y. Shetzer, A. Molchadsky, M. Charni, S. Rabani, G. Koifman and O. Tarcic (2018). "Mutant p53 gain of function underlies high expression levels of colorectal cancer stem cells markers." Oncogene **37**(12): 1669-1684.

Sottocornola, R., C. Royer, V. Vives, L. Tordella, S. Zhong, Y. Wang, I. Ratnayaka, M. Shipman, A. Cheung, C. Gaston-Massuet, P. Ferretti, Z. Molnar and X. Lu (2010). "ASPP2 binds Par-3 and controls the polarity and proliferation of neural progenitors during CNS development." Dev Cell **19**(1): 126-137.

Souza, R. F., X. Huo, V. Mittal, C. M. Schuler, S. W. Carmack, H. Y. Zhang, X. Zhang, C. Yu, K. Hormi-Carver, R. M. Genta and S. J. Spechler (2009). "Gastroesophageal reflux might cause esophagitis through a cytokine-mediated mechanism rather than caustic acid injury." Gastroenterology **137**(5): 1776-1784.

Spechler, S. J. (1999). "The role of gastric carditis in metaplasia and neoplasia at the gastroesophageal junction." Gastroenterology **117**(1): 218-228.

Spechler, S. J. (2002). "Barrett's esophagus and esophageal adenocarcinoma: pathogenesis, diagnosis, and therapy." Med Clin North Am **86**(6): 1423-1445, vii.

Spechler, S. J. (2013). "Barrett esophagus and risk of esophageal cancer: a clinical review." Jama **310**(6): 627-636.

Spechler, S. J. (2018). "Cardiac metaplasia: follow, treat, or ignore?" Digestive diseases and sciences **63**(8): 2052-2058.

Spechler, S. J. and R. K. Goyal (1996). "The columnar-lined esophagus, intestinal metaplasia, and Norman Barrett." Gastroenterology **110**(2): 614-621.

Spechler, S. J., P. Sharma, R. F. Souza, J. M. Inadomi and N. J. Shaheen (2011). "American Gastroenterological Association technical review on the management of Barrett's esophagus." Gastroenterology **140**(3): e18-52; quiz e13.

Srivastava, A., R. D. Odze, G. Y. Lauwers, M. Redston, D. A. Antonioli and J. N. Glickman (2007). "Morphologic features are useful in distinguishing Barrett esophagus from carditis with intestinal metaplasia." Am J Surg Pathol **31**(11): 1733-1741.

Stachler, M. D., N. D. Camarda, C. Deitrick, A. Kim, A. T. Agoston, R. D. Odze, J. L. Hornick, A. Nag, A. R. Thorner and M. Ducar (2018). "Detection of mutations in Barrett's esophagus before progression to high-grade dysplasia or adenocarcinoma." Gastroenterology **155**(1): 156-167.

Stachler, M. D., A. Taylor-Weiner, S. Peng, A. McKenna, A. T. Agoston, R. D. Odze, J. M. Davison, K. S. Nason, M. Loda, I. Leshchiner, C. Stewart, P. Stojanov, S. Seepo, M. S. Lawrence, D. Ferrer-Torres, J. Lin, A. C. Chang, S. B. Gabriel, E. S. Lander, D. G. Beer, G. Getz, S. L. Carter and A. J. Bass (2015). "Paired exome analysis of Barrett's esophagus and adenocarcinoma." Nat Genet **47**(9): 1047-1055.

Stringer, E. J., I. Duluc, T. Saandi, I. Davidson, M. Bialecka, T. Sato, N. Barker, H. Clevers, C. A. Pritchard and D. J. Winton (2012). "Cdx2 determines the fate of postnatal intestinal endoderm." Development **139**(3): 465-474.

Su, Z., L. J. Gay, A. Strange, C. Palles, G. Band, D. C. Whiteman, F. Lescai, C. Langford, M. Nanji and S. Edkins (2012). "Common variants at the MHC locus and at chromosome 16q24. 1 predispose to Barrett's esophagus." Nature genetics **44**(10): 1131-1136.

Suda, K., H. Nakaoka, K. Yoshihara, T. Ishiguro, R. Tamura, Y. Mori, K. Yamawaki, S. Adachi, T. Takahashi and H. Kase (2018). "Clonal expansion and diversification of cancer-associated mutations in endometriosis and normal endometrium." Cell reports **24**(7): 1777-1789.

Sugimoto, S., Y. Ohta, M. Fujii, M. Matano, M. Shimokawa, K. Nanki, S. Date, S. Nishikori, Y. Nakazato and T. Nakamura (2018). "Reconstruction of the human colon epithelium in vivo." Cell Stem Cell **22**(2): 171-176. e175.

Sullivan, A. and X. Lu (2007). "ASPP: a new family of oncogenes and tumour suppressor genes." British journal of cancer **96**(2): 196-200.

Sun, L., Z. Zhang, J. Xu, G. Xu and X. Liu (2017). "Dietary fiber intake reduces risk for Barrett's esophagus and esophageal cancer." Critical reviews in food science and nutrition **57**(13): 2749-2757.

Takahashi, K., K. Tanabe, M. Ohnuki, M. Narita, T. Ichisaka, K. Tomoda and S. Yamanaka (2007). "Induction of pluripotent stem cells from adult human fibroblasts by defined factors." cell **131**(5): 861-872.

Tamai, Y., R. Nakajima, T.-o. Ishikawa, K. Takaku, M. F. Seldin and M. M. Taketo (1999). "Colonic Hamartoma Development by Anomalous Duplication in Cdx2Knockout Mice." Cancer research **59**(12): 2965-2970.

Tata, A., R. D. Chow and P. R. Tata (2021). "Epithelial cell plasticity: breaking boundaries and changing landscapes." EMBO Rep **22**(7): e51921.

Thomas, T., K. Abrams, J. De Caestecker and R. Robinson (2007). "Meta analysis: cancer risk in Barrett's oesophagus." Alimentary pharmacology & therapeutics **26**(11-12): 1465-1477.

Thota, P. N., P. Vennalaganti, S. Vennelaganti, P. Young, S. Gaddam, N. Gupta, D. Lieberman, R. Sampliner, G. W. Falk and S. Mathur (2017). "Low risk of high-grade dysplasia or esophageal adenocarcinoma among patients with Barrett's esophagus less than 1 cm (irregular Z line) within 5 years of index endoscopy." Gastroenterology **152**(5): 987-992.

Thrift, A. P. (2021). "Global burden and epidemiology of Barrett oesophagus and oesophageal cancer." Nature Reviews Gastroenterology & Hepatology **18**(6): 432-443.

Thrift, A. P. and H. B. El-Serag (2020). "Burden of gastric cancer." Clinical Gastroenterology and Hepatology **18**(3): 534-542.

Thrift, A. P. and D. Whiteman (2012). "The incidence of esophageal adenocarcinoma continues to rise: analysis of period and birth cohort effects on recent trends." Annals of oncology **23**(12): 3155-3162.

Toh, B.-H., J. W. Sentry and F. Alderuccio (2000). "The causative H+/K+ ATPase antigen in the pathogenesis of autoimmune gastritis." Immunology today **21**(7): 348-354.

Tomasetto, C., R. Masson, J. L. Linares, C. Wendling, O. Lefebvre, M. P. Chenard and M. C. Rio (2000). "pS2/TFF1 interacts directly with the VWFC cysteine-rich domains of mucins." Gastroenterology **118**(1): 70-80.

Tomita, H., Y. Yamada, T. Oyama, K. Hata, Y. Hirose, A. Hara, T. Kunisada, Y. Sugiyama, Y. Adachi and H. Linhart (2007). "Development of gastric tumors in ApcMin/+ mice by the activation of the β-catenin/Tcf signaling pathway." Cancer research **67**(9): 4079-4087.

Tomkova, M., J. Tomek, S. Kriaucionis and B. Schuster-Böckler (2018). "Mutational signature distribution varies with DNA replication timing and strand asymmetry." Genome biology **19**(1): 1-12.

Tordella, L., S. Koch, V. Salter, A. Pagotto, J. B. Doondeea, S. M. Feller, I. Ratnayaka, S. Zhong, R. D. Goldin and G. Lozano (2013). "ASPP2 suppresses squamous cell carcinoma via RelA/p65–mediated repression of p63." Proceedings of the National Academy of Sciences **110**(44): 17969-17974.

Tosh, D. and J. M. Slack (2002). "How cells change their phenotype." Nat Rev Mol Cell Biol **3**(3): 187-194.

Treuting, P. M., M. J. Arends and S. M. Dintzis (2018). Upper gastrointestinal tract. Comparative Anatomy and Histology, Elsevier**:** 191-211.

Trisno, S. L., K. E. Philo, K. W. McCracken, E. M. Catá, S. Ruiz-Torres, S. A. Rankin, L. Han, T. Nasr, P. Chaturvedi and M. E. Rothenberg (2018). "Esophageal organoids from human pluripotent stem cells delineate Sox2 functions during esophageal specification." Cell stem cell **23**(4): 501-515. e507.

Trunova, G., O. Makarova, M. Diatroptov, I. Bogdanova, L. Mikchailova and S. Abdulaeva (2011). "Morphofunctional characteristic of the immune system in

BALB/c and C57BL/6 mice." Bulletin of experimental biology and medicine **151**(1): 99-102.

Ubertini, V., G. Norelli, D. d'Arcangelo, A. Gurtner, E. Cesareo, S. Baldari, M. Gentileschi, G. Piaggio, P. Nisticò and S. Soddu (2015). "Mutant p53 gains new function in promoting inflammatory signals by repression of the secreted interleukin-1 receptor antagonist." Oncogene **34**(19): 2493-2504.

Van der Burgh, A., J. Dees, W. Hop and M. Van Blankenstein (1996). "Oesophageal cancer is an uncommon cause of death in patients with Barrett's oesophagus." Gut **39**(1): 5-8.

van der Flier, L. G., A. Haegebarth, D. E. Stange, M. van de Wetering and H. Clevers (2009). "OLFM4 is a robust marker for stem cells in human intestine and marks a subset of colorectal cancer cells." Gastroenterology **137**(1): 15-17.

van der Kooy, D., Weiss and Samuel (2000). "Why stem cells?" Science **287**(5457): 1439-1441.

van Es, J. H., M. E. van Gijn, O. Riccio, M. van den Born, M. Vooijs, H. Begthel, M. Cozijnsen, S. Robine, D. J. Winton, F. Radtke and H. Clevers (2005). "Notch/gamma-secretase inhibition turns proliferative cells in intestinal crypts and adenomas into goblet cells." Nature **435**(7044): 959-963.

van Nieuwenhove, Y., H. Destordeur and G. Willems (2001). "Spatial distribution and cell kinetics of the glands in the human esophageal mucosa." Eur J Morphol **39**(3): 163-168.

Van Nieuwenhove, Y. and G. Willems (1998). "Gastroesophageal reflux triggers proliferative activity of the submucosal glands in the canine esophagus." Diseases of the Esophagus **11**(2): 89-93.

VanDussen, K. L., J. M. Marinshaw, N. Shaikh, H. Miyoshi, C. Moon, P. I. Tarr, M. A. Ciorba and T. S. Stappenbeck (2015). "Development of an enhanced human gastrointestinal epithelial culture system to facilitate patient-based assays." Gut **64**(6): 911-920.

Vega, M. E., V. Giroux, M. Natsuizaka, M. Liu, A. J. Klein-Szanto, D. B. Stairs, H. Nakagawa, K. K. Wang, T. C. Wang and J. P. Lynch (2014). "Inhibition of Notch signaling enhances transdifferentiation of the esophageal squamous epithelium towards a Barrett's-like metaplasia via KLF4." Cell Cycle **13**(24): 3857-3866.

Verzi, M. P., H. Shin, H. H. He, R. Sulahian, C. A. Meyer, R. K. Montgomery, J. C. Fleet, M. Brown, X. S. Liu and R. A. Shivdasani (2010). "Differentiation-specific histone modifications reveal dynamic chromatin interactions and partners for the intestinal transcription factor CDX2." Developmental cell **19**(5): 713-726.

Verzi, M. P., M. N. Stanfel, K. A. Moses, B.-M. Kim, Y. Zhang, R. J. Schwartz, R. A. Shivdasani and W. E. Zimmer (2009). "Role of the homeodomain transcription factor Bapx1 in mouse distal stomach development." Gastroenterology **136**(5): 1701-1710.

Vives, V., J. Su, S. Zhong, I. Ratnayaka, E. Slee, R. Goldin and X. Lu (2006). "ASPP2 is a haploinsufficient tumor suppressor that cooperates with p53 to suppress tumor growth." Genes Dev **20**(10): 1262-1267.

von Furstenberg, R. J., J. Li, C. Stolarchuk, R. Feder, A. Campbell, L. Kruger, L. M. Gonzalez, A. T. Blikslager, D. M. Cardona, S. J. McCall, S. J. Henning and K. S. Garman (2017). "Porcine Esophageal Submucosal Gland Culture Model Shows Capacity for Proliferation and Differentiation." Cell Mol Gastroenterol Hepatol **4**(3): 385-404.

Von Rahden, B. H., H. J. Stein, K. Becker, D. Liebermann-Meffert and J. R. Siewert (2004). "Heterotopic gastric mucosa of the esophagus: literature-review and proposal of a clinicopathologic classification." Official journal of the American College of Gastroenterology| ACG **99**(3): 543-551.

Wallner, B., A. Sylvan and K.-G. Janunger (2002). "Endoscopic assessment of the "Z-line"(squamocolumnar junction) appearance: reproducibility of the ZAP classification among endoscopists." Gastrointestinal endoscopy **55**(1): 65-69.

Walters, S., U. Nur, B. Rachet, E. Gordon, N. Jakomis, G. Edgar and M. Coleman (2010). "Office for National Statistics: Cancer survival in England: one year and five year survival for 21 common cancers, by sex and age." Newport, UK: Office for National Statistics.

Wang, D. H. (2017). "The Esophageal Squamous Epithelial Cell—Still a Reasonable Candidate for the Barrett's Esophagus Cell of Origin?" Cellular and Molecular Gastroenterology and Hepatology **4**(1): 157-160.

Wang, D. H. and R. F. Souza (2016). "Transcommitment: paving the way to Barrett's metaplasia." Stem Cells, Pre-neoplasia, and Early Cancer of the Upper Gastrointestinal Tract: 183-212.

Wang, T., K. G. Yeoh and M. Salto-Tellez (2012). "Lgr5 expression is absent in human premalignant lesions of the stomach." Gut **61**(12): 1777-1778.

Wang, T. C., C. A. Dangler, D. Chen, J. R. Goldenring, T. Koh, R. Raychowdhury, R. J. Coffey, S. Ito, A. Varro and G. J. Dockray (2000). "Synergistic interaction between hypergastrinemia and Helicobacter infection in a mouse model of gastric cancer." Gastroenterology **118**(1): 36-47.

Wang, X., H. Ouyang, Y. Yamamoto, P. A. Kumar, T. S. Wei, R. Dagher, M. Vincent, X. Lu, A. M. Bellizzi, K. Y. Ho, C. P. Crum, W. Xian and F. McKeon (2011). "Residual embryonic cells as precursors of a Barrett's-like metaplasia." Cell **145**(7): 1023-1035.

Wang, Y., F. Bu, C. Royer, S. Serres, J. R. Larkin, M. S. Soto, N. R. Sibson, V. Salter, F. Fritzsche and C. Turnquist (2014). "ASPP2 controls epithelial plasticity and inhibits metastasis through β-catenin-dependent regulation of ZEB1." Nature cell biology **16**(11): 1092-1104.

Wang, Z., P. Dollé, W. V. Cardoso and K. Niederreither (2006). "Retinoic acid regulates morphogenesis and patterning of posterior foregut derivatives." Developmental biology **297**(2): 433-445.

Wapenaar, M. C., A. J. Monsuur, J. Poell, R. V. T. Slot, J. W. R. Meijer, G. A. Meijer, C. J. Mulder, M. L. Mearin and C. Wijmenga (2007). "The SPINK gene family and celiac disease susceptibility." Immunogenetics **59**(5): 349-357.

Weaver, J. M. J., C. S. Ross-Innes, N. Shannon, A. G. Lynch, T. Forshew, M. Barbera, M. Murtaza, C. A. J. Ong, P. Lao-Sirieix, M. J. Dunning, L. Smith, M. L. Smith, C. L. Anderson, B. Carvalho, M. O'Donovan, T. J. Underwood, A. P. May, N. Grehan, R. Hardwick, J. Davies, A. Oloumi, S. Aparicio, C. Caldas, M. D. Eldridge, P. A. W. Edwards, N. Rosenfeld, S. Tavare, R. C. Fitzgerald and O. Consortium (2014). "Ordering of mutations in preinvasive disease stages of esophageal carcinogenesis." Nature Genetics **46**(8): 837-843.

Willet, S. G., M. A. Lewis, Z. F. Miao, D. Liu, M. D. Radyk, R. L. Cunningham, J. Burclaff, G. Sibbel, H. Y. G. Lo and V. Blanc (2018). "Regenerative proliferation of differentiated cells by mTORC 1-dependent paligenosis." The EMBO journal **37**(7): e98311.

Wilson, R. L. and C. E. Stevenson (2019). Anatomy and Physiology of the Stomach. Shackelford's Surgery of the Alimentary Tract, 2 Volume Set, Elsevier**:** 634-646.

Winkelstein, A., B. S. Wolf, M. L. Som and R. H. Marshak (1954). "Peptic esophagitis with duodenal or gastric ulcer." J Am Med Assoc **154**(11): 885-889.

Wölffling, S., A. A. Daddi, A. Imai-Matsushima, K. Fritsche, C. Goosmann, J. Traulsen, R. Lisle, M. Schmid, M. del Mar Reines-Benassar and L. Pfannkuch (2021). "EGF and BMPs govern differentiation and patterning in human gastric glands." Gastroenterology **161**(2): 623-636. e616.

Woo, J., I. Miletich, B.-M. Kim, P. T. Sharpe and R. A. Shivdasani (2011). "Barx1-mediated inhibition of Wnt signaling in the mouse thoracic foregut controls tracheo-esophageal septation and epithelial differentiation." PLoS One **6**(7): e22493.

Woods, Y. L. and F. A. Carey (2014). "Pathology and histology of the oesophagus and stomach." Surgery (Oxford) **32**(11): 575-580.

Wu, C., Y. Xie, F. Gao, Y. Wang, Y. Guo, H. Tian, Y. Li and W. Fan (2013). "Lgr5 expression as stem cell marker in human gastric gland and its relatedness with other putative cancer stem cell markers." Gene **525**(1): 18-25.

Wu, W.-B., Y.-Y. Chen, B. Zhu, X.-M. Peng, S.-W. Zhang and M.-L. Zhou (2015). "Excessive bile acid activated NF-kappa B and promoted the development of alcoholic steatohepatitis in farnesoid X receptor deficient mice." Biochimie **115**: 86-92.

Xu, M., J. Horrell, M. Snitow, J. Cui, H. Gochnauer, C. M. Syrett, S. Kallish, J. T. Seykora, F. Liu and D. Gaillard (2017). "WNT10A mutation causes ectodermal dysplasia by impairing progenitor cell proliferation and KLF4-mediated differentiation." Nature communications **8**(1): 1-21.

Xu, X., S. G. Brodie, X. Yang, Y.-H. Im, W. T. Parks, L. Chen, Y.-X. Zhou, M. Weinstein, S.-J. Kim and C.-X. Deng (2000). "Haploid loss of the tumor suppressor Smad4/Dpc4 initiates gastric polyposis and cancer in mice." Oncogene **19**(15): 1868-1874.

Xu, X., J. LoCicero III, E. Macri, M. Loda and F. H. Ellis Jr (2000). "Barrett's esophagus and associated adenocarcinoma in a mouse surgical model." Journal of Surgical Research **88**(2): 120-124.

Yamamoto, Y., X. Wang, D. Bertrand, F. Kern, T. Zhang, M. Duleba, S. Srivastava, C. C. Khor, Y. Hu, L. H. Wilson, H. Blaszyk, D. Rolshud, M. Teh, J. Liu, B. E. Howitt, M. Vincent, C. P. Crum, N. Nagarajan, K. Y. Ho, F. McKeon and W. Xian (2016). "Mutational spectrum of Barrett's stem cells suggests paths to initiation of a precancerous lesion." Nat Commun **7**: 10380.

Yang, A., R. Schweitzer, D. Sun, M. Kaghad, N. Walker, R. T. Bronson, C. Tabin, A. Sharpe, D. Caput and C. Crum (1999). "p63 is essential for regenerative proliferation in limb, craniofacial and epithelial development." Nature **398**(6729): 714-718.

Yang, D., M. Yao, Y. Yan, Y. Liu, X. Wen, X. Chen and F. Lu (2021). "Deoxycholic acid Upregulates serum Golgi protein 73 through activating NF-κB pathway and destroying Golgi structure in liver disease." Biomolecules **11**(2): 205.

Yang, Y., M. Xiao, Y. Song, Y. Tang, T. Luo, S. Yang, W. He, Q. Cheng, L. Ma and Y. Zhang (2019). "H-score of 11β-hydroxylase and aldosterone synthase in the histopathological diagnosis of adrenocortical tumors." Endocrine **65**(3): 683-691.

Yizhak, K., F. Aguet, J. Kim, J. M. Hess, K. Kübler, J. Grimsby, R. Frazer, H. Zhang, N. J. Haradhvala and D. Rosebrock (2019). "RNA sequence analysis reveals macroscopic somatic clonal expansion across normal tissues." Science **364**(6444): eaaw0726.

Yousef, F., C. Cardwell, M. M. Cantwell, K. Galway, B. T. Johnston and L. Murray (2008). "The incidence of esophageal cancer and high-grade dysplasia in Barrett's esophagus: a systematic review and meta-analysis." American journal of epidemiology **168**(3): 237-249.

Yu, W.-Y., J. M. Slack and D. Tosh (2005). "Conversion of columnar to stratified squamous epithelium in the developing mouse oesophagus." Developmental biology **284**(1): 157-170.

Zhang, F., N. K. Altorki, Y. C. Wu, R. A. Soslow, K. Subbaramaiah and A. J. Dannenberg (2001). "Duodenal reflux induces cyclooxygenase-2 in the esophageal mucosa of rats: evidence for involvement of bile acids." Gastroenterology **121**(6): 1391-1399.

Zhang, G., J. Zheng, L. Zheng, S. Yu, C. Jiang, W. Lin, D. Li, L. Qu and W. Wang (2021). "Gastric intestinal metaplasia assessment between linked color imaging based on endoscopy and pathology." Scand J Gastroenterol **56**(1): 103-110.

Zhang, P., M. Yang, Y. Zhang, S. Xiao, X. Lai, A. Tan, S. Du and S. Li (2019). "Dissecting the single-cell transcriptome network underlying gastric premalignant lesions and early gastric cancer." Cell reports **27**(6): 1934-1947. e1935.

Zhang, Y., D. Bailey, P. Yang, E. Kim and J. Que (2021). "The development and stem cells of the esophagus." Development **148**(6).

Zhang, Y., M. Jiang, E. Kim, S. Lin, K. Liu, X. Lan and J. Que (2017). "Development and stem cells of the esophagus." Semin Cell Dev Biol **66**: 25-35.

Zhang, Y., Y. Yang, M. Jiang, S. X. Huang, W. Zhang, D. Al Alam, S. Danopoulos, M. Mori, Y.-W. Chen and R. Balasubramanian (2018). "3D modeling of esophageal development using human PSC-derived basal progenitors reveals a critical role for notch signaling." Cell stem cell **23**(4): 516-529. e515.

Zheng, H., D. M. Pritchard, X. Yang, E. Bennett, G. Liu, C. Liu and W. Ai (2009). "KLF4 gene expression is inhibited by the notch signaling pathway that controls goblet cell differentiation in mouse gastrointestinal tract." Am J Physiol Gastrointest Liver Physiol **296**(3): G490-498.

Zhou, H., M. A. Greco, F. Daum and E. Kahn (2001). "Origin of cardiac mucosa: ontogenic consideration." Pediatric and developmental pathology **4**(4): 358-363.